Supplying Europe with Hydrogen and Negative Emissions – A Model-Based Assessment

Zur Erlangung des akademischen Grades eines
Doktors der Wirtschaftswissenschaften
(Dr. rer. pol.)

von der KIT-Fakultät für Wirtschaftswissenschaften
des Karlsruher Instituts für Technologie (KIT)

genehmigte

DISSERTATION

von

M.Sc. Benjamin Lux

Tag der mündlichen Prüfung:	21. März 2023
Referent:	Prof. Dr. Martin Wietschel
Korreferent:	Prof. Dr. Wolf Fichtner

Karlsruhe März 2023

Contents

Acknowledgments

The publication of this dissertation is akin to reaching the peak of a mountain after a challenging climb. Without the invaluable help and encouragement of numerous individuals, the peak would still be an indistinct shape visible only through binoculars.

First and foremost, I would like to express my gratitude to my supervisor, Prof. Dr. Martin Wietschel, for his constructive and pragmatic support throughout my academic journey. I am also grateful to Prof. Dr. Wolf Fichtner for serving as the second referee of my thesis.

To my mentors, Dr. Ben Pfluger and Dr. Frank Sensfuß, I owe a special debt of gratitude. Their guidance and direction were instrumental in helping me navigate the complex terrain of my research. Being part of their rope team provided me with the safety and freedom to push for new heights.

I would also like to extend my appreciation to my colleagues at the Fraunhofer Institute for Systems and Innvoation Research for the welcoming and productive environment. I am particularly grateful to Miriam Schöfer for her help with formatting and all other aspects of life, Anja Klotz for proofreading, and Stefan Poslowsky, Niklas Schneck, and Miriam Frömel for their good work. I would also like to thank Vasilios Anatolitis, Matthias Kühnbach, Fabian Voswinkel, Christiane Bernath, Katja Franke, Pia Manz, Jose Ordonez, and Markus Fritz for their great company.

I cannot thank my family enough for their love and support. My parents, Friederike and Manfred, provided me with unwavering encouragement. My deepest gratitude goes to Susi. She has been my lighthearted partner on this journey, believing in me at every step. Enno's genuine cheerfulness and cheekiness brought pure joy during challenging moments towards the end.

Climbing this academic mountain would not have been possible without your support and encouragement. Thank you for being part of this journey with me.

Karlsruhe, March 2023

Benjamin Lux

Abstract

Electrolytic hydrogen and captured and subsequently stored CO_2 from ambient air (DACCS) are two options for implementing ambitious climate protection strategies in Germany and Europe. Electricity-based hydrogen can potentially replace fossil fuels in many processes and applications of the classical energy demand sectors and act as seasonal energy storage in the conversion sector. Negative emissions via DACCS can compensate for unavoidable residual emissions, e.g., from agriculture, and compete economically with alternative greenhouse gas mitigation strategies. Both options interact strongly with a transforming energy supply system. Therefore, this dissertation aims to quantitatively analyze the interactions of hydrogen systems with the conversion sector and the provision of negative emissions via DACCS in the context of a greenhouse gas-neutral European energy system.

To address this research topic, the cost minimization model *Enertile*, which used to focus on the representation of electricity and heat supply, is extended to a multidirectional energy supply model. The core of the methodological development is modeling the interactions of hydrogen and DACCS technologies with future renewable electricity and heat systems. The potentials of hydrogen and DACCS and essential drivers for their use are determined in scenario studies.

For hydrogen, the model results show that Europe has a substantial hydrogen production potential and can largely supply itself cost-efficiently. Electrolysis and hydrogen power plants become central flexibility providers in the optimized renewable electricity system. Hydrogen production follows cost-efficient renewable power generation. In cost minimization, hydrogen storage – with a seasonal balancing of supply and demand – and hydrogen transport networks – with a supraregional balancing of supply and demand – fulfill fundamental tasks in the energy system.

In the model results for Europe, there are DACCS potentials at costs between 60 and 270 €/t_{CO2}. Compared to the literature, these technical negative emissions can compete with relatively expensive alternative greenhouse gas abatement options. In the optimization, Sweden, the Iberian Peninsula, Norway, and Finland fulfill key requirements for suitable DACCS sites: vacant electricity generation and geological storage potentials.

This dissertation is based on my research conducted at the Fraunhofer Institute for Systems and Innovation Research (ISI) and supervised by Prof. Dr. Martin Wietschel at the Institute for Industrial Production (IIP) at the Karlsruhe Institute of Technology (KIT). Dr. rer. pol. is the envisaged degree.

Kurzfassung

Elektrolysewasserstoff und aus der Umgebungsluft abgeschiedenes und anschließend eingespeichertes CO_2 (DACCS) sind zwei Optionen für die Umsetzung ambitionierter Klimaschutzstrategien in Deutschland und Europa. Strombasierter Wasserstoff kann dabei potentiell fossile Energieträger in vielen Prozessen und Anwendungen der klassischen Energienachfragesektoren ersetzen und im Umwandlungssektor als saisonaler Energiespeicher fungieren. Negative Emissionen mittels DACCS können unvermeidbare Restemissionen, z. B. aus der Landwirtschaft, kompensieren und in ökonomische Konkurrenz mit alternativen Treibhausgasminderungsstrategien treten. Beide Optionen interagieren stark mit einem im Wandel befindlichen Energieangebotssystem. Ziel dieser Dissertation ist deshalb die quantitative Analyse der Wechselwirkungen des Wasserstoffsystems mit dem Umwandlungssektor und der Bereitstellung von Negativemissionen mittels DACCS im Kontext eines treibhausgasneutralen europäischen Energiesystems.

Zur Adressierung des Forschungsgegenstandes wird das auf die Abbildung von Strom- und Wärmebereitstellung ausgerichtete Kostenminimierungsmodell *Enertile* zu einem multidirektionalen Energieangebotsmodell erweitert. Kern der methodischen Weiterentwicklung ist die Modellierung der Interaktionen von Wasserstoff- und DACCS-Technologien mit zukünftig auf erneuerbare Energien ausgelegten Strom- und Wärmesystemen. An Hand von Szenariostudien werden Potentiale von Wasserstoff und DACCS bestimmt und wesentliche Treiber für ihre Nutzung identifiziert.

Für Wasserstoff zeigen die Modellergebnisse, dass Europa ein substantielles Wasserstofferzeugungspotential hat und sich in großen Teilen kosteneffizient selbstversorgen kann. Elektrolyseure und Wasserstoffkraftwerke werden zu zentralen Flexibilitätsgebern im optimierten erneuerbaren Stromsystem. Die Wasserstofferzeugung folgt dabei der kostengünstigen erneuerbaren Stromerzeugung. In der Kostenminimierung übernehmen Wasserstoffspeicher mit einem saisonalen und Wasserstofftransportnetze mit einem überregionalen Ausgleich von Angebot und Nachfrage fundamentale Aufgaben im Energiesystem.

In den Modellergebnissen für Europa gibt es DACCS-Potentiale zu Kosten zwischen 60 und 270 €/t_{CO2}. Im Literaturvergleich können diese technischen Negativemissionen mit vergleichsweise teuren, alternativen Treibhaugasminderungsoptionen konkurrieren. In der Optimierung erfüllen Schweden, die Iberische Halbinsel, Norwegen, und Finnland zentrale Voraussetzungen für geeignete DACCS-Standorte: Ungenutzte Stromerzeugungs- und geologische Speicherpotentiale.

Diese Dissertation wurde im Rahmen meiner Forschungsarbeit am Fraunhofer-Institut für System- und Innovationsforschung (ISI) erstellt und von Prof. Dr. Martin Wietschel am Institut für industrielle Produktion (IIP) des Karlsruher Instituts für Technologie (KIT) betreut. Dr. rer. pol. ist der angestrebte Abschluss.

Part I

1 Introduction

1.1 Background and motivation

The "urgent action to combat climate change and its impacts" (UN 2015b) is one of the United Nations Sustainable Development Goals. To achieve this overarching goal, 196 parties of the United Nations Framework Convention on Climate Change (UNFCC), representing over 98% of global greenhouse gas (GHG) emissions, agreed in the legally binding "Paris Agreement" to limit the global temperature increase preferably to 1.5 °C compared to the pre-industrial mean temperature (UN 2015a; UNCC 2016). The "European Green Deal" outlines how the European Commission (EC) intends to contribute to achieving these global goals (EC 2019). A core element of this strategy is a GHG-neutral economy in the European Union (EU) by 2050 (EC 2019; European Parliament et al. 2021). At the national level, the German federal government committed itself to the EC's climate protection targets in the amended Climate Protection Act and aims for net GHG neutrality by 2045 (BMJ et al. 2021). The German and European climate protection acts aim at negative GHG balances after 2050. (BMJ et al. 2021; European Parliament et al. 2021).

Two central pillars of both the European and the German climate protection strategies are an increase in energy efficiency (the so-called "efficiency first principle") and direct use of renewable energies (BMUV 2016; European Parliament et al. 2018a, 2018b). The third pillar relies on renewable electricity. It contributes to GHG reduction either directly through the electrification of end-use applications or indirectly through the generation and use of electricity-based energy carriers (e-fuels) (BMUV 2016; EC 2018a). These e-fuels include hydrogen produced via electrolysis and its derivatives synthetic hydrocarbons and synthetic ammonia. To reduce emissions through synthetic hydrocarbons, only GHG-neutral carbon sources – e.g., the ambient air or biogenic sources – must be used in their synthesis. The appeal of using e-fuels is that they reduce GHG emissions by directly replacing their fossil counterparts while retaining established applications and infrastructures. Some GHG mitigation strategies using e-fuels involve the substitution of hydrocarbons with electricity-based hydrogen. In this case, end-use applications and infrastructures must be repurposed or replaced, and the benefit of "GHG reduction by switching only the fuel supply" without process conversions diminishes. However, generating e-fuels using renewable electricity is associated with conversion losses and additional costs. Electrification of applications and processes is most often more efficient due to the direct use of electricity but usually requires changing end-use applications and strengthening electricity infrastructures. Beyond the use of hydrogen and hydrocarbons as feedstock – which require physical energy carriers – there are, therefore, some processes and applications for which it has not yet been decided whether their emissions will be mitigated through electrification or e-fuels.

1 Introduction

Russia's war of aggression against Ukraine challenges the current European and German supply of fossil energy carriers. Russia was the largest supplier of fossil natural gas and oil in 2020: about 65% (39%) of the natural gas (eurostat 2022a) and 30% (23%) of the oil (eurostat 2022b) consumed in Germany (the EU) were of Russian origin. However, the start of Russia's war in Ukraine has led to a sharp reduction and temporary suspension in the supply of these energy carriers. Consequently, the EU is facing an energy shortage and high energy prices in 2022. In response, the German government has been seeking and signing energy partnerships with alternative exporting countries – e.g., Qatar (BMWK 9/14/2022) – to avoid strong dependencies on Russian fossil fuels. Hence, new fossil supply routes are being established today, ideally considering Germany's future supply of renewable hydrogen or synthetic hydrocarbons.

In addition to reducing GHG emissions through more efficient energy use, the utilization of renewable energies, and the direct or indirect use of renewable electricity, an increase in GHG sinks can contribute to achieving GHG neutrality. Despite extensive decarbonization efforts, Wohland et al. (2018), Fasihi et al. (2019), and Realmonte et al. (2019) expect that reaching GHG neutrality in 2050 will require negative emission technologies (NET). In addition to offsetting unavoidable residual emissions in the net-zero emissions equilibrium state, NETs are an option to offset previous emission overshoots – and associated temperature overshoots – by net negative CO_2 emissions (Riahi et al. 2022). Many current scenarios rely on these long-term net negative emissions to return the global temperature increase to 1.5 °C after temporary overshoots (Johansson et al. 2020; Rogelj et al. 2019). Overall, NETs are still in their infancy. Among the various approaches to achieve negative emissions, previous decarbonization scenario studies have mainly examined bioenergy combined with carbon capture and storage (BECCS) (Rogelj et al. 2018). Among others, Smith et al. (2016) formulate sustainability and resource availability concerns with this approach. Therefore, technical solutions with direct air capture plants and subsequent permanent storage of the captured CO_2 (DACCS) are gaining more attention. Key challenges with DACCS are the low CO_2 concentration in the atmosphere causing high energy demands in the capture process (Fuhrman et al. 2020) and a negative public perception of carbon capture and storage (CCS) activities in Germany and other countries (Anderson et al. 2012; Bradbury 2012; Brunsting et al. 2011; Dütschke 2011; Dütschke et al. 2016).

Both e-fuels and DACCS as GHG mitigation strategies rely on renewable energies and interact strongly with the conversion sector. This dissertation aims to consider these interactions and analyze the supply of e-fuels and negative CO_2 emissions via the DACCS pathway in the context of a GHG-neutral European energy supply system. The analysis of e-fuels focuses on hydrogen. The energy system model *Enertile* (Fraunhofer ISI 2021) as the primary research tool for these analyses is successively enhanced in this dissertation. The enhanced model version can cover the supply of electricity, heat, hydrogen, synthetic methane, and negative CO_2 emissions via the DACCS pathway. For simplicity, these supplies are referred to as the "energy supply system" in the remainder of this thesis. Other segments, such as refineries, which are part of this expression in other definitions, are not included within this text.

The energy system model *Enertile* (cf. section 2.2) geographically covers the member states of the EU, Norway, Switzerland, the United Kingdom, Bosnia and Herzegovina, Serbia, Montenegro, Albania, and North Macedonia. For convenience, the modeled territory is referred to as "Europe" in the remainder of this dissertation.

Taking a system perspective, direct addressees of the analyses are political decision-makers concerned with the design of the future German and European energy systems. The focus is on the system integration of the GHG mitigation options hydrogen and negative CO_2 emissions via the DACCS route. The aim is to identify robust characteristics in cost-optimized GHG-neutral target systems. The applied perspective excludes taxes, levies, and subsidies from the analysis. The design of these instruments to achieve the developed target system is out of the scope of this work.

1.2 Structure of the thesis

This cumulative dissertation is structured as shown in Figure 1-1. Section 1 identifies the research questions. Four stand-alone research papers accepted in internationally recognized scientific journals constitute the core of the thesis and are presented in sections 5 - 8. Section 2 summarizes the methodological advancements of the energy system model *Enertile* in all four publications. Section 3 synthesizes the individual publications' results following the formulated research questions. Finally, section 4 derives key conclusions. Superordinately, sections 1-4 constitute the framework chapters in Part 1 of the dissertation. The research papers in sections 5-8 are Part 2.

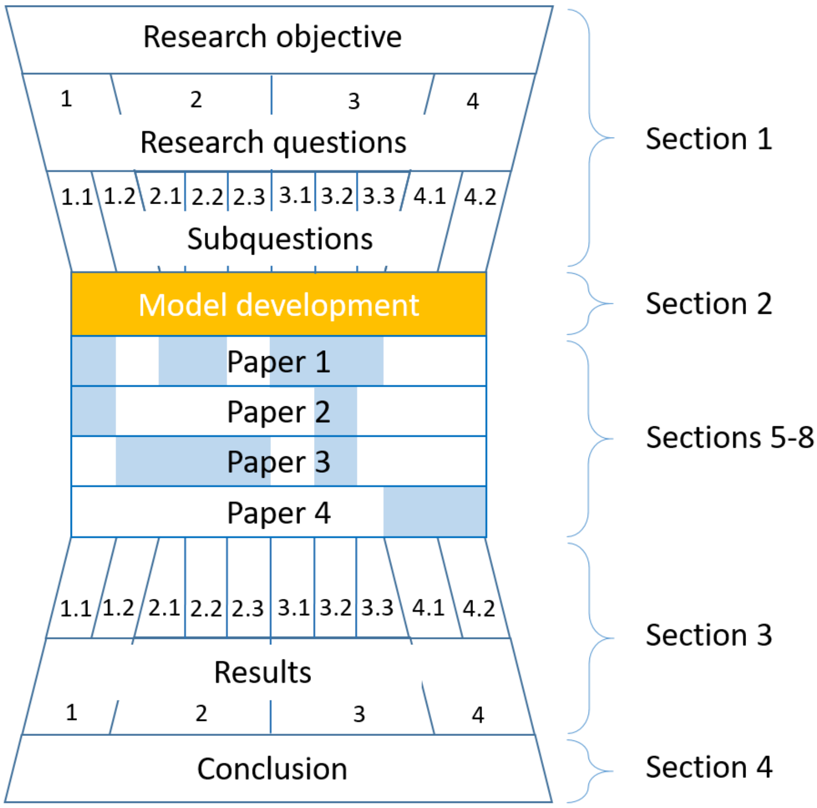

Figure 1-1 Structure of the thesis.

1.3 Research questions

It is an open question to which extent hydrogen and synthetic hydrocarbons will be used in the future GHG-neutral European or German energy system and what they will be used for. The discussion about the most viable GHG reduction strategy and to what extent e-fuels are part of it is particularly dynamic in the traditional energy demand sectors industry, transport, and buildings (in the sectors services and households).

Today, the demand for hydrogen is concentrated almost exclusively in the industrial sector and is met almost entirely from fossil sources (IEA 2021). Agora Energiewende et al. (2021) define three distinct categories of hydrogen application in the industry: firstly, as feedstock in synthesis processes with products containing molecular bound hydrogen; secondly, as a reactant in processes with final products that do not contain molecular bound hydrogen; thirdly, as an energy carrier for heat generation. The first category mainly includes the production of basic chemicals like ammonia, methanol, and olefins, as well as the use of hydrogen in refineries. In these processes, replacing fossil hydrogen with renewable hydrogen can realize GHG reductions (Bazzanella et al. 2017; Neuwirth et al. 2022). If needed (e.g., for methanol and olefin synthesis), carbon would have to be provided either from GHG-neutral sources or via chemical recycling (Wachsmuth et al. 2021). The second category mainly comprises steel production. Reducing iron with hydrogen could replace today's predominant process route in primary steel production, reducing iron ore with coke in blast furnaces to reduce GHG emissions (IRENA 2020; Neuwirth et al. 2022). Alternatively, synthetic methane can act as a direct reducing agent in steelmaking. The third category covers using hydrogen to provide steam and process heat in the industry (e.g., heat provision for cement kilns). This future energetic use of hydrogen is subject to greater uncertainties than in the other two categories and may depend on the temperature level of the required heat. In particular, hydrogen competes with other GHG-neutral low-temperature heat sources such as heat pumps (Wachsmuth et al. 2021). Synthetic methane could also contribute to GHG reductions for the generation of heat. In the 1.5 °C compatible scenarios underlying the EC's long-term strategic vision, industry demands in 2050 for hydrogen in the EU range between 300 TWh/a and 338 TWh/a and for synthetic methane between 150 TWh/a and 164 TWh/a (EC 2018b). The current four major scenario studies achieving GHG neutrality in Germany identify industrial e-fuel demands between 109 TWh/a and 359 TWh/a in the GHG-neutral target state[1] (SCI4climate.NRW 2022) based on (BCG 2021; dena 2021; Fraunhofer ISI et al. 2021; Prognos et al. 2021).

The diffusion of hydrogen as a fuel in the transport sector has been considered a central entry point to a hydrogen-based economic system – the "hydrogen economy" – for a long time (Bashmakov et al. 2022). When the low energy density of batteries and long charging times limited the effective range of battery electric vehicles to 150 km, fuel cell vehicles promised to be an attractive solution for the market segment of long-distance travel (Plötz 2022). Today, as battery-electric vehicles offer 400 km real-world ranges and high-power fast battery charging, Plötz (2022) and Davis et al. (2018) assume that passenger cars and light-duty vehicles will mainly be battery-electric. For the medium- and heavy-duty truck sector, anticipated developments in the literature are less clear-cut. Evaluating the total cost of ownership, Hunter et al. (2021) show for this market segment that the most feasible zero-emission powertrain depends on the operating conditions. The authors conclude that battery electric powertrains may be best suited for truck operation on short ranges or if dwell times are not pivotal for the business case. Fuel cell power trains, on the other hand, offer advantages for truck operation on long ranges or business cases with limited dwell times in this analysis. Mauler et al. (2022) find that advances in autonomous driving could shift the feasibility of fuel cell trucks towards short-range applications as mandatory breaks and rest times for drivers can be omitted, and refueling times are substantially shorter than for battery electric powertrains. Since battery-electric trucks have a head start in development, Plötz (2022), however, concludes that the window of opportunity for fuel-cell electric trucks to become the dominant zero-emission powertrain in the truck segment is closing. In international shipping and aviation, biogenic or hydrogen-based synthetic energy carriers will probably become the dominating energy forms due to their high energy density (Jaramillo et al. 2022). Progress in battery technology could make all-electric aircraft an option for short distances (Schäfer et al. 2019). In the 1.5 °C compatible scenarios underlying the EC's long-term strategic vision, transport demands for

[1] In 2021, the target year for GHG neutrality in Germany was shifted from 2050 to 2045 in an adjustment to the Climate Protection Act ((BMJ et al. 2021)). Not all cited studies published in 2021 have implemented this adjustment and show the demands accordingly for 2045 or 2050.

hydrogen in the EU are between 327 TWh/a and 369 TWh/a in 2050; the demand for synthetic hydrocarbons ranges between 366 TWh/a and 710 TWh/a in 2050 (EC 2018b). The current four major scenario studies achieving GHG neutrality in Germany identify e-fuel demands for transport between 19 TWh/a and 197 TWh/a in the GHG neutral target state[1] (SCI4climate.NRW 2022) based on (BCG 2021; dena 2021; Fraunhofer ISI et al. 2021; Prognos et al. 2021).

Buildings are responsible for the highest energy demand in the EU, with demand for space heating and hot water alone currently amounting to about 3,600 TWh (Fraunhofer ISI et al. 2017; Peters et al. 2020). Natural gas is the main energy carrier in building heat supply in the EU today (Peters et al. 2020). Especially for existing buildings, GHG reductions in heat generation are a major and complex challenge, as possible solutions depend on the renovation status, available infrastructure, and ownership structure of individual buildings (SRU 2021). E-fuels are controversially discussed as a potential solution. The use of synthetic methane for decentralized heat generation has the advantage that existing natural gas transmission and distribution networks and gas-based heating technologies in buildings can be retained. Compared to hydrogen, this advantage may be offset by the conversion losses and costs associated with the additional synthesis step (Fraunhofer IKTS et al. 2021). The decentralized use of hydrogen for building heat generation comes with the challenge that both the transport and distribution infrastructure must be built, existing gas networks must be repurposed, and all end-use applications within a network must be replaced – possibly simultaneously (Fraunhofer IKTS et al. 2021). Blending electricity-based hydrogen with natural gas in the gas networks to reduce emissions in building heat supply is limited to the maximum permissible blending limits. Today, Germany's hydrogen admixture limit is 10% by volume (Wissenschaftliche Dienste des Deutschen Bundestages 2019). While current projects (e.g. (Arcadis Nederland et al. 2020; SGN 2022)) are testing the provision of decentralized heat in buildings using hydrogen, the IEA (2021) and Cabeza et al. (2022) assume that heat demands can be met more efficiently and at lower cost by electrical solutions and that hydrogen will rather play a minor role in the building sector. In the 1.5 °C compatible scenarios underlying the EC's long-term strategic vision, building demands for hydrogen in the EU are between 79 TWh/a and 80 TWh/a in 2050; synthetic methane demands range between 300 TWh/a and 306 TWh/a in 2050 (EC 2018b). The current four major scenario studies achieving GHG neutrality in Germany identify building demands for e-fuel between 0 TWh/a and 178 TWh/a in the GHG neutral target state[1] (SCI4climate.NRW 2022) based on (BCG 2021; dena 2021; Fraunhofer ISI et al. 2021; Prognos et al. 2021).

In addition to using hydrogen as an energy carrier and feedstock in the traditional energy demand sectors, hydrogen can also serve as an energy carrier in the conversion sector. Flexible hydrogen conversion can meet electricity and heat demand at low renewable energy supply times in an energy supply system based on renewable energies. For example, in the 1.5 °C compatible scenarios underlying the EC's long-term strategic vision, hydrogen demand for electricity and heat supply in the EU ranges between 88 TWh/a and 105 TWh/a in 2050. The conversion sector has no synthetic methane demand in the EC's scenarios (EC 2018b). The current four major scenario studies achieving GHG neutrality in Germany identify e-fuel demand in the conversion sector between 24 TWh/a and 152 TWh/a in the GHG neutral target state[1] (SCI4climate.NRW 2022) based on (BCG 2021; dena 2021; Fraunhofer ISI et al. 2021; Prognos et al. 2021).

This overview of the EU's and Germany's e-fuels demands in the various sectors for different GHG-neutral scenarios shows that both applications and energy quantities of these energy forms vary widely. In many cases, it will depend on the cost of e-fuels, whether they are considered part of a GHG reduction strategy, or whether alternative mitigation strategies are employed. Since all e-fuels have electricity-based hydrogen as a key ingredient, the remainder of the analysis focuses on hydrogen. Only the synthetic methane supply in the Middle East and North Africa (MENA) is analyzed in depth in Paper 2.

Based on these preliminary considerations, the first research question is:

Research question 1.: **What does electricity-based hydrogen cost, and how can the European hydrogen demands be met cost-efficiently in the GHG-neutral target state?**

In their hydrogen strategy, the EC identifies North Africa as a potential export region for supplying Europe with electricity-based "green" hydrogen (EC 2020). The asset of the MENA region is its enormous and relatively inexpensive renewable power generation potential. Timmerberg et al. (2019b) find that even as electricity demand in these countries increases, the available renewable potential exceeds that demand by at least an order of magnitude. Potentially, hydrogen can therefore be produced cheaply in this region and subsequently transported to Europe. For export to Europe, however, transport costs and possible risk premiums must also be considered. Before the work in this dissertation, there were few studies investigating the hydrogen production potential in MENA (Hank et al. 2020; Timmerberg et al. 2019a; Ueckerdt et al. 2021), and none comparing it with a consistent methodological approach to an inner-European supply. This gap in the literature will be addressed by evaluating Subquestion 1.1.:

Subquestion 1.1: *Under which circumstances are hydrogen imports to Europe from regions with favorable renewable power generation conditions economically efficient?*

For the investigation of Subquestion 1.1., one approach relies on the determination of European hydrogen supply potentials. This analysis finds that the hydrogen production potential varies greatly between European countries (Lux et al. 2020). Husarek et al. (2021) show that hydrogen imports are key for supplying Germany with hydrogen in 2050. In their analysis, other European countries become important hydrogen trading partners for Germany. Krieg (2012) designed and analyzed a hydrogen pipeline infrastructure within Germany to supply hydrogen fueling stations for road transport. However, before this dissertation, there was a lack of studies considering the interactions of European hydrogen transport infrastructures with the European conversion sector. Whether a European hydrogen transport network is beneficial for offsetting this imbalance in hydrogen supply between individual countries, therefore, is the subject of Subquestion 1.2:

Subquestion 1.2: *Which hydrogen transport routes are economically efficient in Europe?*

Unless Europe imports all hydrogen, the role of hydrogen in the conversion sector is more complex than in the other sectors: Hydrogen is produced from renewable electricity and used to supply electricity and heat in the conversion sector. Fluctuating renewable energies are expected to become the central pillar of electricity generation in a GHG-neutral European power system (Pfluger 2014). The weather dependency of renewable energies – especially solar and wind-based technologies – creates the need for flexibility options continually balancing electricity supply and demand (Huber et al. 2014; Kondziella et al. 2016). Electricity-based hydrogen allows for temporal shifting (combination of upward and downward flexibility) and end-use flexibility (Fraunholz 2021; Li et al. 2021): Electrolytic hydrogen production can integrate an oversupply of renewable electricity. As hydrogen is readily storable in geological formations, it can either be reconverted into electricity during periods of high residual loads – i.e., a shortfall in electricity supply from renewables – or supply hydrogen demands from other sectors. There is a growing body of studies evaluating hydrogen as a flexibility option. However, as shown in a literature review in Paper 3 (cf. section 7), there is a lack in the existing literature analyzing the sector coupling option hydrogen in the context of a spatially, temporally, and technologically detailed assessment of the European energy supply system. Research question 2 addresses this gap following the dimensions of upward flexibility (Subquestion 2.1), downward flexibility (Subquestion 2.2), and time-shifting flexibility (Subquestion 2.3).

Research question 2.: **What role can electricity-based hydrogen play as a storage medium and flexibility option in a GHG-neutral electricity system?**

Subquestion 2.1: *How are electrolyzers dimensioned, where are they positioned, and how are they operated in an optimized renewable electricity system?*

Subquestion 2.2: *How are hydrogen power plants dimensioned, where are they positioned, and how are they operated in an optimized renewable electricity system?*

Subquestion 2.3: *How are hydrogen storages dimensioned and operated over a year in an optimized renewable energy supply system?*

In addition to the overarching issues of hydrogen supply in Germany and Europe, research question 3 examines the determinants of hydrogen production costs. As relevant dimensions, the techno-economic characteristics of electrolyzers (Subquestion 3.1.), renewable electricity costs (Subquestion 3.2.), and other electricity demands (Subquestion 3.3.) are identified.

Research question 3.: **Which variables influence hydrogen production costs in a renewable European energy supply system?**

Subquestion 3.1: *How do hydrogen production costs change with variations in the techno-economic characteristics of electrolyzers?*

Subquestion 3.2: *How do hydrogen production costs change with variations in renewable electricity supply costs?*

Subquestion 3.3: *How do hydrogen production costs change with variations in other electricity demands?*

Some process-related emissions – especially in cement and lime production – cannot be completely avoided by alternative processes. Consequently, a certain amount of GHG emissions, for example, from agriculture, are quasi-unavoidable and need to be compensated by GHG sinks. Accordingly, the EC considers carbon capture and storage (CCS) as one of seven strategy components for a net-zero GHG economy. Its 1.5 °C compatible scenarios deploy CCS in the EU with a volume of 80 - 298 Mt_{CO2}/a (EC 2018b). All four current major scenario studies for GHG neutrality in Germany consider CCS with a volume between 24 Mt_{CO2}/a and 73 Mt_{CO2}/a inevitable to achieve the climate protection goals (SCI4climate.NRW 2022) based on (BCG 2021; dena 2021; Fraunhofer ISI et al. 2021; Prognos et al. 2021). Hitherto, DACCS has been studied mainly from a technological point of view or as a backstop technology option in global energy scenarios with limited techno-economic resolution. For this reason, it is necessary to analyze the provision of carbon dioxide removal (CDR) via the DACCS route in the context of a spatially, temporally, and technologically detailed assessment of the European energy supply system. Research question 4 addresses this gap.

Research question 4.: **Do economically feasible potentials for DACCS exist in Europe?**

Depending on the cost of DACCS, negative emissions may be considered an alternative CO_2 abatement strategy across sectors beyond offsetting unavoidable emissions. However, the cost spread for DACCS in the literature ranges from 30 \$/t_{CO2} to 1,000 \$/t_{CO2} (Fuss et al. 2018). Recognizing the wide range of CO_2 capture costs via the DACCS pathway in the literature and taking a conservative approach due to the novelty of the technology, Subquestion 4.1 reads as follows:

Subquestion 4.1: *What does CO_2 capture and storage via the DACCS route cost in an optimized European energy system?*

For the supply of hydrogen, the analyses in Papers 1 to 3 show that electrolytic hydrogen production strongly depends on low-cost, available renewable electricity generation potential. DACCS is likely to be energy intensive (Fuhrman et al. 2020) and, therefore, dependent on the availability of renewable energies, too. The supply of hydrogen and negative emissions via the DACCS pathway are also similar in being relatively flexible in their generation patterns throughout the year and their ability to adapting the conditions in the renewable electricity generation system. In combination, this infers Subquestion 4.2:

Subquestion 4.2: *Where are DACCS plants positioned in an optimized renewable European energy supply system?*

2 Methods

The quantitative assessment of the supply of electricity-based hydrogen and negative emissions via the DACCS route is complex. There are strong interactions between these supply processes and other components of the conversion sector. Hydrogen has a twofold effect on the conversion sector. Firstly, electrolysis requires electricity to meet the hydrogen demands from other sectors. Secondly, hydrogen can be used as a storage medium within the conversion sector, generating both time-dependent electricity demands and electricity and heat supplies. DACCS can also interact with the conversion sector in two ways. Firstly, DAC plants need renewable electricity or renewable heat to remove the remaining emissions of all sectors from the atmosphere. Secondly, the conversion sector can temporarily increase the required negative emissions by using GHG-active energy sources to generate electricity or heat. To manage this complexity, science and politics develop and use a variety of energy models to understand the fundamental mechanics of the energy system. Different modeling approaches are available depending on the perspective and the issue under investigation. In section 2.1, the most important existing model types are presented, and a suitable approach for addressing the research questions raised in section 1.3 is identified. Afterward, the chosen modeling platform is described in section 2.2.

2.1 Model theory and choice of methods

The subsequent characterization of modeling approaches follows closely what has already been described in Enzensberger (2003), Sensfuss (2007), Pfluger (2014), Deac (2019), and Bernath (2023).

Many model classification schemes divide energy system models in first order based on their focus: they distinguish so-called top-down and bottom-up models (e.g., Enzensberger (2003), Sensfuss (2007), Herbst et al. (2012), Prina et al. (2020)). The description of top-down models focuses on the interactions between the energy sector and other segments of an entire economy (Connolly et al. 2010; Deac 2019). These models try to assess the impact of energy and climate policies on public welfare, employment, or economic growth (Prina et al. 2020). Due to their holistic view, their technical detail is usually low. Typically, technological developments are only captured through policy instruments. These instruments are either price-based, such as taxes, surcharges, or subsidies, or regulatory-based, such as technical standards or technology bans (Herbst et al. 2012). In contrast, bottom-up models focus on a detailed techno-economic description of the energy system's components (Deac 2019) and interconnections. The high level of technical detail allows for studying both the impact of different technologies on the energy system (Prina et al. 2020) and of exogenous framework conditions and policies on the development of individual technologies within the energy system (Enzensberger 2003). However, bottom-up models are usually partial models and do not allow for feedback from other macroeconomic sectors (Prina et al.

2020). The research questions developed in section 1.3 focus on analyzing the integration of hydrogen and DACCS systems in a European or German GHG-neutral energy supply system. A detailed description of the individual hydrogen and DACCS technologies is necessary to capture their interactions with the conversion sector. Therefore, a bottom-up approach is predestined for a model-based investigation of the central research questions.

In the second order, Sensfuss (2007) identifies optimization models and simulation models as important sub-classes of bottom-up models. The key characteristic of an optimization model is one central objective function (Ventosa et al. 2005). In energy system models, the objective typically is the least cost system that meets technical, economic, and political constraints. These models make decisions based purely on economic criteria (Enzensberger 2003). Implicitly, the system optimization approach assumes perfectly competitive markets (Enzensberger 2003). There are two approaches in optimization models to deal with time-dependent information (Prina et al. 2020): In the perfect-foresight approach, a decision is made simultaneously for all time steps. A single optimization problem contains complete information for the entire time horizon. This includes time-dependent information on the developments of techno-economic parameters, policy targets, and demand variations. In contrast, the myopic approach divides long time horizons into a series of optimization problems. Decisions are made stepwise, based on information available only at the respective time step of the series. The structure and characteristics of optimization models cause weaknesses. The perfect market assumption includes that characteristics of real markets, like transaction costs, information costs, and market failures, are not modeled. As a result, the costs of a system change tend to be underestimated (Sensfuss 2007; Zhang et al. 1998). Optimization approaches also have the issue of the so-called "Bang bang" or "Penny-switching" effect (Held 2011; Pfluger 2014). It is characterized by substantial changes in the results due to small changes in the input parameters. In the third order, Sensfuss (2007) distinguishes system dynamics models, game-theoretic approaches, and agent-based modeling as sub-categories of simulation models. In system dynamics models, the interactions between individual components of a system are represented through differential equation systems (Enzensberger 2003). In contrast to pure optimization models, this modeling approach allows the representation of market imperfections and the strategic behavior of individual agents (Enzensberger 2003). However, especially when analyzing long periods and structural changes, this modeling approach can lead to implausible results (Enzensberger 2003; Pfluger 2014). The main characteristic of agent-based models is that individual market participants are modeled by so-called agents (Pfluger 2014). These agents are characterized by their strategic behavior – implemented by specific objective functions – and the adaptation of their strategic behavior to market events – based on learning algorithms – in the model (Enzensberger 2003). This approach allows for considering market power and imperfect or asymmetric information (Pfluger 2014). However, agent-based models often yield unrealistic prices as agents use their full market power. In reality, exercising market power beyond certain thresholds would cause interventions by regulators (Pfluger 2014). Game-theoretic approaches are mainly used to study market designs and market power (Sensfuss 2007). Based on the supply curves of different market actors, so-called Nash equilibria are determined (Enzensberger 2003). No actor can improve at these equilibrium points by deviating from the chosen strategy. However, according to Day et al. (2002), convergence is only assured for simple models. Moreover, Nash equilibria are often ambiguous.

This dissertation systematically investigates the interactions of hydrogen systems with the conversion sector and the supply of negative emissions via the DACCS route. Depending on the specific question, both simulation and optimization models could be considered for this analysis. If, for example, the attractiveness of the market environment of hydrogen is to be investigated from the perspective of different actors, simulation models are to be preferred. They offer the possibility of representing the short- to medium-term return options and the strategic decision-making behavior of the players under the given regulatory framework in detail. In general, simulations are almost inevitable for practically all questions that require a representation of concrete market mechanisms and rules since optimization models cannot represent them or can only do so in a highly simplified way. However, the focus of this work is on the long-term technological design of an energy supply system. Within a defined framework, it is considered which technical changes to the existing energy system can lead to an optimal energy system from the point of view of political decision-makers. Additional aspects that can be taken into account in simulations are only secondarily relevant to this question; for the analysis of an optimal system from a techno-economic point of view, it is often helpful to abstract from current market rules and stakeholder structures. For the given research questions, an optimization model is, therefore, the appropriate analysis tool.

A variety of optimization models are used to study energy systems. Hence, it is necessary to identify a suitable model platform for answering the research questions raised in section 1.3. The following criteria may be applied:

1. Both GHG mitigation options, hydrogen and DACCS, can be powered by renewable electricity. Yet, the renewable electricity supply by wind and solar power plants depends on the weather at a given location at a given time. Therefore, a high technological, spatial, and temporal resolution for the renewable electricity generation potentials is essential to adequately determine the expansion and deployment of the two investigated mitigation options.
2. Both electrolyzers and DAC units compete for cheap electricity with other consumers. However, they can be applied comparatively flexibly. Likewise, hydrogen power plants can supply electricity flexibly and compete with other supply technologies. Therefore, to adequately represent this competition, a good representation of alternative flexible and inflexible electricity consumers and suppliers in the model is required.
3. If necessary, the power transmission grid can compensate weather-related, temporary, regional power supply shortages. Bernath et al. (2019) show that the option of balancing electricity over a large geographic area has an impact on the utilization of renewable energy and heat pumps in heat grids. Therefore, covering as large a geographic area as possible with the option of transmission grid expansion increases the accuracy of the results.
4. Investment decisions affect the entire technical lifetime of a system component. Therefore, to get an accurate picture of the evolution of an energy system on its transformation

path to GHG neutrality, the optimization should take into account investment decisions at different time steps in addition to the dispatch of energy system components.

The energy system model *Enertile* (Fraunhofer ISI 2021), developed at the Fraunhofer Institute for Systems and Innovation Research ISI, meets these criteria sufficiently. In *Enertile*, renewable power generation technologies are modeled with a high resolution. The representation of fluctuating technologies includes onshore wind, offshore wind, ground-mounted PV, rooftop PV, and concentrated solar power (CSP). The potentials of these electricity supplies are calculated on an hourly basis using real weather data on a grid with an edge length of 6.5 x 6.5 km. *Enertile* enables a detailed representation of the conversion sector. Different power generation, demand, transmission, and storage technologies are part of the model decision. In particular, the linkage of the power system with heat systems allows for a high degree of flexibility (Deac 2019). The geographical coverage of *Enertile* is sufficiently large. In the past, studies have been carried out on Europe (Pfluger 2014) and the MENA region (Godron et al. 2014). In *Enertile*, integrated optimization calculations for several simulation years are possible. Both investment and dispatch decisions are taken into account. As the defined key criteria are met by the existing model *Enertile*, it is further developed and improved to answer the research questions outlined in section 1.3.

2.2 The optimization model *Enertile*

Section 2.2.1 describes the state of the energy system model *Enertile* before the start of this dissertation. A more comprehensive documentation of this initial model can be found in (Bernath et al. 2019; Deac 2019; Pfluger 2014; Pfluger et al. 2017). An overview of the model extensions and enhancements in the context of this dissertation is given in section 2.2.2. The mathematical formulation of the resulting model is shown in section 2.2.3.

2.2.1 Existing model

The energy system model *Enertile* has been used for long-term analysis of electricity and heat (via heat pumps and heat grids) supply infrastructures. In GHG-reduction scenarios, a linear optimization problem describes the supplies of electricity and heat in European countries. The goal of the optimization is to minimize system costs. Therefore, the objective function sums the annualized investments and operating and maintenance costs of relevant electricity and heat generation units, transmission networks, and storage technologies. Both capacity expansion and dispatch decisions are considered. To some extent, load shifts through controlled charging of battery electric vehicles and plug-in hybrids are part of the optimization. The combined optimization of electricity and heat supply allows for an adequate representation of combined heat and power (CHP) plants. Moreover, it creates additional flexibility for integrating renewable energies into the electricity system with heat pumps, electric boilers, and heat grids.

The key constraints of the cost minimization require (Lux et al. 2020; Pfluger et al. 2017)

- that exogenously given hourly electricity and heat demands are met in each model region (so-called balance equations),
- that the utilization of electricity and heat supply infrastructures do not violate installed capacities,
- and that political targets, e. g., CO_2 reduction or renewable energy expansion targets, are met.

Other key input parameters include:

- Existing installed capacities of electricity and heat generation, transmission, and storage technologies.
- Technical parameters of existing and expandable electricity and heat infrastructures, like conversion efficiency, losses, or technical lifetime.
- Economic parameters of existing and expandable electricity and heat infrastructures, like specific investments and operation and maintenance costs.
- Prices for energy carriers and CO_2 certificates.
- Highly resolved potentials of the fluctuating renewable electricity generation technologies, onshore wind, offshore wind, ground-mounted PV, rooftop PV, and CSP.

The optimization results provide the cost-efficient expansion and hourly dispatch of renewable and conventional electricity and heat generation, transmission, and storage technologies. Further results are the system costs, the shadow prices of the central demand constraints, the emissions of conventional power and heat generation, and fuel usage (Lux et al. 2018).

Enertile has a high temporal and spatial resolution. It usually covers the simulation years 2030, 2040, and 2050 in hourly resolution in a single model run using perfect foresight. Depending on the research question at hand, *Enertile* can cover Europe, the Middle East and North Africa (MENA), and China. The spatial resolution for the energy supply optimization is mostly at the country level, but it is possible to aggregate small and geographically proximate national states and to split countries for more detailed analyses.

The core of the energy system model *Enertile* is a software package for formulating the linear optimization problem. This software is written in the programming language Java and is linked to a MySQL database for data management. The linear problem is solved with the commercial software *ILOG CPLEX Optimization Studio* (CPLEX) of the company IBM.

2.2.2 Overview of the model enhancements in this dissertation

To investigate the research questions outlined in section 1.3, this dissertation extends the existing linear optimization model *Enertile* to capture the supply of electricity-based hydrogen, synthetic methane, and carbon dioxide removal via the DACCS route. Like electricity and heat, each of these new goods has its own balancing space in the modeling. Figure 2-1 shows a simplified schematic representation of the balance spaces and their interactions. Colors (hydrogen, synthetic methane, negative CO_2 emissions) highlight the model extensions developed in this dissertation. Since the supplies of hydrogen, synthetic methane, and captured and sequestered CO_2 interact closely with conditions in the conversion sector, the extension of *Enertile* has two key advantages: Firstly, it can draw on the existing detailed modeling of renewable energy potentials. The availability of renewable electricity is a key requirement for the supply of goods studied in this dissertation. Secondly, the feedback of the new balance spaces on the conversion sector also improves the level of detail of the old model.

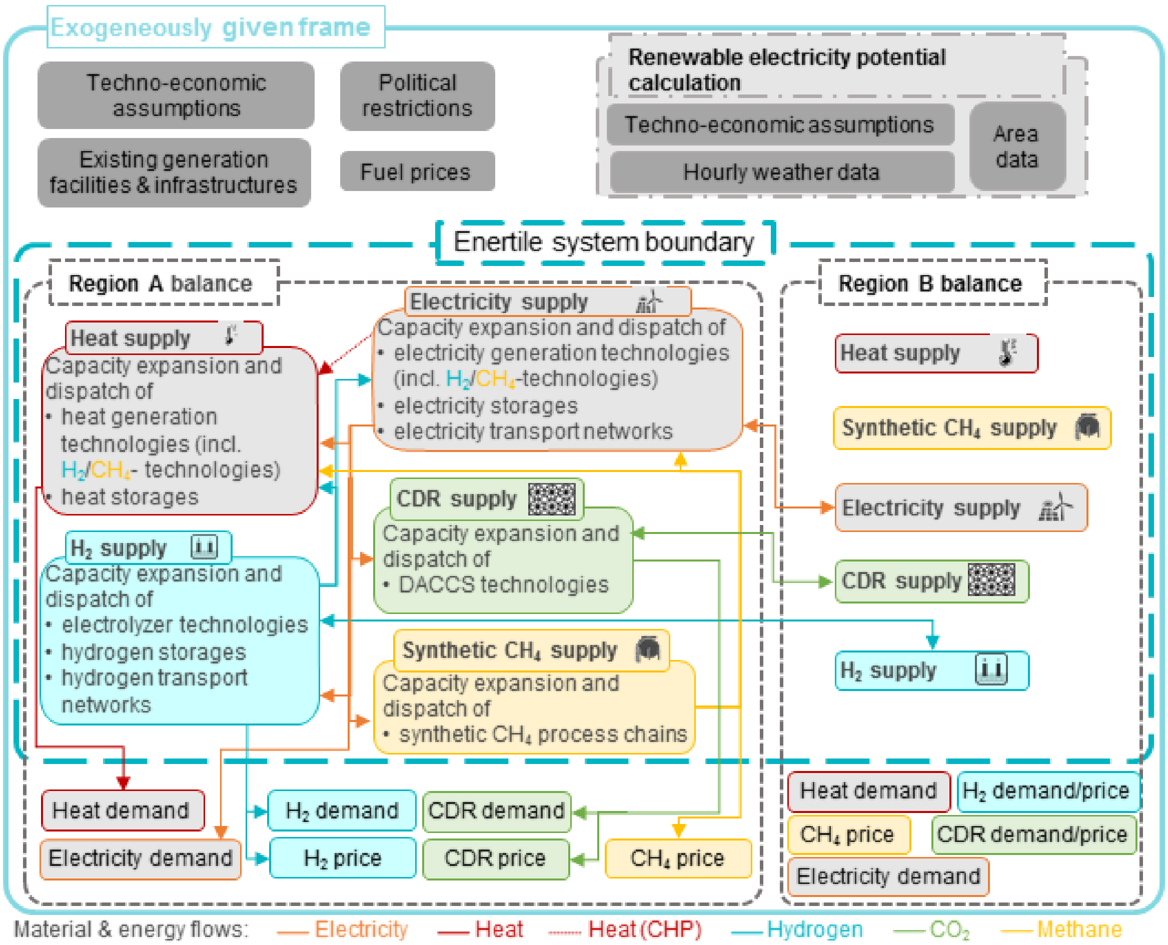

Figure 2-1 Schematic representation of the extended model version of *Enertile*. New and existing modules' extensions are highlighted in color (hydrogen, synthetic methane, negative CO_2 emissions).

2.2.2.1 Multi-balance structure

In the code that generated the linear problem of the old model version, the interconnection or interaction of different balancing spaces – which in some cases is equivalent to a representation of sector coupling – was limited to two balancing spaces. An example of such a connection is a heat pump, which contributes to the heat supply in a region's district heating network and is an electricity consumer in the electricity balance of the same region. The advancement in this dissertation now allows for linking together any number of balances. This has the advantage that the increasing interactions between the supply of electricity, heat, hydrogen, fossil, and synthetic hydrocarbons, and CO_2 capture in renewables-based energy systems can be captured and evaluated more accurately. One concrete application case in this dissertation is hydrogen CHP, which appears as a demand technology in the hydrogen balance and as a supply technology in both the electricity and the heat balance of a region.

2.2.2.2 Hydrogen

This dissertation establishes a new hydrogen module (cf. Figure 2-1). Its goal is to meet both externally imposed hydrogen demands, which may originate from the sectors industry, transport, services, and households, and endogenous hydrogen demands arising in conjunction with the conversion sector represented in the existing model. The modeling includes

- electrolyzers and imports originating from outside Europe as hydrogen supplies,
- different hydrogen power plants (incl. CHP) and hydrogen boilers for electricity and heat generation as model endogenous hydrogen demands,
- geological hydrogen storage facilities as seasonal storage options,
- and transport pipeline networks between model regions for hydrogen transport.

The model was developed successively to address specific research questions in the respective journal publications. The modeling of electrolyzers, hydrogen reconversion technologies, excluding CHP, and geological hydrogen storage, is described in more detail in Paper 1 (section 5.2). Special hydrogen export chains for the MENA region were developed in Paper 2 (section 6.2). Modeling of hydrogen CHP plants, European hydrogen transport networks, and hydrogen imports from outside Europe is applied in Paper 3 (section 7.2).

2.2.2.3 Synthetic methane

This dissertation establishes a new synthetic methane module (cf. Figure 2-1). Its goal is to meet both externally imposed synthetic methane demands, which may originate from the sectors industry, transport, services, and households, and endogenous synthetic methane demands arising in conjunction with the conversion sector represented in the existing model. Synthetic methane serves as a representative example of synthetic hydrocarbons. Due to limited computing power, only the simplest hydrocarbon is considered in the analysis. The modeling includes

- power-to-methane process chains as synthetic methane supplies,
- different power plants (incl. CHP) and boilers for electricity and heat generation as model endogenous synthetic methane demands,
- and geological methane storage facilities as seasonal storage options.

The modeling of the synthetic methane module was done for Paper 2 and is described in more detail in section 6.2.

2.2.2.4 CO_2 capture and sequestration via the DACCS route

This dissertation establishes a new CO_2 capture and sequestration module (cf. Figure 2-1). Its goal is to meet both externally imposed carbon dioxide removal demands, which may originate from the sectors agriculture, industry, transport, services, and households, as well as endogenous CDR demands arising in conjunction with the conversion sector represented in the existing model. The modeling includes

- DAC and sequestration units that capture CO_2 from the atmosphere and permanently store it underground for CDR supply,
- feedbacks from the usage of fossil fuels in the conversion sector increasing model endogenous CDR demands,
- and virtual transfers of removed CO_2 between model regions.

The modeling of CO_2 capture and sequestration was developed to address the research questions in Paper 4 and is described in more detail in section 8.2.

2.2.2.5 Sales instance

Enertile is a partial model that calculates the cost-efficient supply of energy. The central approach to take into account demands for electricity, heat, hydrogen, synthetic methane, or negative CO_2 emissions from other sectors in the supply optimization is to specify them as hourly demand constraints. To meet these demands, cost minimization determines the least cost system design. However, there is no feedback of supply costs to exogenously given demands from other sectors. Therefore, this dissertation establishes a second mechanism that indirectly represents demands for hydrogen, synthetic methane, or negative CO_2 emissions. This mechanism assumes that there is a certain willingness to pay for one of these goods. This willingness to pay is offered to the supply model as a sales price. In the model, the sale of hydrogen, synthetic methane, or compensated CO_2 reduces the system's total cost in the objective function. The supply model decides which supply infrastructure – i.e., electricity supply infrastructure and electrolyzers, synthetic methane generation units, or DACCS plants – it can build and use to sell certain amounts of one of these goods at a given price. The last megawatt hour of hydrogen or synthetic methane or the last ton of compensated CO_2 sold by the model generates production costs at the applied sales price; the marginal generation unit of this good is determined. The equivalence of marginal production costs and prices holds only for the assumption of perfect competition. Section 4.3 discusses that this assumption probably does not hold for real gas or hydrogen markets. Applying different selling prices in different model runs allows for determining supply curves for the respective goods. This approach is only suitable because the demand for hydrogen, synthetic methane, and compensated CO_2 can easily be shifted in time. Hydrogen and synthetic methane are storable at low cost, so generation and demand do not need to be strictly synchronized in time. Offsetting emissions via the DACCS route is even more time-elastic than synchronizing e-fuel demand and supply.

The sales instance was first developed and described to determine European hydrogen supply curves in Paper 1 (section 5). It is also used to determine hydrogen and synthetic methane supply curves in Paper 2 (section 6) as well as supply curves for negative CO_2 emissions in Paper 4 (section 8).

2.2.3 A mathematical formulation of the resulting optimization model

In line with what has been described in Paper 1 (Lux et al. 2020) and Paper 3 (Lux et al. 2022), the objective function of the resulting "linear cost minimization problem for supplying electricity el, heat ht, hydrogen $H2$ [, synthetic methane $CH4$, and negative CO_2 emissions $CO2$] in an energy system is formulated in equation (1). It sums the cost of all included generation, transmission, and storage infrastructures [minus the remunerations for the sales of hydrogen, synthetic methane, or compensated CO_2] in all regions $r \in R$ and all hours $h \in H$ of all considered simulation years $a \in A$." (Lux et al. 2022) New model extensions introduced in this dissertation are highlighted in the same colors as in Figure 2-1. The objective function contains three types of decision variables: firstly $\vec{X}$ describing installed capacities of considered infrastructures, secondly $\vec{x}$ describing the unit dispatch of these infrastructures, and thirdly $\vec{y}$ describing the sales volumes of hydrogen, synthetic methane, and negative CO_2 emissions. "Costs for the supply of electricity, heat, ... hydrogen [, synthetic methane, and negative CO_2 emissions] are the coefficients of the various decision variables and are grouped into fixed costs and variable costs. Fixed cost $c^{fix}_{\{i,j,k[,l,m]\}}$ contain annuitized investments, capital costs, and fixed operation and maintenance costs of respective technologies. Variable cost $c^{var}_{\{i,j,k[,l,m,seq]\}}$ contain fuel cost, CO_2 emission certificate cost, and variable operation and maintenance cost. The technology portfolio I for the provision of electricity contains conventional electricity generation technologies (including CHP and hydrogen power plants), renewable electricity generation technologies, electricity storage technologies, and simplified electricity transmission networks. The set of technologies J for the provision of heat contains conventional heat generation technologies (including hydrogen boilers), renewable heat generation technologies, electric heat generators, and heat storages. The technology set K for the provision of hydrogen contains electrolyzers, hydrogen storage technologies, and simplified hydrogen transport networks." (Lux et al. 2022) The technology portfolio L for the provision of synthetic methane contains different fully integrated power-to-methane process chains, i.e., these process chains represent black boxes for the model that convert electricity into synthetic methane. The parameterization of these process chains takes into account the underlying technologies of seawater desalination (if necessary), electrolysis, CO_2 capture, and methanation. The technology set M contains DAC plants. In this modeling approach, the transport and long-term storage of CO_2 are only considered with variable costs $c^{var}_{\{seq\}}$. Selling prices for hydrogen p^{hy}, synthetic methane p^{CH4}, and sequestered CO_2 p^{CO2} can be considered as the willingness to pay for these goods by sectors outside the system boundaries of *Enertile*. Selling the respective goods at the defined price leads to reduced system costs in *Enertile*.

$$\min_{\vec{X},\vec{x},\vec{y}} \sum_{a\in A}\left[\sum_{r\in R}\left\{ \sum_{i\in I}\left(\underbrace{\left(c_{a,i}^{fix}\cdot X_{a,r,i}^{el}\right)}_{capacity\ expansion\ electricity\ supply} + \underbrace{\sum_{h\in H} c_{a,i}^{var}\cdot x_{a,r,i.h}^{el}}_{electricity\ generation}\right)\right.\right.$$
$$+\sum_{j\in J}\left(\underbrace{\left(c_{a,j}^{fix}\cdot X_{a,r,j}^{ht}\right)}_{capacity\ expansion\ heat\ supply} + \underbrace{\sum_{h\in H} c_{a,j}^{var}\cdot x_{a,r,j,h}^{ht}}_{heat\ generation}\right)$$
$$+\sum_{k\in K}\left(\underbrace{\left(c_{a,k}^{fix}\cdot X_{a,r,k}^{H2}\right)}_{capacity\ expansion\ H2\ supply} + \underbrace{\sum_{h\in H} c_{a,k}^{var}\cdot x_{a,r,k.h}^{H2}}_{H2\ generation}\right)$$
$$+\sum_{l\in L}\left(\underbrace{\left(c_{a,l}^{fix}\cdot X_{a,r,l}^{CH4}\right)}_{capacity\ expansion\ syn.\ CH4\ supply} + \underbrace{\sum_{h\in H} c_{a,l}^{var}\cdot x_{a,r,l.h}^{CH4}}_{syn.\ CH4\ generation}\right) \tag{1}$$
$$+\sum_{m\in M}\left(\underbrace{\left(c_{a,m}^{fix}\cdot X_{a,r,m}^{CO2}\right)}_{capacity\ expansion\ DAC} + \underbrace{\sum_{h\in H}\left(c_{a,m}^{var}+c_{a,seq}^{var}\right)\cdot x_{a,r,m.h}^{CO2}}_{CO2\ capture\ and\ sequestration}\right)$$
$$\left.\left.-\underbrace{\begin{Bmatrix} p^{H2}\cdot y_r^{H2} \\ p^{CH4}\cdot y_r^{CH4} \\ p^{CO2}\cdot y_r^{CO2} \\ 0 \end{Bmatrix}}_{sales\ of\ H2,\ syn.\ CH4\ or\ compensated\ CO2\ to\ demand\ sectors}\right\}\right]$$

"The central constraints of the cost minimization – the so-called demand-supply equations $DS_{\{el,hg,b,H2[,CH4,CO2]\}}$ – are region- and hour-specific balancing equations for electricity, heat, hydrogen [, synthetic methane, and compensated CO_2 emissions]. These equations ensure that the demands of these goods are met. There are two types of demands: Firstly, exogenous demands from other sectors for electricity D^{el}, heat $D^{ht}_{\{hg,b\}}$ in heat grids hg and buildings b, ... hydrogen D^{H2} [, synthetic methane D^{CH4}, and CO_2 removal D^{CO2}]. Secondly, model endogenous demands that result from interdependencies of the different balancing spaces modeled in Enertile." (Lux et al. 2022)

"Equation (2) shows the electricity demand-supply equation DS_{el}. It ensures that the sum of model endogenous electricity demands for heat supply in heat girds and buildings, ... for hydrogen supply via electrolysis [, for synthetic methane production, and for capturing CO_2 from ambient air] along with the exogenously specified electricity demand D^{el} is met for each hour h of a simulation year

a and each region r by the net electricity generation of technologies I. Supplying heat in heat grids HG or buildings B with electrical technologies increases electricity demands. Electric boilers eb convert electricity into heat with efficiency γ_{eb}. The electric conversion efficiencies $\gamma_{\{hpg,hpb\}}$ of both heat pumps for heat grids hpg and buildings hpb depend on the prevailing ambient temperature. The supply of hydrogen with electrolyzers ely increases the electricity demand as a function of the electrolyzer efficiency γ_{ely}." (Lux et al. 2022) Power-to-methane process chains l increase electricity demands by producing synthetic methane with overall conversion efficiency γ_l. Capturing CO_2 from ambient air with DAC plant m causes model endogenous electricity demands. The factor γ_m specifies how much electricity is required to capture one ton of CO_2 from the atmosphere.

[DS$_{el}$]

$$\sum_{i \in I} x^{el}_{a,r,i,h} = D^{el}_{a,r,h} + \sum_{hg \in HG} \left(\frac{1}{\gamma_{a,r,hpg,h}} \cdot x^{ht}_{a,r,hg,hpg,h} + \frac{1}{\gamma_{a,eb}} \cdot x^{ht}_{a,r,hg,eb,h} \right) + \sum_{b \in B} \frac{1}{\gamma_{a,r,hpb,h}} \cdot x^{ht}_{r,b,hpb,h} + \sum_{ely} \frac{1}{\gamma_{a,ely}} \cdot x^{H2}_{a,r,ely,h} + \sum_{l \in L} \frac{1}{\gamma_{a,l}} \cdot x^{CH4}_{a,r,l,h} + \sum_{m \in M} \gamma_{a,m} \cdot x^{CO2}_{a,r,m,h} \qquad \forall a,r,h \qquad (2)$$

"Equations (3) and (4) show the heat demand-supply equations. The demand-supply equation for heat in heat grids DS$_{hg}$ (3) ensures that the exogenously specified heat demand in heat grids D^{ht}_{hg} is met for each hour h of a simulation year a and each region r by the net heat generation of technologies $N \subset J$ and $Q \subset I$. The technology set N includes pure heat generation technologies and heat storage systems suitable for use in heat grids; the technology set Q includes hydrogen CHP plants whose heat generation for heat grids is coupled to electricity generation via the power-to-heat ratio $\gamma^{chp,ht}_q$. The demand-supply equation for heat in buildings DS$_b$ (4) ensures that the exogenously specified heat demand in buildings D^{ht}_b is met for each hour h of a simulation year a and each region r by the net heat generation of the subset of heating technologies $O \subset J$ suitable for supplying buildings.

[DS$_{hg}$]

$$\sum_{n \in N} x^{ht}_{a,r,hg,n,h} + \sum_{q \in Q} \gamma^{chp,ht}_{a,q} \cdot x^{el,chp}_{a,r,q,h} = D^{ht}_{a,r,hg,h} \qquad \forall a,r,hg,h \qquad (3)$$

[DS$_b$]

$$\sum_{o \in O} x^{ht}_{a,r,b,o,h} = D^{ht}_{a,r,b,h} \qquad \forall a,r,b,h \qquad (4)$$

Equation (5) shows the hydrogen demand-supply equation DS$_{H2}$. It ensures for each hour h of a simulation year a and each region r that the net hydrogen supply of technology portfolio K meets the model endogenous hydrogen demands and either explicitly specified exogenous hydrogen demands from other sectors D^{H2} or implicitly imposed hydrogen demands [by the sale of hydrogen y^{H2} at price p^{H2}]. Endogenous hydrogen demands include the provision of heat in heat grids

HG using hydrogen boilers $hyb \in N$ with conversion efficiency γ_{hyb}, the reconversion of hydrogen into electricity using the portfolio of pure hydrogen-to-electricity reconversion technologies $P \subset I$ with associated conversion efficiencies γ_p, and the co-generation of electricity and heat using the portfolio of CHP reconversion technologies $Q \subset I$ with associated conversion efficiencies $\gamma_q^{chp,H2}$." (Lux et al. 2022)

[DS$_{H2}$]
$$\sum_{k \in K} x^{H2}_{a,r,k,h} = \sum_{hg \in HG} \frac{1}{\gamma_{a,hyb}} \cdot x^{ht}_{a,r,hg,hyb,h} + \sum_{p \in P} \frac{1}{\gamma_{a,p}} \cdot x^{el}_{a,r,p,h} + \sum_{q \in Q} \frac{1}{\gamma^{chp,H2}_{a,q}} \cdot x^{el,chp}_{a,r,q,h} + \begin{cases} y^{H2}_{a,r,h} \\ D^{H2}_{a,r,h} \end{cases} \quad \forall a,r,h \qquad (5)$$

Equation (6) shows the synthetic methane demand-supply equation DS$_{CH4}$. It ensures for each hour h of a simulation year a and each region r that the net synthetic methane supply of technology portfolio L meets the model endogenous synthetic methane demands consisting of the provision of heat in heat grids HG using boilers $meb \in N$ with conversion efficiency γ_{meb} and the reconversion of synthetic methane into electricity using the portfolio of reconversion technologies $S \subset I$ with associated conversion efficiencies γ_s. Additionally, the "sale" of synthetic methane y^{CH4} to external demand sectors requires synthetic methane generation.

[DS$_{CH4}$]
$$\sum_{l \in L} x^{CH4}_{r,q,h} = \sum_{hg \in HG} \frac{1}{\gamma_{a,meb}} \cdot x^{ht}_{a,r,hg,meb,h} + \sum_{s \in S} \frac{1}{\gamma_{a,s}} \cdot x^{el}_{a,r,s,h} + y^{CH4}_{a,r,h} \quad \forall a,r,h \qquad (6)$$

Equation (7) shows the carbon dioxide removal demand-supply equation DS$_{CO2}$. It ensures for each hour h of a simulation year a and each region r that the net supply of removed CO_2 from the atmosphere by the technology portfolio M meets the model endogenous CDR demands and either explicitly specified exogenous CDR demands from other sectors D^{CO2} or implicitly imposed CDR demands by the sale of removed CO_2 y^{CO2} at price p^{CO2}. Endogenous CDR demand arises when fossil technologies are used to generate electricity $T \subset I$ or heat in heat grids $U \subset N$. The emissions released by the use of fossil fuels are included in the balance via the emission factor e_f of the fuel and the efficiency $\gamma^{el/ht}$of the technology used. The net supply of removed CO_2 includes the removal of DAC and sequestration plants and the net virtual transfer of CO_2 removal from other regions.

[DS$_{CO2}$]
$$\sum_{m \in M} x^{CO2}_{a,r,m,h} = \sum_{hg \in HG} \sum_{u \in U} \frac{e_f}{\gamma^{ht}_u} \cdot x^{ht}_{a,r,hg,u,h} + \sum_{t \in T} \frac{e_f}{\gamma^{el}_t} \cdot x^{el}_{a,r,t,h} + \begin{cases} y^{CO2}_{a,r,h} \\ D^{CO2}_{a,r,h} \end{cases} \quad \forall a,r,h \qquad (7)$$

3 Results

The core results of this dissertation are summarized below. They are based on the findings presented in the journal publications in sections 5 to 8 and are structured along the research questions formulated in section 1.3.

3.1 Research question 1.: What does electricity-based hydrogen cost, and how can the European hydrogen demands be met cost-efficiently in the GHG-neutral target state?

This research question is addressed in Paper 1, Paper 2, and Paper 3, each focusing on different aspects of the question. One difficulty in identifying economically efficient hydrogen supply strategies is that hydrogen supply and demand are mutually dependent. In the market equilibrium, an economically efficient tuple consists of a hydrogen quantity and a hydrogen price. The market price settles at the intersection of the supply and demand curve. With a few exceptions, the optimization model *Enertile*, which is used in this dissertation, covers only the energy supply side. Consequently, assumptions must be made regarding the hydrogen demand that needs to be met. This difficulty is partially circumvented in Paper 1 and Paper 2 by calculating hydrogen supply curves with *Enertile* for Europe and the MENA region. In Paper 3, a different approach is taken: Based on given region-specific hydrogen demands in Europe, *Enertile* identifies the least-cost energy supply system that meets these demands. The comparison of different scenario narratives with consistent assumptions for the energy demand and supply modeling illuminates robust developments of an inner-European hydrogen infrastructure in more detail. In both approaches, the electricity demand for electrolysis coexists and competes with other electricity demands that must be met.

3.1.1 Subquestion 1.1: Under which circumstances are hydrogen imports to Europe from regions with favorable renewable power generation conditions economically efficient?

To investigate Subquestion 1.1, European hydrogen supply curves were calculated in Paper 1, and hydrogen export curves from the MENA region to Europe were calculated in Paper 2. The MENA countries represent world regions with favorable renewable power generation conditions. In addition, these states have the advantage of geographic proximity to Europe, allowing for pipeline connections and transport by ship. Therefore, comparing the supply curves from the two regions allows for a techno-economic evaluation of Subquestion 1.1: *Under which circumstances are* *hydrogen imports to Europe from regions with favorable renewable power generation conditions economically efficient?*

Technically, the supply curves were determined using the novel sales module of the *Enertile* model described in section 2.2.2.5 for a European and a MENA set-up, respectively. In particular, the following aspects characterize the supply curves and associated analyses:

- While for the calculations for Europe, only an interest rate of 7% was used, the calculations for the MENA region used both interest rates of 7% and 12%. Investment decisions relating to electricity and hydrogen technologies depend on the return on invested capital for investors and the default probability for creditors. Higher investment risks are usually accompanied by higher expected returns or risk premiums. For the assessment of hydrogen import projects, it is particularly relevant that investment risks differ regionally. The "DESERTEC" project shows that energy import projects from the MENA region to Europe can fail, among other things, due to expected risks associated with geopolitical stability. The project's goal was to supply both the MENA region and Europe with electricity using large-scale solar power plants in the MENA desert. Schmitt (2018) identifies the political turbulences of the so-called "Arabellion" as one reason for the failure of the initiative. The political instabilities resulted in slower administrative processes and changing responsibilities, making investments more burdensome and risky. However, there is currently no consistent and comprehensive approach to derive financing costs and risks on a country-specific basis (Wietschel et al. 2021). Therefore, the consortium of dena, giz, Navigant, and adelphi determined on behalf of the German Federal Ministry for Economics four interest rate categories for green hydrogen projects based on publicly available data: low (5%), medium (8%), high (11%), and very high (15%) (Jensterle et al. 2020). The analyses in Paper 2 for the MENA region applied an interest rate similar to the calculations in Europe in one case and an increased interest rate reflecting potentially higher investment risks in another case.
- For the European calculations, supply curves are generated with different techno-economic parameterizations for electrolyzers. The MENA calculations do not include such variation. The influence of the techno-economic electrolyzer parameters on hydrogen production costs is discussed in more depth in section 3.3.
- In addition to pure hydrogen production costs, the export curves include transportation cost surcharges from the MENA region to Europe.
- This approach does not consider costs for the distribution of hydrogen within Europe.
- Hydrogen used as a seasonal storage medium in the conversion sector is part of the model decisions, but the hydrogen quantities used for electricity and heat generation are intentionally excluded from the supply curves.

Figure 6-13 displays the hydrogen supply curves determined by the optimization model *Enertile* for the year 2050 showing the competitive situation between inner-European hydrogen production and hydrogen imports from the MENA region in the context of a GHG-neutral European energy system. The comparison of the analyzed supply strategies shows that meeting European hydrogen demands using production sites in MENA is only cost-efficient in certain cases. Given the assumptions made in Paper 1 and Paper 2, the intra-European hydrogen supply is cost-efficient up to a hydrogen production volume of 488 TWh_{H2} in all analyzed cases. This hydrogen quantity is provided at marginal generation costs of 90 €/MWh_{H2}. The results in Paper 2 indicate that mere hydrogen production costs in the MENA region profit from high full load hours of the technologies PV and CSP. However, this cost advantage is offset by the transportation costs from the MENA region to Europe. For higher hydrogen quantities, the dominant supply strategy depends on the assumed interest rate and techno-economic parametrization of electrolyzers. If an interest rate of 7% is assumed for Europe and the MENA region, a supply of Europe by hydrogen imports is cost-efficient, starting above demand quantities between 488 TWh_{H2} and 1,118 TWh_{H2}. The range emerges from variations in the techno-economic assumptions for electrolyzers. If a higher interest rate of 12% is assumed for the MENA region, imports from the MENA region are cost-efficient, starting above hydrogen demand quantities between 2,044 TWh_{H2} and 3,571 TWh_{H2}. These intersections of the supply curves assume gaseous, pipeline-bound imports. The import of liquefied hydrogen transported by ships is not cost-efficient for demand quantities below 4,111 TWh_{H2}.

These hydrogen supply curves can be put into perspective with the demand figures of the ECs' long-term strategic vision. Meeting the 1.5°C target, the EC expects hydrogen demands to range between 794 TWh_{H2} (1.5LIFE scenario) and 892 TWh_{H2} (1.5TECH scenario) in 2050 (EC 2018a). In the least-cost case, these hydrogen quantities result in supply cost of 86 €/MWh_{H2} and 88 €/MWh_{H2}, respectively. The comparison of the supply strategies presented above shows that with a five percentage point difference in interest rates between the MENA region and Europe, these European hydrogen demands can be met more cost-efficiently by domestic production within Europe. If there is a lower interest rate spread between the two regions, the results of the model calculations imply that part of these hydrogen demands can be met cost-efficiently from MENA. Still, even at equal interest rates, most hydrogen would be supplied from Europe, applying a cost-minimizing strategy.

In response to Subquestion 1.1, these analyses indicate that hydrogen imports from the MENA region to Europe are only economically feasible under very specific conditions: Firstly, financing conditions for hydrogen production projects in the MENA region must be similar to those in Europe. In the calculations, an interest rate spread of five percentage points translated into higher hydrogen supply costs for imports than domestic European hydrogen production. Secondly, hydrogen transportation costs for pipeline transport must be at the cheap end of current literature values. Transport costs to Europe neutralize most of the cost savings of hydrogen production in the MENA region due to low-cost renewable electricity production. Imports by ship would not be part of a least-cost solution.

Irrespective of this techno-economic assessment, hydrogen may need to be imported in Europe in the future, if obstacles and acceptance problems impede a high expansion of renewable energies. Acceptance problems are only considered to a very limited extent in the cost optimization of the energy supply system. Energy imports could circumvent greater limitations on the renewable power generation potential in Europe. From a techno-economic perspective, the MENA region would be a suitable candidate for exports in this case. It has very large hydrogen export potentials in the PWh range (cf. Figure 6-9), comparatively favorable renewable power generation conditions, and a short distance to Europe. However, based on experience gained in the DESERTEC project, the risk of political instability must be taken into account when setting up hydrogen partnerships.

3.1.2 Subquestion 1.2: Which hydrogen transport routes are economically efficient in Europe?

The investigations on Subquestion 1.1 showed that an inner-European hydrogen supply is economically efficient in many cases. However, the domestic transport of hydrogen within Europe was neglected. Optimizing the supply side of the European energy system with *Enertile*, Paper 3 takes into account the supraregional balancing via a hydrogen transport network. This paper examines five different scenarios, each describing consistent pathways for Europe toward a GHG-neutral target system. The chosen scenarios differ in three dimensions that are characterized by high uncertainties in their future development and potentially high impact on the design of hydrogen infrastructures: one, the composition of energy demands; two, the composition of the renewable electricity generation portfolio; and three, the extent of the electricity grid expansion. The energy demand variations use detailed sector model results for the industry, transport, households, and services sectors. Along consistent storylines towards GHG neutrality, these models develop three demand variants with either pronounced electricity, hydrogen, or synthetic hydrocarbon use. The scenario tree (cf. Figure 7-1) distinguishes two variants for the composition of the renewable electricity generation portfolio. In particular, the expansion of onshore wind faces acceptance hurdles (Guo et al. 2015; Reusswig et al. 2016). Therefore, in one scenario, the available area for onshore wind power expansion is halved compared to a reference portfolio. Similarly, two scenario variants are distinguished by the option of expanding the electricity transmission grid. To compensate for regional, weather-induced fluctuations in power generation, the electricity transmission grid is a key flexibility option in the renewable power system (Child et al. 2019). However, similar to an onshore wind expansion, new electricity transmission lines face public acceptance hurdles (Komendantova et al. 2016). Therefore, deviating from a reference parametrization, one scenario imposes tight restrictions on grid expansion: only the transmission grid expansions envisaged in the Ten Year Network Development Plan 2018 (entsoe 2019) and the German Grid Development Plan 2030 (Bundesnetzagentur 2019) are implemented. Expansions beyond these plans are inhibited in this scenario. Comparing the scenario results allows for evaluating Subquestion 1.2: *Which hydrogen transport routes are economically efficient in Europe?* The energy supply system model covers all European countries, but the analysis focuses on Germany.

This analysis relies on the new hydrogen module of *Enertile,* including a simplified representation of a European hydrogen transport grid. This module is introduced in section 2.2.2.2.

Within Germany, a hydrogen grid infrastructure between northern and western Germany is robust in all scenarios. Except for the scenario with reduced onshore wind potentials, hydrogen transport between northern and southern Germany is robust, too. For a GHG-neutral energy system in 2050, Figure 7-8 shows that net annual hydrogen flows between northern and western Germany range between 23 TWh_{H2} and 154 TWh_{H2} and require a transport capacity between 3 GW_{H2} and 18 GW_{H2} in the optimization results. In scenarios without additional restrictions for the expansion of onshore wind, annual hydrogen flows between northern and southern Germany range between 68 TWh_{H2} and 164 TWh_{H2}. These hydrogen flows lead to pipeline capacities between 8 GW_{H2} and 19 GW_{H2} in the optimization results.

At the European level, the model uses hydrogen transport networks in scenarios that allow for their expansion. Due to overall low hydrogen demand, a Europe-wide hydrogen transport network expansion is not included in modeling the scenario variant with pronounced use of synthetic hydrocarbons. Based on the scenario results, four robust hydrogen transport routes can be identified: Firstly, there is a strong connection between the British Isles and Germany. If onshore wind potentials are not subject to additional restrictions, scenario results show annual hydrogen transport flows between 147 TWh_{H2} and 220 TWh_{H2}, and associated pipeline capacities between 17 GW_{H2} and 25 GW_{H2} between the two regions in 2050. As the British Isles have good wind power conditions, limited land availability for onshore wind electricity generation reduces hydrogen exports substantially. In the respective scenario variant, annual hydrogen transport flows between the British Isles and Germany are reduced to 9 TWh_{H2} using a pipeline capacity of 1 GW_{H2}. Secondly, the Scandinavian countries become hydrogen exporters for Germany and the Benelux Union. Hydrogen pipeline capacities along this route add up to between 18 GW_{H2} and 32 GW_{H2} and transport between 162 TWh_{H2} and 280 TWh_{H2} in 2050, depending on the scenario. Thirdly, hydrogen exports take place from the Iberian Peninsula to France and Italy. This supply arm reaches as far as Germany in case of high hydrogen demands. The hydrogen pipelines leaving the Iberian Peninsula to the northeast have a transport capacity of between 5 GW_{H2} and 22 GW_{H2} and transport between 44 TWh_{H2} and 194 TWh_{H2} in the scenario results for 2050. The highest hydrogen exports occur on this route in the scenario with reduced onshore wind potential. At reduced wind power generation, electrolyzers are increasingly powered by solar power. Since the Iberian Peninsula has comparatively long sunshine hours and large areas of suitable grass- and shrubland, electricity-based hydrogen production is shifted to this region. Fourthly, hydrogen flows from the Baltic States and Poland to Germany, the Czech Republic, and Austria. The transport capacities of the hydrogen pipelines along this route amount to 7 GW_{H2} to 14 GW_{H2} and transport between 60 TWh_{H2} and 121 TWh_{H2} in 2050 in the scenarios.

The scenario comparison in Paper 3 allows identifying four determinants for the expansion of a hydrogen transport infrastructure on pathways toward GHG neutrality in Europe. One, cost minimization in *Enertile* uses pipelines to offset regional imbalances between hydrogen demand and available cheap renewable electricity generation potentials for electrolytic hydrogen production. The intra-German hydrogen transport grid connects the hydrogen demand hubs in southern and western Germany with the northern German zones characterized by high hydrogen production from wind power at the coasts (cf. Figure 7-7). Moreover, the German network distributes hydrogen imports, especially from the British Isles and Scandinavia. In the European context, the scenario results show a star-shaped hydrogen infrastructure: it creates a balance between regions with vacant, cheap renewable electricity generation potentials at the edges of Europe and regions in Central Europe with exhausted cheap electricity generation potentials by other electricity demands (cf. Figure 7-9). Two, the extent of hydrogen flows and pipeline capacity is largely determined by the extent of hydrogen demand. Comparing the optimization results of the three investigated energy demand variations shows that increased hydrogen demand leads to increased hydrogen transport infrastructure requirements. Three, constraints in the electricity transmission grid increase hydrogen flows and pipeline capacities. The scenario variant with reduced expansion options for the electricity grid shows that the direction of energy flows between model regions is maintained. However, increased constraints in electricity transmission shift energy trade from electricity to hydrogen. To circumvent bottlenecks in the electricity grid in this scenario in Germany, more electricity is converted to hydrogen via electrolysis, transported by the hydrogen grid passing the bottleneck, and reconverted to electricity. Four, the expansion of renewable electricity generation technologies determines the hydrogen flow directions in Europe. The scenario with reduced onshore wind power potential shows that hurdles in the expansion of individual renewable power generation technologies can substantially change hydrogen flows and associated pipeline capacities. In this case, sunny regions, e.g., the Iberian Peninsula, replace substantial hydrogen production in windy regions, e.g., British Isles. Other obstacles or stimuli to the expansion of renewable energies can lead to similar changes in specific hydrogen flows.

In response to Subquestion 1.2, the results in Paper 3 show that the expansion of hydrogen transport pipelines is economically efficient in GHG-neutral scenarios. This is evident at both the German and the European level. In Germany, the resulting hydrogen network connects windy electrolyzer sites in the north with hydrogen demand centers in the west and south. In Europe, a star-shaped hydrogen pipeline infrastructure transports hydrogen from the edges to central Europe in the scenario results. Regional imbalances of hydrogen demand and renewable energy supply, the level of hydrogen demand, the extent of the electricity transmission grid expansion, and the composition of the renewable electricity generation portfolio are important determinants for the design of the European hydrogen transport network.

3.2 Research question 2.: What role can electricity-based hydrogen play as a storage medium and flexibility option in a GHG-neutral electricity system?

This research question is addressed with different foci in research Papers 1 and 3. Paper 1 examines hydrogen supply curves for a GHG-neutral European energy system. Behind each point of such a supply curve is a calculation of the energy system model *Enertile*. The comparison of the energy systems behind different points on the supply curve allows for insights into the expansion of renewable energies, the curtailment of renewable electricity, and the expansion and use of various flexibility options in the electricity system for different hydrogen supply volumes. Paper 3 examines the hourly balancing of electricity supply and demand in GHG-neutral German power systems. For the weather year 2010, the paper investigates under which conditions the optimization model uses hydrogen infrastructures in the power system. Subsequently, three subquestions discuss results on the dimensioning, positioning, and utilization of electrolyzers, hydrogen storage, and hydrogen power plants.

3.2.1 Subquestion 2.1: How are electrolyzers dimensioned, where are they positioned, and how are they operated in an optimized renewable electricity system?

The two approaches in Papers 1 and 3 enable analyses regarding Subquestion 2.1: *How are electrolyzers dimensioned, where are they positioned, and how are they operated in an optimized renewable electricity system?*

The scenario comparison in Paper 3 shows for the GHG-neutral target state electrolyzer capacities ranging between 41 GW_{el} and 75 GW_{el} in Germany. Based on the analyzed scenarios, there are three main drivers for increased electrolyzer capacity: One, high hydrogen demand in Germany increases domestic hydrogen production and electrolyzer capacity. Two, restrictions in the electricity transmission grid expansion limit a key flexibility and supra-regional balancing option in the renewable electricity system. Electrolyzers can provide the missing demand flexibility and integrate renewables. The transport function of the electricity transmission grid can be taken over by expanding hydrogen transport pipelines. Three, constraints on the onshore wind potential lead to increased use of solar energy sources. The model employs increased electrolyzer capacities to integrate the increased PV peaks at midday.

The full load hours of electrolyzers in the fully decarbonized electricity system in Germany in 2050 range between 2,700 h and 3,500 h. The scenario characterized by high PV capacities due to limited onshore wind potential achieves the lowest full load hours; the scenario with the highest hydrogen demand has the highest electrolyzer full load hours. Figure 7-11 presents the hourly electrolyzer dispatch in Germany for four weeks representing the four seasons in 2050. The dispatch results show that the optimization uses electrolyzers to integrate both wind and solar power. In the spring and fall weeks, electrolyzers use steady, high wind electricity generation to produce hydrogen. The storage level trajectories in Figure 7-10 show that seasonal hydrogen storage is mainly filled in these seasons. In the summer week, the optimizer uses electrolyzers to integrate high electricity generation from PV in the midday hours. The electrolyzers run only for a few hours in the winter week due to high residual loads and constant electricity imports. Section 3.3 gives a more detailed analysis of the drivers of electrolytic hydrogen production.

In Germany, the optimization results show a concentration of electrolyzer sites in northern Germany. Across all scenarios, at least 71% of hydrogen in Germany is produced in windy coastal regions. Conversely, hydrogen demand is concentrated at industrial and power plant sites in western and southern Germany in all scenarios (cf. Figure 7-7). These hydrogen demand hubs have relatively low electrolytic hydrogen production. Hence, cost minimization positions electrolyzers close to low-cost renewable electricity potentials rather than close to hydrogen demand. The local integration of renewable energies using electrolysis prevents additional electricity grid expansion. The specific costs for pipeline-bound hydrogen transport are lower than the specific electricity transport costs. Due to the conversion losses of electrolysis, the amount of transported energy is also reduced when transporting hydrogen.

The results on European hydrogen supply curves in Paper 1 allow more generalized findings on the interactions of electrolyzers and the renewable power system. The comparison of the energy supply systems behind different points on the hydrogen supply curve shows that the amount of electricity curtailed in the European energy system decreases with an increased hydrogen supply for the demand sectors at low hydrogen quantities. In this analysis, the system cost minimization decides on the amount of curtailed renewable electricity. This means that the curtailment decision considers alternative integration measure costs. Concerning electrolyzers, cost minimization weighs whether cheap electricity is available over sufficient hours to compensate for the investment in additional electrolyzer capacity. If low-cost electricity incentivizes only a few operating hours for electrolyzers, the fixed cost components dominate the hydrogen production costs, and curtailment of renewable electricity can be overall more cost-efficient. In the optimization result, the curtailed renewable electricity at 0 TWh_{H2} hydrogen supply to the demand sectors amounts to 36 TWh_{el}. This curtailment represents less than 1% of the annual electricity generation in Europe. Therefore, the optimized energy supply system can provide only small amounts of so-called "surplus electricity" for hydrogen production. However, due to its spatial resolution, the modeling is not able to capture curtailments in case of bottlenecks in the electricity distribution grid. In reality, these bottlenecks could increase curtailment. Moving along the hydrogen supply curve, the amount of curtailed electricity decreases to 29 TWh_{el} at 468 TWh_{H2} hydrogen supply (cf. Figure 5-6). Therefore, the hydrogen supply to the demand sectors integrates electricity that would otherwise be curtailed. With further increased hydrogen generation, the amount of electricity curtailed increases again as a new economic equilibrium results from additional renewable energy and electrolyzer capacities. The model results indicate that it is not cost-efficient to scale the electrolyzer capacity to meet peak renewable electricity generation. A comparison of the installed renewable capacities at different points on the hydrogen supply curve in Paper 1 shows that the production of substantial electricity-based hydrogen amounts requires substantial additional renewable capacities (cf. Figure 5-5). For the supply of 2,524 TWh_{H2} – which covers direct and indirect hydrogen demands via synthetic hydrocarbons by the demand sectors in the EC's long-term strategic vision – the model results show additional installed capacities of 766 GW_{el} wind power and 865 GW_{el} solar energy.

In response to Subquestion 2.1, the overall results in Paper 1 and Paper 3 show that the arrangement of electrolyzers is largely driven by renewables. In cost-minimized energy supply systems, excess electricity that electrolyzers can use is rather limited and amounts to only a few terawatthours across Europe. Instead, the model results show that substantial amounts of electricity-based hydrogen require substantial amounts of electricity and, therefore, an expansion of renewable capacities. Throughout the year, the flexible use of electrolyzers is cost-efficient to integrate high wind and PV capacities. System optimization positions electrolyzers close to renewable electricity sources rather than to hydrogen demand. In Germany, this leads to a concentration of electrolyzer capacity at windy sites in northern Germany.

3.2.2 Subquestion 2.2: How are hydrogen power plants dimensioned, where are they positioned, and how are they operated in an optimized renewable electricity system?

In Paper 1 and Paper 3, the use of hydrogen as an electricity storage medium and, consequently, the capacity expansion of hydrogen technologies for electricity and heat generation is a model decision. Depending on the setting, these hydrogen technologies compete on the electricity and heat supply side with alternative supply technologies, and on the hydrogen demand side, with alternative use of hydrogen in other sectors. By comparing different scenarios, conclusions can be drawn regarding Subquestion 2.2: *How are hydrogen power plants dimensioned, where are they positioned, and how are they operated in an optimized renewable electricity system?*

The model results in Paper 3 show an expansion and deployment of hydrogen power plants in all investigated scenarios in Germany (cf. Figure 7-5). This is particularly true for the PtG/PtL scenario, which explicitly focuses on using synthetic hydrocarbons in various applications. In the optimization results of energy supply infrastructures, the fuel switch from fossil gas power plants to synthetic, GHG-neutral methane is considered too expensive. Therefore, methane-based power plants are eliminated from the electricity generation mix; instead, the optimization builts hydrogen power plants.

In the GHG-neutral energy systems of the different scenarios in Paper 3, the hydrogen power generation capacity is between 26 GW_{el} and 82 GW_{el} in Germany. The extent of hydrogen reconversion capacity differs in the model results mainly due to three driving factors: One, increased hydrogen demand in other sectors leads to reduced hydrogen power plant capacities in the conversion sector. In Paper 3, both the capacity and utilization of hydrogen power plants for electricity and heat generation in Germany is lowest in the scenario with the highest hydrogen demand. The relatively high hydrogen demands of the sectors industry, transport, services, and households in this scenario lead to increased model endogenous prices for hydrogen compared to the other scenarios. In the cost optimization, this higher hydrogen price leads to reduced hydrogen use in the conversion sector, favoring alternative electricity and heat supply options. Paper 1 shows similar results on the European level using an alternative incentive mechanism for hydrogen production. Figure 5-6 shows that if the demand sectors' willingness to pay for hydrogen increases, the amount of hydrogen supplied to these sectors also increases, while the hydrogen usage for reconversion in the conversion sector decreases. Two, an increased electricity demand – especially inflexible electricity demand – increases the need for dispatchable power plants. Due to the pronounced use of imported synthetic hydrocarbons in all sectors, the PtG/PtL scenario in Paper 3 shows the lowest electricity demand across scenarios. In the optimization result, this scenario also has the lowest hydrogen combustion capacity. In contrast, scenarios achieving GHG reductions in the demand sectors through electrification wherever possible show the highest electricity demand and hydrogen combustion capacity. As inflexible loads increase, peak residual load - i. e., peaks in demand not directly met by renewables - and dispatchable power generation increase, too. Optimization considers hydrogen power plants a cost-efficient option to meet these residual loads. Three, similarly to electrolyzers on the electricity demand side, hydrogen power plants can compensate for missing flexibility on the electricity supply side caused by an inhibited transmission grid expansion: Instead of meeting electricity demands supraregionally using the electricity transmission grid, stored hydrogen can be converted to electricity. Therefore, in cost minimization, limitations in the power grid expansion lead to an increase in hydrogen power generation capacity.

Except for the scenario with a diminished electricity grid, the dispatch results for Germany in Figure 7-10 and Figure 7-11 of Paper 3 show that hydrogen in the conversion sector is used almost exclusively in the winter months to meet high residual electricity and heat loads. High residual loads in winter are due to two effects: Firstly, solar power, an important component of the renewable portfolio, is less available during this season. Secondly, colder temperatures in winter increase the heating demand. In the modeled GHG-neutral German energy system, increased heat demand also leads to increased electricity demand from electric heating devices in buildings and heating grids. The optimization offsets these increased residual electricity and heat loads in November, December, January, and February by converting hydrogen to electricity and heat. In the remaining months of the year, cost minimization uses substantial amounts of hydrogen in the conversion sector only in the diminished electricity grid scenario. In this scenario, the use of hydrogen power plants additionally balances grid bottlenecks.

In the optimization results for 2050, the hydrogen demand of the conversion sector in Germany is concentrated in western and southern Germany (cf. Figure 7-7). In all scenarios examined in Paper 3, more than two-thirds of the hydrogen conversion capacity is located in these two regions. In both regions, electricity demand exceeds the local renewable electricity generation potential. Consequently, southern and western Germany depend on energy imports. Hydrogen power plants close the supply shortage at times of high residual load and import bottlenecks in the transmission grid.

In response to Subquestion 2.2, the model results in Paper 1 and Paper 3 show that hydrogen power plants are considered cost-efficient as backup capacities for hours of high residual electricity and heat loads in a GHG-neutral energy system. Hydrogen power plants replace natural gas power plants in this respect. The extent of hydrogen power plant capacities and their utilization depends on the level of hydrogen demand, the level of electricity demand, and bottlenecks in the electricity transmission grid. In cost minimization, hydrogen power plants are primarily installed at sites where high electricity demand meets low renewable electricity generation potential.

3.2.3 Subquestion 2.3: How are hydrogen storages dimensioned and operated over a year in an optimized renewable energy supply system?

Paper 3 analyzes the use of hydrogen storages over a year in a GHG-neutral German energy system for five different scenarios and one weather year. Based on the model calculations, it is possible to investigate Subquestion 2.3: *How are hydrogen storages dimensioned and operated over a year in an optimized renewable energy supply system?*

All scenarios investigated in Paper 3 show the use of hydrogen as a seasonal storage medium in a GHG-neutral German energy system. For the weather year 2010, the hydrogen storage levels in the model results of the five scenarios show a structurally similar profile over the year (cf. Figure 7-10). While the hydrogen storage facilities are emptied in the winter due to comparatively high hydrogen demands for electricity and heat generation and reduced availability of renewable electricity for electrolytic hydrogen production, the storage facilities are refilled in spring and fall due to the integration of high wind electricity generation via electrolysis.

To fulfill the seasonal balancing of hydrogen demand and supply, the model builds hydrogen storage facilities with a scenario-dependent working gas volume of between 42 TWh_{H2} and 104 TWh_{H2} (cf. Figure 7-10). In the optimization results, there is one central driver for the size of hydrogen storage in Germany: The level of hydrogen demand with a pronounced seasonal profile. Scenarios with high seasonal differentiation and comparatively high hydrogen demand in winter show high storage volumes in cost minimization. In the analyzed scenarios, only the hydrogen demand from the conversion sector has this seasonal profile; the demands from industry, transport, and buildings are parameterized with a flat profile. In turn, there are three key drivers in the optimization results that increase hydrogen demand of the conversion sector in winter: a low level of hydrogen demand in other sectors, a high level of electricity demand, and bottlenecks in the electricity transmission grid (cf. section 3.2.2).

Salt caverns are considered particularly suitable for subsurface hydrogen storage (Michalski et al. 2017; Ozarslan 2012). Of the 94 PWh_{H2} hydrogen storage potential in Germany (Caglayan et al. 2020), a volume sufficient to store 45 TWh_{H2} of hydrogen is currently being used as natural gas storage (Kühn et al. 2020). Thus, the existing hydrogen storage volume in salt caverns covers the lower end of the storage requirement in the scenario results. On the other hand, the geological storage potential for salt caverns clearly exceeds the storage demand in all scenarios.

In response to Subquestion 2.3, the model results in Paper 3 show that the core task of hydrogen storage in a GHG-neutral German energy system is a seasonal energy transfer from spring and autumn to winter. In the scenario results, a seasonal hydrogen demand pattern characterized by high consumption in winter is the key driver for hydrogen storage size. A comparison with the literature shows that Germany has a sufficiently large geological storage potential to meet seasonal hydrogen shifts. A major part of the necessary storage capacity could be achieved by rededicating existing natural gas storage facilities.

3.3 Research question 3.: Which variables influence hydrogen production costs in a renewable European energy supply system?

Results from Paper 1, Paper 2, and Paper 3 can be used to address this research question. One challenge in determining hydrogen production costs is the assumption about the full load hours of the electrolyzers and the associated procurement costs for renewable electricity. If the electrolyzers' operating concept relies on cheap surplus electricity, operating costs can be kept low. In turn, this low-cost electricity is not permanently available, and the investment for the electrolyzer must be distributed over only a few operating hours. Alternatively, an electrolyzer can be operated with higher full load hours and correspondingly higher costs for renewable electricity. In this case, the investments for the electrolyzer are allocated to more hours. The optimization approach in *Enertile* decides on the operating hours of the electrolyzer from a system cost perspective. It eliminates the need to make assumptions about the interrelated variables of full load hours and electricity procurement costs. Parameter variations – either on the electrolyzer parameterization itself or the rest of the energy supply system – can be used to measure the respective influences on hydrogen production costs.

3.3.1 Subquestion 3.1: How do hydrogen production costs change with variations in the techno-economic characteristics of electrolyzers?

In Paper 1, hydrogen supply curves are calculated with varying electrolyzer parameters in the context of a GHG-neutral European electricity system. In the parameter study, the specific investments, the technical lifetime, and the conversion efficiency of the electrolyzers are varied. A comparison of the supply curves provides insights into the influence of the individual electrolyzer parameters on electrolytic hydrogen production. This analysis allows for evaluating Subquestion 3.1: *How do hydrogen production costs change with variations in the techno-economic characteristics of electrolyzers?*

Figure 5-8 in Paper 1 shows the shift of the European hydrogen supply curves, given a 10% variation of the specific investment, the technical lifetime, the conversion efficiency, and the combination of these three electrolyzer parameters. With an average increase of 13% in hydrogen production costs, given the decrease in electrolyzer efficiency, this parameter has the highest impact on hydrogen production costs. In the model results, a change in efficiency has a disproportionate effect on hydrogen production costs. This is based on the fact that with higher efficiency, less electricity has to be used to produce the same amount of hydrogen and that, in particular, the most expensive hours of electricity procurement can be avoided. On average, the reduction of the technical lifetime and the increase of the specific investment lead to an increase of the hydrogen production costs of only 1% each.

In response to Subquestion 3.1, the model results in Paper 1 show that an increase in electrolyzer efficiency leads to substantial reductions in hydrogen production costs. Reductions in specific investments or increases in the technical lifetime only have relatively small effects on the production costs.

3.3.2 Subquestion 3.2: How do hydrogen production costs change with variations in renewable electricity supply costs?

In Paper 1 and Paper 2, hydrogen supply curves for GHG-neutral energy systems in Europe and the MENA region are determined. In both cases, the cost components for hydrogen production are investigated. For the European case, the impact of variations in the levelized cost of electricity (LCOE) of the main renewable electricity generation technologies on hydrogen production costs is investigated, too. The LCOE of onshore wind, offshore wind, PV, and CSP are varied in respective model runs. Paper 3 considers the dispatch of renewable energies for hydrogen production in different GHG-neutral German energy systems. Combined, these analyses offer insight regarding Subquestion 3.2: *How do hydrogen production costs change with variations in renewable electricity supply costs?*

The analyses in Paper 1 and Paper 2 show that electricity procurement costs account for the largest share of hydrogen production costs in the optimization result (cf. Figure 5-9 and Figure 6-10). This applies to both hydrogen production in Europe and the MENA region.

For the European case, Figure 5-11 in Paper 1 shows the shifts in hydrogen supply curves when the LCOE of different renewable electricity generation technologies are varied by 10%. If the electricity production costs of both wind and solar energy increase by 10%, this causes an average increase in the hydrogen production costs of 8% in the model results. Due to the increase in renewable electricity production costs, hydrogen production costs increase slightly less than proportionally. This results from the fact that both electricity supply and electrolyzers are affected by other cost components. In addition to the LCOE of renewable technologies, electricity procurement costs for hydrogen production depend on grid and storage costs. Likewise, electrolyzers have other fixed and variable cost components in addition to electricity supply costs.

In the model results in Paper 1 and Paper 3 are three indications that wind power is beneficial to produce electricity-based hydrogen in Germany cost-efficiently: One, for Europe, the results in Paper 1 show that changes in the electricity production costs of wind energy have stronger leverage on the hydrogen production costs than changes in the electricity production costs from solar energy. A 10% increase in the LCOE of wind energy leads to an average increase of 6% in hydrogen production cost. A 10% increase in the LCOE of solar energy leads to an average increase of only 2% in hydrogen production cost. Two, in the analyzed scenarios in Paper 3, electrolyzers' full load hours in Germany range between 2,700 h and 3,500 h. This electrolyzer deployment exceeds the average PV full load hours of 925 h in the scenario results. On average, onshore wind reaches 2,667 h and offshore wind 4,360 h in the optimization. Three, in all scenarios in Paper 3 the optimization concentrates electrolyzer capacities close to the best wind potentials in Germany at the coasts.

Although the model results show that large amounts of wind energy are converted to hydrogen, electrolyzers are also important in integrating PV power. Figure 7-11 in Paper 3 shows that the optimization uses high electrolyzer capacity to handle PV peaks at midday in summer.

In response to Subquestion 3.2, the findings in Paper 1, Paper 2, and Paper 3 show that renewable electricity costs are the most important component of electrolytic hydrogen production costs. Furthermore, the results show that wind energy has a greater impact on hydrogen production costs in Europe – and particularly Germany – than solar energy. Especially cost reductions in wind power translate considerably into reductions in hydrogen production costs.

3.3.3 Subquestion 3.3: How do hydrogen production costs change with variations in other electricity demands?

In Paper 1, hydrogen supply curves are calculated with varying other electricity demands in the context of a GHG-neutral European energy system. Both flexible and inflexible demands are varied. Comparing the supply curves allows for evaluating Subquestion 3.3: *How do hydrogen production costs change with variations in other electricity demands?*

The model results in Figure 5-12 in Paper 1 show only minor shifts in the hydrogen supply curves with changes in other European electricity demands. A 10% increase in European electricity demand increases the hydrogen production costs in the optimization results by 2% at most. Increases in electricity demand result in the utilization of more expensive electricity generation potentials (cf. Figure 5-2). In the analyzed segment of the potential curve, LCOE increases less than proportionally to the associated increase in electricity generation.

In response to Subquestion 3.3, the model results in Paper 1 show that hydrogen production costs are not very sensitive to changes in other electricity demands. Increases in electricity demand lead to higher hydrogen production costs as a result of exploiting more expensive electricity generation potentials.

3.4 Research question 4.: Do economically feasible potentials for DACCS exist in Europe?

In Paper 4, supply curves for negative CO_2 emissions via the DACCS route are calculated. The calculation of CO_2 capture potentials is carried out in the context of a GHG-neutral European energy system and therefore provides ambitious but realistic framework conditions for evaluating this research question.

3.4.1 Subquestion 4.1: What does CO_2 capture and storage via the DACCS route cost in an optimized European energy system?

The commercial rollout of DAC systems is still in its infancy. Therefore, the system cost minimization in Paper 4 uses different parameter sets of DAC plants to address Subquestion 4.1: *What does CO_2 capture and storage via the DACCS route cost in an optimized European energy system?*

Technically, the supply curves were determined using the novel sales module (section 2.2.2.5) and the novel DACCS module (section 2.2.2.4) of the *Enertile* model.

The supply curves for carbon dioxide removal via the DACCS pathway in Figure 8-6 of Paper 4 show that Europe's conversion sector has the potential to provide electricity for capturing CO_2 from ambient air to offset emissions from other sectors, including agriculture, industry, transport, services, and households. This even applies to a GHG-neutral European energy system with high overall electricity demand. The costs for compensated CO_2 in the model results depend on the parameter values of DAC plants and the CO_2 compensation quantities. In the system cost minimization, the geological storage potential in Europe caps the annual CO_2 capture volume. The model calculations assume that only 1% of the available potential can be used per year (about 1 Gt_{CO2}/a). If current techno-economic literature values for DAC plants are applied, the range of CO_2 compensation cost lies between 160 €/t_{CO2} and 270 €/t_{CO2}. If technical progress is anticipated for DAC plants, the CO_2 compensation costs can be reduced to between 60 €/t_{CO2} and 140 €/t_{CO2}.

The comparison of these DACCS costs with the global, cross-sectoral marginal abatement cost curve (MACC) for CO_2 of Della Vigna et al. (2021) shows that most abatement measures are less expensive than DACCS. However, this MACC also displays abatement measures with a global potential of about 2 Gt_{CO2}/a which are more expensive than the DACCS costs in Paper 4. This even applies to the conservative parametrization of the DAC plants.

In response to Subquestion 4.1, the model results in Paper 4 show that DACCS in a GHG-neutral European energy system could cost between 60 €/t_{CO2} and 270 €/t_{CO2} depending on the future development of DAC plants and the required negative emissions. These compensation costs are competitive with expensive alternative abatement strategies.

3.4.2 Subquestion 4.2: Where are DACCS plants positioned in an optimized renewable European energy supply system?

In addition to determining DACCS supply curves, Paper 4 examines how a fixed CO_2 compensation demand equal to 5% of the EU's 1990 emissions can be met cost-efficiently with DACCS. In one scenario branch, the cost optimization can decide on the locations of DACCS units to supply the required negative emissions; i.e., German emissions could be compensated by Norway. Therefore, this approach is suitable for analyzing Subquestion 4.2.: *Where are DACCS plants positioned in an optimized European energy supply system?*

Assuming that the heat required in the CO_2 capture process is provided electrically, the analyses in Paper 4 show that the availability of renewable electricity is pivotal to the operation of DACCS plants. The breakdown of cost components in Figure 8-7 shows that electricity costs are the major cost component of DACCS costs in the model results. Furthermore, a comparison of the European power generation systems with and without a given CDR demand of 288 Mt_{CO2}/a (i.e., 5% of the European 1990 emissions) in Figure 8-9 shows that – depending on the DAC parameterization – an additional 385 TWh_{el} to 495 TWh_{el} of electricity must be generated for CO_2 compensation. In the optimization results, this additional electricity generation requires an increase in installed capacities of renewable energies – mainly onshore wind and PV – by 5% to 8% compared to the reference system.

The cost minimization results for providing negative emissions equal to 5% of the EU's 1990 emissions in Figure 8-8 show that the operation of DACCS plants is most feasible in Finland, Sweden, Norway, the Iberian Peninsula, and the Baltic States. These states have both geological CO_2 storage potentials and – even in an electricity-intensive scenario with a GHG-neutral energy system – vacant, low-cost renewable electricity generation potentials. In contrast, Germany, Denmark, or the British Isles cannot contribute to the supply of negative emissions in this scenario as their potential of onshore wind and ground-mounted PV are fully exploited for meeting other energy demands. In Austria, although the PV potential is not fully exploited in the underlying scenario, the country has not reported any geological CO_2 storage potential and can, therefore, not contribute to the CDR supply.

In response to Subquestion 4.2, the model results in Paper 4 show that the cost minimization positions DACCS plants close to vacant renewable electricity generation potentials and geological storage capacities. In a GHG-neutral European energy system with overall high electricity demand, the optimization chooses Finland, Sweden, Norway, the Iberian Peninsula, and the Baltic States.

4 Conclusions, critical assessment, and outlook

Electrolytic hydrogen and captured and subsequently stored CO_2 from ambient air are two options for pursuing ambitious climate protection strategies in Germany and Europe. Electricity-based hydrogen is attributed two central functions: Firstly, it can replace fossil fuels in many processes and applications in the classical energy demand sectors. Secondly, it can act as a seasonal energy storage and flexibility provider in the conversion sector. Likewise, negative emissions via DACCS can become relevant in two ways: Firstly, they can compensate for unavoidable residual emissions, e. g. from agriculture. Secondly, they can economically compete with alternative GHG mitigation strategies. Both options interact strongly with a transforming energy supply system. Therefore, the aim of this dissertation is to quantitatively analyze the interactions of hydrogen with the conversion sector and the provision of negative emissions via DACCS in the context of a GHG-neutral European energy system.

4.1 Key conclusions

The research topic is addressed with a linear cost minimization approach for the European energy supply system. Within given framework conditions, the goal of the optimization is to identify the least cost supply infrastructure mix capable of meeting hourly electricity, heat, hydrogen, and DACCS demands. The cost minimization makes expansion and dispatch decisions for relevant supply infrastructures. Where applicable, the optimization simultaneously considers multiple simulation years up to the GHG-neutral target state. The modeling takes a system perspective; its results can support policymakers in designing energy and climate protection strategies. To analyze the research objective, the existing cost minimization model *Enertile* is enhanced in this dissertation. *Enertile* used to focus on the electricity and heat supply, with a high level of detail in representing fluctuating renewable energies. This dissertation extends *Enertile* to a multidirectional energy supply model. The core of the methodological advancement is the modeling of the interactions of hydrogen and DACCS technologies with future renewable electricity and heat supply systems. For hydrogen, the modeling now includes electrolyzers and imports from outside Europe as hydrogen supplies, different hydrogen power plants (incl. CHP) and hydrogen boilers as model endogenous hydrogen demands, geological hydrogen storage facilities, and transport pipeline networks between model regions. For DACCS, the modeling now includes DAC and sequestration units for capturing and permanently storing CO_2 underground for carbon dioxide removal supply and feedback from the usage of fossil fuels in the conversion sector, increasing model endogenous CO_2 removal demands. These extensions of *Enertile* yield methodological improvements in two directions: Firstly, renewable electricity is a key input for the supply of hydrogen and negative emissions via the

DACCS route. Drawing on the spatially, temporally, and techno-economically highly resolved potentials of renewable energies in the existing model allows for a high level of detail in the provision of both analyzed goods. Secondly, modeling hydrogen and DACCS technologies improves the representation of the conversion sector in the existing model. This is particularly the case for investigating pathways towards GHG neutrality with high penetration of fluctuating renewables. Hydrogen technologies can provide both supply- and demand-side flexibility in a renewable energy system: electrolyzers can serve as flexible electricity demands; hydrogen power plants and boilers can serve as flexible electricity and heat suppliers. Likewise, DACCS plants can be dispatched flexibly at times of low residual loads. In essence, the optimization model created in this dissertation is capable of adequately describing the supply of electricity, heat, hydrogen, and negative emissions via the DACCS route in a GHG-neutral European energy system.

Based on the synthesis of the results in the four scientific papers in section 3, the following conclusions and policy recommendations can be formulated.

The model calculations show that domestic European hydrogen production is cost-efficient in many cases. Based on the example of the MENA region, the results show that hydrogen imports from outside Europe are limited in their economic feasibility by two factors. Firstly, geographical cost advantages of hydrogen production in the MENA region due to cheaper renewable electricity generation potentials are diminished by transport costs to Europe. Although shipping is more expensive due to the high energy demand for liquifying hydrogen, this feasibility constraint applies to both gaseous pipeline imports and liquid hydrogen imports by ship. Secondly, increased financing costs for hydrogen production projects outside Europe may further reduce the feasibility of hydrogen imports. The failure of the DESERTEC project aiming at electricity imports from the MENA region to Europe shows that investments in infrastructure projects outside Europe may be associated with higher risks and, thus, risk premiums and expected returns. In the cost minimization results, a five percentage points higher interest rate for the MENA region compared to Europe translates into pipeline-bound hydrogen imports to Europe becoming cost-efficient for demands exceeding 2,000 TWh_{H2}. Therefore, to meet European hydrogen demands, expanding renewable power generation plants, electrolyzers, and hydrogen transport infrastructure should focus on Europe first.

The regional ratios of energy demand and renewable energy supply are unevenly distributed in Europe. In Germany, in particular, the ratio of electricity demand and low-cost renewable electricity generation potential is less favorable than, for example, in Scandinavia, on the British Isles, or the Iberian Peninsula. In GHG-neutral scenarios that avoid synthetic hydrocarbons and therefore have substantial hydrogen demands, European hydrogen transport networks are used in the cost minimization to compensate for these regional imbalances. Moreover, the model uses the European hydrogen network to circumvent bottlenecks in the European electricity transmission network caused by inhibited grid expansion: energy trading is shifted from electricity to hydrogen. In the scenario results, Europe has a star-shaped pipeline infrastructure transporting hydrogen from the edges to central Europe. Since international infrastructure projects are complex and affect the interests of several countries, an EU-wide hydrogen strategy should be harmonized, the planning of European hydrogen transport infrastructure initiated quickly, and approval procedures accelerated. The high hydrogen transfers between countries in the cost minimization results imply substantial renewable capacity expansions in exporting regions used quasi-exclusively for hydrogen exports. In addition to the techno-economic aspects presented in this dissertation, the large-scale expansion of renewables entails acceptance issues. The development of the European hydrogen strategy should, therefore, match these cost-minimized results with acceptance potentials.

In the optimization results of all GHG-neutral scenarios studied, hydrogen is used extensively as a seasonal storage medium and flexibility provider in the conversion sector in Germany. To utilize these functions of hydrogen, a strategy must be developed that organizes the transition from natural gas-based technologies to hydrogen-based technologies in the conversion sector. This strategy must cover four fields of action and achieve the following goals. Firstly, existing natural gas storage facilities should be converted into hydrogen storage facilities. The scenario calculations show that the storage volumes of natural gas cavern storage facilities may not be sufficient, and additional new hydrogen storage facilities must be built. Secondly, electrolyzers should ideally be installed near low-cost renewable electricity generation potentials. The optimization results show that in Germany, electrolyzer sites on the coasts with high wind power generation are particularly attractive. Overall, electrolyzers offer the flexibility to integrate high power generation from wind and PV. Thirdly, hydrogen power plants should be built to take over the function of natural gas power plants in meeting peak loads. The model results show that hydrogen power plants are necessary as backup power plants for hours of low renewable power generation and high loads. In the system cost minimization, hydrogen power plants are the cheaper alternative to synthetic methane-based power plants. Fourthly, a hydrogen transport network should also be established within Germany to link hydrogen supply in the north and demand in the west and south. For this purpose, natural gas pipelines can be converted to hydrogen pipelines. A challenge in formulating a strategy to achieve the outlined target picture is that all four fields of action must be considered simultaneously and cannot be worked out one after the other.

Flexibility and conversion efficiency are two key properties of electrolyzers from a system perspective. The scenario results show for the GHG-neutral energy system in Germany that electrolyzers are used in the cost minimization between 2,700 and 3,500 hours. This implies that they should be able to react as flexibly as possible to the conditions in the power system. A parameter study shows that the electrolyzer efficiency has a substantially higher impact on the hydrogen production costs than the specific investments and the technical lifetime. Therefore, subsidies for electrolyzer development should focus on its flexible applicability and conversion efficiency.

Due to quasi-unavoidable emissions, e. g. in agriculture, negative emissions are likely to be needed to achieve GHG neutrality across all sectors. The calculations in this dissertation show that DACCS in Europe could cost between 60 €/t_{CO2} and 270 €/t_{CO2} in 2050. Therefore, DACCS can compete with expensive alternative GHG mitigation strategies. Since the technology is still in its infancy and potentially a global backstop technology with implications for many process transformations discussed today, research efforts on DACCS need to be intensified. Besides the technical advancement and cost degression of DAC facilities, this also includes the safety aspects of long-term geological CO_2 storage. Moreover, it is of major importance to address and overcome political barriers and public concerns regarding the development of a CO_2 storage infrastructure. In the optimization results, the utilization of DACCS is concentrated in Sweden, the Iberian Peninsula, Norway, and Finland. In a scenario with a high degree of electrification across sectors, these regions offer important characteristics for DACCS use: vacant renewable electricity generation potentials and geological CO_2 storage reservoirs. Particularly for countries with low DACCS potentials, this concentration on a few countries implies that European and international cooperations should be initiated.

4.2 Critical assessment

This dissertation investigates the interactions of hydrogen systems with the conversion sector and the provision of negative emissions via the DACCS route in a GHG-neutral European energy system using a linear cost minimization model. The structural peculiarities and limitations of this analytical approach must be considered when evaluating the results.

Modeling always implies a major simplification of a complex reality. This becomes apparent, for example, in the selection of modeled parameters and the choice of input data for these parameters. For example, the techno-economic characterization of electrolyzers in the *Enertile* model is carried out along the following parameters: specific investment, fixed and variable operating and maintenance costs, conversion efficiency, and lifetime. However, other technical parameters, such as start-up times and required pressure and temperature levels, or economic parameters, such as taxes, levies, and expected profits of the electrolyzer operators, are not taken into account. In reality, the input data for these modeled parameters are plant-specific, subject to dispersion in the literature, and their future development is subject to uncertainty. Uncertainties in the description of the future energy system arise not only from the development of individual techno-economic parameters but also from overarching social, economic, and geopolitical trends. The consequences of Russia's war of aggression against Ukraine have shown that the basic premises of the European energy supply can change rapidly. These types of shocks are virtually impossible to capture in the modeling. In this work, the complexity and uncertainty in the choice of input data are addressed by applying different scenario narratives and data variations as sensitivity analyses for decisive parameters wherever feasible.

The deployed and expanded *Enertile* model shares the systematic limitations of cost-minimizing, supply-side energy system models. Firstly, the hourly balancing of supply and demand for electricity, heat in heat grids, hydrogen, synthetic methane, or compensated CO_2 in so-called demand-supply equations implicitly assumes perfect markets. These idealized market conditions, which assume, for example, perfect information, no market power, and the fully rational behavior of market participants, do not exist in real markets. Secondly, the model can only decide between potential solutions already known today. Structurally novel, previously unknown options cannot be considered. Thirdly, the assumption of perfect foresight is, per se, unrealistic. No market actor can predict the impact of an investment decision today for decades to come. Lastly, cost minimization tends towards highly centralized solutions with large plant types. In reality, the variety is much greater, and smaller decentralized projects are also implemented.

The cost minimization approach used to design the energy system in this dissertation makes it difficult to consider acceptance issues. The social costs of individual technologies are difficult to quantify and are not included in the model's parameterization. However, acceptance issues are implicitly considered for modeling renewable electricity generation potentials to a certain degree. Depending on the land use category, only part of the usable area is allowed for renewable electricity generation. Beyond the cost minimization results, it will be crucial in reality whether, for example, the Norwegian population is willing to expand wind power plants, PV plants, DACCS plants, and geological CO_2 storage facilities that only serve to compensate for German emissions.

Russia's war of aggression against Ukraine clearly demonstrates that Europe's dependency on energy imports from single states can be problematic. This is especially true for autocratic trading partners. For the assessment of the European hydrogen supply results in this dissertation, three first-order consequences result from this: Firstly, diversification of trading partners increases resilience. However, system cost minimization always chooses the cheapest option, even if there are only small cost deltas between possible solutions. Therefore, in reality, the tradeoff between the additional costs of the different options and the diversification of import strategies must be evaluated. The second-best solutions can be valid options. Secondly, cost minimization considers criteria such as political stability to a very limited extent. In this dissertation, the modeling of higher investment default probabilities was limited to variations of the interest rate in the MENA region. Beyond cost considerations, the optimizer's preferred solution of an intra-European hydrogen supply has the advantage of being anchored in the EU. Due to its economic and socio-cultural interdependencies, this union stands for a high degree of reliability. Further diversification through non-European imports can further increase resilience, but the political stability of supply countries and the resulting additional costs must be taken into account. Thirdly, fossil-compensated – blue – hydrogen from Russia as competition to electricity-based hydrogen has become less likely.

The computational power of the machines on which the linear cost minimization problem is set up and solved is limited. A resulting optimization problem contains more than 40 million variables and over 35 million constraints. On the available computers, solving this problem takes more than 87 hours. Among other aspects, this limits the temporal and spatial resolution of the calculations. The temporal resolution of the calculations is 8,760 hours per simulation year. Process distinctions - such as the flexibility of alkaline electrolyzers versus PEM electrolyzers - that exist on shorter time scales cannot be resolved. The spatial resolution for balancing supply and demand for electricity, heat in heat grids, hydrogen, and compensated CO_2 is based on the national states of the EU. Only Germany is further subdivided into six sub-regions. This spatial aggregation level has, among other effects, the consequence that distribution grid losses can only be taken into account as a lump sum, and bottlenecks in the distribution grid cannot be taken into account at all. Detailed network analyses – which include the distribution grid – must be considered in downstream models suitable for this purpose.

4.3 Outlook

This dissertation has focused on the cost-efficient supply of electrolytic hydrogen in a GHG-neutral European energy system. This focus leaves space for subsequent research opportunities. Firstly, the transition to this GHG-neutral target system and related conflicts of objectives can be addressed more thoroughly. One result of this dissertation is that hydrogen production is cost-efficient close to renewable electricity production. However, this supply scheme only works if there is an infrastructure to transport the hydrogen from the electrolyzers to the hydrogen demand sites. Therefore, in the absence of hydrogen pipelines, electrolyzers may initially be installed close to consumption. The integrated ramp-up of hydrogen demand, electrolyzers, pipelines, and storage facilities should therefore be investigated. Secondly, the repurposing potential of existing gas infrastructures could be considered and investigated in more detail. Thirdly, in addition to electricity-based hydrogen, fossil-compensated hydrogen could also play a role in hydrogen supply. This competition or complementarity between different hydrogen types should be further investigated.

The modeling in this dissertation assumes perfect markets when determining the prices for hydrogen or captured and sequestered CO_2. The market price results from the intersection of the supply and demand curves. Under this premise, the market price corresponds to the marginal production cost of the last unit of the respective good. Drawing an analogy to real energy markets, such as the oil or gas market, Wietschel et al. (2021) argue that prices for hydrogen and its derivatives are unlikely to settle based on production costs alone. Real markets show that imperfect information, product differentiation, regulatory intervention, market power, and strategic behavior of individual players have a major impact on prices. Future work should, therefore, consider and analyze these influences on price formation.

The results of this dissertation show that DACCS can potentially be an important CO_2 mitigation strategy. In reality, however, this technology is still in its infancy, and only a few projects are trying to implement it. Besides the need for further technological developments, future research work is required to discover how the ramp-up of this technology can be designed. Furthermore, the DAC process can also be used to produce synthetic hydrocarbons instead of negative emissions. The competition or complementarity between permanent storage and the use of captured CO_2 has been little explored.

The analyses in this dissertation aim at a cost-minimized European energy system. Policy instruments that enable the achievement of the key elements of this target system need to be investigated in subsequent works.

References

Agora Energiewende; AFRY Management Consulting (2021): No-regret hydrogen: Charting early steps for H2 infrastructure in Europe.

Anderson, C.; Schirmer, J.; Abjorensen, N. (2012): Exploring CCS community acceptance and public participation from a human and social capital perspective. In: Mitigation and Adaptation Strategies for Global Change, 17 (6), pp. 687–706. https://doi.org/10.1007/s11027-011-9312-z.

Arcadis Nederland; BAM Infra Energie Water; Bekaert Combustion Technology; Cogas; DHV Nederland; DNV-GL Netherlands; Enexis Netbeheer; GasTerra; Gasunie; Green Planet Pesse; Hanze University of Applied Sciences Groningen; Institute of Physical Safety; JP-Energy Systems; Liander; N-TRA/RENDO; Nedstack; New Energy Coalition; Province of Drenthe; Royal Haskoning; Stork Netherlands; Visser & Smit Hanab; Municipality of Hoogeveen (2020): Plan voor waterstof in Hoogeveen.

Bashmakov, I. A.; Nilsson, L. J.; Acquaye, A.; Bataille, C.; Cullen, J. M.; La Rue Can, S. de; Fischedick, M.; Geng, Y.; Tanaka, K.; Bauer, F.; Hasanbeigi, A.; Levi, P.; Myshak, A.; Perczyk, D.; Philibert, C.; Samadi, S. (2022): IPCC AR6 WGIII. Chapter 11: Industry. https://doi.org/10.1093/owc/9780198840831.003.0012.

Bazzanella, A. M.; Ausfelder, F. (2017): Low carbon energy and feedstock for the European chemical industry. DECHEMA Gesellschaft für Chmische Technik und Biotechnologie e.V.

Bernath, C. (2023): Auswirkungen der Sektorkopplung von Strom und Wärme durch Wärmenetze auf das europäische Stromerzeugungssystem. Eine modellbasierte Szenarioanalyse. Karlsruhe: Karlsruher Institut für Technologie (KIT). https://doi.org/10.5445/IR/1000155704.

Bernath, C.; Deac, G.; Sensfuss, F. (2019): Influence of heat pumps on renewable electricity integration: Germany in a European context. In: Energy Strategy Reviews, 26, p. 100389. https://doi.org/10.1016/j.esr.2019.100389.

Boston Consulting Group (2021): KLIMAPFADE 2.0. Ein Wirtschaftsprogramm für Klima und Zukunft.

Bradbury, J. A. (2012): PUBLIC UNDERSTANDING OF AND ENGAGEMENT WITH CCS. In: Markusson, N.; Shackley, S.; Evar, B. (Eds.): The social dynamics of carbon capture and storage. Understanding CCS representations, governance and innovation. London: Routledge. ISBN: 9781136311253.

Brunsting, S.; Best-Waldhober, M. de; Feenstra, C.; Mikunda, T. (2011): Stakeholder participation practices and onshore CCS: Lessons from the dutch CCS case barendrecht. In: Energy Procedia, 4, pp. 6376–6383. https://doi.org/10.1016/j.egypro.2011.02.655.

Bundesministerium der Justiz und für Verbraucherschutz; Bundesamt für Justiz (Eds.) (2021): Bundes-Klimaschutzgesetz. KSG. Available at https://www.gesetze-im-internet.de/ksg/BJNR251310019.html.

Bundesministerium für Umwelt, Naturschutz und nukleare Sicherheit (2016): Klimaschutzplan 2050 - Klimaschutzpolitische Grundsätze und Ziele der Bundesregierung.

Bundesnetzagentur für Elektrizität, Gas, Telekommunikation, Post und Eisenbahnen (2019): Bestätigung des Netzentwicklungsplans Strom für das Zieljahr 2030. Bedarfsermittlung 2019-2030.

Cabeza, L. F.; Bai, Q.; Bertoldi, P.; Kihila, J.; Lucena, A. F.; Mata, É.; Mirasgedis, S.; Novikova, A.; Saheb, Y.; Berrill, P.; Caldas, L. R.; Chàfer, M.; Hu, S.; Khosla, R.; Lamb, W. F.; Vérez, D.; Wanemark, J. (2022): IPCC AR6 WGIII. Chapter 9: Buildings. https://doi.org/10.1016/j.jclepro.2018.08.299.

Caglayan, D. G.; Weber, N.; Heinrichs, H. U.; Linßen, J.; Robinius, M.; Kukla, P. A.; Stolten, D. (2020): Technical potential of salt caverns for hydrogen storage in Europe. In: International Journal of Hydrogen Energy, 45 (11), pp. 6793–6805. https://doi.org/10.1016/j.ijhydene.2019.12.161.

Child, M.; Kemfert, C.; Bogdanov, D.; Breyer, C. (2019): Flexible electricity generation, grid exchange and storage for the transition to a 100% renewable energy system in Europe. In: Renewable Energy, 139, pp. 80–101. https://doi.org/10.1016/j.renene.2019.02.077.

Connolly, D.; Lund, H.; Mathiesen, B. V.; Leahy, M. (2010): A review of computer tools for analysing the integration of renewable energy into various energy systems. In: Applied Energy, 87 (4), pp. 1059–1082. https://doi.org/10.1016/j.apenergy.2009.09.026.

Davis, S. J.; Lewis, N. S.; Shaner, M.; Aggarwal, S.; Arent, D.; Azevedo, I. L.; Benson, S. M.; Bradley, T.; Brouwer, J.; Chiang, Y.-M.; Clack, C. T. M.; Cohen, A.; Doig, S.; Edmonds, J.; Fennell, P.; Field, C. B.; Hannegan, B.; Hodge, B.-M.; Hoffert, M. I.; Ingersoll, E.; Jaramillo, P.; Lackner, K. S.; Mach, K. J.; Mastrandrea, M.; Ogden, J.; Peterson, P. F.; Sanchez, D. L.; Sperling, D.; Stagner, J.; Trancik, J. E.; Yang, C.-J.; Caldeira, K. (2018): Net-zero emissions energy systems. In: Science (New York, N.Y.), 360 (6396). https://doi.org/10.1126/science.aas9793.

Day, C. J.; Hobbs, B. F.; Pang, J.-S. (2002): Oligopolistic competition in power networks: A conjectured supply function approach. In: IEEE Transactions on Power Systems, 17 (3), pp. 597–607. https://doi.org/10.1109/TPWRS.2002.800900.

Deac, G. (2019): Auswirkung der Kopplung von Strom- und Wärmemarkt auf die künftige Integration der erneurbaren Energien und die CO2-Emissionen in Deutschland.

Della Vigna, M.; Stavrinou, Z.; Gandolfi, A.; Snowdon, N.; Young, P.; Tylenda, E.; Chetwode, S.; Singer, B.; Bingham, D. R.; Jones, E. (2021): Carbonomics. Introducing the GS net zero carbon models and sector frameworks.

Deutsche Energie-Agentur GmbH (Ed.) (2021): dena-Leitstudie Aufbruch Klimaneutralität.

Dütschke, E. (2011): What drives local public acceptance–Comparing two cases from Germany. In: Energy Procedia, 4, pp. 6234–6240. https://doi.org/10.1016/j.egypro.2011.02.636.

Dütschke, E.; Wohlfarth, K.; Höller, S.; Viebahn, P.; Schumann, D.; Pietzner, K. (2016): Differences in the public perception of CCS in Germany depending on CO 2 source, transport option and storage location. In: International Journal of Greenhouse Gas Control, 53, pp. 149–159. https://doi.org/10.1016/j.ijggc.2016.07.043.

entsoe (Ed.) (2019): TYNDP 2018 Executive Report Appendix. Final version after public consultation and ACER opinion.

Enzensberger, N. (2003): Entwicklung und Anwendung eines Strom- und Zertifikatmarktmodells für den europäischen Energiesektor. Düsseldorf: VDI-Verl. ISBN: 3183159163.

European Commission (Ed.) (2018a): COMMUNICATION FROM THE COMMISSION TO THE EUROPEAN PARLIAMENT, THE EUROPEAN COUNCIL, THE COUNCIL, THE EUROPEAN ECONOMIC AND SOCIAL COMMITTEE, THE COMMITTEE OF THE REGIONS AND THE EUROPEAN INVESTMENT BANK COM(2018) 773. A Clean Planet for all A European strategic long-term vision for a prosperous, modern, competitive and climate neutral economy. Available at https://eur-lex.europa.eu/legal-content/EN/TXT/?uri=CELEX:52018DC0773, accessed 28.12.2019.

European Commission (Ed.) (2018b): In-depth analysis in support for the commission communication COM(2018) 773. A European long-term strategic vision for a prosperous, modern, competitive and climate neutral economy. Brüssel.

European Commission (Ed.) (2019): The European Green Deal. Brussels.

European Commission (Ed.) (2020): A hydrogen strategy for a climate-neutral Europe. Communication from the Commission to the European Parliament, the Council, the European Economic and Social Committee and the Committee of the Regions. Brussels.

European Parliament; Council of the European Union (Eds.) (2018a): DIRECTIVE (EU) 2018/ 2001 OF THE EUROPEAN PARLIAMENT AND OF THE COUNCIL - of 11 December 2018 - on the promotion of the use of energy from renewable sources. Available at https://eur-lex.europa.eu/legal-content/EN/TXT/PDF/?uri=CELEX:32018L2001&from=EN.

European Parliament; Council of the European Union (Eds.) (2018b): DIRECTIVE (EU) 2018/ 2002 OF THE EUROPEAN PARLIAMENT AND OF THE COUNCIL - of 11 December 2018 - amending Directive 2012/ 27/ EU on energy efficiency. Available at https://eur-lex.europa.eu/legal-content/EN/TXT/PDF/?uri=CELEX:32018L2002&from=EN.

European Parliament; Council of the European Union (Eds.) (2021): Regulation (EU) 2021/1119 of the European parliament and of the council of 30 June 2021 establishing the framework for achieving climate neutrality and amending regulations (EC) No 401/2009 and (EU) 2018/1999. European Climate Law. Available at http://data.europa.eu/eli/reg/2021/1119/oj.

eurostat (2022a): Imports of natural gas by partner country. Available at https://ec.europa.eu/eurostat/databrowser/view/NRG_TI_GAS__custom_2508592/default/table, accessed 14.09.2022.

eurostat (2022b): Imports of oil and petroleum products by partner country. Available at https://ec.europa.eu/eurostat/databrowser/view/NRG_TI_OIL__custom_3366166/default/table, accessed 14.09.2022.

Fasihi, M.; Efimova, O.; Breyer, C. (2019): Techno-economic assessment of CO2 direct air capture plants. In: Journal of Cleaner Production, 224, pp. 957–980. https://doi.org/10.1016/j.jclepro.2019.03.086.

Fraunhofer Institut für System- und Innovationsforschung (2021): Enertile. Available at https://www.enertile.eu/enertile-en/index.php.

Fraunhofer Institut für System- und Innovationsforschung; Consentec GmbH (Consentec); ifeu - Institut für Energie- und Umweltforschung Heidelberg GmbH; Lehrstuhl für Energie- und Ressourcenmanagement der TU Berlin (2021): Langfristszenarien. Available at https://www.langfristszenarien.de/enertile-explorer-de/, accessed 17.06.2021.

Fraunhofer Institut für System- und Innovationsforschung; Universiteit Utrecht; TEP Energy; ARMINES (2017): Heating and cooling facts and figures. The transformation towards a low-carbon heating & colling sector. Heat Raodmap Europe.

Fraunhofer-Institut für Keramische Technologien und Systeme IKTS; Fraunhofer-Einrichtung für Energieinfrastrukturen und Geothermie IEG; Fraunhofer Institut für System- und Innovationsforschung (2021): H2-Masterplan für Ostdeutschland.

Fraunholz, C. (2021): Market Design for the Transition to Renewable Electricity Systems. Dissertation.

Fuhrman, J.; McJeon, H.; Patel, P.; Doney, S. C.; Shobe, W. M.; Clarens, A. F. (2020): Food–energy–water implications of negative emissions technologies in a +1.5 °C future. In: Nature Climate Change, 10 (10), pp. 920–927. https://doi.org/10.1038/s41558-020-0876-z.

Fuss, S.; Lamb, W. F.; Callaghan, M. W.; Hilaire, J.; Creutzig, F.; Amann, T.; Beringer, T.; Oliveira Garcia, W. de; Hartmann, J.; Khanna, T.; Luderer, G.; Nemet, G. F.; Rogelj, J.; Smith, P.; Vicente, J. L. V.; Wilcox, J.; del Mar Zamora Dominguez, M.; Minx, J. C. (2018): Negative emissions—Part 2: Costs, potentials and side effects. In: Environmental Research Letters, 13 (6), p. 63002. https://doi.org/10.1088/1748-9326/aabf9f.

Godron, P.; Neubarth, J.; Soyah, M.; Asceri, V.; Callegari, G.; Cova, B.; Banez, F.; Olmos, L.; Ramos, A.; Rivier, M.; Muhme, K.; Ruderer, D.; Youssef, A. (2014): Desert power: Getting connected. Starting the debate for the grid infrastructure for a sustainable power supply in EUMENA.

Guo, Y.; Ru, P.; Su, J.; Anadon, L. D. (2015): Not in my backyard, but not far away from me: Local acceptance of wind power in China. In: Energy, 82, pp. 722–733. https://doi.org/10.1016/j.energy.2015.01.082.

Hank, C.; Sternberg, A.; Köppel, N.; Holst, M.; Smolinka, T.; Schaadt, A.; Hebling, C.; Henning, H.-M. (2020): Energy efficiency and economic assessment of imported energy carriers based on renewable electricity,

Held, A. M. (2011): Modelling the future development of renewable energy technologies in the European electricity sector using agent-based simulation. Stuttgart: Fraunhofer Verlag. ISBN: 3839602211.

Herbst, A.; Toro, F.; Reitze, F.; Jochem, E. (2012): Introduction to Energy Systems Modelling. In: Swiss Society of Economics and Statistics, (148), pp. 111–135.

Huber, M.; Dimkova, D.; Hamacher, T. (2014): Integration of wind and solar power in Europe: Assessment of flexibility requirements. In: Energy, 69, pp. 236–246. https://doi.org/10.1016/j.energy.2014.02.109.

Hunter, C.; Penev, M.; Reznicek, E.; Lustbader, J.; Birky, A.; Zhang, C. (2021): Spatial and Temporal Analysis of the Total Cost of Ownership for Class 8 Tractors and Class 4 Parcel Delivery Trucks. National Renewable Energy Laboratory. Available at https://www.nrel.gov/docs/fy21osti/71796.pdf, accessed 22.04.2022.

Husarek, D.; Schmugge, J.; Niessen, S. (2021): Hydrogen supply chain scenarios for the decarbonisation of a German multi-modal energy system. In: International Journal of Hydrogen Energy. https://doi.org/10.1016/j.ijhydene.2021.09.041.

International Energy Agency (2021): Global Hydrogen Review 2021.

International Renewable Energy Agency (2020): Reaching zero with renewables: Eliminating CO2 emissions from industry and transport in line with the 1.5°C climate goal.

Jaramillo, P.; Ribeiro, S. K.; Newman, P.; Cavalett, O.; Craig, M.; Creutzig, F.; Cumpsty, N.; Figueroa, M. J.; Held, M.; Hung, C.; Jenn, A.; Kishimoto, P.; Lamb, W. F.; Mittal, S.; Muri, H.; Pathak, M.; Posen, D.; Robertson, S.; Santos, A.; Seto, K.; Sharma, R.; Sovacool, B.; Steg, L.; Usai, L.; Venkatesh, A.; Yeh, S.; Kuzu-ya, T. (2022): IPCC AR6 WGIII. Chapter 10: Transport. https://doi.org/10.1093/owc/9780198814269.003.0011.

Jensterle, M.; Narita, J.; Piria, R.; Schröder, J.; Steinbacher, K.; Wahabzada, F.; Zeller, T.; Crone, K.; Löchle, S. (2020): Grüner Wasserstoff: Internationale Kooperationspotenziale für Deutschland.

Johansson, D. J. A.; Azar, C.; Lehtveer, M.; Peters, G. P. (2020): The role of negative carbon emissions in reaching the Paris climate targets: The impact of target formulation in integrated assessment models. In: Environmental Research Letters, 15 (12), p. 124024. https://doi.org/10.1088/1748-9326/abc3f0.

Komendantova, N.; Battaglini, A. (2016): Beyond Decide-Announce-Defend (DAD) and Not-in-My-Backyard (NIMBY) models? Addressing the social and public acceptance of electric transmission lines in Germany. In: Energy research & social science, 22, pp. 224–231. https://doi.org/10.1016/j.erss.2016.10.001.

Kondziella, H.; Bruckner, T. (2016): Flexibility requirements of renewable energy based electricity systems – a review of research results and methodologies. In: Renewable and Sustainable Energy Reviews, 53, pp. 10–22. https://doi.org/10.1016/j.rser.2015.07.199.

Krieg, D. (2012): Konzept und Kosten eines Pipelinesystems zur Versorgung des deutschen Straßenverkehrs mit Wasserstoff. Forschungszentrum Jülich GmbH. ISBN: 978-3-89336-800-6.

Kühn, M.; Nakaten, N. C.; Kempka, T. (2020): Geological storage capacity for green excess energy readily available in Germany. In: Advances in Geosciences, 54, pp. 173–178. https://doi.org/10.5194/adgeo-54-173-2020.

Li, X.; Mulder, M. (2021): Value of power-to-gas as a flexibility option in integrated electricity and hydrogen markets. In: Applied Energy, 304, p. 117863. https://doi.org/10.1016/j.apenergy.2021.117863.

Lux, B.; Deac, G.; Kiefer, C. P.; Kleinschmitt, C.; Bernath, C.; Franke, K.; Pfluger, B.; Willemsen, S.; Sensfuss, F. (2022): The role of hydrogen in a greenhouse gas-neutral energy supply system in Germany. In: Energy Conversion and Management, 270, p. 116188. https://doi.org/10.1016/j.enconman.2022.116188.

Lux, B.; Pfluger, B. (2020): A supply curve of electricity-based hydrogen in a decarbonized European energy system in 2050. In: Applied Energy, 269, p. 115011. https://doi.org/10.1016/j.apenergy.2020.115011.

Lux, B.; Pfluger, B.; Sensfuss, F. (2018): Wasserstoff als Flexibilitätsoption im europäischen Stromsektor. 15. Symposium Energieinnovation. Available at https://www.tugraz.at/fileadmin/user_upload/Events/Eninnov2018/files/lf/Session_G2/824_LF_Lux.pdf, accessed 04.02.2022.

Mauler, L.; Dahrendorf, L.; Duffner, F.; Winter, M.; Leker, J. (2022): Cost-effective technology choice in a decarbonized and diversified long-haul truck transportation sector: A U.S. case study. In: Journal of Energy Storage, 46, p. 103891. https://doi.org/10.1016/j.est.2021.103891.

Michalski, J.; Bünger, U.; Crotogino, F.; Donadei, S.; Schneider, G.-S.; Pregger, T.; Cao, K.-K.; Heide, D. (2017): Hydrogen generation by electrolysis and storage in salt caverns: Potentials, economics and systems aspects with regard to the German energy transition. In: International Journal of Hydrogen Energy, 42 (19), pp. 13427–13443. https://doi.org/10.1016/j.ijhydene.2017.02.102.

Neuwirth, M.; Fleiter, T.; Manz, P.; Hofmann, R. (2022): The future potential hydrogen demand in energy-intensive industries - a site-specific approach applied to Germany. In: Energy Conversion and Management, 252, p. 115052. https://doi.org/10.1016/j.enconman.2021.115052.

Ozarslan, A. (2012): Large-scale hydrogen energy storage in salt caverns. In: International Journal of Hydrogen Energy, 37 (19), pp. 14265–14277. https://doi.org/10.1016/j.ijhydene.2012.07.111.

Peters, D.; van der Leun, K.; Terlouw, W.; van Tilburg, J.; Berg, T.; Schimmel, M.; van der Hoorn, I.; Buseman, M.; Staats, M.; Schenkel, M.; Mir, G. U. R. (2020): Gas Decarbonisation Pathways 2020-2050. Gas for Climate.

Pfluger, B. (2014): Assessment of least-cost pathways for decarbonising Europe's power supply. A model-based long-term scenario analysis accounting for the characteristics of renewable energies. Karlsruhe.

Pfluger, B.; Tersteegen, B.; Franke, B.; Bernath, C.; Bossmann, T.; Deac, G.; Elsland, R.; Fleiter, T.; Kühn, A.; Ragwitz, M.; Rehfeldt, M.; Steinbach, J.; Cronenberg, A.; Ladermann, A.; Linke, C.; Maurer, C.; Willemsen, S.; Kauertz, B.; Pehnt, M.; Rettenmaier, N.; Hartner, M.; Kranzl, L.; Schade, W.; Catenazzi, G.; Jakob, M.; Reiter, U. (2017): Langfristszenarien für die Transformation des Energiesystems in Deutschland. Modul 2: Modelle und Modellverbund. Fraunhofer Institut für System- und Innovationsforschung; ifeu - Institut für Energie- und Umweltforschung Heidelberg GmbH; TU Wien; TEP Energy; M-Five GmbH (M-Five); Consentec GmbH (Consentec).

Plötz, P. (2022): Hydrogen technology is unlikely to play a major role in sustainable road transport. https://doi.org/10.1038/s41928-021-00706-6.

Prina, M. G.; Manzolini, G.; Moser, D.; Nastasi, B.; Sparber, W. (2020): Classification and challenges of bottom-up energy system models - A review. In: Renewable and Sustainable Energy Reviews, 129, p. 109917. https://doi.org/10.1016/j.rser.2020.109917.

Prognos; Ökö-Institut e. V.; Wuppertal-Institut (Eds.) (2021): Klimaneutrales Deutschland 2045. Wie Deutschland seine Klimaziele schon vor 2050 erreichen kann. Langfassung im Auftrag von Stiftung Klimaneutralität, Agora Energiewende und Agora Verkehrswende.

Realmonte, G.; Drouet, L.; Gambhir, A.; Glynn, J.; Hawkes, A.; Köberle, A. C.; Tavoni, M. (2019): An inter-model assessment of the role of direct air capture in deep mitigation pathways. In: Nature communications, 10 (1), p. 3277. https://doi.org/10.1038/s41467-019-10842-5.

Reusswig, F.; Braun, F.; Heger, I.; Ludewig, T.; Eichenauer, E.; Lass, W. (2016): Against the wind: Local opposition to the German Energiewende. In: Utilities Policy, 41, pp. 214–227. https://doi.org/10.1016/j.jup.2016.02.006.

Riahi, K.; Schaeffer, R.; Arango, J.; Calvin, K.; Guivarch, C.; Hasegawa, T.; Jiang, K.; Kriegler, E.; Matthews, R.; Peters, G.; Rao, A.; Robertson, S.; Sebbit, A. M.; Steinberger, J.; Tavoni, M.; van Vuuren, D. P. (2022): IPCC AR6 WGIII. Chapter 3: Mitigation Pathways Compatible with Long-Term Goals.

Rogelj, J.; Huppmann, D.; Krey, V.; Riahi, K.; Clarke, L.; Gidden, M.; Nicholls, Z.; Meinshausen, M. (2019): A new scenario logic for the Paris Agreement long-term temperature goal. In: Nature, 573 (7774), pp. 357–363. https://doi.org/10.1038/s41586-019-1541-4.

Rogelj, J.; Shindell, D.; Jiang, K.; Fifita, S.; Forster, P.; Ginzburg, V.; Handa, C.; Kheshgi, H.; Kobayashi, S.; Kriegler, E.; Mundaca, L.; Séférian, R.; Vilarino, M. V. (2018): Mitigation Pathways Compatible with 1.5°C in the Context of Sustainable Development.

Sachverständigenrat für Umweltfragen (2021): Wasserstoff im Klimaschutz: Klasse statt Masse. Stellungnahme. Berlin: Sachverständigenrat für Umweltfragen.

Schäfer, A. W.; Barrett, S. R. H.; Doyme, K.; Dray, L. M.; Gnadt, A. R.; Self, R.; O'Sullivan, A.; Synodinos, A. P.; Torija, A. J. (2019): Technological, economic and environmental prospects of all-electric aircraft. In: Nature Energy, 4 (2), pp. 160–166. https://doi.org/10.1038/s41560-018-0294-x.

Schmitt, T. M. (2018): (Why) did Desertec fail? An interim analysis of a large-scale renewable energy infrastructure project from a Social Studies of Technology perspective. In: Local Environment, 23 (7), pp. 747–776. https://doi.org/10.1080/13549839.2018.1469119.

SCI4climate.NRW (Ed.) (2022): Quantitativer Vergleich aktueller klimaschutzszenarien für Deutschland. Available at https://www.energy4climate.nrw/fileadmin/Service/Publikationen/Ergebnisse_SCI4climate.NRW/Szenarien/2022/samadi-2022-vergleich-aktueller-klimaschutzszenarien-fuer-deutschland-cr-sci4climatenrw.pdf, accessed 12.12.2022.

Sensfuss, F. (2007): Assessment of the impact of renewable electricity generation on the German electricity sector. An agent-based simualtion approach.

SGN Scotland Gas Network (2022): H100 Fife | Future of Gas | SGN. Available at https://h100fife.co.uk/about-h100/, accessed 27.04.2022.

Smith, P.; Davis, S. J.; Creutzig, F.; Fuss, S.; Minx, J. C.; Gabrielle, B.; Kato, E.; Jackson, R. B.; Cowie, A.; Kriegler, E.; van Vuuren, D. P.; Rogelj, J.; Ciais, P.; Milne, J.; Canadell, J. G.; McCollum, D.; Peters, G.; Andrew, R.; Krey, V.; Shrestha, G.; Friedlingstein, P.; Gasser, T.; Grübler, A.; Heidug, W. K.; Jonas, M.; Jones, C. D.; Kraxner, F.; Littleton, E.; Lowe, J.; Moreira, J. R.; Nakicenovic, N.; Obersteiner, M.; Patwardhan, A.; Rogner, M.; Rubin, E.; Sharifi, A.; Torvanger, A.; Yamagata, Y.; Edmonds, J.; Yongsung, C. (2016): Biophysical and economic limits to negative CO2 emissions. In: Nature Climate Change, 6 (1), pp. 42–50. https://doi.org/10.1038/nclimate2870.

Timmerberg, S.; Kaltschmitt, M. (2019a): Hydrogen from renewables: Supply from North Africa to Central Europe as blend in existing pipelines – Potentials and costs. In: Applied Energy, 237, pp. 795–809. https://doi.org/10.1016/j.apenergy.2019.01.030.

Timmerberg, S.; Sanna, A.; Kaltschmitt, M.; Finkbeiner, M. (2019b): Renewable electricity targets in selected MENA countries – Assessment of available resources, generation costs and GHG emissions. In: Energy Reports, 5, pp. 1470–1487. https://doi.org/10.1016/j.egyr.2019.10.003.

Ueckerdt, F.; Bauer, C.; Dirnaichner, A.; Everall, J.; Sacchi, R.; Luderer, G. (2021): Potential and risks of hydrogen-based e-fuels in climate change mitigation. In: Nature Climate Change, 11 (5), pp. 384–393. https://doi.org/10.1038/s41558-021-01032-7.

United Nation Climate Change (2016): Report of the Conference of the Parties on its twenty-first session, held in Paris from 30 November to 11 December 2015. Part one: Proceedings. Part one: Proceedings. Available at https://unfccc.int/documents/9097, accessed 15.06.2022.

United Nations (Ed.) (2015a): Paris Agreement. Available at https://unfccc.int/sites/default/files/english_paris_agreement.pdf.

United Nations (2015b): Transforming our world: the 2030 Agenda for Sustainable Development,

Ventosa, M.; Baíllo, Á.; Ramos, A.; Rivier, M. (2005): Electricity market modeling trends. In: Energy Policy, 33 (7), pp. 897–913. https://doi.org/10.1016/j.enpol.2003.10.013.

Wachsmuth, J.; Aydemir, A.; Döscher, H.; Eckstein, J.; Proganietz, W.-R.; Francois, D.-E.; Scheer, D. (2021): The potential of hydrogen for decarbonising EU industry.

Wietschel, M.; Eckstein, J.; Riemer, M.; Zheng, L.; Lux, B.; Neuner, F.; Breitschopf, B.; Fragoso, J.; Kleinschmitt, C.; Pieton, N.; Nolden, C.; Pfluger, B.; Thiel, Z.; Löschel, A. (2021): Import von Wasserstoff und Wasserstoffderivaten: von Kosten zu Preisen. HYPAT Working Paper 01/2021. Karlsruhe.

Wissenschaftliche Dienste des Deutschen Bundestages (2019): Grenzwerte für Wasserstoff (H2) in der Erdgasinfrastruktur. Sachstand. Aktenzeichen: WD 8 - 3000 - 066/19.

Wohland, J.; Witthaut, D.; Schleussner, C.-F. (2018): Negative Emission Potential of Direct Air Capture Powered by Renewable Excess Electricity in Europe. In: Earth's Future, 6 (10), pp. 1380–1384. https://doi.org/10.1029/2018EF000954.

Zhang, Z.; Folmer, H. (1998): Economic modelling approaches to cost estimates for the control of carbon dioxide emissions. In: Energy Economics, 20 (1), pp. 101–120.

Part II

5 A supply curve of electricity-based hydrogen in a decarbonized European energy system in 2050

[Start of Paper 1]

A supply curve of electricity-based hydrogen in a decarbonized European energy system in 2050

Benjamin Lux[1,*] and Benjamin Pfluger[1]

1 Fraunhofer Institute for Systems and Innovation Research ISI, Breslauer Straße 48, 76139 Karlsruhe, Germany

*corresponding author: Benjamin Lux, benjamin.lux@isi.fraunhofer.de, phone: +49-721-6809-474

Paper published in:

Applied Energy 269, Article No. 115011, DOI: 10.1016/j.apenergy.2020.115011

Abstract

Alongside substituting fossil fuels with renewable energies and increasing energy efficiency, the utilization of electricity-based hydrogen or its derived synthetic fuels is a potential strategy to meet ambitious European climate protection targets. As synthetic hydrocarbons have the same chemical properties as their fossil substitutes, existing infrastructures and well-established application technologies can be retained while CO_2 emissions in energy conversion, transport, industry, and residential and services can be reduced. However, the conversion processes, especially the generation of hydrogen necessary for all e-fuels, are associated with energy losses and costs. To evaluate the techno-economic hydrogen production potential and the impact of its utilization on the rest of the energy system, a supply curve of electricity-based hydrogen in a greenhouse gas emission-free European energy system in 2050 was developed. It was found that hydrogen quantities of the order of magnitude envisaged in the 1.5 °C scenarios by the European Commission's long-term strategic vision (1,536 - 1,953 TWh_{H2}) induce marginal hydrogen production costs of over 110 $€_{2020}/MWh_{H2}$ and electrolyzer capacities of more than 615 GW_{el}. Although the generation of these amounts of hydrogen using electrolysis provides some flexibility to the electricity system and can integrate small amounts of local surplus electricity, an additional 766 GW_{el} of wind power and 865 GW_{el} of solar power must be installed to cover the additional electricity demand for hydrogen production. It was furthermore found that the most important techno-economic properties of electrolyzers used in an energy system dominated by renewable energies are the ability to operate flexibly and the *conversion efficiency of electricity into hydrogen. It is anticipated that the shown analysis is valuable for both policy-makers, who need to identify research, subsidy and infrastructure requirements for a future energy system, and corporate decision-makers, whose business models will be significantly affected by the future availability of electricity-based fuels.*

Keywords: Cost of hydrogen; Power-to-Gas; Energy system modeling; Electricity system flexibility; Sector coupling; Electrolysis;

Highlights:

- Hydrogen supply curve for decarbonized European energy system 2050
- E-fuels do not restrain benefits of the expansion of the electricity transport grid
- Flexibility and efficiency become the most important properties of electrolyzers
- Marginal hydrogen generation costs of 110 EUR/MWh_{H2} for 1407 TWh_{H2} in Europe 2050
- Excess electricity is not sufficient to provide substantial amounts of hydrogen

5.1 Introduction

To counter the threats of global warming, the international community of states agreed in the 2015 Paris Agreement to limit the global temperature increase to well below 2 °C above pre-industrial levels (UN 2015). Therefore, the European Commission (EC) reconfirmed the objective of reducing greenhouse gas (GHG) emissions in the European Union (EU) by 80% to 95% compared to 1990 by 2050 (Council of the European Union 2009; EC 2018a). The key strategies of the EU for reducing GHG emissions include an increase in energy efficiency of at least 32.5% by 2030 (European Parliament et al. 2018b) and a renewable energy target of at least 32% of total energy consumption by 2030 (European Parliament et al. 2018a). While energy efficiency measures and substituting fossil fuels with renewable energy sources (RES) are broadly accepted decarbonization strategies, the role of electricity-based hydrogen and other synthetic fuels in reducing GHG emissions remains a topic of discussion.

Hydrogen produced by electrolysis using renewable electricity offers the potential to reduce GHG emissions across sectors. In the electricity sector, wind and solar power are expected to dominate electricity supply in the long run due to their overall generation potential and their economic feasibility (Pfluger 2014). Given the weather-dependent availability of these energy sources, flexibility measures are required to synchronize electricity supply and demand at all times (Huber et al. 2014; Kondziella et al. 2016). Electricity-based hydrogen can potentially provide flexibility: in hours of negative residual loads, i.e. an oversupply of renewable electricity generation, surplus electricity can be converted into hydrogen by electrolysis. Conversely, stored hydrogen can be converted back into electricity by hydrogen turbines, fuel cells, or other reconversion technologies in hours of high residual loads, i.e. hours of both low renewable electricity generation and high electricity demands. With its long-term storage property, hydrogen is suitable as a seasonal electricity storage medium (Crotogino 2016).

Apart from the electricity sector, hydrogen produced from renewable electricity is an option for a GHG emission-free energy supply in transport (Navas-Anguita et al. 2019; Runge et al. 2019), residential and services (Boait et al. 2019), and as an energy and feedstock supply in industry (Chen et al. 2019; Palm et al. 2016). In these demand sectors hydrogen can either be used directly or after being synthesized into methane (power-to-methane) or liquid hydrocarbons (power-to-liquid)[2]. These electricity-based fuels (e-fuels) provide a substitute for fossil fuels while being potentially climate-neutral, depending on the carbon source used in the synthesis processes (Graves et al. 2011; Zeman et al. 2008) and on the assumption that only renewable electricity is used. As all these e-fuels – hydrogen, synthetic methane and synthetic liquid hydrocarbons – have

[2] Throughout the article the following naming convention is used: "E-fuels" is the umbrella term for all gaseous and liquid secondary energy sources produced from electricity. "Power-to-gas" includes all gaseous secondary energy sources produced from electricity, i.e. hydrogen (power-to-hydrogen) and synthetic methane (power-to-methane). "Power-to-liquid" describes all liquid secondary energy sources produced from electricity, e.g. synthetic methanol.

the same chemical properties as their fossil substitutes, CO_2 emissions in the demand sectors can be reduced while maintaining well-established application technologies. In the cases of synthetic hydrocarbons, most existing infrastructures can be retained.

However, the conversion of electricity into secondary fuels is associated with energy losses and costs. Therefore, the use of hydrogen and its derived synthetic fuels is in competition with alternative flexibility options and decarbonization strategies in the different sectors. In the electricity sector, hydrogen as a storage medium competes with other storage technologies, performant European electricity grids and demand-side management for the most cost-efficient provision of flexibility (Brouwer et al. 2016). In transport, industry, residential and services, where e-fuels can be both energy carriers and industrial feedstock, direct-electric processes and the use of biogenic energy sources are alternative de-fossilization options[3]. The deployment of e-fuels depends decisively on their costs and available quantities. The costs, in turn, depend to a large extent on the techno-economic properties of the generation processes of these fuels.

Several existing studies (Glenk et al. 2019; Gorre et al. 2019; Götz et al. 2016; McDonagh et al. 2018; Reuß et al. 2017; Schiebahn et al. 2015) examine the production costs of e-fuels to evaluate their future role in the energy system. These studies focus on the techno-economic properties of the e-fuel production units and neglect the interactions of these production units with the rest of the energy system. Yet the actual costs and potential applications of these fuels can only be assessed with due consideration of their competition with alternative decarbonization and flexibility options.

Based on these preliminary considerations and due to hydrogen being the basis of all e-fuels, the central research questions in this paper are:

- What is the techno-economic generation potential of electricity-based hydrogen?
- How does the generation of electricity-based hydrogen interact with this energy system?

Addressing these questions allows a better understanding of the technical requirements of hydrogen generation facilities, e.g. in terms of flexibility requirements and for weighing specific investment against conversion efficiency. Realistic long-term cost projections are necessary for determining potential uses of e-fuels and comparisons with other de-fossilization alternatives.

The analysis is performed for a de-fossilized European electricity system in 2050. In such a system the electricity used for hydrogen generation is by definition entirely renewable. This prevents from second order effects of increased electricity generation from fossil fuels in the interconnected electricity grid.

[3] Given the availability of permanent CO2 storage facilities, there are fossil supply concepts that do not increase the CO2 concentration in the atmosphere. Here, the CO2 released during the use of fossil fuels must be extracted from the flue gas stream or the atmosphere and subsequently stored. These concepts are not considered in this paper.

An energy system optimization model is used to determine a European supply curve of electricity-based hydrogen for the demand sectors. This systemic approach makes it possible to understand the interactions between renewable energies, electricity-based hydrogen production and other flexibility options in the electricity and heat system. Through parameter variations, different technological development paths of electrolysis are taken into account.

The paper is structured as follows: Section 5.2 introduces the modeling approach, scenario design, and most important input parameters of our analysis. The modeling results are shown in Section 5.3. In Section 5.4, findings are summarized and conclusions are drawn.

5.2 Methodology and Data

5.2.1 Methodology

The working point of this analysis is a de-fossilized European energy system in 2050. In such a system the generation of electricity, heat, and hydrogen is interdependent and ultimately based on weather-dependent renewable energies. Therefore, the energy system optimization model *Enertile* (Fraunhofer ISI 2019) is applied to determine the production cost of electricity-based hydrogen. *Enertile* provides both an integrated perspective on the supply of all three energy forms and a high temporal and spatial resolution of RES in Europe.

5.2.1.1 Optimization model *Enertile*

Enertile is a detailed techno-economic optimization model for large, interlinked energy systems. Within a scenario framework, it identifies cost-efficient pathways for the development of the systems up to the year 2050. For every scenario year considered, *Enertile* determines the cost-minimal generation and infrastructure mix to meet exogenously specified electricity, heat and hydrogen demands; this includes both capacity expansion and unit dispatch of renewable energies, conventional power plants, electricity transport, heat and hydrogen generation technologies, energy storage facilities, and demand-side flexibility.

This paper focuses on the supply of hydrogen in an emission-free European energy system in 2050. This limitation with regard to emission requirements and the time frame is reflected in the settings of the model, i.e. only a single year is considered and no fossil generation technologies are available. It should be noted that neither the applied model nor the analysis in general draws conclusions on how the de-fossilization is achieved in terms of policy measures. The model or its parameterization is intentionally free of technological preferences, choosing the system components solely based on cost-efficiency and technical properties. In reality, different policy mixes could reach the resulting or similar system configurations.

For calculations in this paper, *Enertile* was extended by a sales instance of hydrogen. The resulting model variant of *Enertile* is described below. A more extensive and detailed description of the base version of the model is given in (Bernath et al. 2019), Pfluger (2014), and (Deac 2019).

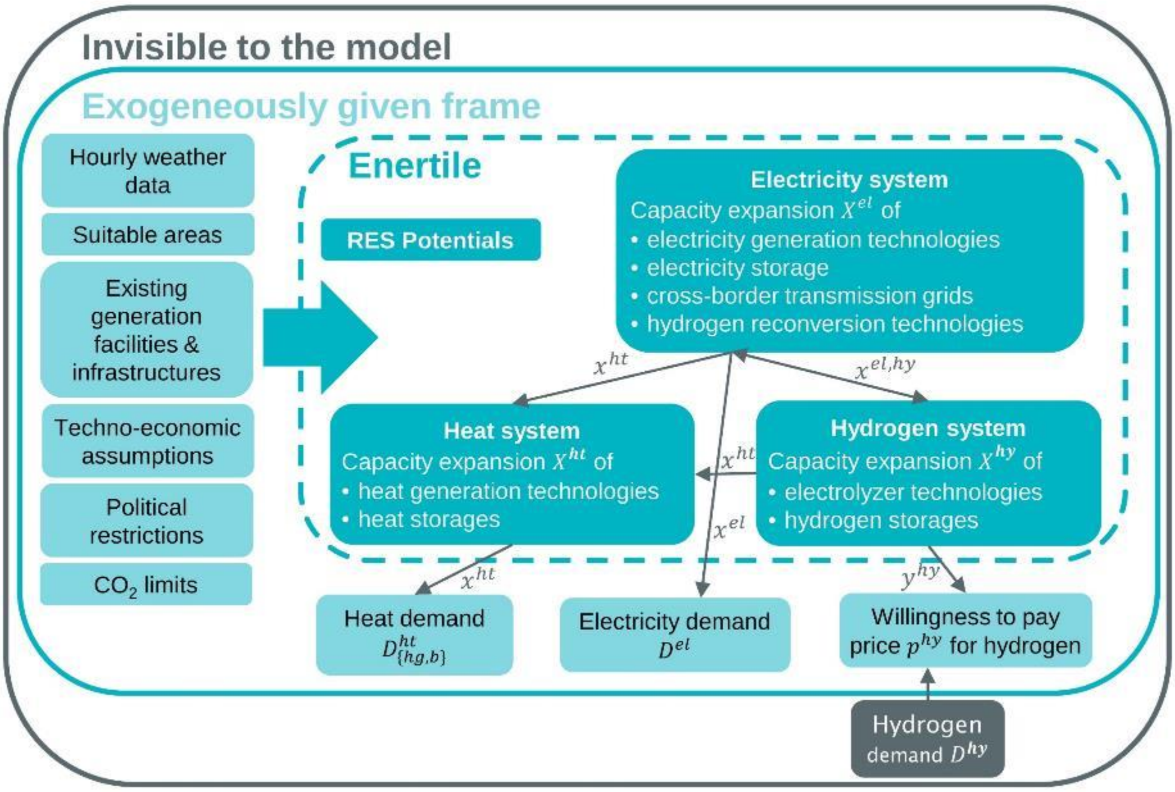

Figure 5-1 Graphical illustration of the coverage and boundaries of the energy system model *Enertile*.

5.2.1.1.1 Objective function

In *Enertile*, the supply of electricity, heat and hydrogen in Europe is described as a linear cost minimization problem of the overall energy system being considered. In the model, costs associated with the decision variables $\vec{X}$ representing installed capacities of relevant infrastructures and their corresponding unit dispatch $\vec{x}$ increase the overall system cost. Taxes and other levies are not included in the evaluation, since the focus is not on the behavior and reactions of individual market actors but on the overall economic perspective.

In the model, hydrogen supply is treated differently to the supply of electricity and heat. While exogenously specified electricity and heat demands need to be met at every hour considered, there is no explicit hydrogen demand (Figure 5-1). Instead, *Enertile* can choose to build electrolyzers that can be used in two ways. Firstly, electrolyzers can be utilized to fill an energy storage unit within the conversion sector. Subsequently, the stored hydrogen can be converted into heat for district heating or reconverted into electricity. Secondly, hydrogen can be sold at price p^{hy} to demand sectors beyond the modeled part of the energy system, .e.g. fuel demand in transport. Potential hydrogen demands of these external sectors are therefore implicitly considered. The hydrogen selling price p^{hy} can be understood as the potential willingness of these sectors to pay for hydrogen. In the model the amount of hydrogen y^{hy} sold to these external demand sectors reduces the total cost of the system. Through the application of different hydrogen sales prices p^{hy}, the resulting hydrogen production potentials display a supply curve for electricity-based hydrogen for the external demand sectors.

The objective function (8) is the sum of costs for the supply of electricity, heat, and hydrogen, minus the remuneration for the sale of hydrogen to external demand sectors, over all regions $r \in R$ and in all 8,760 hours $h \in H$ of the modeled year.

$$\begin{aligned}\min_{\vec{X},\vec{x},y} \sum_{r\in R} \Bigg\{ & \sum_{i\in I}\left(\underbrace{\left(c_i^{fix} \cdot X_{r,i}^{el}\right)}_{capacity\ expansion\ electricity\ supply} + \underbrace{\sum_{h\in H} c_i^{var} \cdot x_{r,i.h}^{el}}_{electricity\ generation} \right) \\ & + \sum_{j\in J}\left(\underbrace{\left(c_j^{fix} \cdot X_{r,j}^{ht}\right)}_{capacity\ expansion\ heat\ supply} + \underbrace{\sum_{h\in H} c_j^{var} \cdot x_{r,j,h}^{ht}}_{heat\ generation} \right) \\ & + \sum_{k\in K}\left(\underbrace{\left(c_k^{fix} \cdot X_{r,k}^{hy}\right)}_{capacity\ expansion\ hydrogen\ supply} + \underbrace{\sum_{h\in H} c_k^{var} \cdot x_{r,k.h}^{hy}}_{hydrogen\ generation} \right) \\ & - \underbrace{p^{hy} \cdot y_r^{hy}}_{hydrogen\ sold\ to\ demand\ sectors} \Bigg\}\end{aligned} \tag{8}$$

Costs for the provision of all three energy forms comprise annuitized fixed costs for capacity expansion and variable costs of all employed technologies. Fixed costs $c_{\{i,j,k\}}^{fix}$ for expanding the capacity of a specific technology include fixed operation and maintenance costs and annuitized specific investments. Variable costs $c_{\{i,j,k\}}^{var}$ of utilizing a specific technology include fuel costs, CO_2 costs, and variable operation and maintenance costs. The underlying technology set I covering electricity supply contains renewable energy technologies, power storage plants, cross-border transmission grids and hydrogen reconversion technologies. The technology portfolio for the supply of heat J includes renewable heating sources, electric boilers, hydrogen boilers, large heat pumps, and heat storage units. Technologies covering the supply of hydrogen are contained in the technology set K and include electrolyzer technologies and hydrogen storage units.

5.2.1.1.2 Constraints

The central constraints of the minimization problem require that electricity, heat and hydrogen demands are met in every region at every hour of the year. On the one hand, exogenous demands for electricity D^{el} and heat in heat grids D_{hg}^{ht} and buildings D_b^{ht} are specified in the model. On the other hand, model endogenous demands can arise from the interdependence of the provision of the different energy forms. The combination of these demands results in so-called demand-supply equations $DS_{\{el,hg,b,hy\}}$ for the various energy forms and applications.

The demand-supply equation for electricity DS_{el} is shown in equation (9). It requires that the sum of net electricity supply of technologies I must match the sum of the exogenously determined electricity demand D^{el}, the electricity demand for heat supply in heating grids and buildings, and the electricity demand for hydrogen generation in each region r and hour h. The net electricity supply includes the pure generation of electricity, the sum of net electricity imports and the net electricity extraction from storage units in a region. The provision of heat in heat grids HG causes electricity demands for the use of heat pumps hpg with conversion efficiency γ_{hpg} and electric boilers eb with conversion efficiency γ_{eb}. Similarly, the provision of heat in buildings B leads to electricity demands if heat pumps hpb with a conversion efficiency γ_{hpb} are used. Hydrogen is generated in the model with a proton exchange membrane electrolyzer pem having a conversion efficiency of γ_{pem}, and increases the electricity demand.

$$[DS_{el}] \qquad \begin{aligned}\sum_{i\in I} x^{el}_{r,i,h} = D^{el}_{r,h} &+ \sum_{hg\in HG}\left(\frac{1}{\gamma_{hpg}}\cdot x^{ht}_{r,hg,hpg,h} + \frac{1}{\gamma_{eb}}\cdot x^{ht}_{r,hg,eb,h}\right) \\ &+ \sum_{b\in B}\frac{1}{\gamma_{hpb}}\cdot x^{ht}_{r,b,hpb,h} + \frac{1}{\gamma_{pem}}\cdot x^{hy}_{r,pem,h}\end{aligned} \qquad \forall r,h \qquad (9)$$

The demand-supply equations for the provision of heat in heat grids DS_{hg} and buildings DS_b are shown in equations (10) and (11). In both cases the equations require that the sum of net heat supply meets the exogenously specified heat demands $D^{ht}_{\{hg,b\}}$ in each region r and hour h. The net heat supply includes both the pure heat generation and the heat extraction from thermal storage units in a region. Different subsets of the heat supply technology portfolio J are available for the heat supplies in heating grids $L \subset J$ and buildings $M \subset J$.

$$[DS_{hg}] \qquad \sum_{l\in L} x^{ht}_{r,hg,l,h} = D^{ht}_{r,hg,h} \qquad \forall r,hg,h \qquad (10)$$

$$[DS_{b}] \qquad \sum_{m\in M} x^{ht}_{r,b,m,h} = D^{ht}_{r,b,h} \qquad \forall r,b,h \qquad (11)$$

Equation (12) shows the demand supply equation of hydrogen DS_{hy}. It requires that the net supply of hydrogen provided by the technology portfolio K must cover the model endogenous hydrogen demands consisting of the following components: The provision of heat in heat grids HG causes hydrogen demands for the use of hydrogen boilers hyb with conversion efficiency γ_{hyb}. The reconversion of hydrogen into electricity uses the portfolio of reconversion technologies $N \subset I$ with the associated conversion efficiencies γ_n. Additionally, the "sale" of hydrogen y^{hy} to external demand sectors requires hydrogen generation. The net hydrogen supply includes both the pure hydrogen generation and the net hydrogen extraction from storage units in a region.

$$[DS_{hy}] \qquad \sum_{k \in K} x^{hy}_{r,k,h} = \sum_{hg \in HG} \frac{1}{\gamma_{hyb}} \cdot x^{ht}_{r,hg,hyb,h} + \sum_{n \in N} \frac{1}{\gamma_n} \cdot x^{el}_{r,n,h} + y^{hy}_r \qquad \forall r, h \qquad (12)$$

Other constraints of the minimization problem require

- that hourly outputs of a generation unit do not exceed the installed capacity of this unit,
- that hourly electricity transfers between regions do not exceed transmission capacities,
- and that storage units only operate within the limits of their technical parameterization; i.e. the amount of energy stored or withdrawn in one time step does not exceed the installed capacity and that the minimum and maximum storage capacity is not violated at any time.

Additionally, political goals such as global or regional CO_2 reduction targets or certain renewable energy expansion targets, as well as technical restrictions such as losses in storage facilities and electricity transport grids can be included as constraints.

5.2.1.1.3 Temporal and spatial resolution

In the applied version of *Enertile,* the energy system of the year 2050 is modeled in an hourly resolution. This high temporal resolution allows for a realistic representation of the challenges in energy systems with a high proportion of renewable energies. Short-term weather-induced fluctuations in the generation of electricity or heat from renewable energies can be captured, as can long-term weather events such as lulls (Pfluger et al. 2017). The model optimizes expansion and dispatch of relevant infrastructures using perfect foresight.

For the analysis of this paper, *Enertile* covers the energy system in Europe. The geographical coverage of such a large area becomes increasingly necessary as the proportion of renewable energy in the system increases. Shortages in the supply of electricity or heat from renewable sources due to local weather conditions can often be compensated for supra-regionally. Therefore, the spatial extension provides sources of system flexibility. The regional resolution of the model varies according to the subject considered: a very high spatial resolution is used for the potential calculation of renewable energies. In order to determine the possible generation of wind and solar energy, GIS-based models are used to determine renewable energy potentials on a grid with an edge length between 1 km and 10 km.

For other aspects of modeling, such as balancing electricity supply and demand, model regions based on the European national states are applied. Small or strongly interconnected national states are aggregated in some cases. A list and map of the resulting model regions can be found in Appendix C. Within a model region, no further locational information is taken into account during the optimization. This means, for example, that potential network restrictions within a model region are invisible to the model.

5.2.1.1.4 Renewable energy potential calculation

The electricity generation potential of renewable energies is represented in the optimization program using cost-potential curves. These cost-potential curves are determined for different renewable electricity generation technologies in detailed preliminary calculations. In these calculations, techno-economic data of the generation technologies, hourly weather data, and land use data are used to determine the possible electricity generation on a fine-grained grid for Europe. A more detailed description of the methodology is given in section 5.2.2.3, along with a graphical representation of the resulting cost-potential curve used in the optimization.

5.2.1.1.5 Electricity grid representation

The representation of electricity grids in *Enertile* is reduced to the exchange of electricity between different model regions. Within a model region, potential grid bottlenecks are not taken into account — a so-called *copper plate* is assumed. Existing possibilities of electricity exchange between model regions are represented by a model of net transfer capacities (NTC), which defines the maximum possible exchange capacity for each border between regions. Besides initially available network capacities, the possible network expansion between model regions is influenced by network expansion cost, network losses and the technical and temporal realization possibilities of expansion projects. For each border, step functions define what network capacity is possible at what costs and in what time periods. On this basis, the model can decide which grid expansion is cost-efficient to cover the electricity demand in the individual regions.

5.2.2 Data

In order to investigate the possible supply of hydrogen in a European energy system in 2050, a parameter study is conducted with the energy system model *Enertile*. The focus of the parameter variation is on possible developments in the polymer electrolyte membrane (PEM) electrolysis technology and a varying willingness to pay for electrolytic hydrogen in the demand sectors. The following section presents the underlying scenario framework and techno-economic assumptions pertaining to the modeled technologies.

5.2.2.1 General framework and scenario design

The following general analysis framework is assumed:

- The cost-minimizing character of our modeling approach makes a substantial use of synthetic fuels at modest decarbonization levels below 80% unlikely. For a lower ambition level, there are more cost-efficient CO_2 reduction measures and flexibility options. This hypothesis was tested with model runs not discussed in this paper. In these scenarios, the resulting CO_2 abatement costs do not reach levels at which electricity-based fuels become competitive with their fossil counterparts. Therefore, the starting point of our analysis is the electricity and heat demands in an 80% decarbonization scenario.
- One option of achieving additional greenhouse gas reductions compared to an 80% decarbonization scenario is by replacing the remaining fossil fuels in the following sectors with e-fuels: energy conversion, transport, industry, residential and services. However, this only applies if the required hydrogen is produced in a CO_2-neutral process. Therefore, the ambition level in the electricity sector is raised and it is assumed that electricity may only be

generated from emission-free sources. This includes an intermediate storage of electricity in the form of hydrogen and subsequent reconversion into electricity.

- In order to capture the competition between the use of synthetic energy carriers in the various applications of the demand sectors and their use in the explicitly modeled heat supply in heat grids, no fossil energy carriers are included in the heat generation mix either. Heat generation is therefore also assumed to be emission-free.
- Demands for hydrogen or other synthetic energy carriers by transport, industry, and residential and services are not explicitly modeled. Instead, the model can reduce system costs by selling hydrogen to the demand sectors. In a parameter study, the associated hydrogen sales price is increased in steps of 10 €$_{2020}$/MWh$_{H2}$.

In summary, a zero-emission generation fleet for electricity, heat and hydrogen is assumed in order to meet the energy demands in an otherwise “80% decarbonization scenario”. This means that the demand for sector coupling options like e-mobility or heat pumps is used widely, but the demand sectors still use a substantial amount of fossil fuels. This setting is chosen to observe the conversion sector at a working point, at which hydrogen or synthetic fuels would come into play. If demands for an almost fully decarbonized energy system were applied, the supply side would already cater for many new needs, e.g. electricity for e-mobility or hydrogen production.

5.2.2.2 Energy demands

The analysis in this paper is primarily based on the energy demands developed in the “Centralized” scenario of the European Union’s Horizon 2020 project “REflex” (REflex 2019). This scenario aims at an 80% reduction in greenhouse gases compared to 1990 across all sectors in Europe. The overarching technological strategy in this scenario is to cover energy demands via central infrastructures if possible. Thus, for example, heat supply in cities is preferably provided by heat grids equipped with large-scale heat storage units and heat pumps.Table 5-1 shows the demand for heat and electricity in the model regions derived from this scenario. Since the REflex project only takes into account the member states of the EU, Norway and Switzerland, energy demands for non-EU countries analyzed in *Enertile* need to be estimated. The demand estimates for these countries are based on the net electricity consumptions in 2016, estimates on the increase in per capita electricity consumption, and projections of the population development until 2050.

The exogenously specified electricity demand in the model is divided into three categories: firstly, the general electricity demand; secondly, the partly flexible electricity demand from the transport sector (i.e. charging of battery electric vehicles (BEV) and plug-in hybrids (PHEV)); and thirdly, the inflexible demand from the transport sector. The inflexible mobility demand includes the electricity demand for inflexible charging of BEV, PHEV and light duty vehicles, and the electricity demands of trolley trains, trolley buses, and trolley trucks. Certain demand profiles are assumed for each of the three categories. The impact of deviating electricity demands on marginal hydrogen generation costs is analyzed in section 5.3.6.

The modeled heat demand includes two categories: firstly, the heat demand in heat grids, and secondly, the heat demand of decentralized heat pumps in buildings.

Table 5-1 Electricity and heat demands in the modeled regions in 2050.

	Electricity (TWh_{el})			Heat (TWh_{th})		Data source
	General[a]	**Flexible mobility**[b]	**Inflexible mobility**[c]	**District heating grids**	**Decentralized heat pump systems**	
Austria	87.6	6.9	1.7	18.5	20.3	(REflex 2019)
Other Balkans[d]	126.4[e]	11.6[f]	2.9[f]	23.0[f]	23.8[f]	
Baltic States	30.3	3.6	0.9	15.6	10.2	(REflex 2019)
Benelux Union	329.7	26.6	6.6	41.7	86.4	(REflex 2019)
Bulgaria & Greece	91.1	10.4	2.6	22.1	14.6	(REflex 2019)
Switzerland	56.2	6.7	1.7	12.7	11.0	(REflex 2019)
Czech Republic	79.9	6.0	1.5	29.1	23.2	(REflex 2019)
Germany	640.4	58.4	14.6	131.7	136.7	(REflex 2019)
Denmark	40.6	5.7	1.4	21.9	18.6	(REflex 2019)
Finland	103.7	6.3	1.6	24.6	25.0	(REflex 2019)
France	531.3	62.3	15.5	35.6	138.3	(REflex 2019)
Hungary & Slovakia	90.3	6.0	1.5	34.0	24.8	(REflex 2019)
Iberian Peninsula	354.9	32.1	8.0	10.1	64.6	(REflex 2019)
Italy	374.5	55.8	13.9	106.1	55.4	(REflex 2019)
Norway	114.5	8.2	2.1	8.2	14.5	(REflex 2019)
Poland	192.1	11.9	3.0	34.5	33.6	(REflex 2019)
Romania	78.6	6.3	1.6	24.4	16.6	(REflex 2019)

	Electricity (TWh_{el})			Heat (TWh_{th})		Data source
	General[a]	**Flexible mobility**[b]	**Inflexible mobility**[c]	**District heating grids**	**Decentralized heat pump systems**	
Sweden	167.6	13.7	3.4	31.0	19.4	(REflex 2019)
British Islands	408.4	71.4	17.8	79.7	170.7	(REflex 2019)
Total	**3,898.1**	**409.9**	**102.4**	**704.6**	**907.7**	

[a] The "General" electricity demand is the total of electricity demands from the demand sectors industry, residential and services excluding the electricity demand for heat pumps in buildings.
[b] The electricity demand "Flexible mobility" only contains the electricity demand of cars and assumes that 80% of the cars are charged smartly.
[c] The electricity demand "Inflexible mobility" contains the inflexible load of cars (20%), trolley busses, trains, light duty vehicles, and trolley trucks.
[d] A definition of the model region "Other Balkans" is given in Appendix C.
[e] For member states of the EU "General" electricity demands are taken from the "Centralized" scenario of the REflex project (REflex 2019). Other demand estimates are used for the non-EU countries in "Other Balkans". The basis of these estimates is the total net electricity consumptions in 2016 in these countries (EIA 2016). Population figures (UN 2017) are used to calculate per capita electricity consumptions in these countries. These per capita electricity consumptions are then extrapolated until 2050 using the average increase in per capita electricity consumption between 2017 and 2040 in the Middle East taken from (IEA 2018). With these estimated per capita electricity consumptions in 2050 and projections for population developments (UN 2017) the "General" electricity demands in these countries are calculated.
[f] Electricity demands for mobility and heat demands in "Other Balkans" are determined by applying the respective average European ratios of "General" electricity demand and the other demand categories ("Flexible mobility", "Inflexible mobility, "District heating grids", "Decentralized heat pump systems"). These ratios are used as scaling factors to translate the "General" electricity demand of "Other Balkans" to the other demand categories.

5.2.2.3 Electricity and heat generation

In addition to the exogenously specified electricity and heat demands, techno-economic information on electricity generators and heat suppliers is included in *Enertile* to parameterize the optimization problem. Weather-dependent renewable electricity generation is included using cost-potential curves. These cost-potential curves are determined for four renewable electricity generation technologies in preliminary calculations before the scenario calculations of the energy system model *Enertile*: For solar energy, two different technologies are distinguished: photovoltaics (PV) and concentrating solar power (CSP). For wind energy, both onshore and offshore potentials are considered.

To determine the electricity generation potential of renewable energies, Europe is divided into tiles using a grid structure. Depending on the distance to the equator, these tiles have a size between 100 km^2 and 10 km^2. For each of the approximately 140,000 tiles considered in the analysis of this paper, the renewable generation potential is determined in five steps (Pfluger et al. 2017):

1. Identification of available areas: Based on the terrain (gradient, soil conditions, etc.) and the prevailing land use (nature reserves, buildings, agriculture, military zones, etc.), suitable areas for renewable energy generation are identified.
2. Determination of possible renewable capacities: Based on the available area, a definition of land-use factors for renewable electricity generation, and the specific area required for renewable energies, the possible renewable capacity per tile and technology is determined.
3. Determination of potential renewable electricity generation: Combining the possible renewable capacity with regionally resolved, hourly weather data, possible renewable generation quantities per technology and tile are determined. For wind energy hourly wind speeds over several years are considered. The calculation considers different hub heights, rotor-generator-ratios, wind turbine power characteristics and regional roughness. For solar energy hourly solar irradiation data over several years and module efficiencies are taken into account.
4. Calculation of specific electricity generation costs: The possible generation potentials are weighted with techno-economic data for the individual generation technologies.
5. Aggregation of the potentials within a model region: The renewable generation potentials of single tiles are aggregated according to their specific generation costs; typically, between 3 and 12 cost steps are considered per technology and region.

As a result, regional cost-potential curves for the various renewable generation technologies are available for system optimization, as well as the respective hourly generation profiles. The aggregated results for the modelled regions in 2050 are shown in Figure 5-2.

It has to be noted that all long-term technology cost projections are subject to uncertainty; this is especially the case for relatively young technologies in a dynamic market, as is the case for wind and solar power technologies. In the past, especially projections for solar PV did not manage to foresee the fast cost reductions that were achieved (Creutzig et al. 2017). It is almost impossible to forecast cost developments of RES technologies for the next 30 years accurately. However, electricity costs are the most important cost component of hydrogen generated using electrolysis. Since, this paper does not attempt to cover all potential RES costs developments, a sensitivity analysis is performed to understand how higher or lower electricity generation costs of RES might impact on hydrogen costs. The impact of deviating electricity generation costs on hydrogen production costs is analyzed in section 5.3.5.

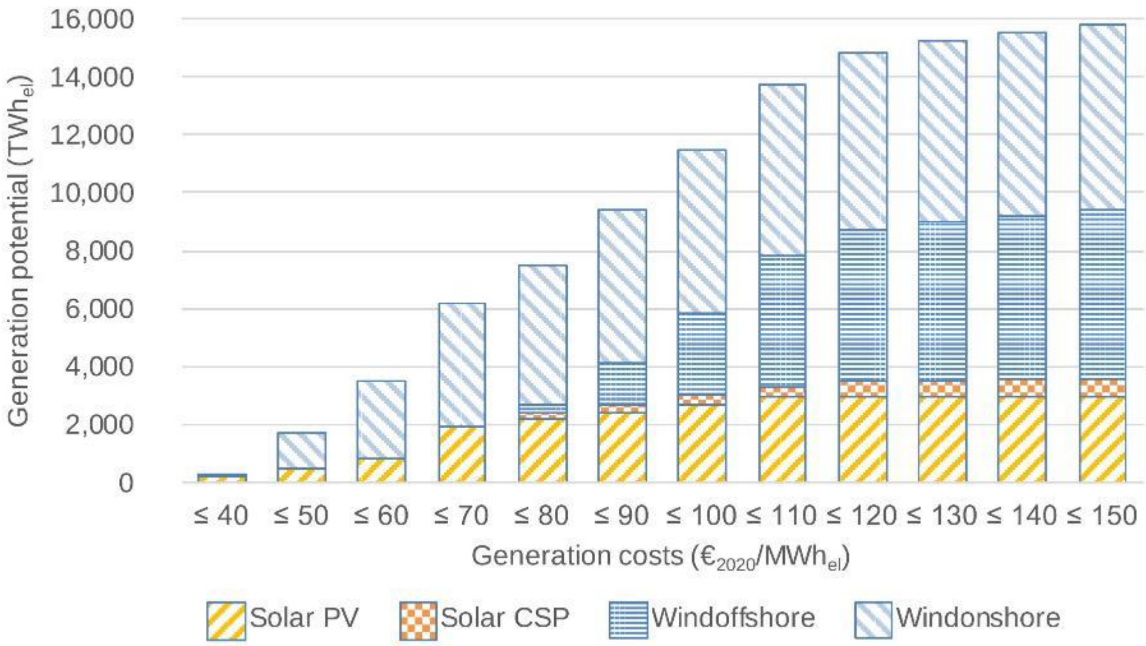

Figure 5-2 Electricity generation potentials of renewable energies in all modeled regions in 2050.

The electricity generation capacities of hydropower and biomass are defined exogenously. In the case of hydropower, a distinction is made between run-of-river, which follows a monthly profile, and storage plants, for which the monthly energy sum is distributed by the model taking into account the installed capacities. Biomass power plants in 2050 are modeled like the storage hydropower plants, i.e. the amount of energy has to be distributed by the model.

Non-renewable electricity and heat generation technologies considered in the model are characterized in Table 5-2. For power generation, hydrogen turbines and combined cycle hydrogen turbines are considered as hydrogen reconversion technologies. At the present time, these technologies do not yet exist for pure hydrogen; however, due to the long experience with combustion processes, it can be assumed that they may be available by 2050. Their techno-economic parameterization in the model is based on comparable combustion plants operated with natural gas. Alternative electricity storage facilities are represented in the model by pumped storage hydropower plants. New nuclear power plants are defined exogenously for the countries that have no phase-out policy in place and see nuclear power as a part of their decarbonization strategy. However, the number of reactors is assumed to decrease compared to today due to their high specific costs.[4]

[4] The high costs are also the reason why the plants have to be defined exogenously; the optimization model chooses the technology only if unrealistically low specific costs are assumed.

For heat generation in the model, Table 5-3 describes techno-economic parameters of hydrogen boilers, electric boilers, large heat pumps and heat storage units. All heating and power generating technologies are characterized by their efficiency, lifetime, specific investment, fixed operation and maintenance cost (fixed O&M) and variable operation and maintenance cost (variable O&M). To convert investment into annual costs in the model, constant weighted average costs of capital of 7% are assumed for all technologies.

Renewable heat generation in heating grids is assumed to account for 20% of the annual heat demand, with solar thermal and geothermal energy each accounting for half of the supply. The solar thermal heat generation follows the solar irradiation profile. The geothermal heat generation profile is assumed to be constant over time.

Table 5-2 Techno-economic parameters of heat generation utilities in 2050 as modeled in Enertile.

	Efficiency (%)	Lifetime (a)	Investment (€$_{2020}$/kW)	Fixed O&M (€$_{2020}$/kW)	Variable O&M (€$_{2020}$/MWh)
Combined cycle hydrogen turbine	60	30	950	11.25	3
Hydrogen turbine	40	30	450	7.5	2.7
Pumped hydro storage	89	40	1100	10	0.5

Table 5-3 Techno-economic parameters of electricity generation utilities in 2050 as modeled in Enertile.

	Efficiency (%)	Lifetime (a)	Investment (€$_{2020}$/kW)	Fixed O&M (€$_{2020}$/kW)
Hydrogen boiler	94	20	50	1.98
Electric heater	95	20	100	5.54
Large heat pump	variable[a]	20	600	2.4
Heat storage	99	20	22	0

[a] The conversion of power depends on the flow temperature and the hourly outdoor temperature.

5.2.2.4 Electrolysis

Currently, there are three main technologies in water electrolysis: Alkaline Electrolysis (AEL), Polymer Electrolyte Membrane Electrolysis (PEMEL) and Solid Oxide Electrolysis (SOEL). The three technologies differ in terms of the electrolyte used, their development stage and their techno-economic properties. From the system perspective that is applied in the analyses presented in this paper, three dimensions of electrolysis characteristics are relevant: firstly, what costs are associated with the technology; secondly, how much energy is used by the technology to produce hydrogen; and thirdly, how flexibly the technology can respond to the fluctuating availability of renewable electricity.

AEL is the most mature electrolysis technology and has been used in industrial applications since the beginning of the 20th century (Kreuter et al. 1998). The electrolyte in AEL is typically an aqueous alkaline solution of sodium hydroxide or potassium hydroxide. Its system efficiency in converting electrical energy into hydrogen is currently in the range of 51% to 60% based on the lower heating value (Buttler et al. 2018). Specific investments for AEL systems currently range between 800 $€_{2020}/kW_{el}$ and 1,500 $€_{2020}/kW_{el}$ (Buttler et al. 2018). Operation with intermittent and fluctuating power sources is possible but leads to problems in pilot plants (Gahleitner 2013). The minimum load of AEL is limited to 20% to 25% of nominal hydrogen production. While its cold start-up time lies between one and two hours, its warm start-up time ranges between one and five minutes (Buttler et al. 2018).

In PEMEL an acidic proton exchange membrane is used as the electrolyte, which requires the use of noble metals as catalysts, anodes, and cathodes to prevent corrosion (Buttler et al. 2018). Due to the high material requirements, this electrolysis technology is currently considerably more expensive than AEL with a specific investment of 1,400 $€_{2020}/kW_{el}$ to 2,100 $€_{2020}/kW_{el}$ (Buttler et al. 2018). It is assumed that production costs comparable to those of AEL can be achieved in the mid-term through the upscaling of electrolyzer production and further developments in the materials used (Brinner et al. 2018; Smolinka et al. 2018). The efficiency of a PEMEL system currently ranges between 46% and 60% based on the lower heating value and is thus similar to an AEL system (Buttler et al. 2018). PEMEL features the most flexible operation of the three technologies, with short cold start-up times of between 5 and 10 minutes, warm start-up times of less than 10 seconds, and without technical limits of minimum load (Buttler et al. 2018).

SOEL is still at the pre-commercial development stage. It is operated at 700 °C to 1,000 °C and uses a ceramic electrolyte. The high operating temperature can reduce the direct power consumption of the technology, if external heat sources are available. The electrical system efficiency can therefore be increased to between 76% and 81% based on the lower heating value (Buttler et al. 2018). If no external heat is available, the SOEL's efficiency is similar to that of AEL or PEMEL. Even though SOEL allows for an operating range of -100% (meaning it operates as a fuel cell) to 100%, its flexible utilization is limited. The high operating temperature causes long cold start-up times of up to 10 hours and relatively long warm start-up times of 15 minutes (Buttler et al. 2018; Smolinka et al. 2018). Material degradation caused by high temperatures and steep temperature gradients currently results in short lifetimes of 8,000 to 20,000 operating hours and an overall unsuitability of SOELs as a system flexibility option (Buttler et al. 2018; Smolinka et al. 2011). Due to the pre-commercial status, estimates on the current specific investment of SOEL are uncertain and range between 1,350 $€_{2020}/kW_{el}$ and 3,250 $€_{2020}/kW_{el}$ (Smolinka et al. 2018).

For the analyses in this paper only PEMEL is considered. It is particularly suitable for flexible operation in combination with fluctuating renewable power sources and has the potential to be the technology with the lowest hydrogen production cost in many potential fields of application by 2050. The techno-economic electrolyzer parameters used for the modeling in 2050 are shown in Table 5-4. Starting from a *central parameter scenario*, the specific investments, the electrical system efficiency, and the lifetime of a PEMEL system are individually varied by 10%. In the *progressive parameter scenario*, all three parameter dimensions are assumed to be simultaneously enhanced by 10%; in the *conservative parameter scenario*, all three parameter dimensions are assumed to be simultaneously weakened by 10%.

Table 5-4 Techno-economic parameter variation of PEMEL as modeled in 2050.

	Efficiency (%)	**Lifetime (a)**	**Investment ($€_{2020}$/kW)**	**Fixed O&M ($€_{2020}$/kW)**
Progressive	**75**	**30**	**459**	**6.3**
Progressive investment	68	27	459	6.3
Progressive efficiency	75	27	510	7
Progressive lifetime	68	30	510	7
Central	**68 (Smolinka et al. 2018)**	**27 (Smolinka et al. 2018)**	**510 (Smolinka et al. 2018)**	**7 (Smolinka et al. 2018)**
Conservative investment	68	27	561	7.7
Conservative efficiency	61	27	510	7
Conservative lifetime	68	24	510	7
Conservative	**61**	**24**	**561**	**7.7**

5.3 Results

Below the hydrogen generation potential in Europe in 2050 resulting from the model runs is presented and analyzed. Of particular interest are the available quantities of hydrogen for the demand sectors of transport, industry, residential and services, the impact of hydrogen production on the electricity system, the regional distribution of electrolyzer capacities in Europe and the techno-economic drivers determining the deployment of electrolyzers.

5.3.1 Hydrogen supply curve for demand sectors in Europe in 2050

The hydrogen supply curves determined by the optimization model for transport, industry, residential and services in an emission-free European energy system in 2050 are shown in Figure 5-3. Hydrogen production quantities for three different techno-economic development statuses of PEM electrolysis and different hydrogen sales prices (as ex works prices)[5] are given. Hydrogen utilized as an electricity storage medium in the conversion sector is included in the scenario runs, but not included in these supply curves.

The optimization results in Figure 5-3 show a disproportional increase in the available quantity of hydrogen for the demand sectors with increasing hydrogen prices. In the *central parameter scenario*, the potential hydrogen supply increases from 0 TWh_{H2} at a sales price of 50 $€_{2020}/MWh_{H2}$ to 4,111 TWh_{H2} at a sales price of 150 $€_{2020}/MWh_{H2}$. In compliance with the 1.5 °C target, the long-term strategic vision of the EC implies a hydrogen demand of about 1,536 TWh_{H2} to 1,953 TWh_{H2}[6] in Europe for industry, transport, residential and services by 2050 (EC 2018a, 2018b). The optimization results indicate that hydrogen demands of this order of magnitude entail marginal hydrogen generation costs between 110 $€_{2020}/MWh_{H2}$ and 130 $€_{2020}/MWh_{H2}$ in the *central parameter scenario*. In the event of a *conservative* techno-economic development of PEM electrolysis, the marginal hydrogen generation costs rise to between 120 $€_{2020}/MWh_{H2}$ and 150 $€_{2020}/MWh_{H2}$ to cover these hydrogen demands. In the opposite case of a *progressive* techno-economic development, the marginal hydrogen generation costs induced by these demands decrease to between 90 $€_{2020}/MWh_{H2}$ and 110 $€_{2020}/MWh_{H2}$. A more detailed analysis of the influence of the different techno-economic drivers on the hydrogen generation potential is given in section 5.3.4.

5 The model answers the question of how much hydrogen the supply sector would produce if the willingness of the demand sectors to pay ex works, i.e. without incurring costs after production, such as transport costs etc., reached a given level.

6 For the 1.5TECH scenario the EU long-term strategy (EC 2018a, 2018b) indicates the following demands for hydrogen-based energy sources for the industrial, residential & services and transport sectors in 2050: 67.7 Mtoe hydrogen, 44.7 Mtoe e-gas, and 40.7 e-liquids. For the 1.5Life scenario the demands in 2050 are: 60.7 Mtoe hydrogen, 40.7 Mtoe e-gas, 19.6 Mtoe e-liquids. In a simple estimation of the required hydrogen for e-gas and e-liquids production, it is assumed that e-gas is equivalent to synthetic methane and that e-liquids are equivalent to synthetic methanol. The necessary quantities of hydrogen are calculated using the demands of e-gas and e-liquids and the stoichiometric ratios in the Sabatier reaction and methanol synthesis.

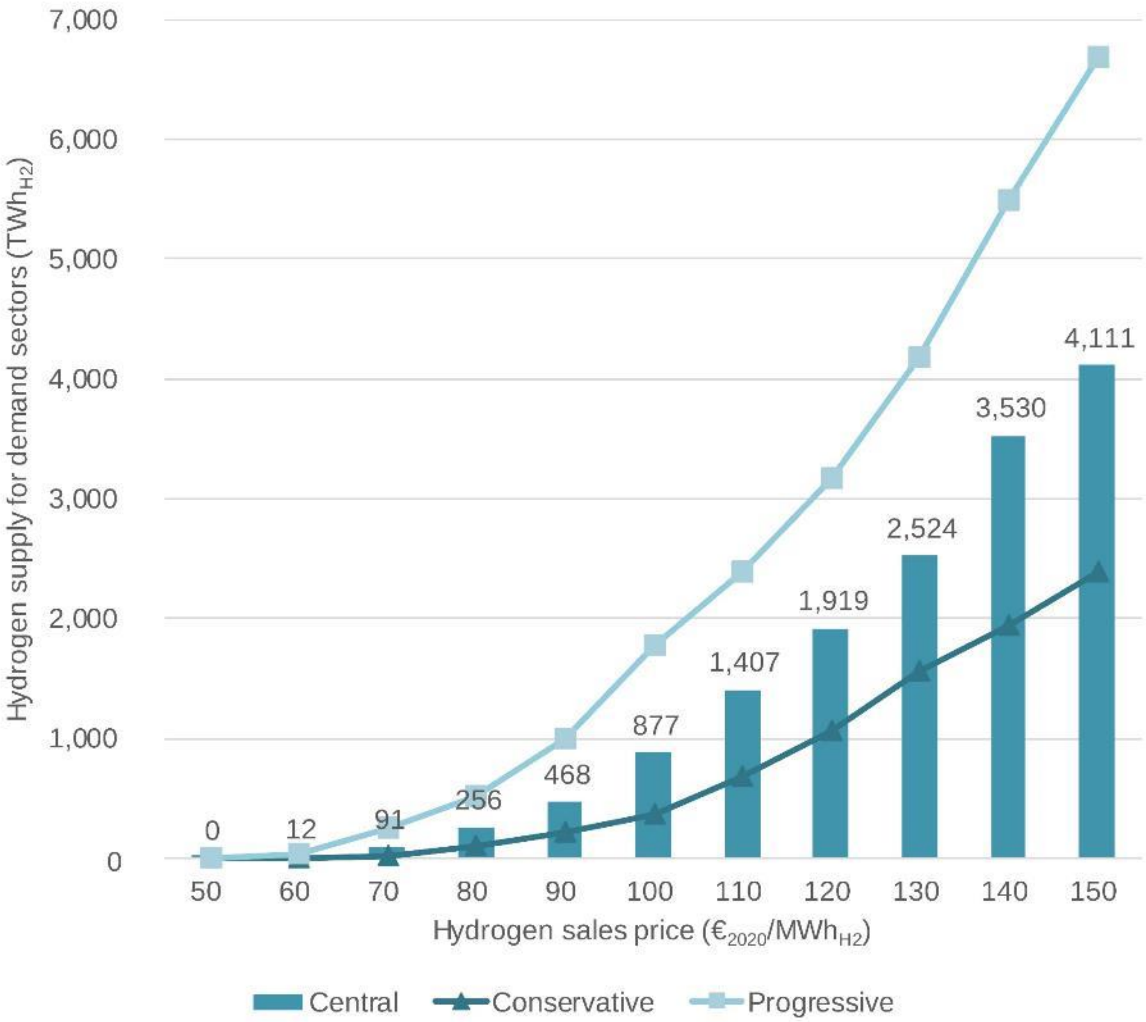

Figure 5-3 Hydrogen supply curves for the demand sectors of transport, industry, residential and services in Europe in 2050. Depicted here are available quantities of electricity-based hydrogen at increasing sales prices (ex works) for three different techno-economic development statuses of PEM electrolysis.

5.3.2 Impacts of hydrogen generation on the electricity sector in Europe in 2050

Besides the potential utilization in the demand sectors, hydrogen can serve as an electricity storage and flexibility option in the conversion sector. In both cases the production of hydrogen using electricity has impacts on the electricity sector.

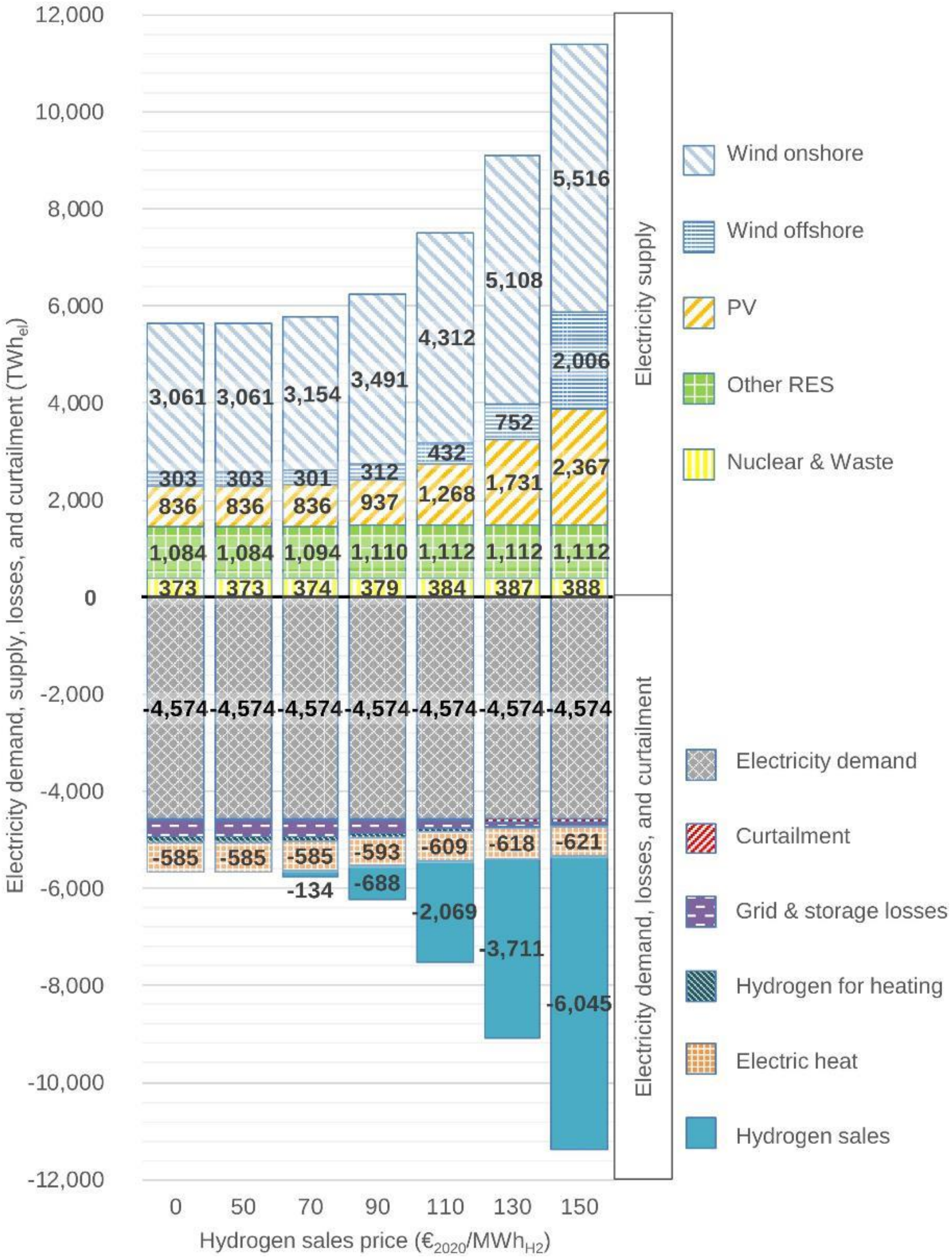

Figure 5-4 Electricity demands and supplies in all modeled regions in 2050 with varying hydrogen supply prices for the demand sectors of transport, industry, residential and services. Optimization results are shown for the central parameter scenario of PEM electrolysis.

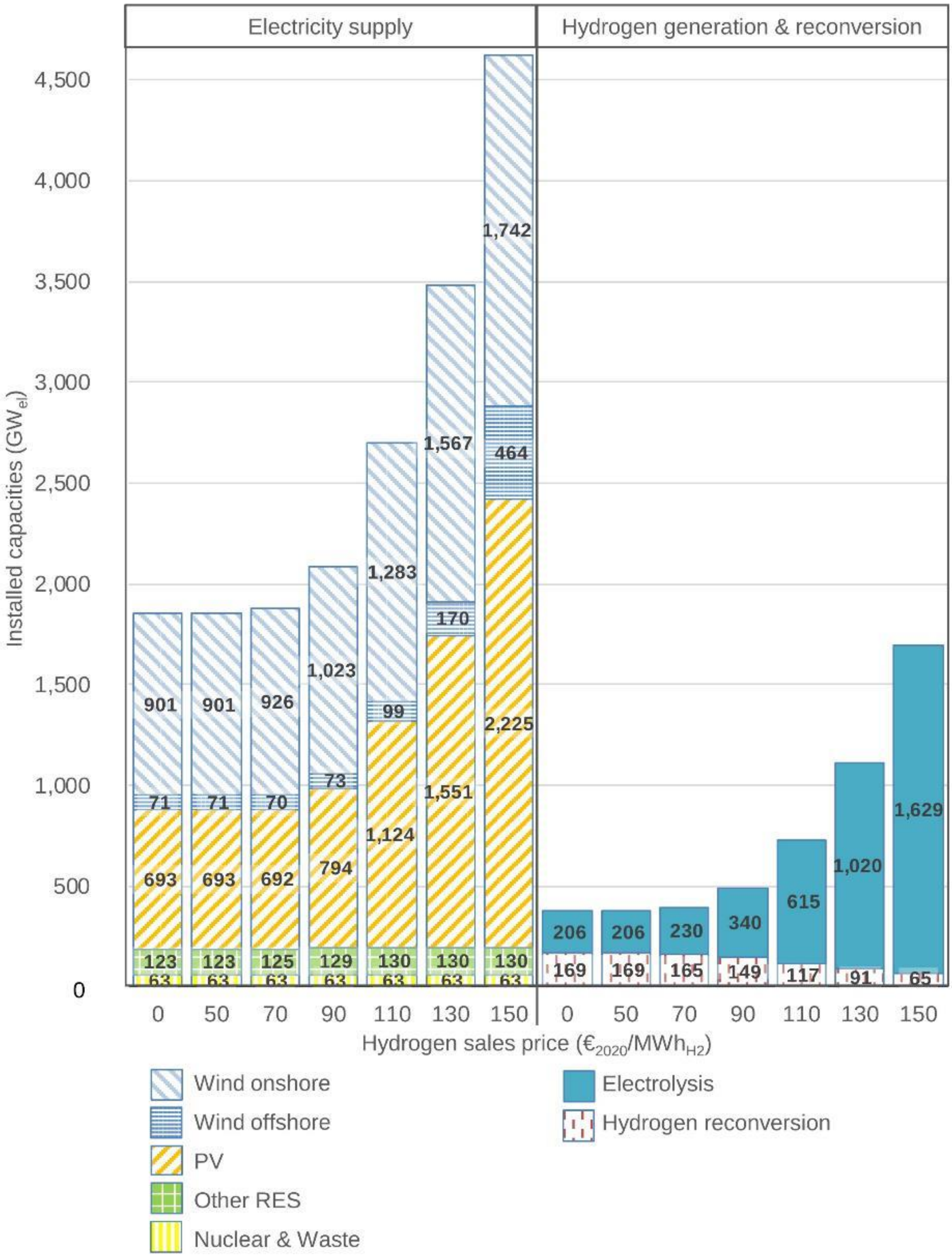

Figure 5-5 Installed electric capacities in all modeled regions in 2050 with varying hydrogen sales prices for the demand sectors of transport, industry, residential and services. Optimization results are shown for the central parameter scenario of PEM electrolysis.

The results of the scenario analysis in Figure 5-4 and Figure 5-5 show that the production of substantial amounts of hydrogen requires a substantial expansion of the renewable electricity generation fleet. The electricity used to generate hydrogen, which is either used as storage for the conversion sector or to supply the demand sectors, increases from 507 TWh_{el} at a hydrogen sales price of 50 $€_{2020}/MWh_{H2}$ to 6,106 TWh_{el} at a hydrogen sales price of 150 $€_{2020}/MWh_{H2}$. At the lower end of the sales prices at 50 $€_{2020}/MWh_{H2,}$ there is no sale of hydrogen to the demand sectors. The electricity consumed by electrolysis at this sales price is ultimately converted back into electricity or heat and therefore remains in the conversion sector. The 146 TWh_{H2} of produced hydrogen is the amount the model considers cost-efficient for balancing a system based largely on fluctuating renewable energy. At a hydrogen sales price of 130 $€_{2020}/MWh_{H2}$ – which is necessary to reliably cover the hydrogen demands in industry, transport, residential and services in the 1.5 °C scenarios of the EC's long-term strategic vision – the overall electricity demand for hydrogen production rises to 3,831 TWh_{el}. This increase in electricity demand for hydrogen production causes a capacity increase of 766 GW_{el} wind power and 865 GW_{el} solar power.

The results show positive effects of a flexible operation of electrolyzers and hydrogen storage units on the integration of fluctuating renewable energies into the energy system. Figure 5-6 indicates that with an increasing hydrogen sales price up to 110 $€_{2020}/MWh_{H2}$ the curtailed renewable electricity is reduced in the model results by between 4% and 18% compared to the curtailment at 50 $€_{2020}/MWh_{H2}$. This happens despite an expansion of the installed renewable generation capacities. Therefore, a certain amount of surplus electricity is used by the model to generate hydrogen. However, hydrogen sales prices exceeding 110 $€_{2020}/MWh_{H2}$ lead to higher amounts of curtailed renewable electricity, as renewable capacities are further expanded.

The utilization of hydrogen as an electricity storage medium in the conversion sector decreases with increasing hydrogen sales prices for the demand sectors. While at a hydrogen sales price of 50 $€_{2020}/MWh_{H2}$ 146 TWh_{el} of electricity are supplied from hydrogen reconversion, at a hydrogen sales price of 150 $€_{2020}/MWh_{H2}$ hydrogen reconversion decreases to 14 TWh_{el} (see Figure 5-6). This can be explained by two effects. Firstly, it is the opportunity costs that determine the type of use of electricity-based hydrogen. The model weighs the potential benefits from the sale of hydrogen to the demand sectors against the value of hydrogen as a storage option in the electricity and heating system. The possible profits from the sale of hydrogen to the demand sectors are determined by the price in the scenario definition. The value of hydrogen as an energy carrier and storage medium in the electricity and heating system is determined endogenously in the model on the basis of the supplies and demands in each hour considered. With increasing scenario-specific hydrogen sales prices for the demand sectors, there is an increasing number of alternatives in the electricity and heating system that can offer a supply below these opportunity costs. Secondly, the increase in hydrogen production is accompanied by an increase in the installed capacity of renewable energies. This additional electrical capacity reduces the residual load in hours of high demand and low supply of renewable energies. Consequently, this decreased residual load reduces the need for hydrogen as an electricity storage medium.

With increasing hydrogen sales prices, the generation of hydrogen for the demand sectors becomes the main flexibility option in the electricity system for dealing with an oversupply of renewable electricity. While the production of hydrogen for transport, industry, residential and services increases, the use of hydrogen for reconversion, pumped hydro storage power plants and cross-regional balancing via the transmission grid to integrate an oversupply in the electricity system decreases (see Figure 5-6). While the installed capacity remains constant, the use of pumped hydro storage power plants at a hydrogen sales price of 150 $€_{2020}/MWh_{H2}$ is reduced by about 69% compared to its utilization at a sales price of 50 $€_{2020}/MWh_{H2}$. The total amount of electricity traded between model regions and thus the grid losses decrease by 53% with an increase in the hydrogen sales price from 50 $€_{2020}/MWh_{H2}$ to 150 $€_{2020}/MWh_{H2}$. However, the total transmission capacity of the grid decreases only slightly by 1%. This implies that at high hydrogen sales prices, local conversion of local electricity surpluses into hydrogen increases and distribution of these surpluses via the electricity grid decreases. Setting aside the regional distribution of hydrogen demands, it also implies that the installed transmission grid capacity is determined by the peaks of the residual loads and not by the provision of hydrogen to the demand sectors. On the other hand, electricity-based heat generation in heat grids increases with rising hydrogen sales prices. While at a hydrogen sales price of 50 $€_{2020}/MWh_{H2}$ 159 TWh_{el} electricity are used to generate heat in heat grids, at a sales price of 150 $€_{2020}/MWh_{H2}$ the electricity demand for heat generation increases to 286 TWh_{el} (see Figure 5-6). This increase in flexible, electrical heat generation is caused by the higher installed capacity of renewable energies at increasing hydrogen production volumes.

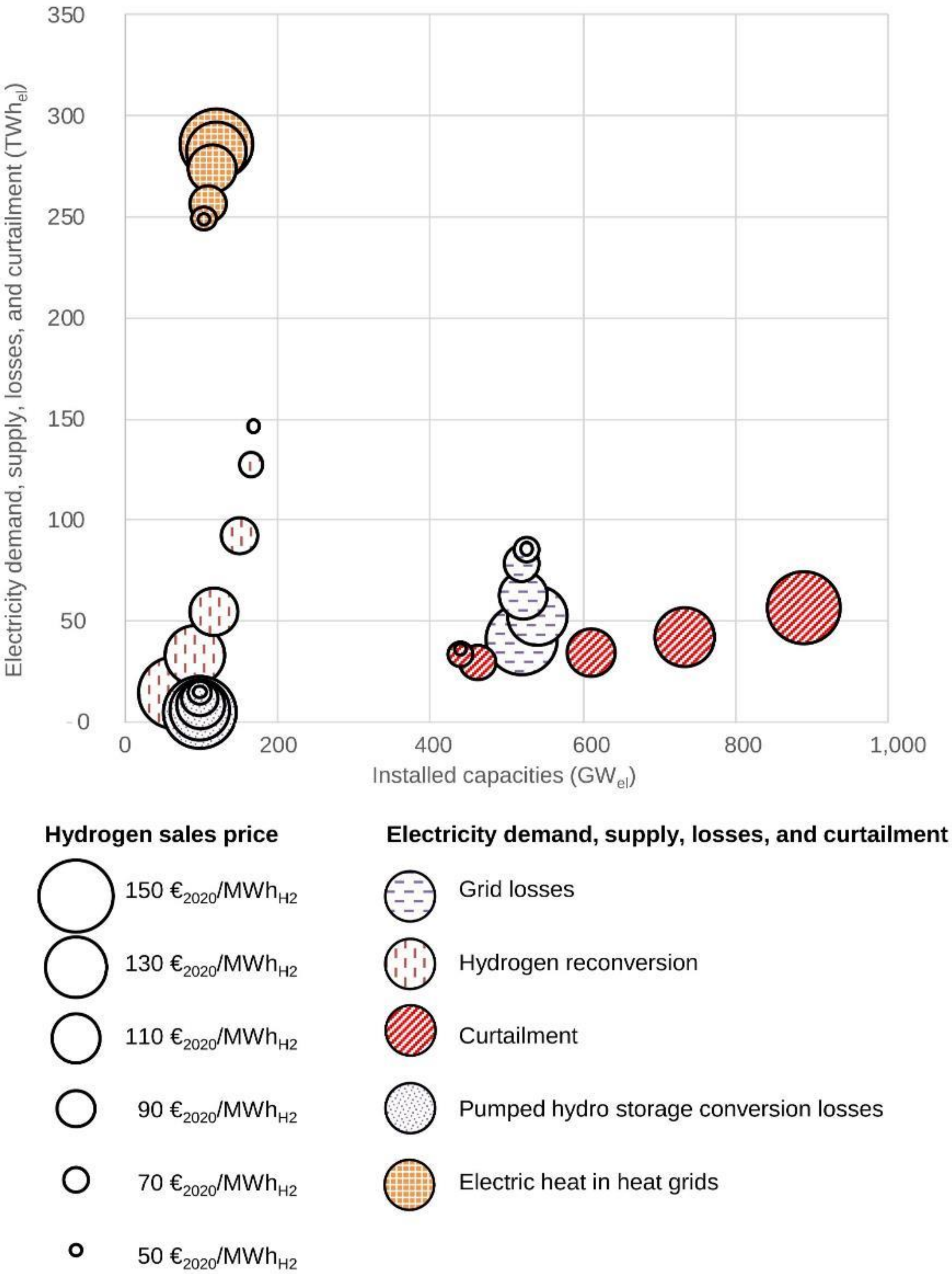

Figure 5-6 Influence of increasing hydrogen production quantities at increasing hydrogen sales prices for the demand sectors on other flexibility options in the conversion sector. Optimization results are displayed shown for the central parameter scenario of PEM electrolysis.

5.3.3 Installed electrolyzer capacities and full load hours

The increased hydrogen generation at higher hydrogen sales prices coincides with increasing electrolyzer capacities. Figure 5-5 shows in the *central parameter scenario* at hydrogen generation costs of 50 $€_{2020}/MWh_{H2}$ an installed electrolyzer capacity of 206 GW_{el} in Europe in 2050. At a hydrogen sales price of 150 $€_{2020}/MWh_{H2}$ the electrolyzer capacity increases to 1,629 GW_{el}. In order to securely meet the hydrogen demands of the demand sectors as postulated in the 1.5 °C scenarios of the EC (EC 2018a, 2018b), the model results indicate that in the *central parameter scenario* between 798 GW_{el} and 1,020 GW_{el} of electrolyzers need to be installed.

The average full load hours (FLH) of the electrolyzers increase with rising hydrogen sales prices. At a hydrogen sales price of 50 $€_{2020}/MWh_{H2}$ the electrolyzers are operated at 1,670 FLH. With a hydrogen sales price of 150 $€_{2020}/MWh_{H2}$ the model uses electrolysis in 2,549 hours of the year: the same FLH result for meeting the sectoral demands of the 1.5 °C scenarios of the EC's long-term strategic vision. This increase in electrolyzer FLH is mainly driven by the additional renewable electricity generation plants that are installed by the model to sell more hydrogen to the demand sectors. These additional power plants are not essential to meet other electricity demands and, increase the full load hours of the electrolyzers. Therefore, the proportion of the electricity used for electrolysis increases for the additional RES capacities built in the scenarios with the higher hydrogen sales prices.

5.3.4 Techno-economic drivers of electrolyzer deployment

The installed electrolyzer capacities and their utilization are strongly dependent on the techno-economic development of the electrolyzer technologies. Figure 5-7 shows the changes in the hydrogen supply potential for the demand sectors if the following parameters are varied: specific investment, lifetime, and efficiency of PEM electrolysis.

In the *conservative parameter scenario*, the hydrogen generation potential for the demand sectors is reduced by 38% to 84% depending on the underlying specific hydrogen generation costs. In the opposite case of the *progressive parameter scenario*, the European hydrogen generation potential for the demand sectors increases between 62% and 168% compared to the central case.

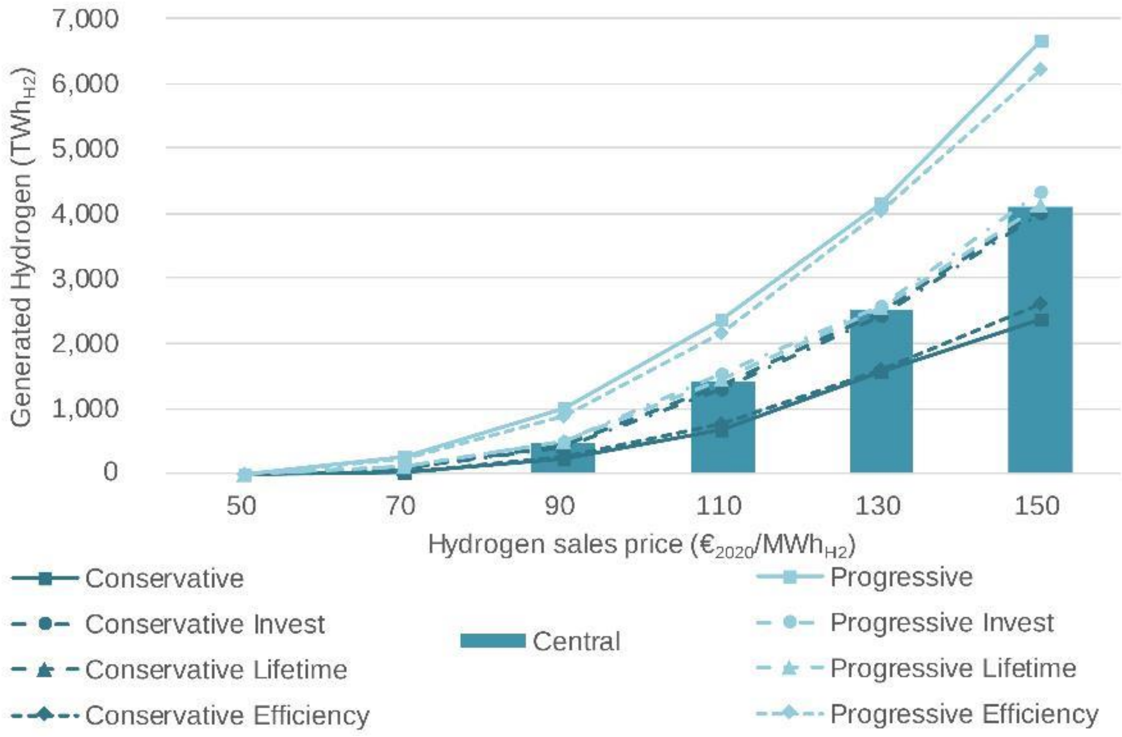

Figure 5-7 Hydrogen supply curves for the demand sectors at different hydrogen sales prices (ex works) and with variations of ±10% in the electric system efficiency, the specific investment, and the lifetime of PEM electrolyzers in Europe in 2050.

The results of the individual parameter variation in Figure 5-7 show that the electric efficiency of electrolyzers is most decisive for its deployment in a European energy system primarily based on renewables. While a variation of the specific investment or the lifetime by ±10% leads to a maximum deviation of 23% in hydrogen generation for the demand sectors compared to the *central parameter scenario*, a variation of the electric efficiency by ±10% causes a deviation in hydrogen production for the demand sectors of between 36% and 131% compared to the *central parameter scenario*.

Alternatively, the model results can be used to estimate the cost reduction of hydrogen production if the electrolyzer parameters are varied. For this purpose, the supply curves in Figure 5-7 are determined by performing linear interpolation between the data points received in the model runs. This allows to determine the distance – i.e. the variation in marginal hydrogen production costs – between the curves for selected hydrogen production quantities. A reduction of the marginal hydrogen production costs would result in a left shift of the supply curve compared to the *central parameter scenario*. Figure 5-8 shows the average variations in marginal hydrogen production costs for different parameter variations of PEM electrolysis. It can be seen that an increase in lifetime or a reduction of the specific investment only slightly reduces the marginal hydrogen production costs. While an increase in lifetime by 10% does not affect specific hydrogen production costs significantly, a reduction of the specific investment by 10% reduces the marginal hydrogen production costs on average by 1%. Conversely, a change in the system efficiency of

PEM electrolyzers has a disproportionally high effect on the marginal hydrogen production costs: An increase in efficiency by 10% reduces the marginal hydrogen production costs on average by 12%. The disproportionately high effect of an increase in efficiency on marginal hydrogen generation costs is mainly based on the fact that an increase in efficiency by 10% reduces the electricity procurement costs of an electrolyzer - i.e. the most important cost component of hydrogen generation - in two ways. Firstly, the higher efficiency reduces the electricity demand of hydrogen production by 9%. Secondly, the average electricity procurement costs of an electrolyzer are reduced. The higher efficiency would allow an electrolyzer to produce the same amount of hydrogen in 9% fewer hours. Thus, the number of hours with high electricity procurement costs can be avoided. Both effects together allow for a disproportionate effect of an efficiency increase on marginal hydrogen production costs.

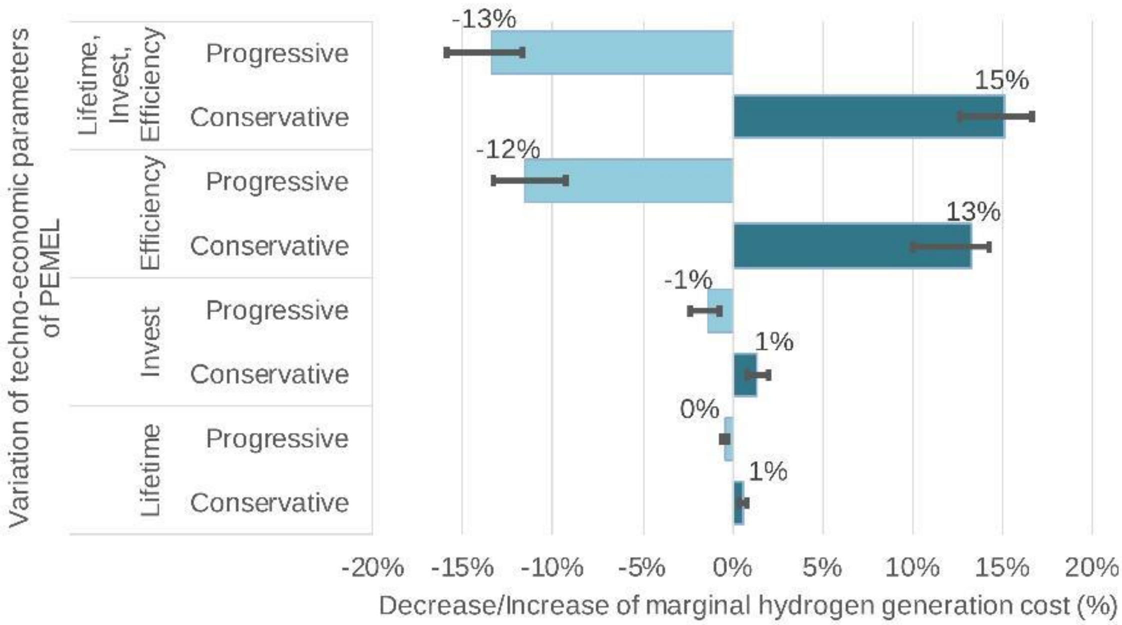

Figure 5-8 Variations of the marginal hydrogen production costs for variations of ±10% in the electric system efficiency, the specific investment, and the lifetime of PEM electrolyzers[7].

[7] The values are determined by calculating the distances between the supply curves of the central parameter scenario and the model results of the parameter variations in Figure 5-7. The distances are calculated for hydrogen production quantities between 500 TWhH2 and 3000 TWhH2 in 500 TWhH2 steps. The bars represent the mean values of the variations determined. The error bars show the minimum and maximum variations.

5.3.5 Impacts of renewable electricity cost on marginal hydrogen generation costs

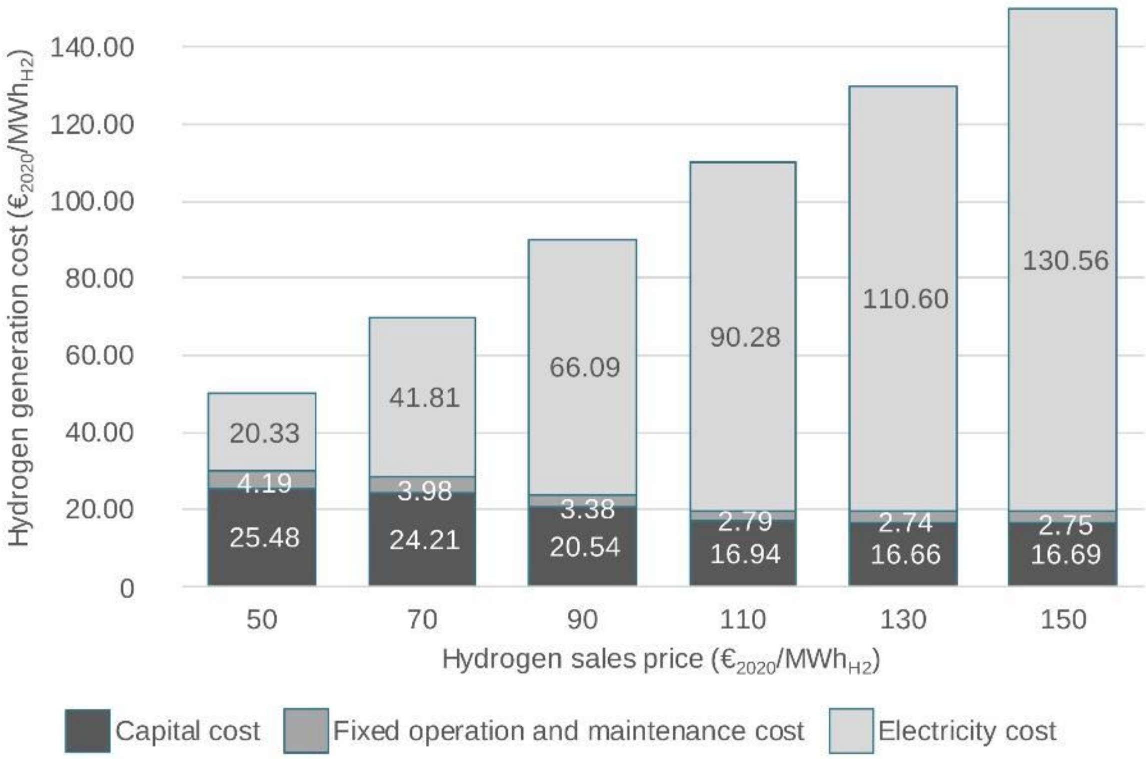

Figure 5-9 Price components of electricity-based hydrogen in the *central parameter scenario* of PEM electrolysis.

The strong dependence of the electrolyzer deployment on the electric efficiency in the model results is based on the dominance of electricity costs in the hydrogen generation costs. Figure 5-9 shows the specific cost components of hydrogen production by electrolysis for increasing hydrogen sales prices in the *central parameter scenario*. The annuitized investments of all electrolyzers – operated to provide both flexibility as electricity storage and supply to the demand sectors – are allocated to the overall amount of hydrogen generated in the model run. The figure shows that the proportion of hydrogen production costs represented by electricity costs increases with increasing hydrogen production from 41% at a hydrogen price of 50 $€_{2020}/MWh_{H2}$ to 87% at a hydrogen price of 150 $€_{2020}/MWh_{H2}$. While low hydrogen production volumes allow the integration of low-cost regional electricity surpluses, increasing production volumes induce the use of electricity with higher procurement costs.

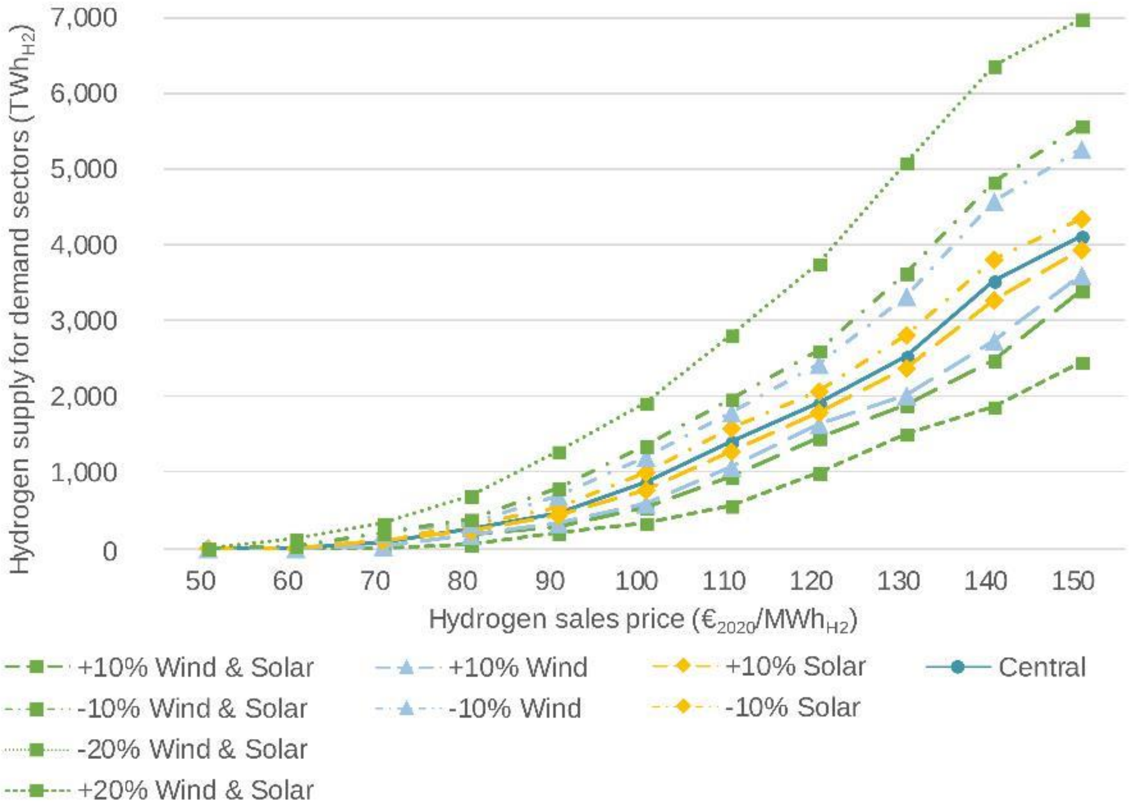

Figure 5-10 Hydrogen supply curves for the demand sectors at different hydrogen sales prices (ex works) and with variations of wind and solar based electricity generation costs by ±10% and ±20% in Europe in 2050.

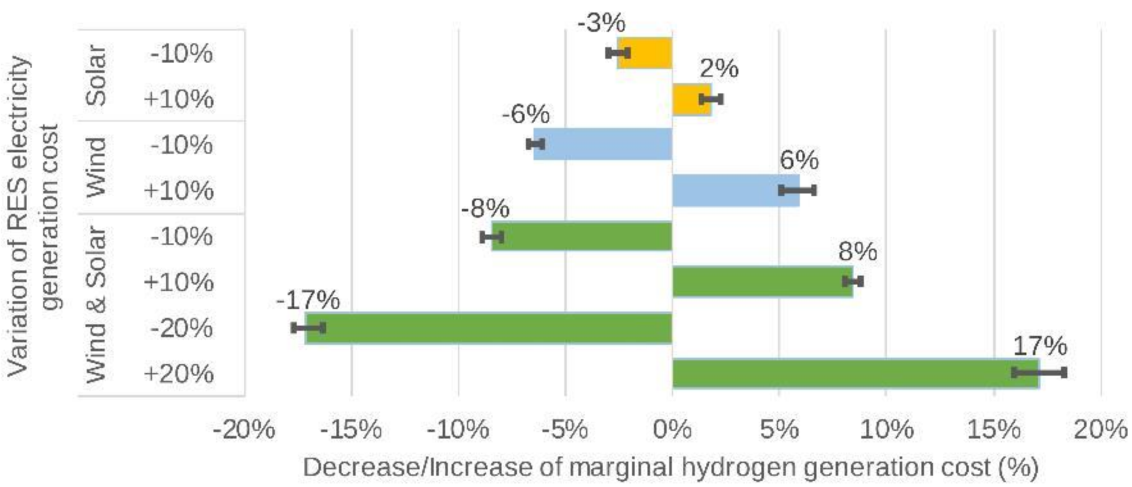

Figure 5-11 Variations of the marginal hydrogen production costs for variations of wind and solar based electricity generation costs. Values are calculated using the hydrogen supply curves in Figure 5-10 and the methodology described in footnote [7].

Electricity costs are the most important component of hydrogen generation costs and the electricity system is dominated by fluctuating renewable electricity generation. Therefore, the calculated hydrogen generation costs are sensitive to deviations from the assumed costs for renewable electricity.

Figure 5-10 shows the deviations in hydrogen generation from the *central parameter scenario* if renewable electricity generation costs are varied. The supply curves between successive data points are determined by linear interpolation. A reduction of the marginal hydrogen production costs would result in a left shift of the supply curve compared to the central parameter scenario. Figure 5-11 shows the average deviations in marginal hydrogen production costs for different changes in RES generation costs, i.e. the distance between the supply curves for selected hydrogen production quantities. The model results in Figure 10 and Figure 11 show that the production costs of weather-dependent renewable energies are – as expected – important determinants of the marginal production costs of electricity-based hydrogen. The marginal hydrogen production costs change slightly under-proportionally in the case of a simultaneous reduction of the electricity generation costs from solar and wind energy. A simultaneous decrease in electricity production costs from both wind and solar energy by 10% leads to a decrease in marginal hydrogen production costs by 8%. An equivalent reduction of these electricity generation costs by 20% leads to a reduction of the marginal hydrogen production costs by 17%. The disproportionately lower reduction of hydrogen production costs compared to the decrease in electricity generation costs has two main reasons. Firstly, hydrogen generation costs have other, fixed cost components (see Figure 5-9). These fixed cost components remain unaffected by a reduction in electricity cost. Secondly, electricity generation costs of RES are the major, but not the only cost component of the electricity system, both in reality and in the model. Additional costs stem for example from expanding and maintaining the electricity grids and electricity storages. Therefore, reducing RES costs by 10% reduces electricity costs of the whole electricity system by less the 10%.

The model results in Figure 10 and Figure 11 also reveal that a change in electricity generation costs from wind energy has a greater influence on marginal hydrogen production costs than changing the costs of solar energy. While a 10% reduction in electricity production costs from wind energy leads to an average reduction in marginal hydrogen production costs of 6%, an equivalent 10% reduction in electricity production costs from solar energy only results in an average reduction in marginal hydrogen production costs of 3%.

5.3.6 Impact of demand variations on marginal hydrogen generation costs

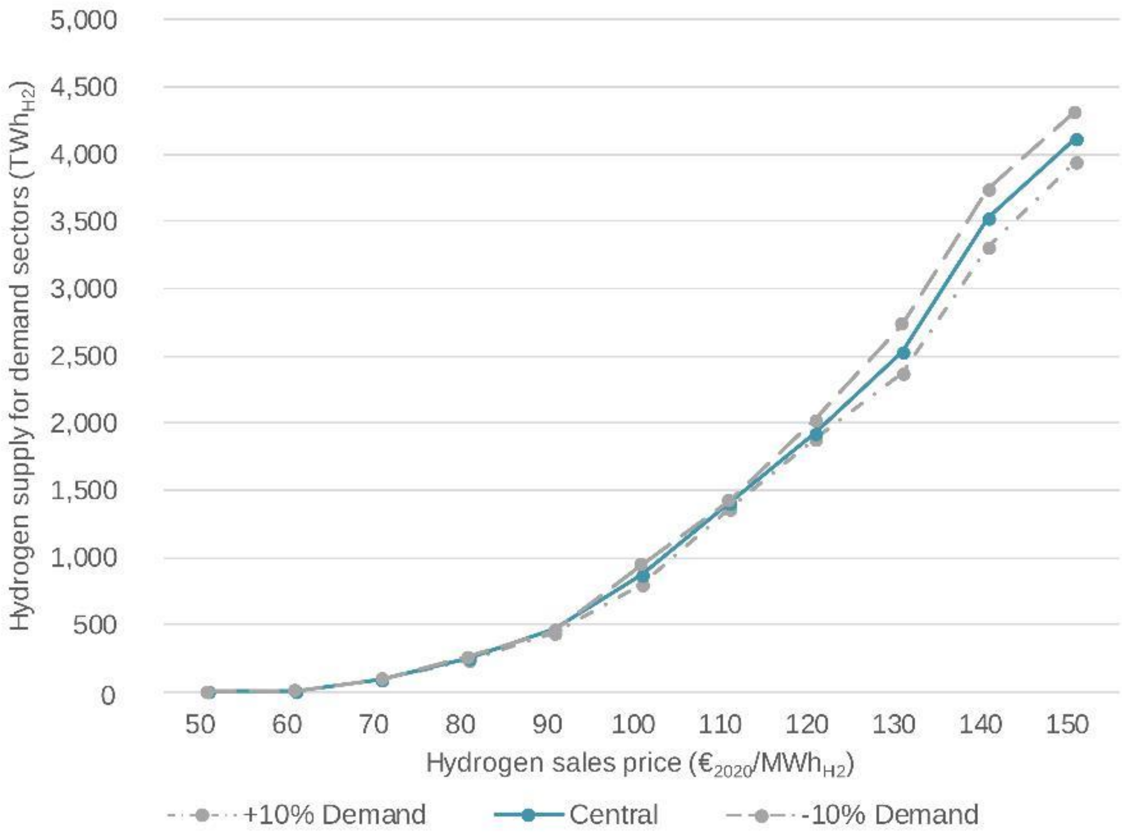

Figure 5-12 Hydrogen supply curves for the demand sectors at different hydrogen sales prices (ex works) and with variations of electricity demands in Europe in 2050.

According to our model results, a change in the total European electricity demand is only expected to have a minor impact on the hydrogen production potential in Europe in 2050. Figure 5-12 shows the deviations in hydrogen quantities generated for the demand sectors with varying electricity demands. Simultaneous variations of 10% of both flexible and inflexible electricity demands (as defined in Table 5-1) are investigated. Applying the same methodology as for the sensitivity analysis of electrolyzer parameters and RES cost – i.e. measuring the side-shift of the supply curve for demand variations – hydrogen generation cost variations are determined. This approach shows that demand variations of ± 10% lead to deviations in hydrogen production costs of up to ± 2%. The deviation of hydrogen generation costs for many points of the supply curve is close to 0%. These results suggest that the generation costs of hydrogen are not substantially depended on other electricity demands and indicate that other parameters have a much higher impact.

5.3.7 Regional distribution of hydrogen generation in Europe in 2050

The hydrogen generation potential to supply the demand sectors varies between regions in Europe. Figure 5-13 shows the regional distribution of these generation potentials in the model results. While in the *central parameter scenario* in Austria and Switzerland no hydrogen is produced for the demand sectors even at a hydrogen sales price of 150 $€_{2020}/MWh_{H2}$, the generation potential at this price in the UK and Ireland is 689 TWh_{H2}.

The regional distribution of the hydrogen generation potential mainly depends on the quality of national RES potentials still available after the prevailing electricity demand is covered. This characteristic allows the regions modeled in *Enertile* to be grouped into two categories. In regions of the first category, the model chooses to meet the prevailing electricity demands by net electricity imports from other regions in addition to exploiting regional RES potentials. These regions have no substantial hydrogen generation potential. In Europe, these countries include Austria, Switzerland, Germany, the Czech Republic, Hungary, Slovakia, Italy, and the countries of the Benelux Union. These are countries with a low or costly renewable electricity generation potential compared to their electricity demand. At a sales price of 130 $€_{2020}/MWh_{H2}$, the hydrogen generation potential for the demand sectors of these countries, at 71 TWh_{H2}, accounts for about 3% of the total generation potential in Europe.

The regions in the second category can be characterized by relatively higher RES generation potentials compared to their electricity demands. At a hydrogen sales price of 50 $€_{2020}/MWh_{H2}$, i.e. when no hydrogen production for the demand sectors occurs, these regions are net electricity exporters to regions with a less beneficial ratio between electricity demands and RES potentials. These exporting regions can be distinguished by the type of RES that is predominantly exploited when hydrogen is produced for the demand sectors at higher sales prices. In the UK, Ireland, Sweden, Poland, Finland, Denmark, France, and the Baltic States the high hydrogen generation potentials are driven by the good wind potentials. In these countries, at a hydrogen sales price of 130 $€_{2020}/MWh_{H2}$, 70% of the additional renewable electricity generated in order to produce hydrogen for the demand sectors originates from wind power. By contrast, in Bulgaria, Slovakia and Romania over 70% of hydrogen generation for the demand sectors at a sales price of 130 $€_{2020}/MWh_{H2}$ is covered by an expansion of electricity generation from solar power. In Norway, Portugal and Spain the origin of additional electricity generation for hydrogen production is, at a sales price of 130 $€_{2020}/MWh_{H2}$, more evenly distributed between wind and solar power.

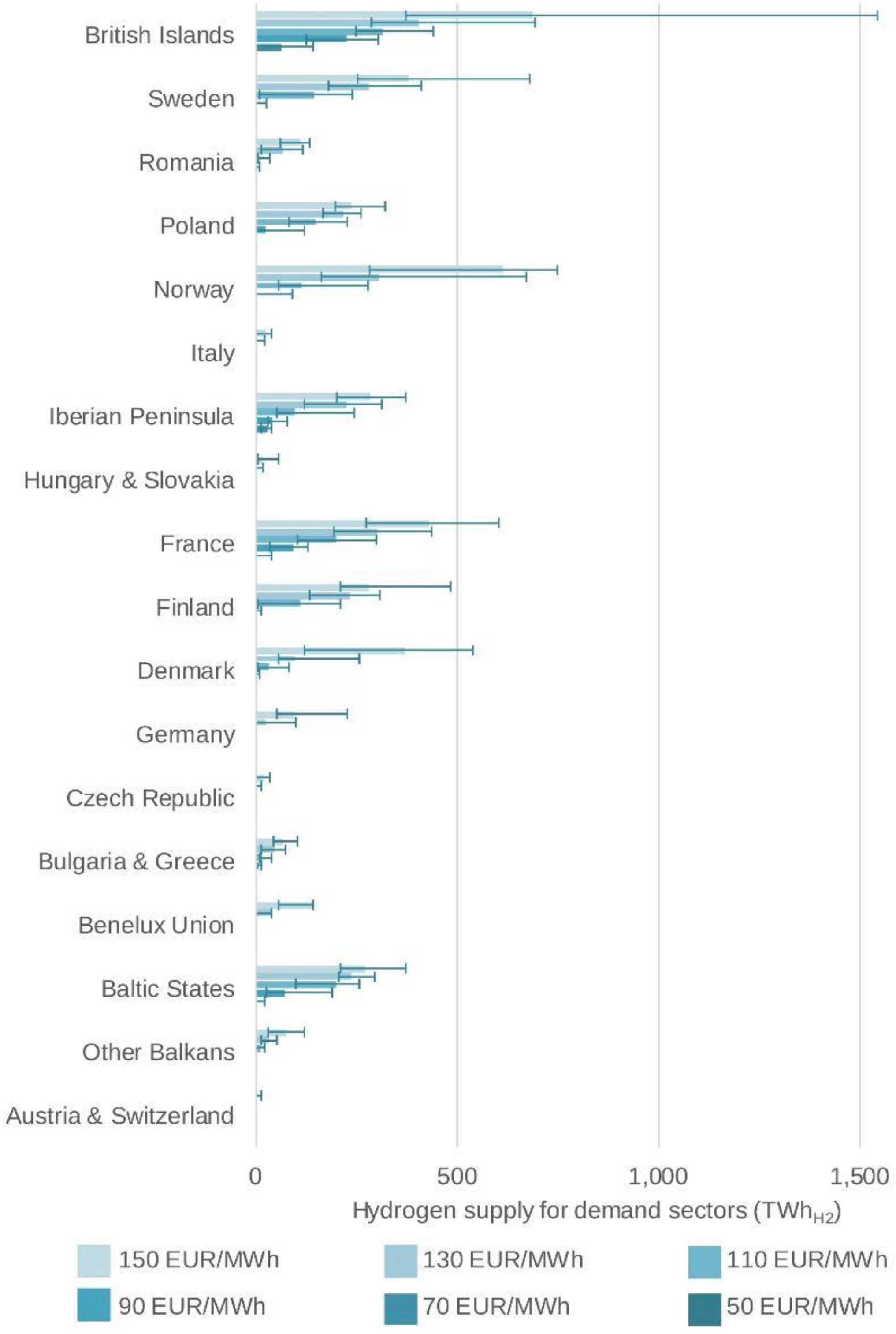

Figure 5-13 Hydrogen generation potential for the demand sectors by region in Europe in 2050. The bars show the optimization results of the *central parameter scenario* of PEM electrolysis, while the error bars show the deviations from that result in the *conservative* and the *progressive parameter scenarios* respectively.

5.4 Summary and Conclusions

This paper examines the production potential for electricity-based hydrogen in a de-fossilized European energy system in 2050. The analysis was carried out using an extended version of the energy system optimization model *Enertile*. The study focuses on possible hydrogen production quantities if certain levels of willingness to pay for hydrogen are assumed. The interactions of the resulting hydrogen production with the rest of the energy system, and the influence of techno-economic electrolyzer characteristics on the hydrogen production potential are analyzed. While the focus of the analysis is on the target state of a de-fossilized European energy system in 2050, the model results allow conclusions on options and needs for action for today's decision makers in politics and economy.

The model results show that hydrogen production of small amounts up to 12 TWh_{H2} starts at marginal production costs of 60 $€_{2020}/MWh_{H2.}$ Hydrogen quantities of at least 1,536 TWh_{H2} as envisaged in the 1.5 °C scenarios by the EC's long-term strategic vision induce marginal hydrogen production costs of over 110 $€_{2020}/MWh_{H2}$. These costs take into account only the costs of hydrogen production and exclude potential costs of transport and distribution infrastructures or the conversion to other energy carriers such as methane. Based on these long-term cost projections, potential uses of e-fuels can be identified and compared to alternative de-fossilization strategies. For example, a steel producer can use this cost estimate to check whether it is feasible to transform the steel production process to direct reduction with hydrogen generated from renewable electricity in Europe.

In order to generate hydrogen amounts of the order of magnitude envisaged in the EC's scenarios in Europe, electrolyzers with a capacity greater than 798 GW_{el} must be installed. Due to the low demand, electrolyzers are currently manufactured on a small scale only. In 2016, the global annual production volume of electrolyzers was estimated to be below 100 MW_{el}/a (Smolinka et al. 2018). If electricity-based hydrogen produced in Europe at the shown costs is to play a substantial role in the future European energy system, both the available electrolyzer sizes and the production capacity of electrolyzers must be significantly increased soon.

The generation of substantial hydrogen quantities has considerable effects on the electricity system. To provide the electricity required for the production of the hydrogen quantities determined in the EC's scenarios, an additional 766 GW_{el} of wind power and 865 GW_{el} of solar power need to be installed. In 2017 the installed capacities in the EU amounted to 169 GW_{el} of wind power and 107 GW_{el} of solar photovoltaic power (Observ'ER et al. 2019); i.e. to cover the additional electricity demand of electrolysis, it would be necessary to increase the installed capacity of wind power by more than four and half times and the installed capacity of solar photovoltaic power by more than eight times. In energy systems dominated by renewable energies the 'fuel' of electrolyzers – electricity – is scarce. Economic evaluations of e-fuel concepts must therefore take into account the competition among electricity consumers for cheap renewable electricity. The expansion of renewable energies should therefore be intensified if e-fuels are to be produced in Europe. Given this order of magnitude of additional renewable energy power plants in the pursuit of strategies with substantial e-fuel quantities, questions of acceptance for these power plants must be addressed.

Due to the long-term storage property of hydrogen and the flexible operation of PEM electrolyzers, a power system dominated by renewable energies can in principle be provided with flexibility through the electrolytic production of hydrogen. The model results show that a high willingness to pay up to 110 $€_{2020}/MWh_{H2}$ for electrolytic hydrogen by the demand sectors can reduce curtailment of renewable energies by 4%, the utilization of electricity transport grids by 27% and the utilization of other storage facilities by 45%. The expansion of grid capacities and installed storage capacities, however, are not reduced in the model results. Therefore, the generation of e-fuels can help to some extent to integrate RES into electricity generation, but it does not undermine the economic benefit of the expansion of electricity transport grids.

The model results show that there are two key techno-economic properties of electrolyzers used in energy systems dominated by renewable energies: Firstly, the technical capability to operate flexibly and secondly, its conversion efficiency of electricity into hydrogen. On the one hand, the results of the system cost minimization show that on average electrolyzers are operated in less than 30 % of the hours of a year across all model regions and that their loads often change quickly. This implies that electrolyzers must be able to react flexibly to the fluctuating conditions in an electricity system dominated by renewables. On the other hand, variations of different techno-economic electrolyzer parameters show that in such an electricity system the conversion efficiency of electrolyzers has the greatest influence on marginal hydrogen production costs. By increasing the efficiency by 10%, the specific hydrogen production costs can be reduced by 12% on average. Equivalent improvements in the specific investment or system lifetime of an electrolyzer have a substantially lower impact on specific hydrogen production costs. For the application of electrolyzers in energy systems dominated by renewable energies, the future technological development of electrolyzers should therefore focus on optimizing flexible operation and increasing conversion efficiencies.

Electricity procurement is the largest cost component for hydrogen produced with electrolysis. In a future decarbonized electricity system, wind and solar energy will dominate electricity supply. However, the cost developments of these technologies in the next 30 years are subject to high uncertainty. Therefore, a sensitivity analysis was performed analyzing the impacts of higher and lower electricity generation costs. Reducing the costs of both wind and solar energy by 10% and 20% leads to a decrease in marginal hydrogen production costs by 8% and 17%, respectively. This shows that a steeper technological learning in renewable electricity generation would also allow substantially reduced hydrogen production costs.

Hydrogen production potential is unevenly distributed across Europe. It correlates with the generation potentials for renewable electricity that are not required to cover the remaining electricity demand. Setting aside a hydrogen transport infrastructure that delivers the produced hydrogen to potential customers, the largest and most cost-efficient hydrogen production potential is in the United Kingdom due to its vast wind energy resources. Given this regionally dispersed hydrogen production potential, a European hydrogen transport infrastructure is potentially necessary and should be further explored.

Considering the obtained hydrogen supply curve, it remains unclear whether substantial amounts of hydrogen will be produced in Europe using electrolysis. Actual European production will also depend on hydrogen procurement costs from alternative sources. Firstly, it is possible to import electricity-based hydrogen from regions with more favorable renewable energy potentials such as the MENA (Middle East and North Africa) region. Secondly, the use of carbon storage systems also makes it possible to use hydrogen obtained from natural gas via steam reformation or similar techniques.

CRediT authorship contribution statement

Benjamin Lux: Conceptualization, Methodology, Software, Investigation, Visualization, Data curation, Writing - original draft.

Benjamin Pfluger: Conceptualization, Methodology, Investigation, Writing - original draft, Supervision.

Declaration of Competing Interest

The authors declare that they have no known competing financial interests or personal relationships that could have appeared to influence the work reported in this paper.

Acknowledgments

This research did not receive any specific grant from funding agencies in the public, commercial, or not-for-profit sectors.

5.5 Appendix

Appendix A.Nomenclature

Table 5-5 Index sets.

Index set	Description
B	Set of building types
H	Set of hours of the year
I	Set of electricity generating technologies, electricity storage technologies, and cross-border transmission grid technologies
J	Set of heat generating technologies and heat storage technologies
K	Set of electrolyzer and hydrogen storage technologies
L	Subset of heat generating technologies and heat storage technologies in heat grids
M	Subset of heat generating technologies and heat storage technologies in buildings
N	Subset of electricity generating technologies for hydrogen reconversion
R	Set of scenario regions
HG	Set of heating grids

Table 5-6 Indices.

Index	Description
b	Building type index
h	Hour of the year index
i	Electricity generation, electricity storage, and cross-border transmission grid technology index
j	Heat generation and heat storage technology index
k	Electrolyzer and hydrogen storage technology index

Index	**Description**
l	Heat generation and storage technology in heat grids index
m	Heat generation and storage technology in buildings index
n	Hydrogen reconversion technology index
r	Region index
eb	Electric boiler (part of heating technologies)
hg	Heat grid index
hpb	Heat pump in building (part of heating technologies)
hpg	Heat pump in heat grid (part of heating technologies)
hyb	Hydrogen boiler (part of heating technologies)

Table 5-7 Parameters.

Parameter	**Description**
p^{hy}	Hydrogen sales price for external demand sectors €$_{2020}$/MWh$_{H2}$
c_i^{fix}	Annuitized specific fixed cost of technology i in €$_{2020}$/MW$_{el}$
c_i^{var}	Specific variable cost of technology i in €$_{2020}$/MWh$_{el}$
c_j^{fix}	Annuitized specific fixed cost of technology j in €$_{2020}$/MW$_{th}$
c_j^{var}	Specific variable cost of technology j in €$_{2020}$/MW$_{th}$
c_k^{fix}	Annuitized specific fixed cost of technology k in €$_{2020}$/MW$_{H2}$
c_k^{var}	Specific variable cost of technology k in €$_{2020}$/MWh$_{H2}$
$D_{r,h}^{el}$	Electricity demand in region r, and hour h in MWh$_{el}$
$D_{r,hg,h}^{ht}$	Heat demand in region r, heat grid hg, and hour h in MWh$_{th}$
$D_{r,b,h}^{ht}$	Heat demand in region r, building b, and hour h in MWh$_{th}$
γ_{hpg}	Conversion efficiency (electricity to heat) of heat pump in heat grids in %

Parameter	Description
γ_{eb}	Conversion efficiency (electricity to heat) of electric boiler in %
γ_{hpb}	Conversion efficiency (electricity to heat) of heat pump in buildings in %
γ_{pem}	Conversion efficiency (electricity to hydrogen) of PEM electrolyzers in %
γ_{n}	Conversion efficiency (hydrogen to electricity) of hydrogen reconversion technology in %
γ_{hyb}	Conversion efficiency (hydrogen to electricity) of hydrogen reconversion technology in %

Table 5-8 Variables.

Variable	Description
$X_{r,i}^{el}$	Capacity of technology i in region r in MW_{el}
$X_{r,j}^{ht}$	Capacity of technology j in region r in MW_{th}
$X_{r,k}^{hy}$	Capacity of technology k in region r in MW_{H2}
$x_{r,i.h}^{el}$	Unit of electricity supplied or demanded by technology i in region r, and hour h in MWh_{el}
$x_{r,n,h}^{el}$	Unit of electricity supplied by hydrogen reconversion technology n in region r, and hour h in MWh_{el}
$x_{r,j,h}^{ht}$	Unit of heat supplied or demanded by technology j in region r, and hour h in MWh_{th}
$x_{r,b,m,h}^{ht}$	Unit of heat supplied by technology m in region r, building b, and hour h in MWh_{th}
$x_{r,hg,eb,h}^{ht}$	Unit of heat supplied by electric boiler eb in region r, heat grid hg, and hour h in MWh_{th}
$x_{r,hg,hpg,h}^{ht}$	Unit of heat supplied by heat pump hpg in region r, heat grid hg, and hour h in MWh_{th}
$x_{r,hg,hyb,h}^{ht}$	Unit of heat supplied by hydrogen boiler hyb in region r, heat grid hg, and hour h in MWh_{th}

$x_{r,k.h}^{hy}$	Unit of hydrogen supplied or demanded by technology k in region r, and hour h in MWh_{H2}
y_r^{hy}	Unit of hydrogen sold to external demand sectors in region r in MWh_{H2}

Appendix B.Abbreviations

Table 5-9 Abbreviations

Abbreviation	Explanation
AEL	Alkaline electrolysis
BEV	Battery electric vehicles
CSP	Concentrating solar power
DS	Demand-supply equation
EC	European Commission
EU	European Union
e-fuels	Electricity-based fuels
FLH	Full load hours
GHG	Greenhouse gas
MENA	Middle East and North Africa
O&M	Operation and maintenance cost
PEM	Polymer electrolyte membrane
PEMEL	Polymer electrolyte membrane electrolysis
PHEV	Plug-in hybrid electric vehicles
PV	Photovoltaics
RES	Renewable energy source
SOEL	Solid oxide electrolysis

Appendix C. Enertile regions

Figure 5-14 Map of regions as modeled in *Enertile*.

Table 5-10 Definition of regions as used in Enertile, Table 5-1, Figure 5-13, and Table 5-D1.

Enertile region code	Countries	Term Table 5-1	Term Figure 5-13/ Table D1
AT	Austria	Austria	Austria
CH	Switzerland	Switzerland	& Switzerland
DE	Germany	Germany	Germany
FR	France	France	France
IBEU	Spain, Portugal	Iberian Peninsula	Iberian Peninsula
BEU	Belgium, Luxembourg	Benelux Union	Benelux Union
HUK	Hungary, Slovakia	Hungary & Slovakia	Hungary & Slovakia
UKI	United Kingdom, Ireland	British Islands	British Islands
PL	Poland	Poland	Poland
BUG	Bulgaria, Greece	Bulgaria & Greece	Bulgaria & Greece
BAK	Slovenia, Croatia, Bosnia and Herzegovina, Serbia, Kosovo, Montenegro, Albania, North Macedonia	Other Balkans	Other Balkans
BAT	Estonia, Lithuania, Latvia	Baltic States	Baltic States
CZ	Czech Republic	Czech Republic	Czech Republic
DK	Denmark	Denmark	Denmark
IT	Italy	Italy	Italy
NO	Norway	Norway	Norway
RO	Romania	Romania	Romania
SE	Sweden	Sweden	Sweden
NL	Netherlands	Benelux Union	Benelux Union

Appendix D. Regional results

Table 5-11 Hydrogen generation potential for the demand sectors by region in all modelled regions in 2050 as shown in Figure 5-13.

	Conservative parameter scenario						Central parameter scenario						Progressive parameter scenario					
	50 €$_{2020}$/MWh	70 €$_{2020}$/MWh	90 €$_{2020}$/MWh	110 €$_{2020}$/MWh	130 €$_{2020}$/MWh	150 €$_{2020}$/MWh	50 €$_{2020}$/MWh	70 €$_{2020}$/MWh	90 €$_{2020}$/MWh	110 €$_{2020}$/MWh	130 €$_{2020}$/MWh	150 €$_{2020}$/MWh	50 €$_{2020}$/MWh	70 €$_{2020}$/MWh	90 €$_{2020}$/MWh	110 €$_{2020}$/MWh	130 €$_{2020}$/MWh	150 €$_{2020}$/MWh
Austria & Switzerland	0	0	0	0	0	0	0	0	0	0	0	0	0	0	0	0	0	12
Other Balkans	0	0	0	11	34	75	0	0	0	0	13	31	0	0	2	21	55	123
Baltic States	0	1	74	199	236	271	0	0	27	98	206	212	0	24	191	260	296	373
Benelux Union	0	0	0	0	39	143	0	0	0	0	0	57	0	0	0	0	39	143
Bulgaria & Greece	0	0	9	14	47	68	0	0	1	11	14	43	0	1	13	42	74	105
Czech Republic	0	0	0	0	0	19	0	0	0	0	0	0	0	0	0	0	16	38
Germany	0	0	0	0	27	98	0	0	0	0	0	54	0	0	0	0	101	226
Denmark	0	0	0	35	97	370	0	0	0	6	55	123	0	0	8	84	259	538
Finland	0	0	2	111	234	280	0	0	0	8	135	209	0	0	13	210	310	484
France	0	0	93	202	303	429	0	0	35	103	196	274	0	40	130	302	437	602
Hungary & Slovakia	0	0	0	0	5	19	0	0	0	0	0	8	0	0	0	0	20	56
Iberian Peninsula	0	27	41	97	224	286	0	15	32	54	122	202	0	39	80	244	314	373
Italy	0	0	0	0	0	26	0	0	0	0	0	0	0	0	0	0	21	39
Norway	0	0	0	116	305	613	0	0	0	57	164	283	0	0	91	280	670	748

	Conservative parameter scenario						Central parameter scenario						Progressive parameter scenario					
	50 €$_{2020}$/MWh	70 €$_{2020}$/MWh	90 €$_{2020}$/MWh	110 €$_{2020}$/MWh	130 €$_{2020}$/MWh	150 €$_{2020}$/MWh	50 €$_{2020}$/MWh	70 €$_{2020}$/MWh	90 €$_{2020}$/MWh	110 €$_{2020}$/MWh	130 €$_{2020}$/MWh	150 €$_{2020}$/MWh	50 €$_{2020}$/MWh	70 €$_{2020}$/MWh	90 €$_{2020}$/MWh	110 €$_{2020}$/MWh	130 €$_{2020}$/MWh	150 €$_{2020}$/MWh
Poland	0	0	25	150	218	238	0	0	0	82	169	200	0	0	123	226	262	322
Romania	0	0	0	13	66	109	0	0	0	6	12	60	0	0	8	34	115	133
Sweden	0	0	0	145	281	380	0	0	0	9	180	254	0	0	26	240	409	682
British Islands	0	63	225	313	406	688	0	0	125	247	289	373	0	141	306	442	692	1,541

References

Bernath, C.; Deac, G.; Sensfuss, F. (2019): Influence of heat pumps on renewable electricity integration: Germany in a European context. In: Energy Strategy Reviews, 26, p. 100389. https://doi.org/10.1016/j.esr.2019.100389.

Boait, P. J.; Greenough, R. (2019): Can fuel cell micro-CHP justify the hydrogen gas grid?: Operating experience from a UK domestic retrofit. In: Energy and Buildings, 194, pp. 75–84. https://doi.org/10.1016/j.enbuild.2019.04.021.

Brinner, A.; Schmidt, M.; Schwarz, S.; Wagener, L.; Zuberbühler, U. (2018): Technologiebericht 4.1 Power-to-gas (Wasserstoff). Gefördert durch: Bundesministerium für Wirtschaft und Energie. Wuppertal.

Brouwer, A. S.; van den Broek, M.; Zappa, W.; Turkenburg, W. C.; Faaij, A. (2016): Least-cost options for integrating intermittent renewables in low-carbon power systems. In: Applied Energy, 161, pp. 48–74. https://doi.org/10.1016/j.apenergy.2015.09.090.

Buttler, A.; Spliethoff, H. (2018): Current status of water electrolysis for energy storage, grid balancing and sector coupling via power-to-gas and power-to-liquids: A review. In: Renewable and Sustainable Energy Reviews, 82, pp. 2440–2454. https://doi.org/10.1016/j.rser.2017.09.003.

Chen, C.; Lu, Y.; Banares-Alcantara, R. (2019): Direct and indirect electrification of chemical industry using methanol production as a case study. In: Applied Energy, 243, pp. 71–90. https://doi.org/10.1016/j.apenergy.2019.03.184.

Council of the European Union (2009): Presidency Conclusions 29-30 October 2009. Brussels. Available at https://ec.europa.eu/regional_policy/sources/cooperate/baltic/pdf/council_concl_30102009.pdf, accessed 12.09.2019.

Creutzig, F.; Agoston, P.; Goldschmidt, J. C.; Luderer, G.; Nemet, G. F.; Pietzcker, R. C. (2017): The underestimated potential of solar energy to mitigate climate change. In: Nature Energy, 2 (9), p. 369. https://doi.org/10.1038/nenergy.2017.140.

Crotogino, F. (2016): Larger Scale Hydrogen Storage. In: Storing Energy, pp. 411–429. https://doi.org/10.1016/B978-0-12-803440-8.00020-8.

Deac, G. (2019): Auswirkung der Kopplung von Strom- und Wärmemarkt auf die künftige Integration der erneurbaren Energien und die CO2-Emissionen in Deutschland.

European Commission (Ed.) (2018a): COMMUNICATION FROM THE COMMISSION TO THE EUROPEAN PARLIAMENT, THE EUROPEAN COUNCIL, THE COUNCIL, THE EUROPEAN ECONOMIC AND SOCIAL COMMITTEE, THE COMMITTEE OF THE REGIONS AND THE EUROPEAN INVESTMENT BANK COM(2018) 773. A Clean Planet for all A European strategic long-term vision for a prosperous, modern, competitive and climate neutral economy. Available at https://eur-lex.europa.eu/legal-content/EN/TXT/?uri=CELEX:52018DC0773, accessed 28.12.2019.

European Commission (2018b): In-depth analysis in support of the commission communication COM(2018) 773. A clean Planet for all - A European long-term strategic vision for a prosperous, modern, competitive and cimate neutral economy. Supplementary information.

European Parliament; Council of the European Union (Eds.) (2018a): DIRECTIVE (EU) 2018/ 2001 OF THE EUROPEAN PARLIAMENT AND OF THE COUNCIL - of 11 December 2018 - on the promotion of the use of energy from renewable sources. Available at https://eur-lex.europa.eu/legal-content/EN/TXT/PDF/?uri=CELEX:32018L2001&from=EN.

European Parliament; Council of the European Union (Eds.) (2018b): DIRECTIVE (EU) 2018/ 2002 OF THE EUROPEAN PARLIAMENT AND OF THE COUNCIL - of 11 December 2018 - amending Directive 2012/ 27/

EU on energy efficiency. Available at https://eur-lex.europa.eu/legal-content/EN/TXT/PDF/?uri=CELEX:32018L2002&from=EN.

Fraunhofer Institut für System- und Innovationsforschung (2019): Enertile. Available at https://www.enertile.eu/enertile-en/index.php, accessed 07.11.2019.

Gahleitner, G. (2013): Hydrogen from renewable electricity: An international review of power-to-gas pilot plants for stationary applications. In: International Journal of Hydrogen Energy, 38 (5), pp. 2039–2061. https://doi.org/10.1016/j.ijhydene.2012.12.010.

Glenk, G.; Reichelstein, S. (2019): Economics of converting renewable power to hydrogen. In: Nature Energy, 4 (3), pp. 216–222. https://doi.org/10.1038/s41560-019-0326-1.

Gorre, J.; Ortloff, F.; van Leeuwen, C. (2019): Production costs for synthetic methane in 2030 and 2050 of an optimized Power-to-Gas plant with intermediate hydrogen storage. In: Applied Energy, 253, p. 113594. https://doi.org/10.1016/j.apenergy.2019.113594.

Götz, M.; Lefebvre, J.; Mörs, F.; McDaniel Koch, A.; Graf, F.; Bajohr, S.; Reimert, R.; Kolb, T. (2016): Renewable Power-to-Gas: A technological and economic review. In: Renewable Energy, 85, pp. 1371–1390. https://doi.org/10.1016/j.renene.2015.07.066.

Graves, C.; Ebbesen, S. D.; Mogensen, M.; Lackner, K. S. (2011): Sustainable hydrocarbon fuels by recycling CO2 and H2O with renewable or nuclear energy. In: Renewable and Sustainable Energy Reviews.

Huber, M.; Dimkova, D.; Hamacher, T. (2014): Integration of wind and solar power in Europe: Assessment of flexibility requirements. In: Energy, 69, pp. 236–246. https://doi.org/10.1016/j.energy.2014.02.109.

IEA International Energy Agency (2018): World Energy Outlook 2018. Paris. https://doi.org/10.1787/weo-2018-en.

Kondziella, H.; Bruckner, T. (2016): Flexibility requirements of renewable energy based electricity systems – a review of research results and methodologies. In: Renewable and Sustainable Energy Reviews, 53, pp. 10–22. https://doi.org/10.1016/j.rser.2015.07.199.

Kreuter, W.; Hofmann, H. (1998): Electrolysis: The important energy transformer in a world of sustainable energy. In: International Journal of Hydrogen Energy, 23 (8), pp. 661–666.

McDonagh, S.; O'Shea, R.; Wall, D. M.; Deane, J. P.; Murphy, J. D. (2018): Modelling of a power-to-gas system to predict the levelised cost of energy of an advanced renewable gaseous transport fuel. In: Applied Energy, 215, pp. 444–456. https://doi.org/10.1016/j.apenergy.2018.02.019.

Navas-Anguita, Z.; García-Gusano, D.; Dufour, J.; Iribarren, D. (2019): Prospective techno-economic and environmental assessment of a national hydrogen production mix for road transport. In: Applied Energy, p. 114121. https://doi.org/10.1016/j.apenergy.2019.114121.

Observ'ER; ECN part of TNO; RENAC; Frankfurt School of Finance and Management; Fraunhofer Institut für System- und Innovationsforschung; Statistics Netherlands (Eds.) (2019): THE STATE OF RENEWABLE ENERGIES IN EUROPE. Edition 2018 18th EurObserv'ER Report. EurObserv’ER consortium.

Palm, E.; Nilsson, L. J.; Åhman, M. (2016): Electricity-based plastics and their potential demand for electricity and carbon dioxide. In: Journal of Cleaner Production, 129, pp. 548–555. https://doi.org/10.1016/j.jclepro.2016.03.158.

Pfluger, B. (2014): Assessment of least-cost pathways for decarbonising Europe's power supply. A model-based long-term scenario analysis accounting for the characteristics of renewable energies. Karlsruhe.

Pfluger, B.; Tersteegen, B.; Franke, B.; Bernath, C.; Bossmann, T.; Deac, G.; Elsland, R.; Fleiter, T.; Kühn, A.; Ragwitz, M.; Rehfeldt, M.; Steinbach, J.; Cronenberg, A.; Ladermann, A.; Linke, C.; Maurer, C.; Willemsen, S.; Kauertz, B.; Pehnt, M.; Rettenmaier, N.; Hartner, M.; Kranzl, L.; Schade, W.; Catenazzi, G.; Jakob, M.; Reiter, U. (2017): Langfristszenarien für die Transformation des Energiesystems in Deutschland. Modul 2:

Modelle und Modellverbund. Fraunhofer Institut für System- und Innovationsforschung; ifeu - Institut für Energie- und Umweltforschung Heidelberg GmbH; TU Wien; TEP Energy; M-Five GmbH (M-Five); Consentec GmbH (Consentec).

REflex (2019): REflex – Analysis of the European Energy System. Available at http://reflex-project.eu/, accessed 07.11.2019.

Reuß, M.; Grube, T.; Robinius, M.; Preuster, P.; Wasserscheid, P.; Stolten, D. (2017): Seasonal storage and alternative carriers: A flexible hydrogen supply chain model. In: Applied Energy, 200, pp. 290–302. https://doi.org/10.1016/j.apenergy.2017.05.050.

Runge, P.; Sölch, C.; Albert, J.; Wasserscheid, P.; Zöttl, G.; Grimm, V. (2019): Economic comparison of different electric fuels for energy scenarios in 2035. In: Applied Energy, 233-234, pp. 1078–1093. https://doi.org/10.1016/j.apenergy.2018.10.023.

Schiebahn, S.; Grube, T.; Robinius, M.; Tietze, V.; Kumar, B.; Stolten, D. (2015): Power to gas: Technological overview, systems analysis and economic assessment for a case study in Germany. In: International Journal of Hydrogen Energy, 40 (12), pp. 4285–4294. https://doi.org/10.1016/j.ijhydene.2015.01.123.

Smolinka, T.; Günther, M.; Garche, J. (2011): Stand und Entwicklungspotenziale der Wasserelektrolyse zur Herstellung von Wasserstoff aus regenerativen Energien. NOW-Studie.

Smolinka, T.; Wiebe, N.; Sterchele, P.; Lehner, F.; Jansen, M.; Kiemel, S.; Miehe, R.; Wahren, S.; Zimmermann, F. (2018): Studie IndWEDe Industrialisierung der Wasser-elektrolyse in -Deutschland: -Chancen und -Herausforderungen für nachhaltigen Wasserstoff für Verkehr, Strom und -Wärme. Berlin.

U.S. Energy Information Administration (2016): International Energy Statistics. Available at https://www.eia.gov/beta/international/rankings/#?prodact=2-2&cy=2016&pid=2&aid=2&tl_id=2-A&tl_type=a&v=B&ug=8, accessed 07.11.2019.

United Nations (Ed.) (2015): Paris Agreement. Available at https://unfccc.int/sites/default/files/english_paris_agreement.pdf.

United Nations (2017): World Population Prospects: The 2017 Revision. Key Findings and Advance Tables. New York: United Nations. Available at https://population.un.org/wpp/Publications/Files/WPP2017_KeyFindings.pdf.

Zeman, F. S.; Keith, D. W. (2008): Carbon neutral hydrocarbons. In: Philosophical transactions. Series A, Mathematical, physical, and engineering sciences, 366 (1882), pp. 3901–3918. https://doi.org/10.1098/rsta.2008.0143.

[end of Paper 1]

6 Supply curves of electricity-based gaseous fuels in the MENA region

[Start of Paper 2]

Supply curves of electricity-based gaseous fuels in the MENA region

Benjamin Lux[1*], Johanna Gegenheimer[2], Katja Franke[1], Frank Sensfuß[1], and Benjamin Pfluger[3]

1 Fraunhofer Institute for Systems and Innovation Research ISI, Breslauer Straße 48, 76139 Karlsruhe, Germany

2 DVGW Research Center at Engler-Bunte-Institut of Karlsruhe Institute of Technology (KIT), Engler-Bunte-Ring 1-9, Building 40.51, 76131 Karlsruhe, Germany

3 Fraunhofer Research Institution for Energy Infrastructures and Geothermal Systems IEG, Breslauer Straße 48, 76139 Karlsruhe, Germany

*corresponding author: Benjamin Lux, benjamin.lux@isi.fraunhofer.de, phone: +49-721-6809-474

Paper published in:

Computers & Industrial Engineering 162, Article No. 107647, DOI: 10.1016/j.cie.2021.107647

Abstract

The utilization of electricity-based fuels (e-fuels) is a potential strategy component for achieving greenhouse gas neutrality in the European Union (EU). As renewable electricity production sites in the EU itself might be scarce and relatively expensive, importing e-fuels from the Middle East and North Africa (MENA) could be a complementary and cost-efficient option. Using the energy system model Enertile, supply curves for hydrogen and synthetic methane in the MENA region are determined for the years 2030 and 2050 to evaluate this import option techno-economically. The model optimizes investments in renewable electricity production, e-fuel production chains, and local electricity transport infrastructures. Analyses of renewable electricity generation potentials show that the MENA region in particular has large low-cost solar power potentials. Optimization results in Enertile show for a weighted average cost of capital of 7% that substantial hydrogen production starts above 100 €/MWhH2 in 2030 and above 70 €/MWhH2 in 2050. Substantial synthetic methane production in the model results starts above 170 €/MWhCH4 in 2030 and above 120 €/MWhCH4 in 2050. The most important cost component in both fuel production routes is electricity. Taking into account transport cost surcharges, in Europe synthetic methane from MENA is available above 180 €/MWhCH4 in 2030 and above 130 €/MWhCH4 in 2050. Hydrogen exports *from MENA to Europe cost above 120 €/MWhH2 in 2030 and above 90 €/MWhH2 in 2050. If exported to Europe, both e-fuels are more expensive to produce and transport in liquefied form than in gaseous form. A comparison of European hydrogen supply curves with hydrogen imports from MENA for 2050 reveals that imports can only be economically efficient if the two following conditions are met: Firstly, similar interest rates prevail in the EU and MENA; secondly, hydrogen transport costs converge at the cheap end of the range in the current literature. Apart from this, a shortage of land for renewable electricity generation in Europe may lead to hydrogen imports from MENA. This analysis is intended to assist in guiding European industrial and energy policy, planning import infrastructure needs, and providing an analytical framework for project developers in the MENA region.*

Key words: E-Fuels; Power-to-Gas; MENA region; Energy system modeling; Cost of hydrogen; Cost of synthetic methane;

Highlights:

- Design of integrated e-fuel production chains for the MENA region
- Electricity-based hydrogen and methane supply curves for MENA in 2030 and 2050
- Integrated optimization of electricity generation and e-fuel production
- Comparison of hydrogen production costs in MENA and Europe

6.1 Introduction

To counter the threats of global warming, the international community of states agreed in the 2015 Paris Agreement to balance greenhouse gas (GHG) emissions and sinks in the second half of the 21st century (UN 2015). Subsequently, the European Commission (EC) sharpened their climate protection target in the European Green Deal and is now aiming for GHG neutrality by 2050 (Council of the European Union 2009; EC 2019). While all scenarios in the EC's underlying in-depth analysis (EC 2018a, 2018b) make strong use of energy efficiency measures and renewable energy sources (RES), the scenarios with net-zero GHG emissions in 2050 also strongly rely on electricity-based hydrogen (H_2) and other synthetic fuels. In its "Hydrogen Strategy" the EC makes hydrogen a key priority to achieve Europe's clean energy transition (EC 2020). Overall, these electricity-based fuels (e-fuels[8]) are climate-neutral substitutes for fossil fuels, assuming that only renewable electricity and balance-neutral carbon sources are used in the synthesis process (Graves et al. 2011; Zeman et al. 2008). Substituting fossil fuels with e-fuels offers the advantage of reducing carbon dioxide (CO_2) emissions across sectors while continuing to use well-established application technologies. For gaseous and liquid hydrocarbons, most existing infrastructures can be retained.

The deployment of e-fuels is heavily dependent on costs and available quantities. These two properties in turn depend on the availability of suitable RES. If e-fuels are to play a substantial role, large additional amounts of renewable electricity are required. In Europe itself, the availability of land for renewable electricity generation to produce e-fuels may be limited due to high electricity demands and low acceptance of renewable generation facilities. Therefore, importing e-fuels might be an alternative, complementary, or even necessary option. In addition, the production of e-fuels in regions close to the equator could be more cost-efficient due to favorable solar conditions. However, other cost factors such as transportation to Europe or the availability of climate-neutral CO_2 for fuel synthesis must be taken into account. For Europe, the MENA (Middle East and North Africa) region is of particular interest as a potential exporter of e-fuels.

Few peer-reviewed studies have examined in detail the generation potential of e-fuels in the MENA region, their generation costs, and their potential export to Europe:

Timmerberg et al. (2019a) investigate the cost and potentials of electricity-based hydrogen in North Africa and its transport to Europe as a blend with natural gas in existing pipelines. Hydrogen production is therefore investigated only in the vicinity of existing natural gas pipelines in North Africa. Using linear optimization, hydrogen supply costs from MENA to Central Europe in 2020 amount to between 54 €/MWh_{H2} and 119 €/MWh_{H2} depending on the underlying parameter scenario. Timmerberg et al. (2019a) find that the existing pipeline capacity is the limiting factor and not the potentials of renewable energies required for hydrogen supply from North Africa to Central Europe.

[8] "E-fuels" is the umbrella term for all gaseous energy carriers produced from electricity considered in this article.

Hank et al. (2020a) develop five Power-to-X (PtX) pathways (methane, methanol, ammonia, liquefied hydrogen, and hydrogen bound in liquid organic hydrogen carriers). In a case study, they evaluate these PtX pathways for an exemplary medium- to large-scale production site in Morocco for the year 2030. The analysis is based solely on local renewable electricity generation. Downstream long-distance transport to Northwestern Europe is part of the cost assessment. Gaseous hydrogen in Morocco has an ex works production cost of 90 €/$MWh_{H2,LHV}$[9]. Additional liquefaction, intermediate storage, and shipping from Morocco to Germany increases the hydrogen supply cost to 126 €/$MWh_{H2,LHV}$. Gaseous synthetic methane (CH_4) is available in Morocco at a production cost of 124 €/$MWh_{CH4,LHV}$. Liquefied transport to Germany increases the methane supply cost to 145 €/$MWh_{CH4,LHV}$.

Ueckerdt et al. (2021) estimate the supply cost of synthetic methane produced in a renewable-rich country and subsequently shipped for about 4,000 km. The basis of their analysis is an average electricity price of 50 €/MWh_{el} in 2030 and 30 €/MWh_{el} in 2050, which reflects the average costs of electricity supply of a wind- and solar PV-based power system in Australia. They determine cost-optimal electrolysis utilization using the electricity price variability of wholesale market data for Australia as of 2019. They assume that their analysis could fit the supply of e-fuels produced in Northwest Africa (e.g. Morocco) and transported to Northwest Europe (e.g. Germany). For 2030 they estimate a synthetic methane supply cost of 114 €/$MWh_{CH4,}$LHV[10] in Europe. For 2050 their estimate is 65 €/$MWh_{CH4,LHV}$[10].

In addition to peer-reviewed literature, there is also grey literature and online tools that address e-fuels generation in the MENA region. The IEA (2019) identifies North Africa and the Middle East as promising areas for electricity-based hydrogen production. It estimates the cost of electrolytic hydrogen in the long-term as 43 €/$MWh_{H2,LHV}$ in the Middle East10[11] and 41 €/$MW_{H2,LHV}$ in North Africa[1011]. Agora Verkehrswende et al. (2018) estimate the final product cost of synthetic methane in North Africa and the Middle East as 140 €/MWh_{CH4} in 2030 and to 110 €/MWh_{CH4} in 2050. They base their cost estimates on PV and hybrid PV-wind power systems. Fraunhofer IEE (2021) has developed a PtX potential atlas in a web application. The atlas shows the generation potential for hydrogen and various synthetic hydrocarbons in 2050 for selected locations worldwide. It also provides information on transport costs from the PtX production site to Europe. As an example, production and liquefaction of hydrogen at a production site in Morocco and subsequent transport to Germany costs on average 102 €/MWh_{H2} in 2050. The export of liquefied synthetic methane costs 127 €/MWh_{CH4} for the same country combination.

[9] The energy content of hydrogen is given in terms of the lower heating value (LHV) of hydrogen, which describes the amount of thermal energy released during the combustion of hydrogen without water condensation.

[10] Values read from a figure.

[11] Values in (IEA 2019) are given in USD/kgH2. Conversion with energy content of hydrogen related to the lower heating value 33.33 kWhH2/kgH2 and the average USD-EURO exchange rate in 2019 of 1 Euro = 1.12 USD.

There is currently no literature that looks in detail at e-fuel generation in the MENA region beyond individual site assessments. Based on these preliminary considerations the central research questions in this paper are:

- What is the techno-economic generation potential of the e-fuels hydrogen and synthetic methane in the MENA region?
- What is the optimal power generation mix for e-fuel production in MENA?
- Which countries offer the most favorable conditions for the production of hydrogen and synthetic methane?
- Which technical components of e-fuel production are decisive for the generation costs?
- How does e-fuel generation in MENA perform compared to Europe, and are exports to Europe feasible?

Addressing these questions will make it possible to derive strategies for future European e-fuel imports, for example by allowing domestic production options in Europe to be weighed against imports. Since the lead time for infrastructures such as gas pipelines is typically several years, an assessment of whether there is a need for transportation infrastructure from the MENA region to Europe is valuable. Additionally, the derived costs are valuable for determining use cases of e-fuels in various sectors and for comparing strategies based on e-fuel against other decarbonization options.

The analysis of the generation potentials of electricity-based hydrogen and synthetic methane in the MENA region is conducted for the years 2030 and 2050 using an energy system optimization model. The approach requires that e-fuel production is based solely on renewable electricity.

The paper is structured as follows: Section 6.2 introduces the modelling approach, scenario design, and most important input parameters including e-fuel production chains. Section 6.3 presents the model results. Section 6.4 summarizes the findings and derives key conclusions.

6.2 Methodology and data

6.2.1 Methodology

E-fuel supply curves in the MENA region are calculated and analyzed using the energy system model *Enertile* (Fraunhofer ISI 2019). *Enertile* is a software package aimed at optimizing the future cost of energy supply in Europe and the MENA region. It combines the interlinked supply of electricity, heat, and electricity-based fuels with highly resolved potentials of solar and wind energy.

6.2.1.1 Energy system model Enertile

Enertile is an optimization model with a high technical, spatial, and temporal resolution. It determines the cost-minimal portfolio of technologies to meet exogenously specified electricity, heat, and e-fuel demands simultaneously. However, calculations in the MENA region use only the electricity and e-fuel supply modules. Figure 6-1 shows a simplified illustration of the model components used in this paper. The optimization includes both capacity expansion and unit dispatch of relevant generation and infrastructure technologies. The portfolio of technologies covers renewable energies, in particular wind and solar energy, conventional power plants, electricity transmission grids, e-fuel generation technologies, energy storage facilities, and demand-side flexibility options. A more detailed and formal description of *Enertile* and how it is used to determine hydrogen supply curves can be found in (Lux et al. 2020). Pfluger (2014) describes the model representation of the electricity system more thoroughly, though for an older version not including e-fuels; Bernath et al. (2019) provide a detailed insight into the heat module of *Enertile* that is used for calculations in Europe. The central extension of *Enertile* in this paper provides a model representation of process chains for the generation of synthetic methane and a regional concept of the MENA region for e-fuel production. The methodology for determining synthetic methane supply curves follows the computational procedure for hydrogen supply curves outlined in Lux et al. (2020). Subsequent paragraphs summarize the key properties of the optimization model for the analysis in this paper.

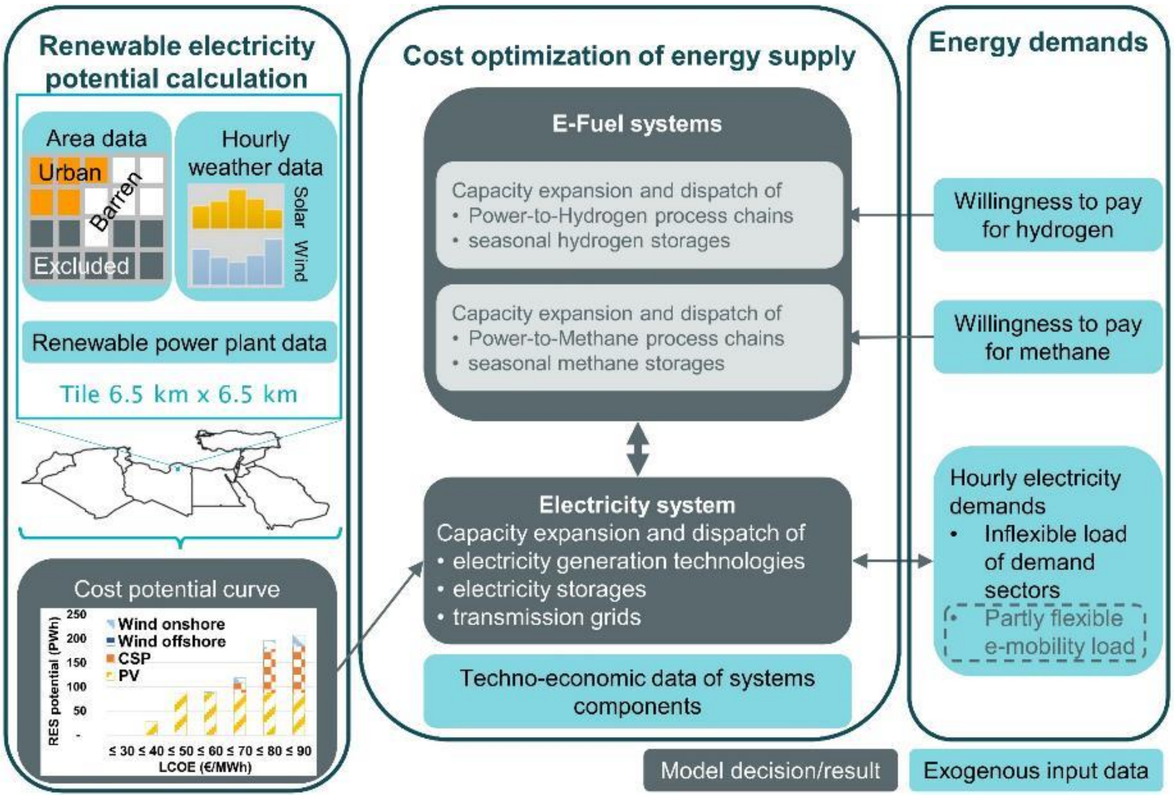

Figure 6-1 Simplified graphical illustration of the components and interactions of the energy system model Enertile as used in this paper. Calculations for Europe, which serve as a benchmark for the results of this paper, additionally cover heat generation in heat grids (cf. Lux et al. (2020)).

The objective function of the optimization model totals the cost of the supply side of the energy system being considered, including electricity transport and storage. Installed capacities of energy infrastructures and their hourly dispatch are the decision variables of the linear problem. These variables are weighted by fixed costs and variable costs in the objective function. Fixed costs for expanding the capacity of a specific technology include annuitized investments and fixed operation and maintenance costs. Utilizing the technology incurs variable costs, including fuel costs, CO_2 emission costs and variable costs for operation and maintenance.

The central constraints of the optimization problem require hourly equilibria of energy supply and demand in balance equations. These balance equations are formulated for electricity and electricity-based fuels for each model region and each hour of a given year. Demands either are given exogenously or arise endogenously as a model decision. An endogenous electricity demand arises, for example, from the model-determined use of electrolyzers. Sector coupling options, energy storages, and grids create connections between individual balancing equations. Sector coupling technologies such as electrolyzers enter the electricity and hydrogen balance of a given region and hour with either a plus or minus sign as appropriate. Storages create intertemporal connections between balancing equations. Electricity transmission grids link electricity balances in different regions. This allows *Enertile* to provide a very detailed picture of the interdependencies of the energy supply side in the optimization process. Other constraints ensure that system components operate within their capacity limits.

The provision of e-fuels plays a special role in the modeling for this paper. In contrast to exogenous electricity demands, there are no e-fuel demands externally imposed on *Enertile*. Instead, the model is offered a selling price for hydrogen or synthetic methane and it decides how much e-fuel it will produce at the given price. Technically, the sale of e-fuels reduces the energy system cost in the objective function. The model installs and uses additional electricity supply infrastructure and e-fuel generation units as long as incurred costs are covered by the revenues of selling these e-fuels. The last megawatt-hour of e-fuels provided and sold creates marginal costs at almost exactly the applied sales price. This mechanism can represent potential e-fuel demands from other sectors in the MENA region or export offers at the relevant sales price. Applying different sales prices in different model runs generates cost-supply curves for the investigated e-fuels. These supply curves interrelate with the rest of the energy system in the scenario design. It is also possible to use e-fuels exclusively for energy storage within the model.

The linear optimization problem is set up and solved for the simulation years 2030 and 2050 in hourly resolution. The expansion and dispatch of energy infrastructures are optimized using perfect foresight. The full hourly resolution of analyzed years combined with the use of real weather data allows an adequate representation of the challenging synchronization between energy demand and fluctuating renewable energy supply. This approach can allow for extreme weather events from the energy system perspective with simultaneous lulls, cold spells, and darkness.

For the analysis in this paper, *Enertile* covers the energy supply system in Morocco, Algeria, Libya, Tunisia, Egypt, Saudi Arabia, Lebanon, Israel, Syria, and Turkey. While renewable potentials are determined on a regionally highly resolved grid with a size of 42.25 km², electricity demands and trade flows are summarized in larger model regions. Due to the extensive geographical area of the countries under consideration, the concentration of population and infrastructures near the coasts, and the generally high aridity of the area, model regions are defined as a function of distance to coast. Figure 6-2 shows that the analyzed countries are divided into 250 km wide strips starting at the coast. Model regions with coastline access and therefore seawater access have a special status, as in the selected modeling approach e-fuels can only be produced here. This means that electrolyzers and subsequent synthesis plants can only be built near the coast and operated with desalinated seawater. This approach is intended to prevent competition for scarce fresh water in the arid MENA region and water transport across the desert.

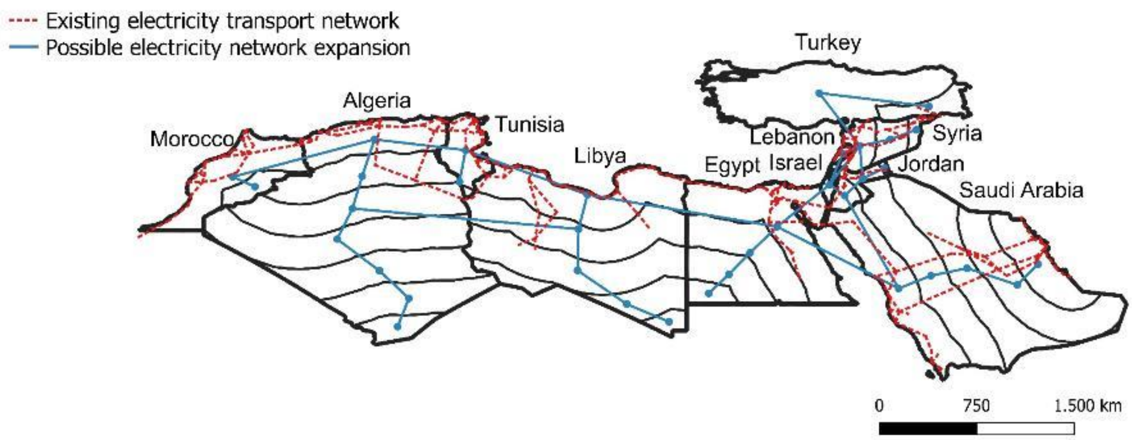

Figure 6-2 Geographic coverage of the modeling approach, existing electricity transport network (Beltaifa 2020), and modelled net transfer capacities as electricity grid between regions.

The electricity transport grid in *Enertile* is modeled as net transfer capacities (NTCs) between different model regions. Figure 6-2 shows the potential grid connections. The modeling of electricity transport grids for the MENA region follows three approaches. Firstly, it enables the expansion of the power grid between model regions already connected through transmission lines. Figure 6-2 shows the existing transmission network connections based on a dataset of Beltaifa (2020). Secondly, grid expansion becomes possible between coastal regions of neighboring countries, regardless of whether connections already exist or not. Thirdly, grid connections between coastal regions and the hinterland can be created or extended. The last two approaches allow for the power supply of e-fuel generation units near the coast and ensure that the entire MENA region can contribute to e-fuel production. Local grid restrictions within model regions are not considered and unlimited flows are allowed within the model regions.

6.2.1.2 Renewable potential calculation

The calculation of the potentials of renewable energies is an upstream process to *Enertile* (cf. Figure 6-1). Geographically resolved power generation potentials are determined on the basis of real weather data, land use data, and techno-economic parameters of renewable power generation technologies. The analysis includes onshore wind, offshore wind, ground-mounted photovoltaics (PV), and concentrated solar power (CSP) technologies. As a result, *Enertile* obtains installable capacities, full load hours of power generation, hourly generation profiles, and levelized costs of electricity for the energy system optimization.

Following the definition of different potential types for renewable energies in (Hoogwijk et al. 2004), the geographical potential, the technical potential, and the economic potential are each determined in turn. The basis of all these potential calculations is the division of the MENA region into a grid with an edge length of 6.5 x 6.5 km. More than 250,000 tiles are evaluated for the entire region under consideration.

The first step is to determine the geographical potential, expressing the area assessable for the installation of renewable energies for each tile of the grid. For this analysis, each grid tile receives information on land use (European Space Agency and Université Catholique de Louvain 2010), elevation and slope (Danielson et al. 2011), and protected areas (UNEP 2014). Tiles located in protected areas or near cities are excluded from the calculation. The approach considers geotechnical limitations such as excessive slopes (e.g. for CSP) or high water depth (e.g. for offshore wind). For each land use type and renewable technology, a utilization factor is defined that determines the proportion allowed for renewable electricity generation. Table 6-1 lists the utilization factors for different land uses and technologies. The available area per tile for a renewable technology is calculated using equation (13). In (13) A_{tile} is the area of each tile (42.25 km²), $share_l$ is the share of the land use type l on this tile and u_l is the utilization factor for this land use and technology. The sum of the available area of the 250,000 tiles results in the geographical potential A_{region} of the model region.

$$A_{region} = \sum^{tile} A_{tile} \cdot share_l \cdot u_l \qquad (13)$$

Table 6-1 Utilization factors for the considered land uses and renewable technologies.

Land use	**Onshore wind** (ID 166 & 168)	**Offshore wind** (ID 104 & 117)	**Ground-mounted PV** (ID 133 & 140)	**Rooftop PV** (ID 97 & 102)	**CSP** (ID 89 & 94)
Barren	0.4	0	0.16	0	0.12
Cropland natural	0	0	0	0	0
Croplands	0.3	0	0	0	0.01
Forest	0.15	0	0	0	0

Land use	**Onshore wind** (ID 166 & 168)	**Offshore wind** (ID 104 & 117)	**Ground-mounted PV** (ID 133 & 140)	**Rooftop PV** (ID 97 & 102)	**CSP** (ID 89 & 94)
Grassland	0.3	0	0.2	0	0.02
Savanna	0.3	0	0.2	0	0.12
Scrubland	0.3	0	0.2	0	0.12
Snow and ice	0.12	0	0.4	0	0
Urban	0	0	0	0.065	0
Water	0	0.9	0	0	0
Wetlands	0	0	0	0	0
Excluded	0	0	0	0	0

Own assumptions.

Renewable power generation potentials are sensitive to assumptions on utilization factors for different land uses and renewable technologies. Throughout the literature, utilization factors vary widely. Franke et al. (2021) analyze the dependency of onshore wind potentials on the chosen utilization factors. This study shows that land utilization factors can have an impact of up to 51% on the calculated results. The utilization factors used in this paper tend to be lower than the values in most literature. As *Enertile* can build different renewable technologies on a single tile, competition for available space can arise for certain technologies and land use categories. The chosen utilization factors are intended to reflect this competition. In reviewed publications (Bosch et al. 2017; Eurek et al. 2017; Feng et al. 2020; He et al. 2014; Hu et al. 2019; Liu et al. 2017; Sebestyén 2017), the utilization factors vary between 0.0 and 0.9 for the land use category "barren". In the MENA region, this category accounts for a high share of up to 80% in Egypt, Libya, and Algeria. The chosen utilization factor for this land use therefore has a huge impact on the calculated potentials. In this study, the chosen utilization factor is low to represent a conservative approach. The actual potential of renewable energies could therefore be higher.

In the second step, the technical potential of renewable energies is determined. The technical potential describes the maximum installable capacity of renewable energy technologies per tile. This is achieved by intersecting the available areas determined in the geographical potential with the technical limitations of the power generation technologies. In the case of wind power, the spacing of the turbines in the field is taken into account to limit the wind shadow effect. The spacing used in this article is 5 rotor diameters within a row and 9 rotor diameters between rows (Gupta 2016; Pfluger et al. 2017). The occupied area of solar power plants is dependent on the efficiency of the solar power plant. The installable capacity of solar power plants varies from 50 MW/km² for a module with an efficiency of 17% to 57 MW/km² for a module with an efficiency of 19% (Fraunhofer ISE 2015). This installable capacity is based upon an analysis of the occupied area by real solar power plants. Different azimuth and tilt angles are also considered (Schubert 2012).

Finally, the economic potentials are determined. The economic potential comprises the levelized cost of electricity per tile and technology. In this step, the technical potential is combined with techno-economic data of renewable power generation technologies and real weather data for a selected weather year. The technology-specific cost data include both specific investments for capacity expansion and the costs of operation and maintenance. For wind power, the installation costs are dependent on the hub height and rotor diameter. In the calculated scenarios, the model can choose between 59 different turbine configurations for onshore wind and seven offshore wind turbines (cf. Appendix Appendix E). For onshore wind, the number of different wind turbine configurations increases from 10 in 2020 to 30 in 2030 and 41 in 2040. In the case of wind turbines, the future cost reduction potential of individual components such as rotors, generators, or towers is limited due to the already high level of technological maturity. Electricity generation from wind could become cheaper in the future if larger plants are built, the rotor-generator ratio increases and the plant can specifically absorb more energy. In this paper, it is assumed that the specific investments show a cost reduction of about 10% between 2020 and 2050. For example, a wind turbine with a hub height of 110 m and a specific area output of 400 W_{el}/m^2 costs 1160 €/kW_{el} in 2020 and 1050 €/kW_{el} in 2050. For PV plants, modules are currently still learning at a rate of 19% (ZSW 2019). There is still potential for cost reductions and efficiency improvements. As module prices fall, other components, such as the rack, become increasingly important. However, the technical learning of these peripheral systems and thus the cost reduction potential is limited and thus slows down the technical learning of the entire system. Reductions in specific investments and operation and maintenance costs are taken into account for each renewable power generation technology considered, as shown in the appendix in Table 6-14 and Table 6-15.

The specific electricity production costs also depend on the assumed full load hours and related electricity generation of the technologies. In this modeling, the operating times are derived from real weather data for the year 2010. For wind power plants, the wind speed at four different heights is considered to calculate the electricity output. For solar plants, the solar irradiation and the temperature are taken into account. Further information on the calculated power output can be found in (Schubert 2012). The data base for hourly wind speed, solar irradiation, and temperature is the ERA5 dataset from the European Centre for Medium-Range Weather Forecasts (Copernicus Climate Change Service 2020).

6.2.2 Data

6.2.2.1 General framework and scenario design

This article examines the supply of electricity-based hydrogen and synthetic methane in the MENA region in the years 2030 and 2050. A fundamental premise is that the electricity used in e-fuel generation originates from RES. To guarantee this renewable origin, the optimization framework differs for the two target years.

According to the politically set expansion targets for renewable energies, the electricity mix of the MENA countries will still be dominated by fossil energies in 2030 (Timmerberg et al. 2019b). Morocco sets the most ambitious target, with renewables accounting for an envisaged 52% of its national electricity production in 2030 (Timmerberg et al. 2019b). A greenfield approach for e-fuel production is therefore assumed with respect to the power system in 2030. The optimizer's expandable technology portfolio is limited to renewable energies, electricity storages, and grid infrastructure. In the optimization problem, the remaining electricity demand of the MENA states and the existing power plant fleet and transport infrastructure are excluded. This ensures the additivity of the renewable power generation units and power infrastructures to be installed for e-fuel production, as they are operated completely independently from the rest of the electricity system, which is not modeled. Consequently, a synergetic utilization of electricity infrastructures to meet electricity demands in MENA and to generate hydrogen or synthetic methane is not possible in this setting.

For 2050, it is assumed that all electricity generation in MENA is greenhouse gas neutral. Fossil generation technologies are prohibited in the modeling approach. The optimization problem addresses the cost-efficient supply of electricity demands in MENA and the supply of electricity-based fuels. Mutual synergies can be exploited.

Demands or exports of hydrogen or synthetic methane are not explicitly modeled. Instead, the model has the option of reducing system costs by generating and selling these e-fuels. No distinction is made between sales to demand sectors in MENA and exports, as the sales price is interpreted as the price ex works. In a parameter study, the associated hydrogen and methane sales prices are increased in steps of 10 $€/MWh_{H2/CH4,LHV}$.

6.2.2.2 Electricity demands in the MENA region in 2050

Electricity demands for each MENA country in 2050 are estimated using historical demands from 2018 (IEA 2020a), average annual load growth rates from the World Energy Outlook 2020 (IEA 2020b), and population projections from the United Nations in 2019 (UN 2019). Figure 6-3 shows the resulting load projections for the MENA region in 2050. The identified electricity demands are distributed among the different model regions within a country according to the population distribution from 2018 (WorldPop 2018). The modeling distinguishes between electricity demands that follow a fixed demand profile and those that have some flexibility. The general load in Figure 6-3 follows a fixed demand profile. Electricity demands for e-mobility have an inflexible and a flexible component. The inflexible mobility demand includes trolley trucks, trolley buses, and battery electric vehicles with inflexible charging behavior. For 50% of battery electric vehicles, it is assumed that they can charge flexibly while complying with their driving profiles.

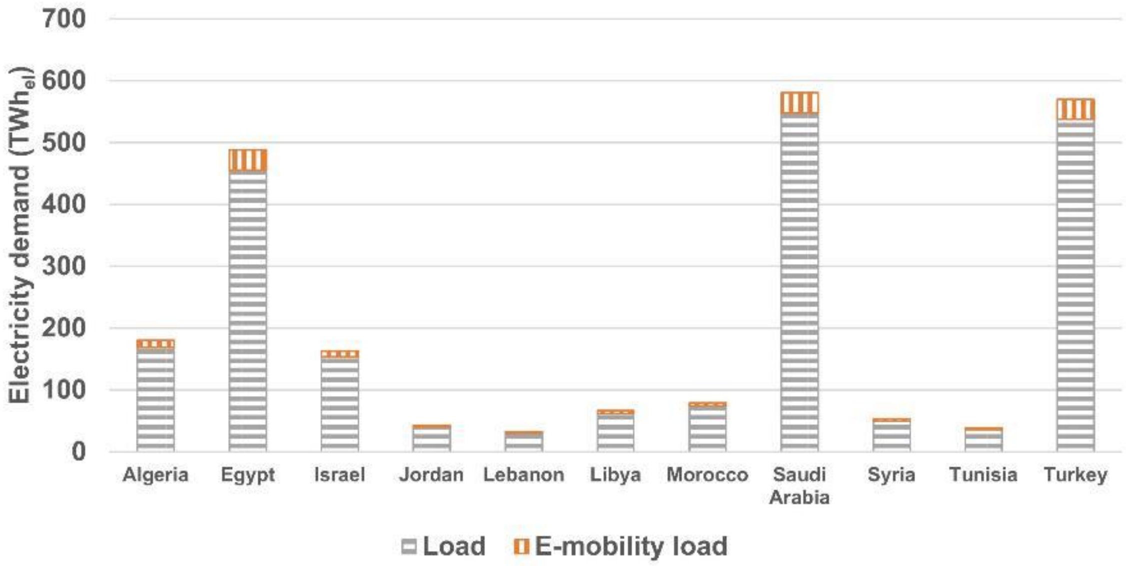

Figure 6-3 Projected electricity demands in the MENA countries in 2050. Electricity demands include a flat surcharge for distribution grid losses of 6.5%.

6.2.2.3 Electricity transport network expansion

The parameterization of the NTCs of the modeled power grid is based on the data in Table 6-2. Specific investments and losses of grid lines are weighted by the distances between geographic centers of connected model regions in the transport network parameterization in *Enertile*.

Table 6-2 Techno-economic characteristics of the transmission grid parametrization in Enertile (Godron et al. 2014).

Technology	CAPEX	Fixed OPEX	Losses
Converter terminal	270 M€	1% of investment p.a.	3% per 1000 km [a]
High-voltage direct current (HVDC) overhead line	300 €/ (MW$_{el}$ km)	1% of investment p.a.	

[a] Own estimations

6.2.2.4 E-fuel production concepts

This section presents the conceptual design of e-fuel production chains in the MENA region. It illustrates eight different generation concepts for electricity-based hydrogen and methane and their techno-economic parametrization in the energy system model *Enertile.*

The efficient conversion of electricity into hydrogen and methane, called the Power-to-Gas (PtG) process, requires the interaction of different technologies. Depending on the final product, these technologies include seawater desalination, water electrolysis, CO_2 supply, methanation and liquefaction units. *Enertile* takes the energy system perspective and is thus unable to resolve these individual components. Therefore, a preliminary analysis assembles four representative production chains for hydrogen (Power-to-Hydrogen, PtH_2) and methane (Power-to-Methane, $PtCH_4$), respectively. These production chains enter the *Enertile* parametrization as an integrated composition characterized by overall efficiencies, summed specific investments, and aggregated operation and maintenance costs. The individual technologies in the production chains and their techno-economic characteristics as described in detail in appendix Appendix D.

Hydrogen and methane production chains are differentiated in two aspects: the electrolyzer technology and the physical state of the final product. The physical state of the chain product can be either gaseous or liquefied. This paper distinguishes between e-fuel production chains with polymer electrolyte membrane electrolysis (PEMEL) and solid oxide electrolysis (SOEL). The analysis of all investigated process chains refers to technical and economic data for the year 2030 or 2050 and for a plant capacity of 100 $MW_{H2/CH4}$. In this article, the plant capacity ($MW_{H2/CH4}$) and plant output ($MWh_{H2/CH4}$) are related to the lower heating value (LHV) of the product (i.e. hydrogen or methane), which describes the amount of thermal energy released during the product's combustion without water condensation. Figure 6-4 and Figure 6-5 show the considered production chains for gaseous hydrogen (at 20 bar) and liquefied hydrogen (L-hydrogen, L-H2) and for methane (L-methane, L-CH4) for the year 2050. Direct input parameters for the *Enertile* model are the overall process efficiency and the specific costs of the entire process chains shown below. The energy balance of the production chains comprises chemical, electrical, and thermal energy inflows and outflows. Except for methanation, all processes within the investigated production chains have relevant electrical energy demands. SOEL and DAC have additional thermal energy demands. Due to the exothermic reaction, methanation releases thermal energy, which covers parts of the thermal energy demands of DAC and SOEL. An electric heater covers the remaining thermal energy requirements.

The overall process efficiency $\eta_{\mathrm{PtH2,LHV}}$ or $\eta_{\mathrm{PtCH4,LHV}}$ of e-fuel production in equations (14) and (15) is defined as the ratio of the chemical energy output $F_{\mathrm{E,chem,H2/CH4,LHV}}$ in the form of hydrogen or methane to the electrical energy input $F_{\mathrm{E,el,total,in}}$. The chemical energy output is defined as the product of the mass flow $F_{\mathrm{M,H2/CH4}}$ and lower heating value of hydrogen or methane $LHV_{\mathrm{H2/CH4}}$.

$$\eta_{\mathrm{PtH2,LHV}} = \frac{F_{\mathrm{E,chem,H2,LHV}}}{F_{\mathrm{E,el,total,in}}} = \frac{F_{\mathrm{M,H2}} * LHV_{\mathrm{H2}}}{F_{\mathrm{E,el,total,in}}} \tag{14}$$

$$\eta_{\mathrm{PtCH4,LHV}} = \frac{F_{\mathrm{E,chem,CH4,LHV}}}{F_{\mathrm{E,el,total,in}}} = \frac{F_{\mathrm{M,CH4}} * LHV_{\mathrm{CH4}}}{F_{\mathrm{E,el,total,in}}} \tag{15}$$

Table 6-3 and Table 6-4 show the overall process efficiencies for the eight investigated PtH_2 and $PtCH_4$ process chains. These efficiencies match well with the literature and real-life data from pilot plants (Drechsler et al. 2021; Frank et al. 2018; Götz et al. 2016; Timmerberg et al. 2019a). Theoretical optimization of the STORE&GO pilot plant in Troia, Italy, with a plant size of approximately 200 kW_{el} electrical input, shows that an overall PtG efficiency of 46% related to the higher heating value (HHV) of the methane output is achievable, without taking into account further energy savings through scaling effects (Schlautmann et al. 2021).

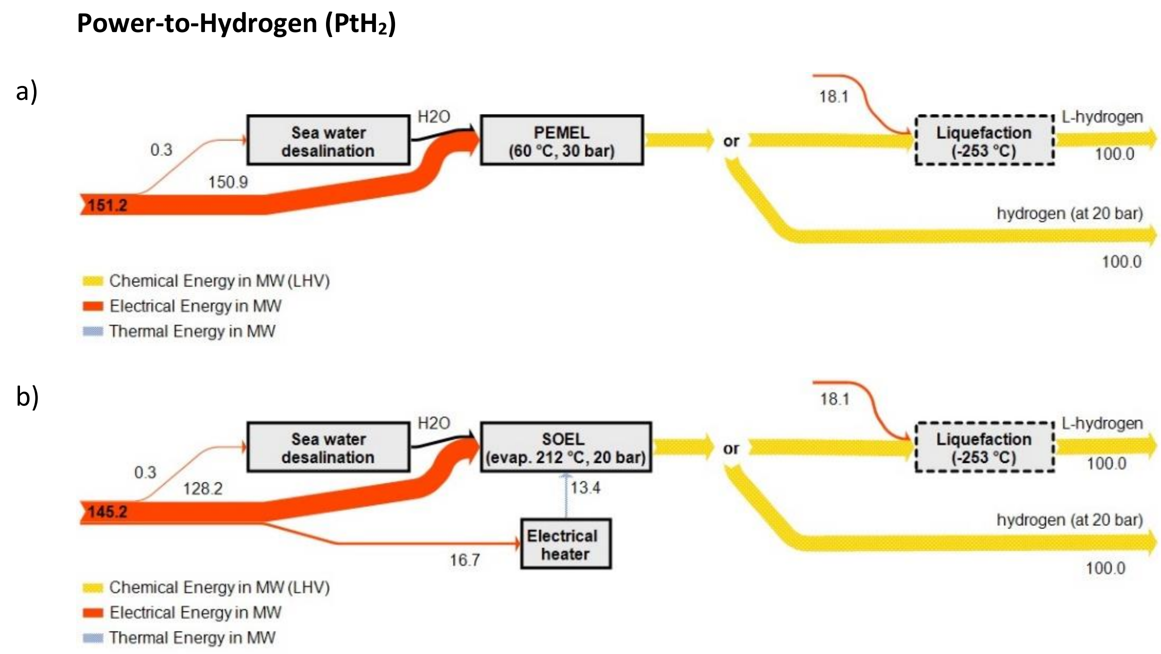

Figure 6-4 Energy flow diagram for a Power-to-Hydrogen process chain in the MENA region with PEMEL (a) or SOEL (b) and optional liquefaction for 100 MW hydrogen output related to the lower heating value (LHV). The process chains are based on technical key data referring to the year 2050. Quantities of energy not shown correspond to energetic losses.

Power-to-Methane (PtCH4)

a)

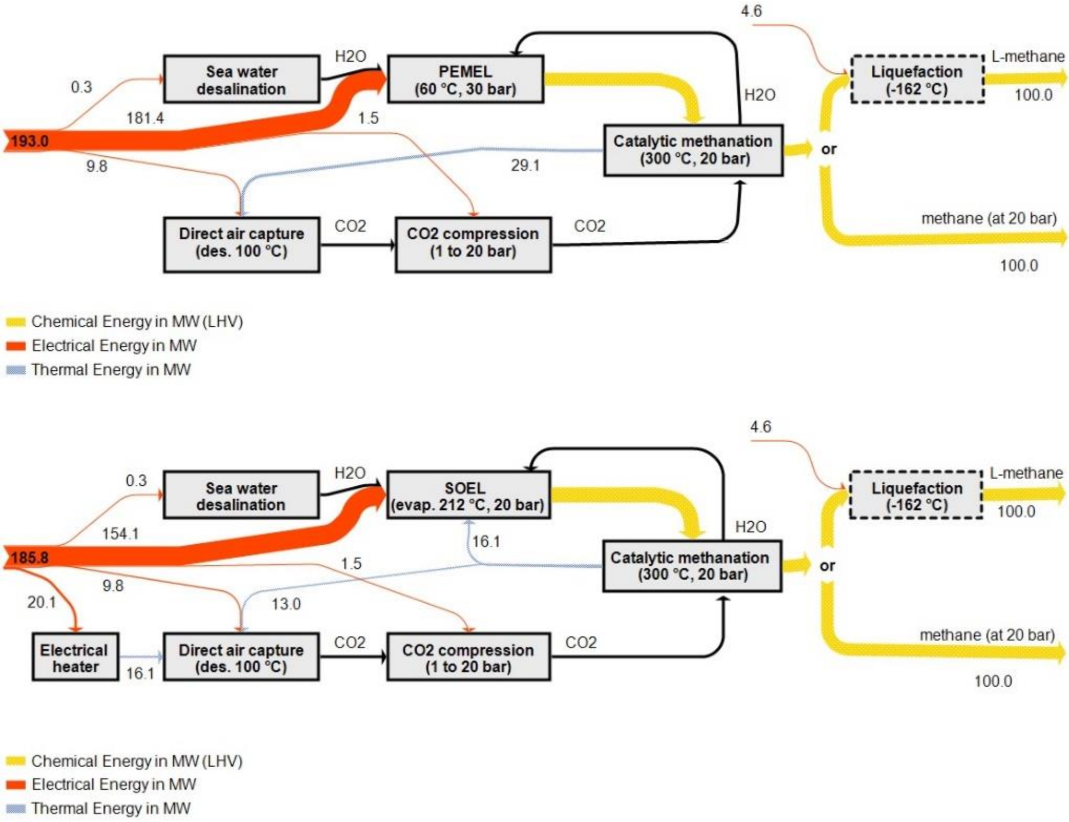

b)

Figure 6-5 Energy flow diagram for a Power-to-Methane process chain in the MENA region with PEMEL (a) or SOEL (b) and optional liquefaction for 100 MW methane output related to the lower heating value (LHV). The process chains are based on technical key data referring to the year 2050. Quantities of energy not shown correspond to energetic losses.

Table 6-3 Overall efficiencies of the four investigated options of Power-to-Hydrogen (PtH2) process chains in MENA. Values are related to the lower heating value (LHV) and take internal heat integration into account. External heat requirements are provided by an electric heater, based on technical key data referring to the years 2030 and 2050.

Power-to-Hydrogen production chain	**Overall efficiency $\eta_{PtCH4,LHV}$ in %**	
	in 2030	**in 2050**
PtH_2-PEMEL	60	66
PtH_2-SOEL	68	69
PtH_2-PEMEL-liquefaction	53	59
PtH_2-SOEL-liquefaction	60	61

Table 6-4 Overall efficiencies of the four investigated options of Power-to-Methane (PtCH4) process chains in MENA. Values are related to the lower heating value (LHV) and take internal heat integration into account. External heat requirements are provided by an electric heater, based on technical key data referring to the years 2030 and 2050.

Power-to-Methane production chain	**Overall efficiency $\eta_{PtCH4,LHV}$ in %**	
	in 2030	**in 2050**
$PtCH_4$-PEMEL	47	52
$PtCH_4$-SOEL	53	54
$PtCH_4$-PEMEL-liquefaction	46	51
$PtCH_4$-SOEL-liquefaction	52	53

Table 6-5 and Table 6-6 show specific capital expenditure (CAPEX) and fixed operating expenditure (OPEX) of the different Power-to-Hydrogen and Power-to-Methane production chains as used in Enertile. Costs to meet electricity demands are determined endogenously by the optimization model.

Today's PtG plants operate on a pilot scale of a few $MW_{H2/CH4}$. Due to the high RES generation potential in MENA, PtG plants on a scale of GW are likely in the future. The economic analyses in this article are examples based on key data for a plant capacity of 100 $MW_{H2/CH4,LHV}$ output. For plants with capacities of several hundred $MW_{H2/CH4}$, the costs may be lower due to degression. However, the CAPEX-intensive PtG technologies, such as electrolysis and DAC, are modular and larger plant capacities are achieved by numbering up. Whether the assumed cost reductions for the PtG technologies will be achieved in 2030 and 2050 depends largely on the actual market ramp-up of PtG. For this reason, the learning rates predicted in the literature may be either under- or over-fulfilled.

Table 6-5 CAPEX and fixed OPEX for entire Power-to-Hydrogen (PtH2) process chains in the MENA region. Underlying economic key data refer to the years 2030 and 2050 and to a plant capacity of 100 MW hydrogen or methane output related to the lower heating value (LHV) as listed in the appendix (Table 6-12 and Table 6-13).

Power-to-Hydrogen production chain		**Specific costs**		
		in 2030	**in 2050**	
PtH_2-PEMEL	CAPEX	689	623	€/kW_{H2}
	fixed OPEX	26	23	€/kW_{H2}/ a
PtH_2-SOEL	CAPEX	1,026	690	€/kW_{H2}
	fixed OPEX	77	37	€/kW_{H2}/ a
PtH_2-PEMEL-Liqufaction	CAPEX	1,756	1,690	€/kW_{H2}
	fixed OPEX	69	65	€/kW_{H2}/ a
PtH_2-SOEL-Liqufaction	CAPEX	2,061	1,757	€/kW_{H2}
	fixed OPEX	120	80	€/kW_{H2}/ a

Table 6-6 CAPEX and fixed OPEX for entire Power-to-Methane (PtCH4) process chains in the MENA region. Underlying economic key data refer to the years 2030 and 2050 and to a plant capacity of 100 MW hydrogen or methane output related to the lower heating value (LHV) as listed in the appendix (Table 6-12 and Table 6-13).

Power-to-Methane production chain		**Specific costs**		
		in 2030	**in 2050**	
$PtCH_4$-PEMEL	CAPEX	1,968	1,516	€/kW_{CH4}
	fixed OPEX	58	45	€/kW_{CH4}/ a
$PtCH_4$-SOEL	CAPEX	2,373	1,595	€/kW_{CH44}
	fixed OPEX	120	63	€/kW_{CH4}/ a
$PtCH_4$-PEMEL-Liqufaction	CAPEX	2,493	2,038	€/kW_{CH4}
	fixed OPEX	90	77	€/kW_{CH4}/ a
$PtCH_4$-SOEL-Liqufaction	CAPEX	2,897	2,119	€/kW_{CH4}
	fixed OPEX	151	94	€/kW_{CH4}/ a

6.2.2.5 Long-distance transport of e-fuels

Hydrogen and methane have low energy densities compared to fossil liquid fuels such as petroleum. To transport these fuels economically, they must be compress or liquefied. Alternatively, hydrogen can be converted to larger molecules, which is not considered in this article.

The logistic concept for pipeline-based transport of hydrogen and synthetic methane essentially includes compressor stations, transport pipelines, and gas storage facilities. The long-distance transport of liquefied hydrogen or methane consists of the sub-steps of liquefaction and intermediate storage, transport via tankers, and regasification on arrival.

The transport costs depend in particular on the distance to be covered. In this article, transport distances are estimated by the center-to-center air distance to e-fuel production regions in the MENA region (cf. section 6.2.1.1 and section Appendix C) and continental Europe. In reality, transport routes are likely to be different.

For large methane volumes, pipeline transport is profitable for shorter distances, while transport of L-methane becomes economically feasible for larger distances (between 2,000 and 5,000 km). Liquid transportation is dominated by liquefaction costs, while pipeline-based transport requires more compressors as the distance increases (Fasold 2010; Homann et al. 2013; Simon Göß 2017). The costs reported in the literature for transporting natural gas via pipelines and via ship vary mainly due to the different assumed capacities and distances. (Fasold 2010; Homann et al. 2013; Julian Deymann 2014; Simon Göß 2017).

Today, hydrogen pipelines are mostly operated locally, e.g. at industrial sites, and a hydrogen tanker is operated only for project purposes (Collins 2019). Due to limited experience, cost values for hydrogen transport vary widely in the literature (Hydrogen Council 2020; IEA 2019; Niermann et al. 2021). One of the main challenges is the low boiling temperature of hydrogen, compared to methane (see Appendix D). The shipping of hydrogen therefore shows higher costs, e.g. for the insulation of the tanks.

The compression of hydrogen is also more energy-intensive than of methane and thus, higher costs are expected for hydrogen pipelines. The transport costs of gaseous hydrogen strongly depend on the assumed pipeline capacities. (Wang et al. 2020) calculate costs for new infrastructure, assuming hydrogen pipelines with a diameter of 0.6 to 1.2 m and a nominal capacity of approximately 13 GW_{H2}. The author's own estimations (Leiblein et al. 2020) agree with the costs given by (Wang et al. 2020). Table 6-7 shows the distance-dependent costs for the transport of hydrogen and synthetic methane from MENA to continental Europe used in this article.

Table 6-7 Levelized transport costs for hydrogen and synthetic methane referring to the lower heating value (LHV) of hydrogen or methane. Costs for transport via ship exclude liquefaction. Costs for transport via pipeline include on-site compression up to 100 bar for hydrogen and up to 80 bar for methane. Costs are based on values for 2020 and rely on a literature review (Fasold 2010; Homann et al. 2013; IEA 2019; Leiblein et al. 2020; Simon Göß 2017).

Logistic chain	**Levelized costs of transport**	
Hydrogen via pipeline	0.69	€ct/(MWh_{H2} km)
Hydrogen via ship	$12.43 \times x^{0.13}, x: distance\ in\ km$	€/MWh_{H2}
Synthetic methane via pipeline	0.17	€ct/(MWh_{CH4} km)
Synthetic methane via ship	$0.11 \times x^{0.38}, x: distance\ in\ km$	€/MWh_{CH4}

6.3 Results

6.3.1 Renewable energy potentials in MENA

The supply of e-fuels decisively depends on the quantity and levelized cost of renewable electricity. This section therefore presents both the spatial distribution of the generation costs of the main renewable power generation technologies of PV, CSP, and onshore wind, and cumulative cost potential curves for renewable electricity for the MENA region.

6.3.1.1 Spatial distribution of renewable energies

Figure 6-6 shows the spatial distribution of levelized cost of electricity (LCOE) for the generation technologies CSP (a), ground-mounted PV (b), and onshore wind (c) in the MENA region in 2050. The results in this figure are based on calculations with a weighted average cost of capital (WACC) of 7%.

Offshore wind is not considered in the following analysis, as the potentials are low in the MENA region. This is firstly due to the restriction that offshore wind can only be installed up to a water depth of 50 m and up to 370 km from the coast. In the Mediterranean Sea adjacent to the MENA region the water depth is mostly greater, so the installable capacities for offshore wind plants are low. Secondly, the full load hours for offshore wind in the regions considered are mainly below 3,000 hours. Overall, the electricity generation of offshore wind starts at a LCOE of 130 €/MWh_{el}.

Due to low installation costs, solar PV is the least expensive power generation technology in MENA in 2050, with a LCOE between 28 €/MWh_{el} and 51 €/MWh_{el}. The uniform coloring of the map shows that the regional differences in LCOE are small. About 90% of the PV generation potential has electricity generation costs below 31 €/MWh_{el}. The overall cheapest 10% of the PV potential is located in Egypt, Libya and Jordan, and lies below 29 €/MWh_{el}. Turkey has on average the highest PV generation cost due to its northern location. Among the model regions with coastlines - and thus e-fuel production model regions - Jordan, Egypt, and Saudi Arabia have the lowest LCOE for PV.

The electricity generation costs of CSP are higher than those of PV, ranging from 47 €/MWh_{el} to 88 €/MWh_{el}. The cheapest 90% of the CSP generation potential has a LCOE below 55 €/MWh_{el}. The regional distribution tends to show a stronger north-south gradient than PV because CSP power plants depend on direct solar irradiation. The overall cheapest 10% of the CSP potential is located in Egypt, and Libya, and lies below 49 €/MWh_{el}. The most expensive CSP power generation takes place in Turkey, northern Morocco, northern Algeria, and northern Tunisia. Larger areas in Turkey, Morocco, and western Saudi Arabia show no CSP potential. These areas were excluded from the potential calculation due to excessive slopes.

Compared to solar power generation technologies, wind potentials exhibit higher generation costs in 2050. The levelized cost of electricity for onshore wind ranges from 43 €/MWh_{el} to well above 140 €/MWh_{el}. The electricity generation costs of onshore wind show stronger local differences than the solar technologies. Small, low-cost wind hotspots exist in western Morocco and eastern Egypt. Larger areas of relatively good wind sites are located in Algeria and Libya.

a)

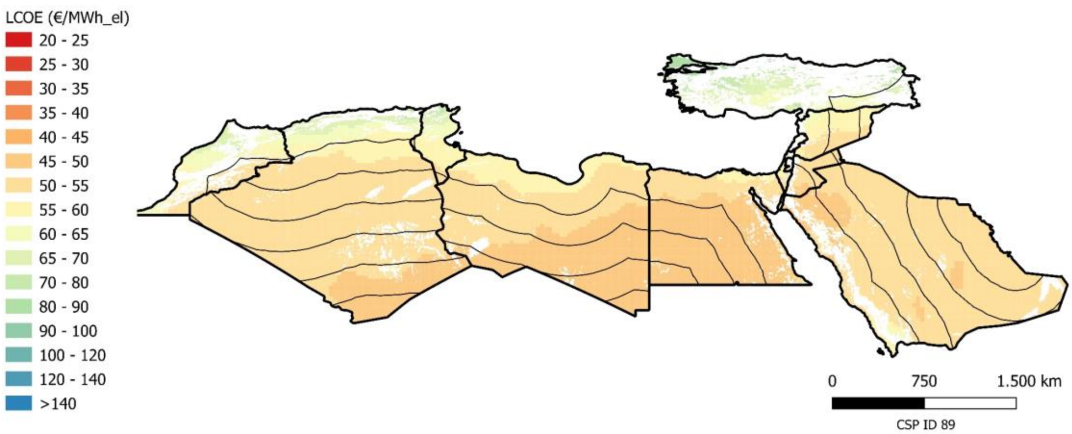
LCOE (€/MWh_el)
20 - 25
25 - 30
30 - 35
35 - 40
40 - 45
45 - 50
50 - 55
55 - 60
60 - 65
65 - 70
70 - 80
80 - 90
90 - 100
100 - 120
120 - 140
>140
0
750
1.500 km
CSP ID 89

b)


LCOE (€/MWh_el)
20 - 25
25 - 30
30 - 35
35 - 40
40 - 45
45 - 50
50 - 55
55 - 60
60 - 65
65 - 70
70 - 80
80 - 90
90 - 100
100 - 120
120 - 140
>140
0
750
1.500 km
SOPV ID 133

c)

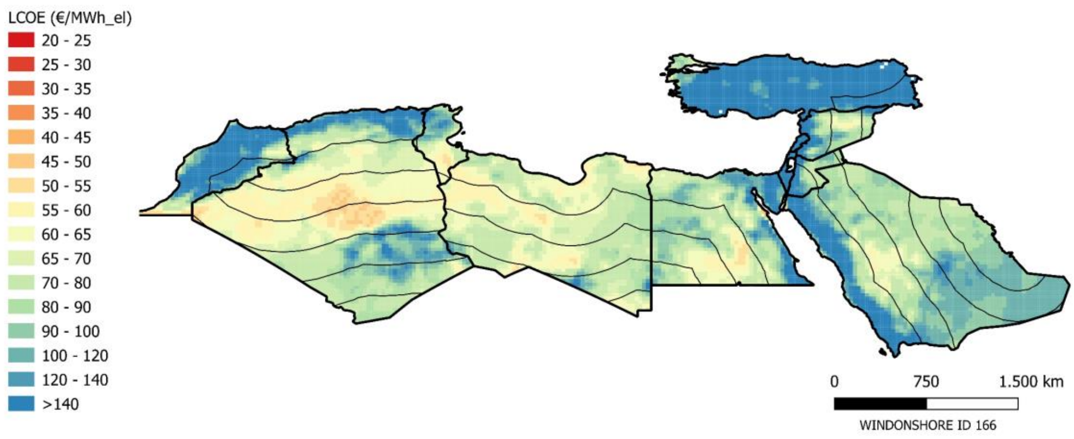

Figure 6-6 Spatial distribution of LCOE for the technologies a) CSP, b) ground mounted PV, and c) onshore wind in 2050 calculated with a WACC of 7%. White spaces are excluded from the potential calculation due to excessive slopes.

6.3.1.2 RES potential curves

Categorizing the LCOE shown in Figure 6-6 in cost steps results in the potential curves illustrated in Figure 6-7. The potential curves show the accumulated generation potential of renewable energies for increasing LCOEs in 2030 and 2050.

In Figure 6-7 a) the generation potential of the renewable technologies considered is illustrated for 2030. The dominance of solar PV in MENA becomes apparent from the high generation potential of about 90,000 TWh_{el} at costs below 45 €/MWh_{el}. At a LCOE of 60 €/MWh_{el}, 2,200 TWh_{el} of onshore wind generation potential becomes exploitable. Solar CSP is more expensive in 2030 than other renewable technologies, such that a CSP generation potential of about 20,000 TWh_{el} is available at costs of 70 €/MWh_{el}. The absolute CSP potential surpasses the solar PV potential at generation costs of 80 €/MWh_{el} with about 90,000 TWh_{el}.

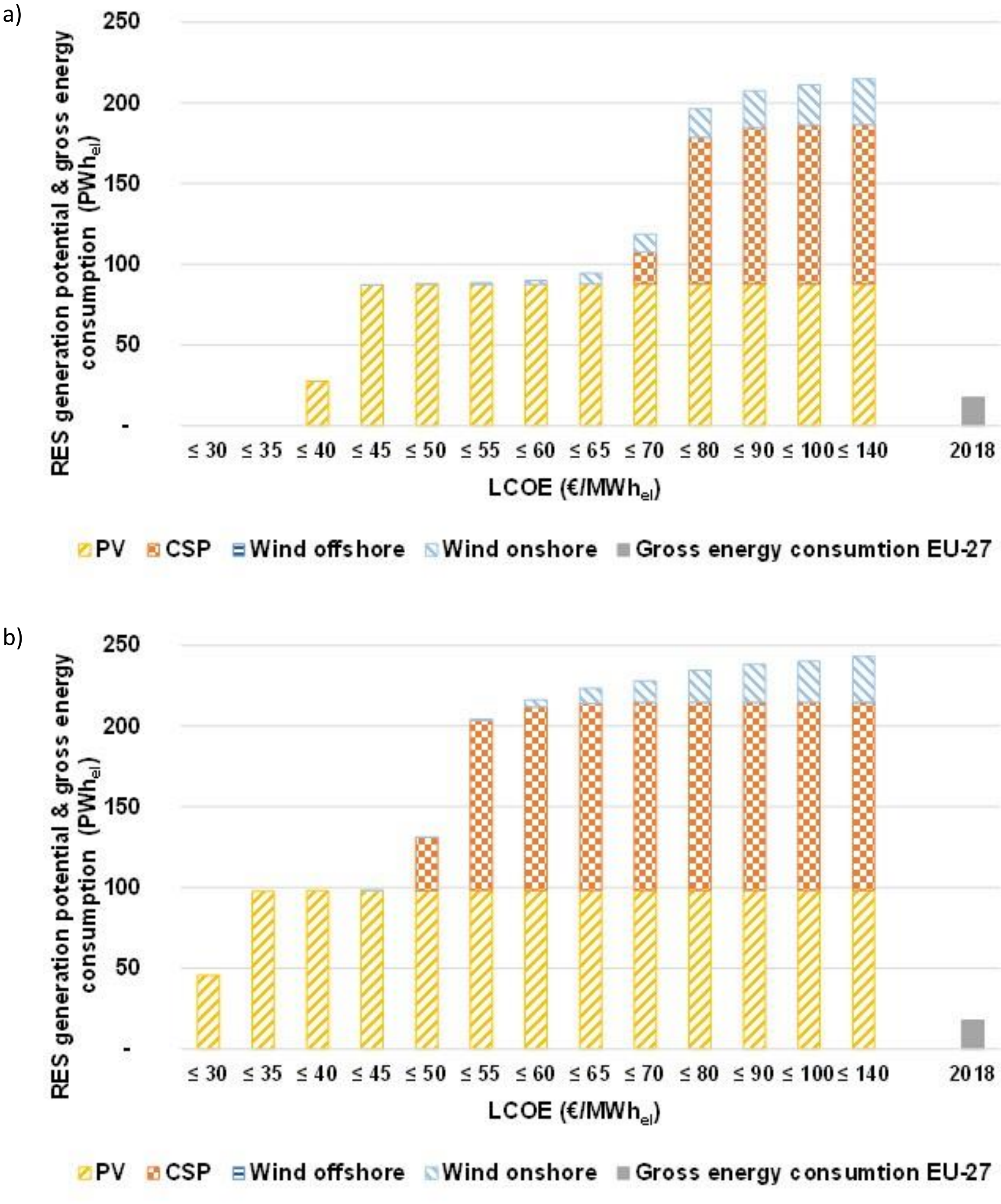

Figure 6-7 Renewable potential curves for the various technologies in the MENA region for the years 2030 (a) and 2050 (b).

Figure 6-7 b) shows the renewable potential curves for the MENA region in 2050. Solar PV is still the dominant technology for both spatial coverages in 2050. Due to a decrease in installation costs, the generation potential of solar PV reaches almost 99,000 TWh$_{el}$ at costs below 35 €/MWh$_{el}$. This is a significant increase compared to 2030, where the generation potential of solar PV below 35 €/MWh$_{el}$ is 0 TWh$_{el}$. At LCOE of 50 €/MWh$_{el}$, CSP power plants become available with a generation potential of 32,980 TWh$_{el}$. At 55 €/MWh$_{el}$, the potential of CSP reaches the potential of solar PV and from 60 €/MWh$_{el}$, the CSP potential surpasses the solar PV potential with a generation potential of 113,000 TWh$_{el}$. At LCOE of 55 €/MWh$_{el}$, onshore wind potential of 895 TWh$_{el}$ becomes exploitable. The number of onshore wind potentials is minor compared to the combined potential of solar PV and CSP. This is due to low wind speeds in the MENA region and high solar irradiation.

Overall, the renewable power generation potential in the MENA region is enormous. A comparison with European gross energy consumption in 2018 shows that in 2050, the generation potential of solar PV alone is six times greater than the gross energy consumption of the EU 27 in 2018.

The renewable potential curves show the theoretically exploitable potential. However, these potential curves are calculated without taking into account existing or potential infrastructures. MENA countries are therefore subdivided into 250 km wide strips to account for the cost of transmission grids between regions with different renewable potentials in the Enertile calculations.

6.3.2 E-fuel production in the MENA region

This section shows the model results of e-fuel production in the MENA region. Due to Europe's contrasting structure, with scarce land for renewable electricity generation coupled with high energy demands, Europe is a potential trading partner for e-fuels with the MENA region. Therefore, this section also considers transportation of e-fuels to Europe. Section 6.3.2 shows e-fuels supply curves for the MENA region including and excluding transportation to Europe and breaks down the resulting cost components of e-fuel production. The electricity system in MENA for the production of electricity-based hydrogen and synthetic methane is described in Section 6.3.3. Section 6.3.5 discusses the competition in the European hydrogen market between imports from the MENA region and European hydrogen production.

6.3.2.1 Supply curves of hydrogen and synthetic methane

Figure 6-8 and Figure 6-9 show supply curves of electricity-based hydrogen and methane determined by the optimization model for the years 2030 and 2050 in the MENA region. The figures show production quantities of these electricity-based fuels for rising sales prices (as ex works prices) and at WACCs of 7% and 12%. In addition to production costs, transportation from MENA to Europe is an important cost component for evaluating the e-fuel export option to Europe. Each supply curve for MENA is therefore supplemented by an export curve to Europe, which includes transportation costs. Hydrogen and methane utilized as electricity storages within the MENA region are included in the scenario runs, but not in the supply curves. It is important to note that the curves represent techno-economic potentials but not necessarily realistic trajectories of expansion. This applies in particular to the period up to 2030, in which higher sales prices result in quantities that would be very difficult to ramp up to in less than a decade.

The optimization results in Figure 6-8 shows steep increases in the production quantities of electricity-based fuels with increasing sales prices in the MENA region. Depending on the interest rate, substantial hydrogen production in 2030 starts above 100 €/$MWh_{H2,LHV}$ (7% WACC) and 130 €/$MWh_{H2,LHV}$ (12% WACC). Taking into account hydrogen pipeline transport costs (cf. section 6.2.2.5), the supply curves of hydrogen produced in MENA for Europe start above 120 €/$MWh_{H2,LHV}$ (7% WACC) and 150 €/$MWh_{H2,LHV}$ (12% WACC). Synthetic methane is more expensive due to the additional synthesis step and the required CO_2 capture. In 2030, substantial methane production starts above sales prices of 170 €/$MWh_{CH4,LHV}$ at 7% WACC and above a sales price of 210 €/$MWh_{CH4,LHV}$ at 12% WACC. Methane pipeline transportation costs to Europe (cf. section 6.2.2.5) mean that the potential MENA supply of synthetic methane to Europe starts above 180 €/$MWh_{CH4,LHV}$ (7% WACC) and 220 €/$MWh_{CH4,LHV}$ (12% WACC). The spread in interest rates between model runs shows that higher interest rates not only shift the supply curves for electricity-based hydrogen and methane each to the right but also flatten their respective trajectories.

Additional liquefaction increases the costs of hydrogen and methane and shifts the supply curves of the electricity-based energy carriers further to the right. In 2030, the production of substantial amounts of liquefied hydrogen starts above a sales price of 150 €/$MWh_{H2,LHV}$ with a WACC of 7%, and above 180 €/$MWh_{H2,LHV}$ with a WACC of 12%. Substantial synthetic liquid methane production starts above a sales price of 180 €/$MWh_{CH4,LHV}$ (7% WACC). A higher WACC of 12% causes the MENA supply curve to start above 230 €/$MWh_{CH4,LHV}$.

Liquid hydrogen and liquid methane are more expensive to export to Europe than their gaseous counterparts. Although the costs of transporting liquid methane by ship are lower than those of transporting gaseous methane by pipeline for the distances considered here (see sections 6.2.2.5 and 6.3.2.2), this cannot compensate for the additional costs of liquefaction. European supply of liquid methane imported from MENA starts above sales prices of 190 €/$MWh_{CH4,LHV}$ (7% WACC) and 240 €/$MWh_{CH4,LHV}$ (12% WACC). Liquid hydrogen from MENA is available in Europe above sales prices of 190 €/$MWh_{H2,LHV}$ (7% WACC) and 220 €/$MWh_{H2,LHV}$ (12% WACC).

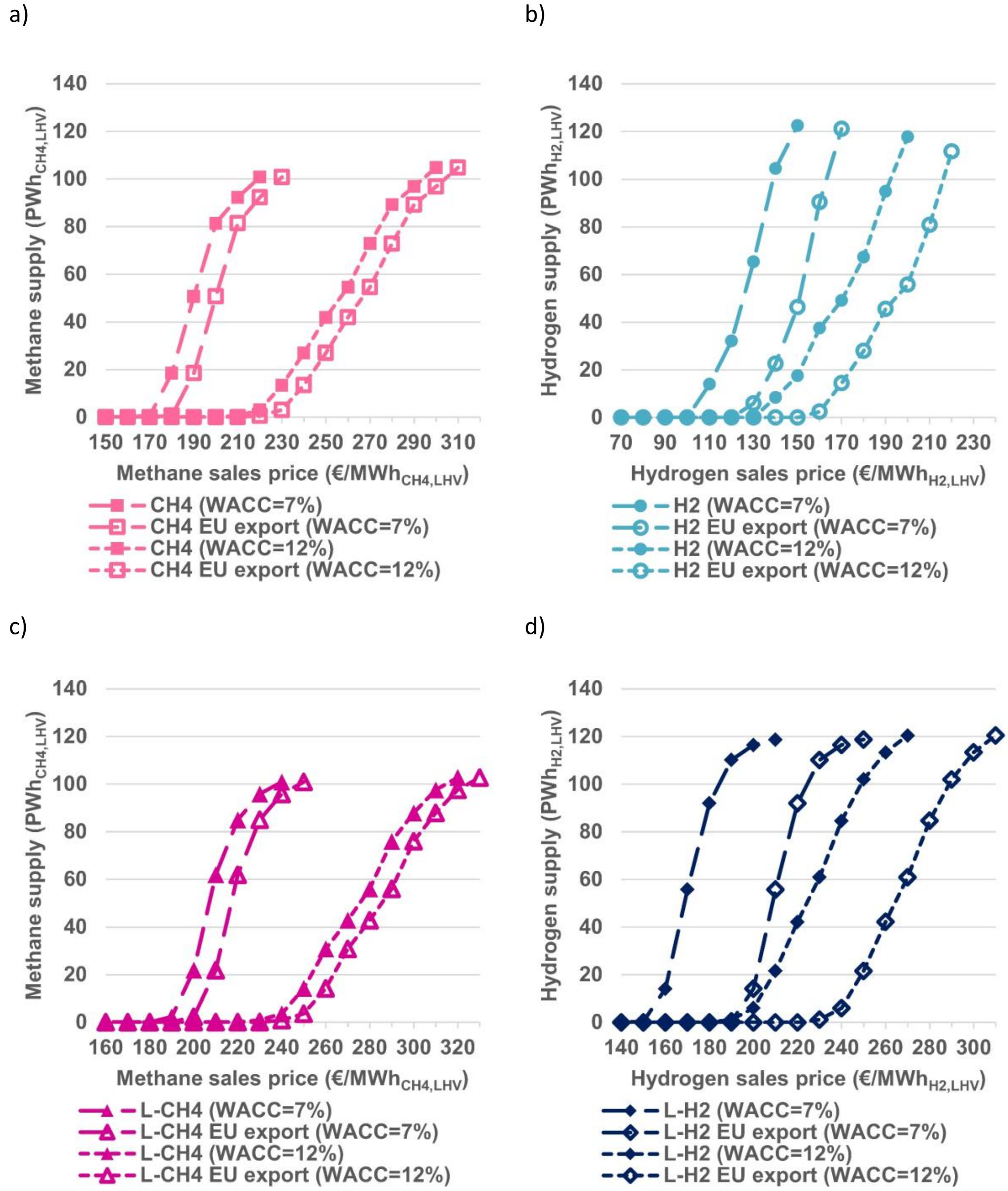

Figure 6-8 Supply curves of e-fuels in the MENA region including and excluding transportation to the EU in 2030. Production and export quantities of a) methane (CH4), b) hydrogen (H2), c) liquefied methane (L-CH4), and d) liquefied hydrogen (L-H2) are shown for a weighted average cost of capital (WACC) of 7% and 12%.

Technological learning reduces the generation costs of e-fuels between 2030 and 2050. This cost reduction affects not only the components of the PtG process chains but also the power generation technologies. Figure 6-9 shows left shifts in the supply curves for 2050 compared to 2030. Substantial hydrogen production in MENA in 2050 starts above sales prices of 70 €/MWh$_{H2,LHV}$ (7%

WACC) and 90 €/MWh$_{H2,LHV}$ (12% WACC), depending on the weighted average cost of capital. Electricity-based methane is available at sales prices starting above 120 €/MWh$_{CH4,LHV}$ (7% WACC) and 160 €/MWh$_{CH4,LHV}$ (12% WACC). The additional liquefaction of hydrogen increases the generation costs by at least 40 €/MWh$_{H2,LHV}$. This shifts the start of the hydrogen supply curve for liquid hydrogen to 110 €/MWh$_{H2,LHV}$ at a WACC of 7% and to 150 €/MWh$_{H2,LHV}$ at a WACC of 12%. In the model results in 2050, substantial liquid methane production starts above 130 €/MWh$_{CH4,LHV}$ (7% WACC) and 180 €/MWh$_{CH4,LHV}$ (12% WACC).

As in 2030, exporting gaseous hydrogen and methane to Europe in 2050 is cheaper than their respective liquid forms when production and transport are taken into account. The supply of substantial amounts of gaseous hydrogen from MENA to Europe starts above a sales prices of 90 €/MWh$_{H2,LHV}$ (7% WACC) and 120 €/MWh$_{H2,LHV}$ (12% WACC). Substantial exports of gaseous methane from MENA to Europe are available starting above sales prices of 130 €/MWh$_{CH4,LHV}$ (7% WACC) and 170 €/MWh$_{CH4,LHV}$ (12% WACC).

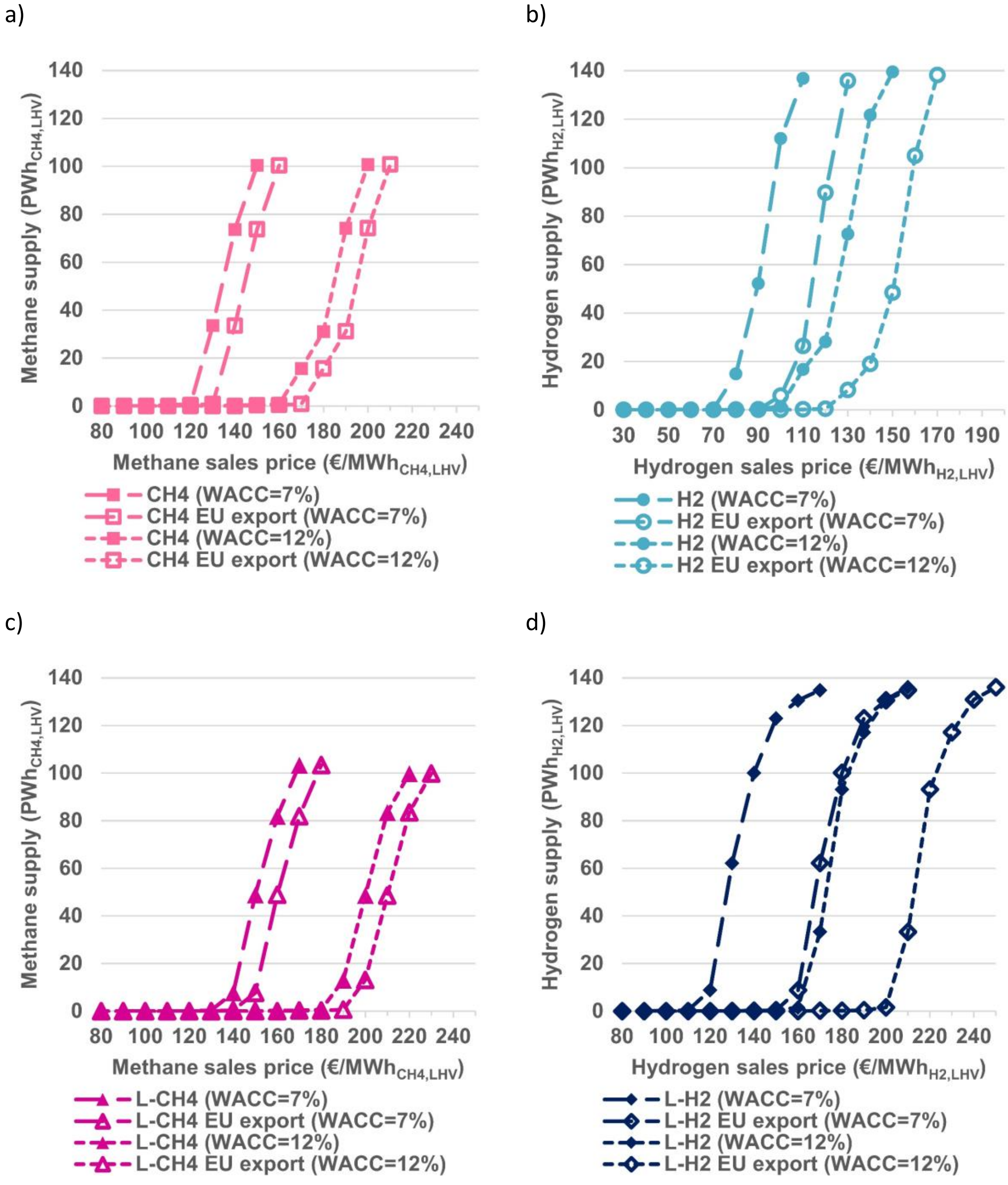

Figure 6-9 Supply curves of e-fuels in the MENA region including and excluding transportation to the EU in 2050. Production and export quantities of a) methane (CH4), b) hydrogen (H2), c) liquefied methane (L-CH4), and d) liquefied hydrogen (L-H2) are shown for a weighted average cost of capital (WACC) of 7% and 12%.

6.3.2.2 Cost components of e-fuel production

Figure 6-10 shows the cost components associated with the production of e-fuels in the MENA region for 2030 and 2050. Each bar corresponds to a point on the supply curves in section 6.3.2.1. Selected supply curve points exceed the hydrogen or synthetic methane production of

1,000 $TWh_{H2/CH4,LHV}$ for the first time. This choice is arbitrary, yet assumes substantial generation quantities and a strong role of the MENA region in a future global e-fuel market. The figure aims at comparability between different e-fuel production concepts. However, a direct consequence of this benchmark approach is that different e-fuel generation volumes lie behind the bars shown in the cost breakdown.

The optimization results show that renewable electricity is the most important cost component for synthetic methane production. Depending on the simulation year, physical state of the product, and assumed WACC, electricity supply accounts for between 65% and 72% of methane production (excluding transportation costs to Europe). Annuitized investments and fixed operation and maintenance costs represent the missing 28% to 35% of methane production costs in MENA. The cost of transport to Europe — accounting for between 2.0 €/$MWh_{CH4,LHV}$ and 2.7 €/$MWh_{CH4,LHV}$ via ship and between 3.5 €/$MWh_{CH4,LHV}$ and 7.3 €/$MWh_{CH4,LHV}$ via pipeline depending on the transport distance — is negligible compared to generation costs.

The technology with the highest cost contributions in methane production is electrolysis. This applies both to electricity costs, where its share is always at least 81%, and to fixed-cost components, with a share of at least 36%. Overall, electrolysis accounts for at least 69% of synthetic methane production costs without transport. The second largest cost contribution derives from CO_2 supply. It accounts for between 10% and 15% of methane production costs depending on the simulation year, physical state of the product, and assumed WACC. The cost contribution of DAC is dominated by fixed-cost components. Seawater desalination and methanation as well as intermediate compression costs lag behind those of electrolysis and DAC and are mainly fixed costs. If methane is liquefied for subsequent transport to Europe, this accounts for 8% to 10% of production cost in MENA, depending on the simulation year and assumed WACC.

The cost composition of electricity-based hydrogen depends strongly on the physical state in which it is provided. Nevertheless, electrolysis — in particular the electricity demand of the electrolysis process — remains the largest cost component in the supply of hydrogen. In the case of gaseous supply, at least 95% of the hydrogen production costs are attributable to electrolysis. At least two thirds of the electrolysis costs are electricity input; the rest are annuitized investments and fixed operation and maintenance costs. If the gaseous hydrogen is subsequently exported to Europe by pipeline, the transport costs account for 9% to 27% of the supply costs in Europe depending on the transportation distance, simulation year, and assumed WACC. If hydrogen is exported to Europe in liquid form, liquefaction and ship transport together account for a substantial part of the supply costs at 35% to 42%. However, in liquid hydrogen production — without transport — electrolysis remains the technology with the largest cost contributions in the production chain. Depending on the simulation year and assumed WACC, electrolysis accounts for between 67% and 69% of liquefied hydrogen production costs. At least 79% of the electrolysis costs are electricity costs. Desalination of seawater is a minor component compared to other process steps.

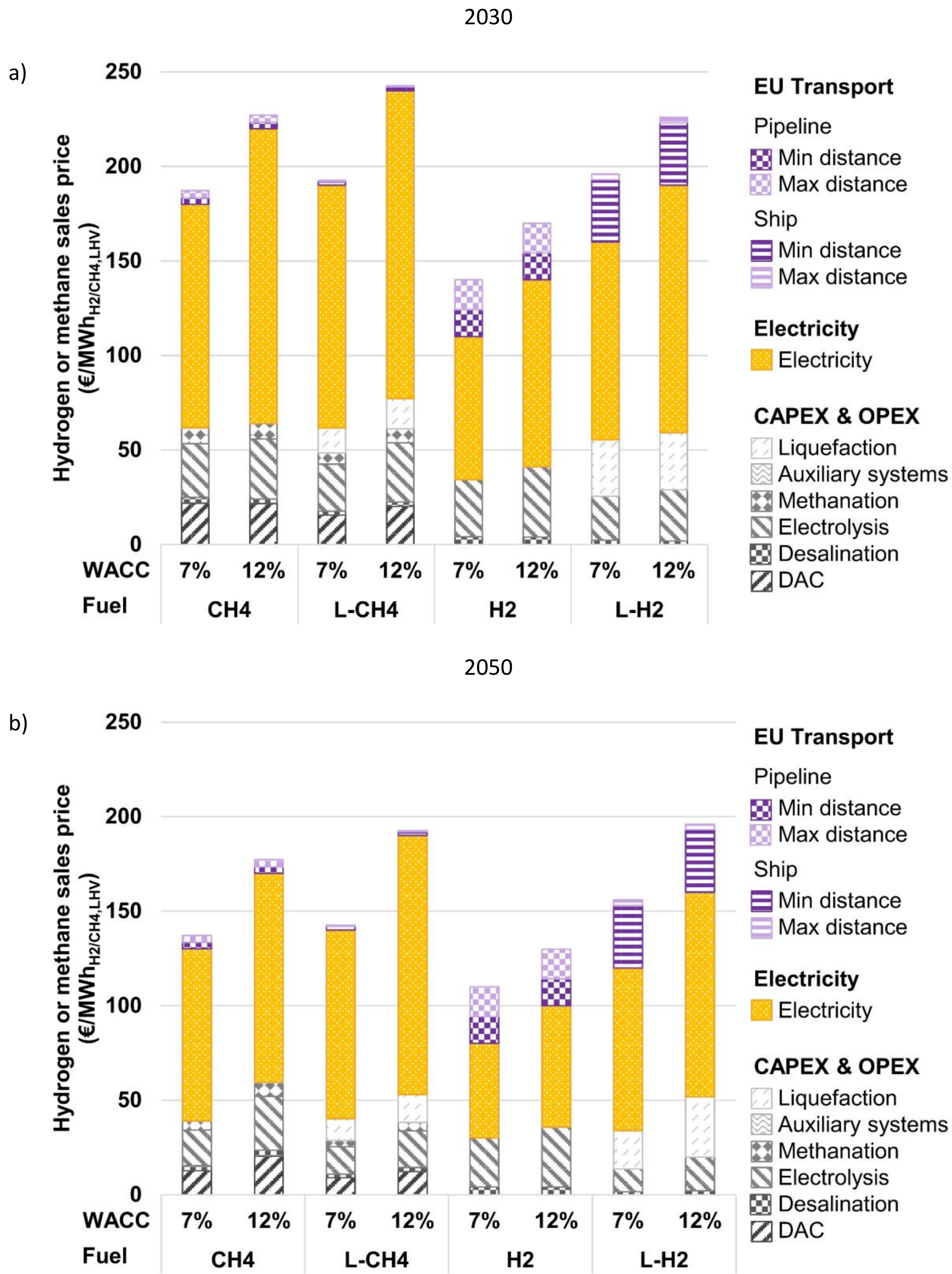

Figure 6-10 Supply cost components of electricity-based hydrogen (H2), liquefied hydrogen (L-H2), methane (CH4), and liquefied methane (L-CH4) at WACC of 7% and 12% in MENA and as exports to Europe in 2030 (a) and 2050 (b). Selected points on the supply curves behind the bars have

in common that the e-fuel generation volume exceeds 1,000 $TWh_{H2/CH4,LHV}$ for the first time. Consequently, bars correspond to different e-fuel production volumes. The range of transportation costs derives from minimum and maximum distances between regions centers of e-fuel production regions in MENA and the European region center.

6.3.2.3 Comparison of PEM-based and SOEC-based e-fuel production

The choice of electrolyzer technology for e-fuels production in the MENA region is subject to high uncertainties. In particular, the PEM and SOEC technologies considered in this article are currently at different stages of development (see section Appendix D). Nevertheless, it is possible to deduce techno-economic characteristics that may be decisive for the choice of electrolysis in the long term from the model results.

The model results for the year 2050 show that process chains with higher overall capital intensities rely more heavily on SOEC electrolysis. Depending on the assumed WACC, the SOEC-based process chain is used on average between 58% (7% WACC) and 82% (12% WACC) for liquid hydrogen production in 2050. For liquid methane production, the average use of the SOEC chain ranges from 61% (7% WACC) to 85% (12% WACC). In the model results, the SOEC chains achieve high full load hours of over 7,500 hours per year regardless of the final product. Overall, capital-intensive process chains therefore benefit from the higher efficiency of SOEC and allocate fixed-cost components over many operating hours.

In contrast, for the production of gaseous hydrogen and methane, the model focuses on the PEM-based process chains. Depending on the assumed WACC, the PEM-based process chain is used on average between 72% (7% WACC) and 75% (12% WACC) for the production of gaseous hydrogen in 2050. For gaseous methane production, the average use of the PEM chain ranges from 52% (7% WACC) to 59% (12% WACC). The full load hours of the PEM chains lie between 2,700 and 4,000 hours per year, depending on the final product. Overall, less capital-intensive process chains are therefore less dependent on the higher efficiency of SOEC and instead rely on the lower fixed costs of PEM.

6.3.3 Electricity system for e-fuel production in the MENA region in 2050

Figure 6-11 shows the optimization result of electricity supply and demand compositions for selected points on the e-fuel supply curves for 2050. The selection of the points aims at substantial e-fuel generation quantities and electricity supply that is as comparable as possible. Consequently, the e-fuel generation quantities behind the bars differ.

On the demand side, Figure 6-11 shows that due to the very high renewable electricity generation potential in the MENA region, the normal load of the MENA countries can potentially be exceeded by a multiple of electricity input for e-fuel generation. For the selected points on the supply curves, the electricity demand for e-fuel production is at least 91% of the total electricity demand. The amount of curtailed electricity in the optimization results is small overall with a maximum of 5% in the case of liquefied hydrogen and a WACC of 12%.

The supply side is dominated by solar generation technologies for all e-fuels and configurations studied. At a WACC of 7%, PV and CSP account for between 97% and 100% of the electricity generation mix. Increasing the WACC from 7% to 12% leads to an increase in the onshore wind share of electricity generation for all four electricity-based energy carriers considered (hydrogen, liquefied hydrogen, synthetic methane, and liquefied synthetic methane). However, the proportion of wind in the electricity mix remains comparatively low with a maximum of 13% for gaseous methane production.

Higher capital intensity in the production of electricity-based fuels increases the share of CSP in the electricity generation mix. Firstly, this can be seen when comparing hydrogen and methane production. The additional synthesis step and technical equipment used in methane production increase the capital intensity compared to similar production routes for electricity-based hydrogen. This leads to higher CSP shares in each case. Secondly, additional liquefaction in particular increases the capital costs of the overall process chains compared to gaseous supply. In the optimization result, liquefaction and the associated increase in capital intensity leads to an increase in the CSP share compared to the gas-based generation routes. This effect can be explained by the higher full load hours of electricity production of CSP compared to PV. The thermal intermediate storage of energy in CSP allows higher investments to be allocated to more operating hours of the PtG process chains.

In the energy systems in Figure 6-11, the model uses battery storages in 400 to 900 hours of a year to increase the full load hours of the PtG generation plants. Battery storage systems exhibit higher utilization in calculations with a WACC of 12%. The batteries allow fixed-cost components of the PtG plants, which are more pronounced at a WACC of 12%, to be allocated to more operating hours.

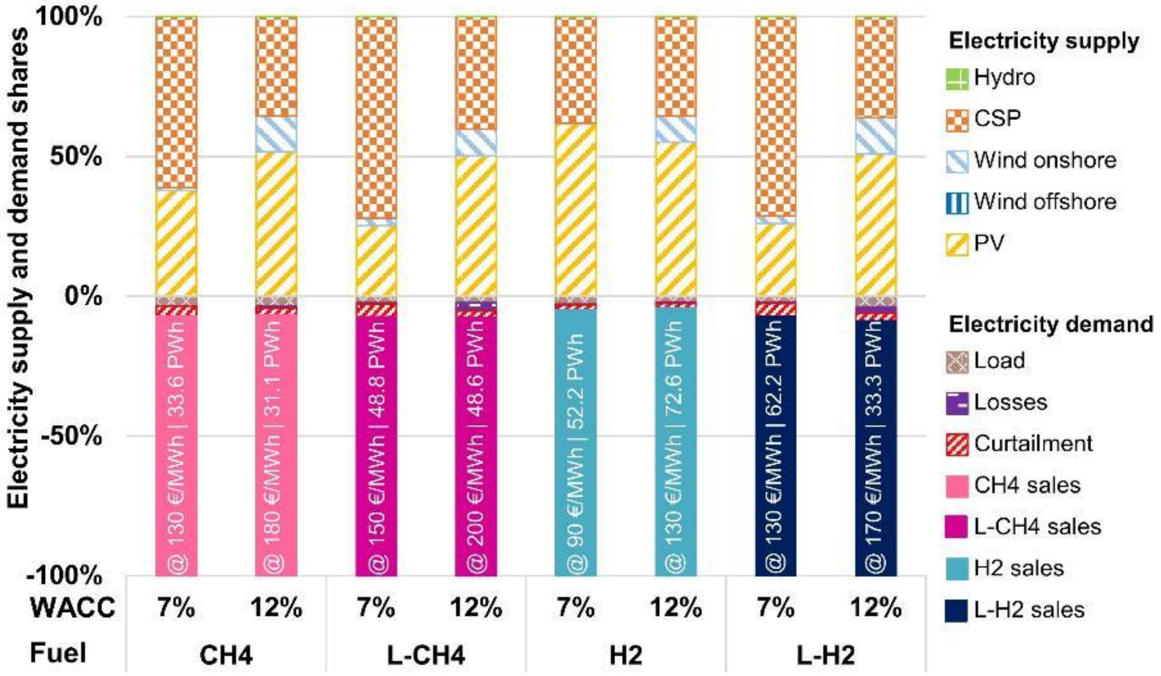

Figure 6-11 Electricity generation and demand mixes in MENA in 2050. Selected bars belong to different production volumes of e-fuels, but aim at comparability of the underlying power systems.

6.3.4 Regional distribution of e-fuel supply

Figure 6-12 shows the evolution of the renewable energy expansion along the supply curve of gaseous synthetic methane at a WACC of 7% for the year 2050. In the optimization results, synthetic methane generation starts with small production quantities at a selling price of 120 €/$MWh_{CH4,LHV}$ in Egypt (439 $TWh_{CH4,LHV}$), Saudi Arabia (219 $TWh_{CH4,LHV}$), Jordan (71 $TWh_{CH4,LHV}$), and Morocco (61 $TWh_{CH4,LHV}$). The division of the MENA countries into sub-regions, where e-fuels can only be generated in the coastal regions and electricity generation in the hinterland is subject to grid penalties, results in a gradual exploitation of the electricity generation potential in the hinterland. This happens despite the flat generation cost structure of renewable energies shown in section 6.3.1. The coloring of the maps shows that at a sales price of 130 €/$MWh_{CH4,LHV}$ methane production is expanded by the optimizer. The first substantial synthetic methane quantities are produced especially in Saudi Arabia (16,404 $THW_{CH4,LHV}$), Egypt (9,269 $THW_{CH4,LHV}$), Libya (5,650 $THW_{CH4,LHV}$), and Morocco (1,006 $THW_{CH4,LHV}$). This results in a roll-out of PV in the coastal regions and the build-up of CSP capacities, which already reach further inland. The expansion of onshore wind power at this methane sales price is limited to the aforementioned individual hotspots in Morocco, Libya, and Egypt. At a methane sales price of 150 €/$MWh_{CH4,LHV}$, the model results are dominated by high power densities for CSP and PV outside of Turkey, Lebanon, and Israel.

Distance-dependent cost premiums for pipeline transport of synthetic methane from MENA to Europe do not change the order of the first exporting countries given the accuracy of our result resolution. Assuming a WACC of 7%, the first substantial exports of gaseous synthetic methane to Europe in 2050 start at a selling price of 140 €/$MWh_{CH4,LHV}$ from Saudi Arabia (16,404 $TWh_{CH4,LHV}$), Egypt (9,269 $TWh_{CH4,LHV}$), and Libya (5.650 $TWh_{CH4,LHV}$).

The first substantial hydrogen production quantities for the MENA region and a WACC of 7% appear in the model results at a sales price of 80 €/$MWh_{H2,LHV}$. At this sales price hydrogen is mainly produced in Saudi Arabia (5,030 $TWh_{H2,LHV}$), Egypt (4,132 $TWh_{H2,LHV}$), and Libya (3,854 $TWh_{H2,LHV}$). Based on our measurement accuracy and using distance-based cost premiums for pipeline transport of gaseous hydrogen from MENA to Europe, the order of exporting countries changes at the beginning of the supply curve. The first substantial hydrogen volumes are provided in Europe at a sales price 100 €/$MWh_{H2,LHV}$ from Libya (3,854 $TWh_{H2, LHV}$) and Morocco (910 $TWh_{H2,LHV}$). Due to the further distance, Saudi Arabia exports substantial amount of hydrogen (5,030 $TWh_{H2,LHV}$) to Europe only starting at a selling price of 110 €/$MWh_{H2,LHV}$.

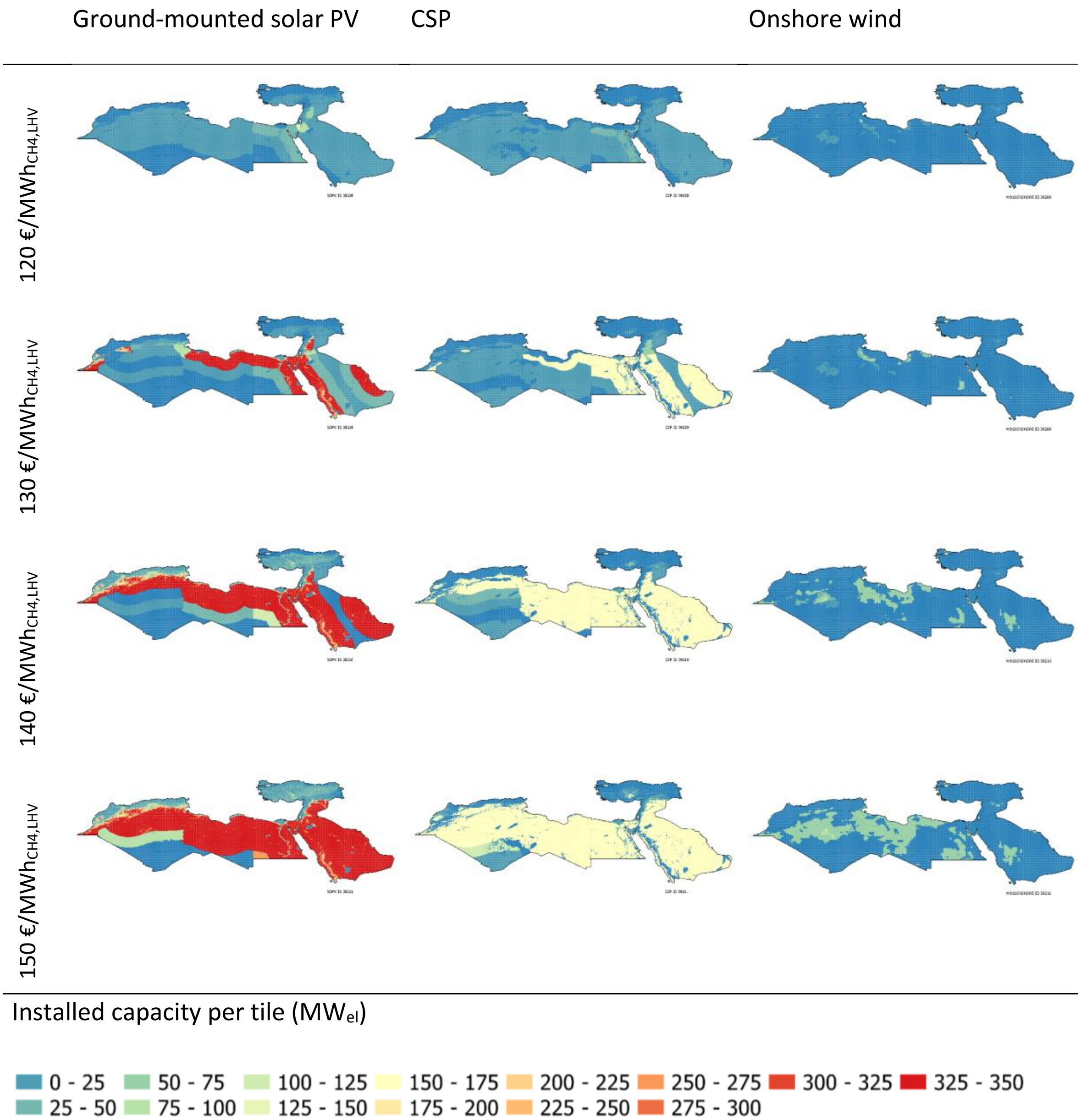

Figure 6-12 Evolution of renewable electric capacities for PV, CSP, and onshore wind for gaseous synthetic methane production at rising sales prices and a weighted average cost of capital of 7% in 2050.

6.3.5 Competition on the European hydrogen market

One criterion for deciding whether hydrogen from the MENA region can become part of the European supply mix is the relationship between the supply costs of European hydrogen and hydrogen imported from MENA.

Figure 6-13 shows a comparison of the supply costs of hydrogen in Europe, which is either produced in Europe itself or imported from MENA. The supply curves of a European production are taken from (Lux et al. 2020). In general, the modeling approach used to calculate European supply curves and the MENA import curves is similar. However, since Lux et al. (2020) was published, there has been a cost update for renewable electricity generation technologies in *Enertile*. The update has resulted in structurally lower renewable electricity generation costs. The European hydrogen supply curves in Figure 6-13 are therefore subject to higher electricity production costs than the hydrogen import curves from the MENA region. A second difference between the model parameterizations in Lux et al. (2020) and scenario runs in this article applies to the used techno-economic data for electrolyzers[12]. In both cases MENA import and European production costs for the local distribution of hydrogen are not considered.

The comparison of the model results shows that the import curves remain below the European supply curves up to a hydrogen price of 90 €/MWh$_{H2,LHV}$. Up to this sales price and corresponding hydrogen quantities, domestic-European hydrogen supply is more cost-efficient. Assuming the same WACC of 7% for Europe and MENA, the import of gaseous hydrogen from the MENA region becomes economically attractive starting at hydrogen demands between 488 TWh$_{H2,LHV}$ and 1,118 TWh$_{H2,LHV}$, depending on the electrolyzer parametrization in Lux et al. (2020). If the import of hydrogen is subject to substantially higher risk premiums or profit margins realized in the model runs by a WACC of 12%, the import of hydrogen is only profitable compared to domestic European production starting above hydrogen quantities between 2,044 TWh$_{H2,LHV}$ and 3,571 TWh$_{H2,LHV}$. The intersection of the supply curves for liquid hydrogen imports from MENA with the European supply occurs above hydrogen sales prices of 150 €/MWh$_{H2,LHV}$ and European hydrogen supplies of 4,111 TWh$_{H2,LHV}$.

In compliance with the 1.5 °C target, the long-term strategic vision of the EC estimates a final energy demand for hydrogen in Europe in 2050 between 794 TWh$_{H2}$ (1.5LIFE scenario) and 892 TWh$_{H2}$ (1.5TECH scenario) (EC 2018a). The comparison of hydrogen supply curves between European production with the central electrolyzer parametrization and MENA imports in Figure 6-13 implies that, from a techno-economic point of view, these demands could be partly met by MENA imports, if Europe and MENA are subject to the same interest rates. For the progressive electrolyzer parametrization in Europe and a WACC of 7% hydrogen demands could be met cost efficiently by an inner European production. If MENA imports are assigned a higher WACC of 12%, these European hydrogen demands would be met by domestic European hydrogen production independently of the electrolyzer parameter scenario in Europe. However, imports could also be necessary if the RES potential in Europe cannot be sufficiently utilized due to lack of public acceptance.

[12] In (Lux et al. 2020), hydrogen supply curves are calculated for three different techno-economic parameterizations of PEM electrolyzers. The conservative version of the electrolysis parameters is not shown in this graph, because it lacks comparability with the parameterization for the MENA region.

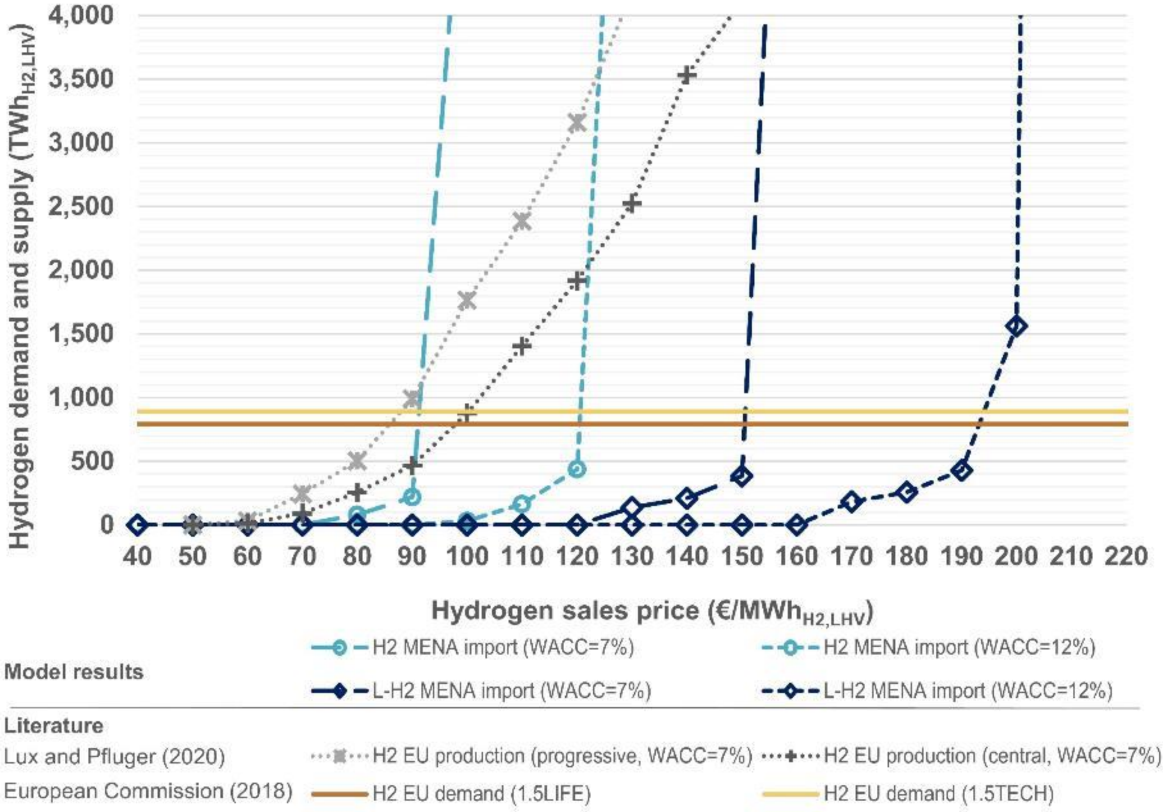

Figure 6-13 Competition on the European hydrogen market in 2050. Modeled export curves from the MENA region are compared with literature values (Lux et al. 2020) for domestic European production. The hydrogen demand from the EC (2018a) for the year 2050 serves as a reference.

6.4 Summary & Conclusions

This article identifies the generation potentials of the electricity-based fuels hydrogen and synthetic methane for the MENA region in 2030 and 2050. For the generation of these e-fuels, it is assumed that only renewable electricity is used. The analysis is performed with the energy system optimization model *Enertile*. Based on the model results, the export of e-fuels from MENA to Europe is also considered using distance dependent transport costs.

The energy system optimization in *Enertile* is based on an assessment of renewable electricity potentials in the MENA region at high resolution. The resulting cost potential curves and the distribution of the considered renewable technologies show that PV and CSP are the most cost-efficient technologies in the MENA region. The wind potential in the MENA region lags behind solar technologies in its suitability for producing e-fuels. Electricity generation by wind at low cost is limited to individual hot spots on the coast and in some inland areas. Cheap renewable power generation potentials in coastal areas are located in Egypt, Saudi Arabia, Libya, and Morocco. Following the scenario architecture, which postulates that e-fuels are only produced in coastal regions, these countries make the first and least expensive contributions to e-fuel production in the model calculations.

The cost potential curves are calculated for two different assumptions regarding the weighted average cost of capital (WACC), 7% and 12%. The model results for the generation of e-fuels show that substantial amounts of gaseous hydrogen can be produced in MENA in 2030 starting above a production cost of 100 €/MWh$_{H2,LHV}$ (7% WACC) and 130 €/MWh$_{H2,LHV}$ (12% WACC). In 2050, the start of the hydrogen supply curves drops to above 70 €/MWh$_{H2,LHV}$ (7% WACC) and 90 €/MWh$_{H2,LHV}$ (12% WACC). As the supply curves progress, they show a steep increase in production volumes. Additional liquefaction increases hydrogen supply cost by at least 40 €/MWh$_{H2,LHV}$.

Due to the additional synthesis step and the required CO_2 capture, the production of synthetic methane is more expensive than electricity-based hydrogen. In the model results, a substantial gaseous methane production in 2030 starts above a generation cost of 170 €/MWh$_{CH4,LHV}$ (7% WACC) and 210 €/MWh$_{CH4,LHV}$ (12% WACC) in MENA. In 2050, the model results show substantial synthetic methane generation volumes above generation costs of 120 €/MWh$_{CH4,LHV}$ (7% WACC) and 160 €/MWh$_{CH4,LHV}$ (12% WACC). The supply curve of methane also shows a steep increase for rising sales prices. Additional liquefaction increases the cost of synthetic methane by at least 10 €/MWh$_{CH4,LHV}$.

A cost comparison shows that exporting gaseous hydrogen and methane to Europe is cheaper than transporting their respective liquid forms. Taking into account methane pipeline transportation costs to Europe, the potential MENA supply of synthetic methane from MENA to Europe starts above 180 €/MWh$_{CH4,LHV}$ (7% WACC) and 220 €/MWh$_{CH4,LHV}$ (12% WACC) in 2030. Equivalent export curves of hydrogen produced in MENA for Europe start above 120 €/MWh$_{H2,LHV}$ (7% WACC) and 150 €/MWh$_{H2,LHV}$ (12% WACC). In 2050, exports of gaseous methane from MENA to Europe are available starting at sales prices above 130 €/MWh$_{CH4,LHV}$ (7% WACC) and 170 €/MWh$_{CH4,LHV}$ (12% WACC). The supply of hydrogen produced in MENA for Europe in 2050 starts at sales prices above 90 €/MWh$_{H2,LHV}$ (7% WACC) and 120 €/MWh$_{H2,LHV}$ (12% WACC), respectively.

The cost of renewable electricity is decisive for e-fuel production costs, accounting for at least 62% of e-fuel generation costs in the production chains examined. For both hydrogen and synthetic methane production, the technology with the highest cost contributions is electrolysis. Regardless of the simulation year and assumed WACC, electrolysis accounts for at least 95% of gaseous hydrogen production costs and at least 69% of the costs in synthetic methane production. The second major cost component in methane production is CO_2 supply from ambient air. It accounts for 10% to 15% of generation costs, depending on the physical state of the product, simulation year, and assumed WACC. The remaining plant components, seawater desalination and methanation, are less prominent in the overall costs. Cost reductions between the simulation years 2030 and 2050 are due to lower costs for renewable electricity and technical learning of the e-fuel production chains.

The production of electricity-based renewable gases is characterized by the large and low-cost solar power generation potentials in the MENA region. PV and CSP account for at least 87% of the electricity mix for e-fuel production in all constellations studied. Increasing capital intensity by liquefying or processing hydrogen into methane increases the share of CSP in the generation mix, due to its relatively high full load hours in electricity generation. Wind energy plays a relatively small role in e-fuel generation in MENA. The maximum share of onshore wind in the generation mix of the MENA region is 13% in the model results.

The comparison of the calculated hydrogen supply in the MENA region with equivalent supply curves in Europe shows that hydrogen trade flows from MENA to Europe can only be cost-efficient within certain limits. In order to have hydrogen export flows from MENA to Europe in a competitive market context, the following two conditions need to be fulfilled. Firstly, there is no interest rate spread or only a low interest rate spread between Europe and the MENA countries. This means that investors are willing to develop projects in MENA at similar financing conditions as in Europe. Secondly, the transportation costs for hydrogen are low. Transportation costs by pipeline account for a substantial proportion of hydrogen supply costs from MENA in Europe. In the current literature, these transportation costs are characterized by large spreads and uncertainties. Nevertheless, an effective shortage of sites for expanding renewable electricity generation in Europe could be a game changer and may lead to hydrogen imports from MENA. This may arise, for example, from high electricity demands accompanied with low acceptance for a widespread expansion of renewable electricity generation units in Europe.

The analysis also has relevance for policy decisions: First of all, it broadens the perspective regarding the costs of e-fuel imports: Several previous publications use somewhat simplified assumptions, for example regarding the price of electricity used in hydrogen production, or assume very low interest rates. The more holistic framework used in this analysis provides a more comprehensive picture of the costs incurred. The higher costs resulting from this show that importing e-fuels to Europe is not a cheap silver bullet to circumvent bottlenecks in renewable energy expansion or achieve supply side transformation. The cost of e-fuels have to be weighed up against other options. The analysis also hints at certain regions that might be most suitable for producing e-fuels for exports. However, the differences in site quality vary within a range, in which other factors might be equally important, such as transport costs and interest rate expectations for individual countries or even projects.

Analyzing e-fuel production chains in detail and considering transport also highlights the complexity and sheer size of these potential projects. Too often hydrogen and e-fuel imports are used as the gap-filler in national energy transformation strategies. The deeper analysis shows that these projects are too large and too costly to happen without strong policy support and without high security that the energy products will be bought long-term at agreed prices. Policy makers aiming at importing hydrogen or e-fuels should start developing policies in this direction soon, as infrastructure projects of the sizes discussed here have a considerable lead time.

Overall, the analysis shows that e-fuel production in the MENA region is indeed attractive, especially due to its high solar potential. However, the question of whether utilizing this potential for Europe's energy supply makes sense from a strictly economic point of view is not answered definitively. Differences in capital costs and transport costs may reduce or even nullify the advantages of the region. Future analysis should analyze these aspects in even greater detail and take price formation on international energy commodity markets into account.

CRediT authorship contribution statement

Benjamin Lux: Conceptualization, Methodology, Investigation, Visualization, Data curation, Writing - original draft, Writing - review & editing.

Johanna Gegenheimer: Data curation, Writing - original draft, Writing - review & editing.

Katja Franke: Methodology, Writing - original draft, Writing - review & editing.

Frank Sensfuß: Supervision.

Benjamin Pfluger: Conceptualization, Writing - original draft, Writing - review & editing, Supervision.

Declaration of Competing Interest

The authors declare that they have no known competing financial interests or personal relationships that could have appeared to influence the work reported in this paper.

Acknowledgments

The main content of the paper is closely related to the research work in the project MethQuest, which received funding from the Federal Ministry for Economic Affairs and Energy on the basis of a decision by the German Bundestag.

For contribution of their extensive experience with Power-to-Gas technologies, the authors thank the following project partners of MethQuest/MethFuel:

- Elogen.
- EIfER - European Institute for Energy Research.
- Karlsruhe Institute of Technology, Engler-Bunte-Institute, Division of Fuel Technology.
- Technical University of Berlin - The Electrochemical Energy, Catalysis and Material Science Group.

The authors also gratefully acknowledge Frank Graf, Friedemann Mörs and Janina Leiblein from the DVGW Research Center at Engler-Bunte-Institut of Karlsruhe Institute of Technology (KIT) for sharing their extensive knowledge in the field of Power-to-Gas and for their valuable comments.

Funding

This work was supported by funding of the German Federal Ministry for Economic Affairs and Energy [O20E-100335368].

6.5 Appendix

Appendix A.Abbreviations

Table 6-8 Abbreviations.

Abbreviation	Explanation
BEV	Battery electric vehicles
BoL	Begin of life
CAPEX	Capital expenditure
CH_4	Methane
CO_2	Carbon dioxide
CSP	Concentrating solar power
DAC	Direct air capture, CO_2 separation from ambient air
EC	European Commission
EU	European Union
e-fuels	Electricity-based fuels
el	electrical
FLH	Full load hours
GHG	Greenhouse gas
H_2	Hydrogen
L-hydrogen	Liquefied hydrogen
L-methane	Liquefied methane
LCOE	Levelized cost of electricity
LHV	Lower heating value
LNG	Liquefied natural gas
MENA	Middle East and North Africa

Abbreviation	**Explanation**
O&M	Operation and maintenance cost
OPEX	Operating expenditure
PEMEL	Polymer electrolyte membrane electrolysis
PtG	Power-to-Gas
PtH_2	Power-to-Hydrogen
$PtCH_4$	Power-to-Methane
PtX	Power-to-X
PV	Photovoltaics
RES	Renewable energy source
SED	Specific energy demand
STP	Standard temperature and pressure (T_{STP} = 0 °C, p_{STP} =1.01325 bar).
SOEL	Solid oxide electrolysis
th	thermal
TRL	Technology readiness level
WACC	Weighted average cost of capital
wt	weight

Appendix B.Substance data

Table 6-9 Substance data.

Substance data		
Density of water (at 0 °C)	999.8	kg/m^3
Higher heating value (HHV) of natural gas	50.0	MJ/kg
HHV of H_2	141.8	MJ/kg
Lower heating value (LHV) of H_2	120.0	MJ/kg
HHV of CH_4	55.5	MJ/kg
LHV of CH_4	50.0	MJ/kg
Molar mass of H_2	2.0	g/mol
Molar mass of CH_4	16.0	g/mol
Molar mass of water	18.0	g/mol
Molar volume at standard temperature and pressure (STP)	22.4	$m^3/kmol$

Appendix C. Model regions and transport distances to Europe

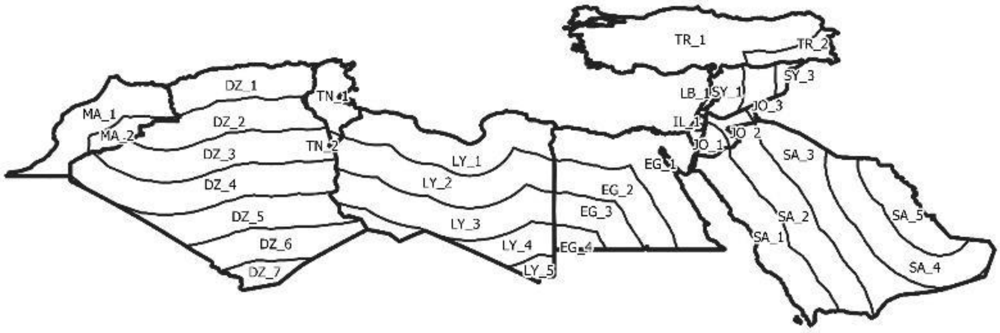

Figure 6-14 Model regions for Enertile calculations in the MENA region.

Table 6-10 Transport distances assumed between e-fuel production regions in MENA and Europe. Transport distances are estimated by the center-to-center air distance of MENA and continental Europe. In reality, transport routes are likely to be different.

Transport distances from e-fuel production regions in MENA to Europe		
DZ_1	2,098	km
EG_1	3,143	km
IL_1	2,981	km
JO_1	3,119	km
LB_1	2,788	km
LY_1	2,507	km
MA_1	2,778	km
SA_1	3,988	km
SA_5	4,344	km
SY_1	2,790	km
TN_1	2,073	km
TR_1	2,232	km

Appendix D. Technologies and techno-economic parameters of PtG process chains

This section covers details of individual PtG technologies within the e-fuel production chains presented in section 6.2.2.4. Table 6-11 shows the specific energy demands of individual PtG technologies. Table 6-12 and Table 6-13 show specific investments and fixed operation and maintenance cost of individual PtG technologies.

Water electrolysis, in which water is electrochemically divided into hydrogen and oxygen, is the main process step for hydrogen production. This paper examines PEMEL and SOEL systems, which differ for example in the type of membrane used and the operating conditions (Adolf et al. 2017; Golling et al. 2019; Smolinka et al. 2018; Töpler et al. 2016; Ursua et al. 2012). Figure 6-4 and Figure 6-5 in section 6.2.2.4 specify the operating temperatures and pressures, chosen for the techno-economic parametrization. As SOEL operates with steam, thermal energy is required at approximately 200 °C for water evaporation. This makes SOEL particularly promising when heat is available at the site. However, PEMEL offers the advantage of operating over a wide load range (Smolinka et al. 2018) and allows a quick response to power fluctuations from RES. PEMEL has already reached a high technology readiness level (TRL) of 9. SOEL is a newer technology (TRL 6) and its development is therefore associated with greater opportunities but also with higher risks (Golling et al. 2019). According to the literature, further optimization of PEMEL and SOEL, e. g. of cell and stack design, will lead to an increase in efficiency over the next 30 years (Smolinka et al. 2018). Efficiencies of electrolyzers given in the literature usually refer to begin of life (BoL). For the *Enertile* parametrization, efficiency reduction for PEMEL and SOEL due to stack degradation is taken into account through the author's own estimations, based on technical key data from the literature (Smolinka et al. 2018) (cf. Table 6-11). Accordingly, replacement of the stacks over the system lifetime of 20 years is included in the fixed OPEX (Table 6-13).

Currently commercially available electrolysis processes require freshwater as feedstock. In the arid MENA region, freshwater is a scarce resource (Hamed et al. 2018). In coastal regions, however, seawater is available. Electrolysis processes that directly use seawater are the subject of current research, but are only at the laboratory testing stage and are not yet commercially available (d'Amore-Domenech et al. 2019). To avoid competition for scarce freshwater in the MENA region and to take advantage of electrolysis technologies already available, seawater desalination is explicitly included in the economic and energy modeling and assessment of e-fuel process chains in this paper (cf. Table 6-11, Table 6-12 and Table 6-13). Various seawater desalination technologies are commercially available today. The most commonly used desalination technology is reverse osmosis (Zhou et al. 2005). It has a TRL of 9 (Zhou et al. 2005). It is used, for example, on a large scale to provide drinking water in Israel (Atkinson 2005). The transport of water from the coastline to the PtG site is not explicitly considered in this work, since transport costs for water are comparably low (Zhou et al. 2005) and PtG production sites are located close to the coast in the modeling approach.

Due to the arid climate, the MENA region offers a low potential for biomass and industry that is only located at coastal areas. For this reason, the use of ambient air as a CO_2 source is obvious (Fasihi et al. 2019). Otherwise, CO_2 can be captured from point sources elsewhere and transported to the e-fuel production site, which is not considered in this paper. (Fasihi et al. 2019) give an overview of different process concepts for the separation of CO_2 from ambient air, so-called Direct Air Capture (DAC). Climeworks GmbH supplies a DAC technology with a relatively high TRL (6 – 9), which is based on the chemisorptive binding of CO_2 molecules to amine-activated cellulose (adsorption) at ambient conditions (40 °C, 1 bar) (Viebahn et al. 2019). At temperatures of approximately 100 °C and vacuum conditions, CO_2 is released again (desorption) and can be fed to the methanation process as an enriched CO_2 gas flow (Fasihi et al. 2019; Mörs et al. 2020; Viebahn et al. 2019). The technology has been tested in several pilot plants, for example at the PtG demo site at Troia within the EU project STORE&GO (Mörs et al. 2020). Based on the experience gained in these projects, a further reduction of thermal SED as well as CAPEX and OPEX is expected in the next decade (Table 6-11, Table 6-12 and Table 6-13).

Before methanation, the reactants (hydrogen and CO_2) must first be brought to operating pressure. Table 6-11 shows the SED for intermediate compression of CO_2 (1 to 20 bar) and hydrogen (9 to 20 bar). In the case of PEMEL, hydrogen exits the electrolysis system at a pressure above 20 bar and hydrogen compression is not necessary. The same assumption applies to SOEL in the year 2050.

In catalytic methanation, CO2 and hydrogen are converted to methane and water. Water can be recycled into the electrolysis, thus reducing the seawater requirement. The methanation is exothermic and releases heat of reaction (165 kJ/mol) at a relatively high temperature level (250 to 500 °C) (Götz et al. 2016; Rönsch et al. 2016; Schildauer et al. 2016). The released thermal energy can either be supplied to the DAC or used to generate steam if SOEL is chosen. For the Enertile parametrization, a decrease in methanation costs is assumed over the next decades. The assumed CAPEX and fixed OPEX for methanation are based on learning curves from the literature (Zauner et al. 2019) and the author's own estimations, including costs for product gas cleaning (Table 6-12 and Table 6-13).

For methane liquefaction, a relatively high amount of energy is required to cool the gas below the boiling temperature (-162 °C, 1 bar) and to remove the enthalpy of condensation (Table 6-11). The energy density is thus increased by a factor of 600 (approx. 5.6 MWhCH4/m³) compared to ambient temperature. Methane liquefaction is well known as an application for natural gas transport, so no further cost reduction is assumed (Table 6-12 and Table 6-13).

The energy demand for hydrogen liquefaction is over three times higher than for methane, related to LHV, due to the low boiling temperature of -253 °C (Table 6-11). The optimization of hydrogen liquefaction is part of current research (Stolzenburg et al. 2013) and development work, so reduction in SED and costs is expected in the medium term (Table 6-12 and Table 6-13).

Table 6-11 Specific electrical (el) and thermal (th) energy demand (SED) for all technologies investigated for electricity-based hydrogen and methane production in MENA. Values refer to the years 2030 and 2050.

Process step	**Specific energy demand**					**Source**
	Electrical (el)		**Thermal (th)**			
	in 2030	**in 2050**	**in 2030**	**in 2050**		
Sea water desalination	5.5	5.5	None	None	$kW_{el}/(m^3/h \text{ purified water})$	(Hafez et al. 2003)
PEMEL	5.0	4.5	None	None	$kW_{el}/(m^3/h\ H_2\ STP)$	a, b,c (Smolinka et al. 2018)
SOEL	3.9	3.8	0.4	0.4	$kW_{el/th}/(m^3/h\ H_2\ STP)$	b (Smolinka et al. 2018)
DAC	1.0	1.0	2.9	2.9	$kW_{el/th}/(m^3/h\ CO_2\ STP)$	(Viebahn et al. 2019)
H_2 compression from 9 to 20 bar	0.03	0.03	None	None	$kW_{el}/(m^3/h\ H_2\ STP)$	a
CO_2 compression from 1 to 20 bar	0.15	0.15	None	None	$kW_{el}/(m^3/h\ CO_2\ STP)$	a
H_2 liquefaction	6.76	6.02	None	None	$kW_{el}/(kg/h\ H_2)$	(Stolzenburg et al. 2013)
CH_4 liquefaction	0.7	0.7	None	None	$kW_{el}/(kg/h\ CH_4)$	(Wärtsilä 2016)

[a] Own estimations, taking into account degradation of the stacks by 3 µV/h for 2030 and 2 µV/h for 2050.
[b] Own estimations, taking into account degradation of the stacks by 7 µV/h for 2030 and 4 µV/h for 2050.
[c] The efficiency of PEMEL is not expected to increase significantly by 2030, because PEMEL electrolysis is in an economic "race to catch up" with alkaline electrolysis. Low CAPEX is prioritized over an increase in efficiency in the development of PEMEL (Smolinka et al. 2018).

Table 6-12 Specific CAPEX for each process step for production of electricity-based hydrogen or methane in terms of plant capacity. Values refer to plant capacities of 100 MW (LHV) hydrogen or methane output.

PtG process step	**Specific CAPEX**			**Source**	
	in 2030	**in 2050**			
Sea water desalination	97	97	€/(l/h fresh water out)	(Hafez et al. 2003)	a
PEMEL	2,000	1,800	€/(m³/h STP H_2 out)	(Smolinka et al. 2018)	b, c
SOEL	2,912	2,002	€/(m³/h STP H_2 out)	(Smolinka et al. 2018)	b, c
H_2 compression (9 to 20 bar)	96	none	€/(m³/h STP H_2 in)	(Chardonnet et al. 2017)	b, c, d
Direct air capture	8,344	5,574	€/(m³/h STP CO_2 out)	(Siegemund et al. 2019)	b, c
CO_2 compression (1 to 20 bar)	238	238	€/(m³/h STP CO_2 in)	(Schäffer et al. 2019)	b, c
Catalytic methanation	2,778	1,815	€/(m³/h STP CH_4 out)	(Zauner et al. 2019)	b, c, e
H_2 liquefaction	35,510	35,510	€/(kg H_2 out)	(Hank et al. 2020b)	b, c
CH_4 liquefaction	7,265	7,265	€/(kg CH_4 out)	(Songhurst 2018)	b

[a] Lifetime 15 years
[b] Lifetime 20 years
[c] And own estimations
[d] Only necessary for PtG chain with SOEL
[e] Product gas cleaning included

Table 6-13 Specific OPEX for each process step for production of electricity-based hydrogen or methane; costs for electricity and heat excluded; in terms of plant capacity; referring to plant capacity of 100 MW (LHV) hydrogen or methane output.

PtG process step	**Specific fixed OPEX**			**Source**	
	in 2030	**in 2050**			
Sea water desalination	19	19	€/(l/h fresh water out)/a	(Hafez et al. 2003)	
PEMEL	37	31	€/(m³/h STP H2 out)/a	(Smolinka et al. 2018)	a

PtG process step	Specific fixed OPEX			Source
	in 2030	in 2050		
SOEL	187	77	€/(m³/h STP H2 out)/a	(Smolinka et al. b 2018)
H2 compression (9 to 20 bar)	Neglected	Neglected	€/(m³/h STP H2 in)/a	
Direct air capture	167	111	€/(m³/h STP CO2 out)/a	(Siegemund et al. 2019)
CO2 compression (1 to 20 bar)	Neglected	Neglected	€/(m³/h STP CO2 in)/a	
Catalytic methanation	100	66	€/(m³/h STP CH4 out)/a	(Zauner et al. c 2019)
H2 liquefaction	1,420	1,420	€/(kg H2 out)/a	(Hank et al. 2020b; Stolzenburg et al. 2013)
CH4 liquefaction	437	437	€/(kg CH4 out)/a	(Songhurst 2018)

[a] And own estimations: stack replacement after 10 years.
[b] And own estimations: stack replacement after maximum lifetime of the stacks.
[c] And own estimations; product gas cleaning included.

Appendix E. Techno-economic parameters of renewable energy technologies

For onshore wind turbines, 59 different configurations are taken into account for the year 2050. The hub heights vary between 80 and 160 m. The specific area output ranges between 270 and 500 W/m². A wind turbine with a hub height of 110 m and a specific area output of 400 W_{el}/m^2 costs 1160 €/kW_{el} in 2020 and 1050 €/kW_{el} in 2050. The costs are based on (Wallasch et al. 2019).

Table 6-14 Hub height, rotor diameter, and specific investments for the considered offshore wind turbines in 2030 and 2050 (Koepp et al. 2019).

Turbine	Hub height (m)	Rotor diameter (m)	Specific investment (€/kW$_{el}$)	
			2030	**2050**
1	100	400	3580	3422
2	100	450	3497	3341
3	110	400	3640	3482
4	120	350	3783	3622
5	120	360	3766	3607
6	120	380	3732	3574
7	120	400	3700	3542

Table 6-15 Specific investments for different solar technologies in 2030 and 2050; the costs are based on solar power plants from 2020 (ZSW 2019) and a learning rate (Fraunhofer ISE 2015).

	Specific investment (€/kW$_{el}$)	
Technology	**2030**	**2050**
Ground-mounted PV	662	500
Roof-top PV	933	765
CSP	2047	1442

References

Adolf, J.; Balzer, C. H.; Louis, J.; Schabla, U.; Fischedick, M.; Arnold, K.; Pastowski, A.; Schüwer, D. (2017): Shell Hydrogen Study Energy of the Future? Sustainable Mobility through Fuel Cells and H2. https://doi.org/10.13140/RG.2.2.31848.57604.

Agora Verkehrswende; Agora Energiewende; Frontier Economics (2018): The Future Cost of Electricity-Based Synthetic Fuels.

Atkinson, S. (2005): World's largest desalination plant begins operating in Israel. In: Membrane Technology, 2005 (12), pp. 9–10. https://doi.org/10.1016/S0958-2118(05)70589-9.

Beltaifa, H. (2020): MENA - Electricity Transmission Network. Available at https://energydata.info/dataset/mena-electricity-transmission-network-2017, accessed 24.02.2021.

Bernath, C.; Deac, G.; Sensfuss, F. (2019): Influence of heat pumps on renewable electricity integration: Germany in a European context. In: Energy Strategy Reviews, 26, p. 100389. https://doi.org/10.1016/j.esr.2019.100389.

Bosch, J.; Staffell, I.; Hawkes, A. D. (2017): Temporally-explicit and spatially-resolved global onshore wind energy potentials. In: Energy, 131, pp. 207–217. https://doi.org/10.1016/j.energy.2017.05.052.

Chardonnet, C.; Vos, L. de; Genoese, F.; Roig, G.; Bart, F.; Lacroix, T. de; Ha, T.; van Genabet, B. (2017): EARLY BUSINESS CASES FOR H2 IN ENERGY STORAGE AND MORE BROADLY POWER TO H2APPLICATIONS: FINAL REPORT. Available at https://www.clean-hydrogen.europa.eu/media/publications/study-early-business-cases-h2-energy-storage-and-more-broadly-power-h2-applications_en.

Collins, L. (2019): World's first liquefied hydrogen carrier launched in Japan: The Suiso Frontier is a key part of the HySTRA demonstration project, which will see hydrogen shipped 9,000 km from southeast Australia to the Japanese city of Kobe: NHST Global Publications AS. Available at https://www.rechargenews.com/transition/worlds-first-liquefied-hydrogen-carrier-launched-in-japan/2-1-722155, accessed 24.03.2021.

Copernicus Climate Change Service (2020): ERA5: Fifth generation of ECMWF atmospheric reanalyses of the global climate: Copernicus Climate Change Service Climate Data Store. Date of access: May 2019. Available at https://cds.climate.copernicus.eu/cdsapp.

Council of the European Union (2009): Presidency Conclusions 29-30 October 2009. Brussels. Available at https://ec.europa.eu/regional_policy/sources/cooperate/baltic/pdf/council_concl_30102009.pdf, accessed 12.09.2019.

d'Amore-Domenech, R.; Leo, T. J. (2019): Sustainable Hydrogen Production from Offshore Marine Renewable Farms: Techno-Energetic Insight on Seawater Electrolysis Technologies. In: ACS Sustainable Chemistry & Engineering, 7 (9), pp. 8006–8022. https://doi.org/10.1021/acssuschemeng.8b06779.

Danielson, J. J.; Gesch, D. B. (2011): Global multi-resolution terrain elevation data 2010 (GMTED2010). In: Open-File Report, (2011-1073). https://doi.org/10.3133/ofr20111073.

Drechsler, C.; Agar, D. W. (2021): Characteristics of DAC operation within integrated PtG concepts. In: International Journal of Greenhouse Gas Control, 105, p. 103230. https://doi.org/10.1016/j.ijggc.2020.103230.

Eurek, K.; Sullivan, P.; Gleason, M.; Hettinger, D.; Heimiller, D.; Lopez, A. (2017): An improved global wind resource estimate for integrated assessment models. In: Energy Economics, 64, pp. 552–567. https://doi.org/10.1016/j.eneco.2016.11.015.

European Commission (Ed.) (2018a): COMMUNICATION FROM THE COMMISSION TO THE EUROPEAN PARLIAMENT, THE EUROPEAN COUNCIL, THE COUNCIL, THE EUROPEAN ECONOMIC AND SOCIAL COMMITTEE, THE COMMITTEE OF THE REGIONS AND THE EUROPEAN INVESTMENT BANK COM(2018) 773. A Clean Planet for all A European strategic long-term vision for a prosperous, modern, competitive and climate neutral economy. Available at https://eur-lex.europa.eu/legal-content/EN/TXT/?uri=CELEX:52018DC0773, accessed 28.12.2019.

European Commission (2018b): In-depth analysis in support of the commission communication COM(2018) 773. A clean Planet for all - A European long-term strategic vision for a prosperous, modern, competitive and cimate neutral economy. Supplementary information.

European Commission (Ed.) (2019): The European Green Deal. Brussels.

European Commission (Ed.) (2020): A hydrogen strategy for a climate-neutral Europe. Communication from the Commission to the European Parliament, the Council, the European Economic and Social Committee and the Committee of the Regions. Brussels.

European Space Agency and Université Catholique de Louvain (2010): GlobCover 2009. Available at http://due.esrin.esa.int/page_globcover.php, accessed 15.07.2020.

Fasihi, M.; Efimova, O.; Breyer, C. (2019): Techno-economic assessment of CO2 direct air capture plants. In: Journal of Cleaner Production, 224, pp. 957–980. https://doi.org/10.1016/j.jclepro.2019.03.086.

Fasold, H.-G. (2010): Langfristige Gasbeschaffung für Europa - Pipelineprojekte und LNG-Ketten. In: gwf-Gas| Erdgas, p. 528.

Feng, J.; Feng, L.; Wang, J.; King, C. W. (2020): Evaluation of the onshore wind energy potential in mainland China—Based on GIS modeling and EROI analysis. In: Resources, Conservation and Recycling, 152, p. 104484. https://doi.org/10.1016/j.resconrec.2019.104484.

Frank, E.; Gorre, J.; Ruoss, F.; Friedl, M. J. (2018): Calculation and analysis of efficiencies and annual performances of Power-to-Gas systems. In: Applied Energy, 218, pp. 217–231. https://doi.org/10.1016/j.apenergy.2018.02.105.

Franke, K.; Sensfuss, F.; Deac, G.; Kleinschmitt, C.; Ragwitz, M. (2021): Factors affecting the calculation of wind power potentials: A case study of China. In: Renewable and Sustainable Energy Reviews, 149, p. 111351. https://doi.org/10.1016/j.rser.2021.111351.

Fraunhofer Institut für System- und Innovationsforschung (2019): Enertile. Available at https://www.enertile.eu/enertile-en/index.php, accessed 07.11.2019.

Fraunhofer-Institut für Energiewirtschaft und Energiesystemtechnik (2021): PtX-Atlas. Available at https://maps.iee.fraunhofer.de/ptx-atlas/, accessed 20.07.2021.

Fraunhofer-Institut für Solare Energiesysteme ISE (2015): Current and Future Cost of Photovoltaics. Long-term Scenarios for Market Development, System Prices and LCOE of Utility-Scale PV Systems. Study on behalf of Agora Energiewende. Available at https://www.agora-energiewende.de/fileadmin/Projekte/2014/Kosten-Photovoltaik-2050/AgoraEnergiewende_Current_and_Future_Cost_of_PV_Feb2015_web.pdf, accessed 23.07.2021.

Godron, P.; Neubarth, J.; Soyah, M.; Asceri, V.; Callegari, G.; Cova, B.; Banez, F.; Olmos, L.; Ramos, A.; Rivier, M.; Muhme, K.; Ruderer, D.; Youssef, A. (2014): Desert power: Getting connected. Starting the debate for the grid infrastructure for a sustainable power supply in EUMENA.

Golling, C.; Heuke, R.; Seidl, H.; Uhlig, J. (2019): Roadmap Power to Gas. Available at https://www.dena.de/fileadmin/dena/Publikationen/PDFs/2019/Roadmap_Power_to_Gas.pdf.

Götz, M.; Lefebvre, J.; Mörs, F.; McDaniel Koch, A.; Graf, F.; Bajohr, S.; Reimert, R.; Kolb, T. (2016): Renewable Power-to-Gas: A technological and economic review. In: Renewable Energy, 85, pp. 1371–1390. https://doi.org/10.1016/j.renene.2015.07.066.

Graves, C.; Ebbesen, S. D.; Mogensen, M.; Lackner, K. S. (2011): Sustainable hydrocarbon fuels by recycling CO2 and H2O with renewable or nuclear energy. In: Renewable and Sustainable Energy Reviews.

Gupta, N. (2016): A review on the inclusion of wind generation in power system studies. In: Renewable and Sustainable Energy Reviews, 59, pp. 530–543. https://doi.org/10.1016/j.rser.2016.01.009.

Hafez, A.; El-Manharawy, S. (2003): Economics of seawater RO desalination in the Red Sea region, Egypt. Part 1. A case study. https://doi.org/10.1016/s0011-9164(02)01122-0.

Hamed, Y.; Hadji, R.; Redhaounia, B.; Zighmi, K.; Bâali, F.; El Gayar, A. (2018): Climate impact on surface and groundwater in North Africa: A global synthesis of findings and recommendations. In: Euro-Mediterranean Journal for Environmental Integration, 3 (1), p. 1163. https://doi.org/10.1007/s41207-018-0067-8.

Hank, C.; Sternberg, A.; Köppel, N.; Holst, M.; Smolinka, T.; Schaadt, A.; Hebling, C.; Henning, H.-M. (2020a): Energy efficiency and economic assessment of imported energy carriers based on renewable electricity,

Hank, C.; Sternberg, A.; Köppel, N.; Holst, M.; Smolinka, T.; Schaadt, A.; Hebling, C.; Henning, H.-M. (2020b): Supplementary Information: Energy efficiency and economic assessment of imported energy carriers based on renewable electricity.

He, G.; Kammen, D. M. (2014): Where, when and how much wind is available? A provincial-scale wind resource assessment for China. In: Energy Policy, 74, pp. 116–122. https://doi.org/10.1016/j.enpol.2014.07.003.

Homann, K.; Reimert, R.; Klocke, B. (2013): The Gas Engineer's Dictionary: Supply Infrastructure from A to Z. DIV.

Hoogwijk, M.; Vries, B. de; Turkenburg, W. C. (2004): Assessment of the global and regional geographical, technical and economic potential of onshore wind energy. In: Energy Economics, 26 (5), pp. 889–919. https://doi.org/10.1016/j.eneco.2004.04.016.

Hu, J.; Harmsen, R.; Crijns-Graus, W.; Worrell, E. (2019): Geographical optimization of variable renewable energy capacity in China using modern portfolio theory. In: Applied Energy, 253, p. 113614. https://doi.org/10.1016/j.apenergy.2019.113614.

Hydrogen Council (2020): Path to hydrogen competitiveness: A cost perspective. Available at https://hydrogencouncil.com/wp-content/uploads/2020/01/Path-to-Hydrogen-Competitiveness_Full-Study-1.pdf.

IEA International Energy Agency (2020a): Electricity Consumption by IEA Data Services. Available at https://www.iea.org/subscribe-to-data-services/world-energy-balances-and-statistics, accessed 24.02.2021.

International Energy Agency (Ed.) (2019): The Future of Hydrogen. Seizing today's opportunities.

International Energy Agency (2020b): World Energy Outlook 2020. https://doi.org/10.1787/557a761b-en.

Julian Deymann (2014): Unkonventionelles Erdgas: Auswirkungen auf den globalen Erdgasmarkt.

Koepp, M.; Krampe, L.; Wendring, P.; Eckstein, J.; Richter, M.; Schäfer-Frey, J.; Umana-Packebusch, M.; Wiemann, J.; Macharey, U.; Svoboda, P.; Wilms, J. (2019): Vorbereitung und Begleitung bei der Erstellung eines Erfahrungsberichts gemäß §97 Erneuerbare-Energien-Gesetz. Teilvorhaben IIf: Windenergie auf See.

Leiblein, J.; Bär, K.; Graf, F.; Kühn, M.; Müller, S.; Bäuerle, M.; Benthin, J. (2020): Roadmap Gas 2050 Deliverable D1.1: Bewertung von alternativen Verfahren zur Bereitstellung von grünem und blauem H2: DVGW-Förderkennzeichen G 201824. Deutscher Verein des Gas- und Wasserfaches e.V.; DBI Gas- und Umwelttechnik GmbH.

Liu, C.; Wang, Y.; Zhu, R. (2017): Assessment of the economic potential of China's onshore wind electricity. In: Resources, Conservation and Recycling, 121, pp. 33–39. https://doi.org/10.1016/j.resconrec.2016.10.001.

Lux, B.; Pfluger, B. (2020): A supply curve of electricity-based hydrogen in a decarbonized European energy system in 2050. In: Applied Energy, 269, p. 115011. https://doi.org/10.1016/j.apenergy.2020.115011.

Mörs, F.; Schlautmann, R.; Gorre, J.; Leonhard, R. (2020): Innovative large-scale energy storage technologies and power-to-gas concepts after optimisation (STORE&GO): D 5.9 Final report on evaluation of technologies and processes. https://doi.org/10.3030/691797.

Niermann, M.; Timmerberg, S.; Drünert, S.; Kaltschmitt, M. (2021): Liquid Organic Hydrogen Carriers and alternatives for international transport of renewable hydrogen. In: Renewable and Sustainable Energy Reviews, 135, p. 110171. https://doi.org/10.1016/j.rser.2020.110171.

Pfluger, B. (2014): Assessment of least-cost pathways for decarbonising Europe's power supply. A model-based long-term scenario analysis accounting for the characteristics of renewable energies. Karlsruhe.

Pfluger, B.; Tersteegen, B.; Franke, B.; Bernath, C.; Bossmann, T.; Deac, G.; Elsland, R.; Fleiter, T.; Kühn, A.; Ragwitz, M.; Rehfeldt, M.; Steinbach, J.; Cronenberg, A.; Ladermann, A.; Linke, C.; Maurer, C.; Willemsen, S.; Kauertz, B.; Pehnt, M.; Rettenmaier, N.; Hartner, M.; Kranzl, L.; Schade, W.; Catenazzi, G.; Jakob, M.; Reiter, U. (2017): Langfristszenarien für die Transformation des Energiesystems in Deutschland. Modul 2:

Modelle und Modellverbund. Fraunhofer Institut für System- und Innovationsforschung; ifeu - Institut für Energie- und Umweltforschung Heidelberg GmbH; TU Wien; TEP Energy; M-Five GmbH (M-Five); Consentec GmbH (Consentec).

Rönsch, S.; Schneider, J.; Matthischke, S.; Schlüter, M.; Götz, M.; Lefebvre, J.; Prabhakaran, P.; Bajohr, S. (2016): Review on methanation - From fundamentals to current projects. In: Fuel, 166, pp. 276–296. https://doi.org/10.1016/j.fuel.2015.10.111.

Schäffer, J.; Ortloff, F.; Lubenau, U.; Imberg, C.; Senner, J. (2019): Bewertung von Quellen und Abtrennungsverfahren zur Bereitstellung von CO2 für PtG-Prozesse: Abschlussbericht G201621, G 1/04/16. Deutscher Verein des Gas- und Wasserfaches e.V.; DBI Gas- und Umwelttechnik GmbH; Gas- und Wärme-Institut Essen e.V.

Schildauer, T. J.; Biollaz, S. M. A. (2016): Synthetic Natural Gas from Coal, Dry Biomass, and Power-to-Gas Applications. Hoboken, New Jersey: John Wiley & Sons Inc. https://doi.org/10.1002/9781119191339.

Schlautmann, R.; Böhm, H.; Zauner, A.; Mörs, F.; Tichler, R.; Graf, F.; Kolb, T. (2021): Renewable Power-to-Gas: A Technical and Economic Evaluation of Three Demo Sites Within the STORE&GO Project. In: Chemie Ingenieur Technik, 9 (7), p. 50. https://doi.org/10.1002/cite.202000187.

Schubert, G. (2012): Modeling hourly electricity generation from PV and wind plants in Europe. In: 2012 9th International Conference on the European Energy Market (2012 9th International Conference on the European Energy Market (EEM 2012)), 5/10/2012 - 5/12/2012, Florence, Italy. [Place of publication not identified], pp. 1–7. https://doi.org/10.1109/EEM.2012.6254782.

Sebestyén, T.-T. (2017): Assessment of Solar PV Power Generation Potential in Centre Development Region of Romania. https://doi.org/10.18178/JOCET.2017.5.4.387.

Siegemund, S.; Trommler, M.; Kolb, O.; Zinnecker, V.; Schmidt, P.; Weindorf, W.; Zittel, W.; Raksha, T.; Zerhusen, J. (2019): The potential of electricity-based fuels for low-emission transport in the EU: E-Fuels study. Berlin: Deutsche Energie-Agentur GmbH; Ludwig-Bölkow-Systemtechnik GmbH. Available at https://www.dena.de/themen-projekte/projekte/mobilitaet/e-fuels-the-potential-of-electricity-based-fuels-for-low-emission-transport-in-the-eu/.

Simon Göß (2017): Tutorial Gasmarkt Teil 6: Erdgastransport und -speicherung. Available at https://blog.energybrainpool.com/tutorial-gasmarkt-teil_6-erdgastransport-und-speicherung/, accessed 08.03.2021.

Smolinka, T.; Wiebe, N.; Sterchele, P.; Palzer, A.; Lehner, F.; Jansen, M.; Kiemel, S.; Miehe, R.; Wahren, S.; Zimmermann, F. (2018): Study IndWEDe: Industrialisation of water electrolysis in Germany: Opportunities and challenges for sustainable hydrogen for transport, electricity and heat. Berlin: Fraunhofer Institut für System- und Innovationsforschung; Fraunhofer-Institut für Produktionstechnik und Automatisierung IPA.

Songhurst, B. (2018): LNG plant cost reduction 2014-18. Oxford Institute for Energy Studies. https://doi.org/10.26889/9781784671204.

Stolzenburg, K.; Berstad, D.; Decker, L.; Elliott, A.; Haberstroh, C.; Hatto, C.; Klaus, M.; Mortimer, N. D.; Mubbala, R.; Mwabonje, O.; Neksa, P.; Quack, H.; Rix, J.; Seemann, I.; Walnum, H. T. (2013): Efficient Liquefaction of Hydrogen: Results of the IDEALHY Project. In: XXth energie-symposium Stralsund.

Timmerberg, S.; Kaltschmitt, M. (2019a): Hydrogen from renewables: Supply from North Africa to Central Europe as blend in existing pipelines – Potentials and costs. In: Applied Energy, 237, pp. 795–809. https://doi.org/10.1016/j.apenergy.2019.01.030.

Timmerberg, S.; Sanna, A.; Kaltschmitt, M.; Finkbeiner, M. (2019b): Renewable electricity targets in selected MENA countries – Assessment of available resources, generation costs and GHG emissions. In: Energy Reports, 5, pp. 1470–1487. https://doi.org/10.1016/j.egyr.2019.10.003.

Töpler, J.; Lehmann, J. (2016): Hydrogen and fuel cell: Technologies and market perspectives. Berlin: Springer. ISBN: 978-3-662-44972-1.

Ueckerdt, F.; Bauer, C.; Dirnaichner, A.; Everall, J.; Sacchi, R.; Luderer, G. (2021): Potential and risks of hydrogen-based e-fuels in climate change mitigation. In: Nature Climate Change, 11 (5), pp. 384–393. https://doi.org/10.1038/s41558-021-01032-7.

United Nations (Ed.) (2015): Paris Agreement. Available at https://unfccc.int/sites/default/files/english_paris_agreement.pdf.

United Nations (2019): World Population Prospects 2019. Online Edition. Rev. 1. Available at https://population.un.org/wpp/Download/Standard/Population/, accessed 24.02.2021.

Ursua, A.; Gandia, L. M.; Sanchis, P. (2012): Hydrogen Production From Water Electrolysis: Current Status and Future Trends. In: Proceedings of the IEEE, 100 (2), pp. 410–426. https://doi.org/10.1109/JPROC.2011.2156750.

Viebahn, P.; Scholz, A.; Zelt, O. (2019): The Potential Role of Direct Air Capture in the German Energy Research Program--Results of a Multi-Dimensional Analysis. In: Energies, 12 (18), p. 3443. https://doi.org/10.3390/en12183443.

Wallasch, A.-K.; Lüers, S.; Heyken, M.; Rehfeldt, K.; Jachmann, H. (2019): Vorbereitung und Begleitung bei der Erstellung eines Erfahrungsberichts gemäß §97 Erneuerbare-Energien-Gesetz. Teilvorhaben IIe): Wind an Land.

Wang, A.; van der Leun, K.; Peters, D.; Buseman, M. (2020): European Hydrogen Backbone: HOW A DEDICATED HYDROGEN INFRASTRUCTURE CAN BE CREATED, accessed 17.08.2020.

Wärtsilä Corporation (2016): LNG Plants Mini-scale Liquefaction Technology. Available at https://www.wartsila.com/marine/build/gas-solutions/liquefaction-bog-reliquefaction/lng-plants-mini-scale-liquefaction-technology, accessed 08.03.2021.

World Conservation Monitoring Centre (2014): World Database on Protected Areas (WDPA). Available at http://www.protectedplanet.net/, accessed 15.07.2020.

WorldPop (2018): Global 1km Population. https://doi.org/10.5258/SOTON/WP00647.

Zauner, A.; Böhm, H.; Rosenfeld, D. C.; Tichler, R. (2019): Innovative large-scale energy storage technologies and Power-to-Gas concepts after optimization: D 7.7 Analysis on future technology options and on techno-economic optimization.

Zeman, F. S.; Keith, D. W. (2008): Carbon neutral hydrocarbons. In: Philosophical transactions. Series A, Mathematical, physical, and engineering sciences, 366 (1882), pp. 3901–3918. https://doi.org/10.1098/rsta.2008.0143.

Zentrum für Sonnenenergie- und Wasserstoff-Forschung Baden-Württemberg (2019): Vorbereitung und Begleitung bei der Erstellung eines Erfahrungsberichts gemäß § 97 Erneuerbare-Energien-Gesetz. Teilvorhaben II c: Solare Strahlungsenergie. Erstellt im Auftrag des Bundesministeriums für Wirtschaft und Energie.

Zhou, Y.; Tol, R. S. J. (2005): Evaluating the costs of desalination and water transport. In: Water Resources Research, 41 (3), p. 18. https://doi.org/10.1029/2004WR003749.

[End of paper 2]

7 The role of hydrogen in a greenhouse gas-neutral energy system in Germany

[Start of Paper 3]

The role of hydrogen in a greenhouse gas-neutral energy system in Germany

Benjamin Lux[1,*], Gerda Deac[1], Christoph P. Kiefer[1], Christoph Kleinschmitt[1], Christiane Bernath[1], Katja Franke[1], Benjamin Pfluger[2], Sebastian Willemsen[3], and Frank Sensfuß[1]

1 Fraunhofer Institute for Systems and Innovation Research ISI, Breslauer Straße 48, 76139 Karlsruhe, Germany

2 Fraunhofer Research Institution for Energy Infrastructures and Geothermal Systems IEG, Breslauer Straße 48, 76139 Karlsruhe, Germany

3 Consentec GmbH, Grüner Weg 1, 52070 Aachen, Germany

*corresponding author: Benjamin Lux, benjamin.lux@isi.fraunhofer.de, phone: +49-721-6809-474

Paper published in:

Energy Conversion and Management 270, Article No. 116188, DOI: 10.1016/j.enconman.2022.116188

Abstract

Hydrogen is widely considered to play a pivotal role in successfully transforming the German energy system, but the German government's current "National Hydrogen Strategy" does not specify how hydrogen utilization, production, storage or distribution will be implemented. Addressing key uncertainties for the German energy system's path to greenhouse gas-neutrality, this paper examines hydrogen in different scenarios. This analysis aims to support the concretization of the German hydrogen strategy. Applying a European energy supply model with strong interactions between the conversion sector and the hydrogen system, the analysis focuses on the requirements for geological hydrogen storages and their utilization over the course of a year, the positioning of electrolyzers within Germany, and the contributions of hydrogen transport networks to balancing supply and demand. Regarding seasonal hydrogen storages, the results show that hydrogen storage facilities in the range of 42 TWh_{H2} to 104 TWh_{H2} are beneficial to shift high electricity generation volumes from onshore wind in spring and fall to winter periods with lower renewable supply and increased electricity and heat demands. In 2050, the scenario results show electrolyzer capacities between 41 GW_{el} and 75 GW_{el} in Germany. Electrolyzer sites were found to follow the low-cost renewable *energy potential and are concentrated on the North Sea and Baltic Sea coasts with their high wind yields. With respect to a hydrogen transport infrastructure, there were two robust findings: One, a domestic German hydrogen transport network connecting electrolytic hydrogen production sites in northern Germany with hydrogen demand hubs in western and southern Germany is economically efficient. Two, connecting Germany to a European hydrogen transport network with interconnection capacities between 18 GW_{H2} and 58 GW_{H2} is cost-efficient to meet Germany's substantial hydrogen demand.*

Key words: Hydrogen supply; Hydrogen storage; German energy transition; Greenhouse gas neutrality; Energy system modeling;

Highlights:

- Cost minimization of European electricity, heat, and hydrogen supply up to 2050
- Hydrogen storage demand in climate-neutral German energy system: 42 - 104 TWh
- Electrolyzer capacity in Germany: 41 - 75 GW
- At least 71% of German electrolyzers at the coast
- Germany's interconnection capacity to European hydrogen grid: 18 - 58 GW

7.1 Introduction

In order to achieve the 1.5 °C target established in the Paris Agreement 2015 (UN 2015), the European Commission (EC) aims for net zero greenhouse gas (GHG) emissions in 2050 in the European Green Deal (EC 2019). The German Federal Government has committed itself to achieving the European targets in Germany's Federal Climate Change Act (BMJ et al. 2021). The transformation of the energy system is pivotal to meeting the stated climate protection targets (BMUV 2016), and the German government assigns GHG-neutral hydrogen a key role in this transformation (BMWi 2020). Following the current trend that sees hydrogen becoming part of the global energy system transition (Capurso et al. 2022), Germany has created a framework to support innovations and investments in hydrogen technologies in its national hydrogen strategy (BMWi 2020). However, this strategy still lacks a concrete outline of future hydrogen supply infrastructures. The design of these hydrogen supply infrastructures depends on various influences.

Firstly, the amount of hydrogen demand has a high impact on hydrogen supply. Lux et al. (2020) show increasing electrolyzer capacities for increasing hydrogen production volumes in Europe in 2050. Similarly, in a parameter study, Husarek et al. (2021) show different configurations of a German hydrogen transport infrastructure for increasing hydrogen demand levels. However, Neuwirth et al. (2022) claim that the level of future hydrogen demand in Germany is largely uncertain. Commissioned by the National Hydrogen Council, a meta-study (Wietschel et al. 2021) of current energy system studies for Germany achieving GHG reductions of at least 90% shows that hydrogen demand in the demand sectors in 2050 ranges between 0 and 316 TWh_{H2} depending on the underlying scenario. Today, robust decisions regarding the development of hydrogen supply infrastructures need to take these uncertainties in the development of hydrogen demand into account.

Secondly, to design suitable hydrogen supply infrastructures, the entire value chain of generation, storage, and transport should be considered. With an analysis of hydrogen supply potentials in Europe and the Middle East and North Africa (MENA), Sens et al. (2022) contribute to this requirement in two respects: First, even though electrolytic hydrogen production costs in the MENA region are cheaper than using electrolyzers in Germany, the export costs for supplying this hydrogen to Germany are in the same order of magnitude as for on-site production within Germany due to transport surcharges. Second, Sens et al. show that the use of salt caverns for seasonal storage of hydrogen can reduce hydrogen supply costs by up to 50%. Consequently, for a comprehensive analysis of hydrogen supply in Germany, it is not sufficient to consider only hydrogen production with electrolyzers; hydrogen storage and transport must be considered too.

Thirdly, the components of these hydrogen supply chains interact strongly with the rest of the energy system. On the one hand, producing high hydrogen quantities using electrolysis translates directly into high electricity demand and additional expansion of renewable power generation technologies (Lux et al. 2020). As a result, hydrogen increasingly competes with other applications for low-cost electricity. On the other hand, flexible hydrogen production with electrolyzers can help to integrate weather-dependent renewable energies (Chen et al. 2021). Gils et al. (2021)

show that hydrogen as a storage medium can offset seasonal effects in renewable electricity generation and electricity demands. In the latter case, renewable electricity is stored in geological formations at negative residual loads, i.e., at times when renewable electricity generation exceeds the load, and is then withdrawn at subsequent positive residual loads, i.e., at times when the load exceeds renewable electricity generation. Consequently, hydrogen supply must be considered in the context of the energy system.

Finally, analyses on the German energy system need to address the European context. Bernath et al. (2019) show that in Germany both the deployment of renewable energies in the electricity system and the decarbonization of district heating grids through heat pumps strongly depend on the integration of Germany into the European energy system. Therefore, the alternative sector coupling technologies of hydrogen supply in Germany should also be investigated in an integrated European energy system.

In summary, the challenges in defining a concrete rollout of hydrogen supply technologies are considering the entire value chain of hydrogen production, storage, and transport simultaneously, the interactions of this value chain with the rest of the German and European energy system, and its dependence on future hydrogen demand. Although there is a rapidly growing body of literature on hydrogen supply, there are only few studies for Germany with a system perspective that consider these aspects at least partly. Lux et al. (2020) develop hydrogen supply curves for a decarbonized European energy system in 2050. The results of this energy system cost minimization show that there is a substantial but regionally heterogeneous hydrogen production potential in Europe. The balancing of these regional differences via a hydrogen network to meet hydrogen demands is however not considered. In a subsequent study (Lux et al. 2021), this European hydrogen supply potential is compared to import curves from the MENA region. Similar to Sens et al. (2022), this comparison shows that low-cost electrolytic hydrogen production at locations with favorable renewable energy potentials in the MENA region is offset by transportation costs. Welder et al. (2018) analyze three different scenarios for power-to-hydrogen supply infrastructures meeting mobility and industry demands in a future German energy system. Applying a mixed integer linear program, they find the cost of hydrogen for mobility is below current hydrogen retail prices. Their results indicate that the utilization of underground hydrogen storages reduces the system costs for a renewable-based German energy system. However their modeling approach has limitations: The temporal resolution is limited to typical days, the geographical scope is limited to Germany, the electricity grid is not part of the optimization, and only onshore wind is considered for renewable power generation. Gils et al. (2021) analyze the interaction of hydrogen infrastructures with other sector coupling technologies in a GHG-neutral German energy system. They apply an integrated optimization of the supplies of electricity, heat, hydrogen, and methane with a strong focus on Germany. Analyzing a single scenario including several sensitivities, they find that flexible hydrogen production is key for the integration of renewables and seasonal balancing. However, they do not analyze sector coupling options or hydrogen transport infrastructures in a European context. Husarek et al. (2021) use a multi-modal energy system model to analyze hydrogen supply chains for Germany in 2050. They show that hydrogen imports are pivotal for meeting German hydrogen demand and that a north-south hydrogen pipeline connection within Germany is a no-regret option. The geographic resolution of their modeling for Germany is high, however, they only estimate hydrogen import potentials based on four exemplary routes taken from literature values. They do not consider interactions of German hydrogen imports with the European power generation system.

The literature review shows that none of the previous studies addresses all the described challenges in defining a concrete strategy for the buildup of hydrogen supply infrastructures. There is the need for technically, spatially, and temporally highly resolved analyses of hydrogen supply as part of an integrated European energy system. This paper aims to close the identified research gap by investigating the interaction of hydrogen supply infrastructures with the energy system in different scenarios that all achieve GHG neutrality in Germany by 2050. The analysis focuses on Germany, but considers this in the wider context of a fully integrated European energy system. Using the energy system model *Enertile* and following the hydrogen supply chain of production, storage, and transport, this paper addresses the following research questions:

- Where should electrolyzers be positioned in Germany?
- What are the requirements for geological hydrogen storages and how are storage facilities managed over the course of a year?
- What contribution can hydrogen transport networks make to balancing supply and demand?

Addressing these questions using a detailed modeling approach and covering a broad solution space with different scenarios aims to provide policy makers with robust guidance for concretizing Germany's hydrogen strategy.

The paper is structured as follows: section 7.2 introduces the modeling approach, scenario design, and most important input parameters. Model results are presented in section 7.3 and discussed in section 7.4. Section 7.5 derives key conclusions.

7.2 Methods and data

This section introduces the overall scenario design (section 7.2.1), presents the employed modeling tools (section 7.2.2), and provides an overview of the input data used (section 7.2.3).

7.2.1 Scenario design

This study focuses on hydrogen supply infrastructures in Germany in the context of a GHG-neutral European energy system. In order to derive robust characteristics of a German hydrogen supply system, the analysis in this paper compares five scenarios. Starting with an *electrification scenario*, the scenario design varies along three main dimensions: Development of energy demands, composition of the renewable electricity generation portfolio, and availability of expansions in the electricity transmission networks. For the energy demand variation, a *hydrogen scenario* assumes an increased hydrogen usage in end-use applications and processes. Likewise, a *power-to-gas/power-to-liquid* (*PtG/PtL) scenario* assumes an increased usage of synthetic hydrocarbons. The composition of energy demand follows consistent scenario storylines across all sectors and results from detailed bottom-up models. For the renewable power generation variation, an *onshore wind scenario* assumes a reduced onshore wind potential in Europe. For the electricity network variation, an *electricity grid scenario* assumes a freeze of the European electricity transmission grid expansion. Figure 7-1 shows an overview of the scenario tree. Subsequent paragraphs describe these variations in more detail.

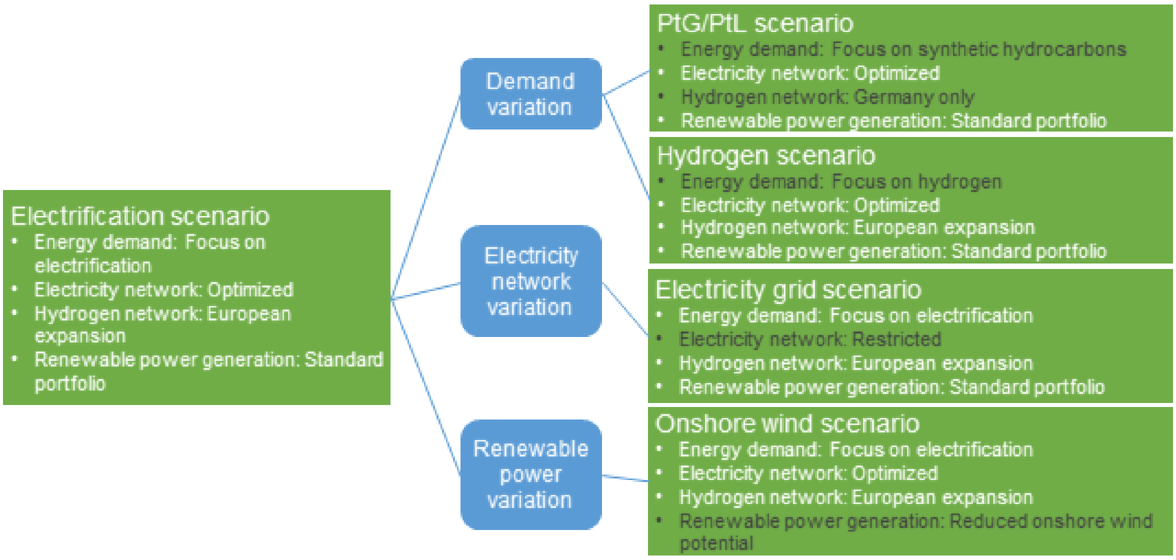

Figure 7-1 Scenario tree.

7.2.1.1 Demand variations

Germany's overarching strategy for reducing GHG emissions is to first reduce energy consumption (the so called “efficiency first principle”), second to directly substitute fossil fuels with renewable energies where possible, and third, to electrify applications and operate them with renewable electricity (BMUV 2016). Nonetheless, there remain processes where a direct use of renewable energy in general or renewable electricity in particular is either not possible or where alternative de-fossilization strategies are being discussed. Currently, there is no consensus on the most efficient CO_2 mitigation strategy for certain industrial processes such as steel production and transport applications such as aviation and long-distance transport (Davis et al. 2018). Reducing GHG emissions in these processes requires the use of carbon-neutral energy or feedstock. In essence, these comprise all energy forms derived from non-fossil sources, or fossil sources for which emissions are fully sequestered and stored, e.g., through carbon capture and storage (CCS). However, the regulatory framework in Germany excludes both nuclear energy, for which a phase-out policy is in place, and CCS. Effectively, the only long-term options for climate-neutral energy in Germany are renewable electricity, hydrogen, or synthetic hydrocarbons. Therefore, this study analyzes three demand variations with a pronounced use of one of these secondary energy forms, deliberately illuminating the corners of the solution space. This section briefly outlines the philosophy of the three scenarios in the demand sectors. German energy demand was determined using independent detailed sector models (Fraunhofer ISI et al. 2021) and use as the input to the supply modeling and analyses in this paper. A detailed presentation of the assumptions and modeling used to determine these demand data is not part of this paper, but section 7.2.3.1 provides a summary of the obtained values. The analysis in the remainder of this paper focuses on how to meet these energy demands – especially for hydrogen – cost efficiently.

The *electrification scenario* relies on a strong use of renewable electricity. The use of hydrocarbons in 2050 is limited to the biomass potential considered sustainable. Nevertheless, a significant amount of hydrogen is needed to achieve the goal of greenhouse gas neutrality in this scenario. In the energy demand sectors of industry, transport, residential and services, applications and processes are shifted towards a direct use of electricity where possible. In the industrial sector, this mainly means that the majority of process heat is provided electrically. Hydrogen is used only where direct electrification is not possible, e.g., because the energy sources are used as feedstocks (e.g. for the production of olefins). In the transport sector, the private car segment and lightweight and medium-sized commercial vehicles are dominated by battery-electric drive systems in the long run. One third of heavy-duty vehicles are also battery-electric. The remaining fleet consists of hybrid trolley trucks wherever possible. In aviation and shipping, biogenic fuels dominate and alternative powertrains are only used to a small extent. In this scenario, heat supply in buildings is mainly provided by heat pumps, district heating, and biomass. Processes and applications in the residential and services sectors are electrified extensively.

The *PtG/PtL scenario* relies on high utilization of synthetic hydrocarbons. The central idea in this scenario is to substitute fossil hydrocarbons with their synthetic or biogenic, GHG-neutral counterparts. This allows the retention of existing infrastructures and processes that are rendered GHG-neutral 'from the outside', i.e., without requiring substantial changes on the usage side. In addition to the use of sustainable biomass, the required amounts of hydrocarbons are imported from regions outside Europe. The structural changes in the industrial sector are less profound than in the other two scenarios. Typically, industrial furnaces are already fired with natural gas. One exception is blast furnaces in steel production, which switch to methane in this scenario. In the transport sector, battery-electric vehicles dominate the segments of passenger cars and small and medium-sized commercial vehicles in this scenario as well. Diesel vehicles continue to be used for heavy-duty vehicles and hydrocarbons continue to be used in international air and sea transport. Gas boilers remain the most important heating technology for buildings, although heat pumps and heat grids make a greater contribution than today.

The *hydrogen scenario* aims at high hydrogen utilization in all sectors, which implies a substantial switch from fossil fuels to hydrogen. This requires a high level of adaptation in applications and infrastructures. In the industrial sector, for example, hydrogen is used as an energy carrier for process heat generation and as a feedstock and reducing medium in steel production. In the transport sector, fuel cell vehicles are increasingly used in addition to battery electric vehicles, with fuel cells especially prevalent in the passenger car and heavy-duty vehicle segments. Decentralized hydrogen boilers are used for heating buildings in this scenario in addition to heat pumps and heat grids.

7.2.1.2 Electricity network variation

Future energy systems based on renewable energies will have an increasing need for flexibility options to compensate for weather effects (Kondziella et al. 2016). Hydrogen as a seasonal storage medium is one flexibility option. The electricity grid is another important option providing supra-regional balancing. These flexibility options are in competition with each other. Therefore, in order to investigate robust results for a hydrogen supply infrastructure, this study varies the electricity grid expansion option in the optimization. The *electricity grid scenario* only realizes the Ten Year Network Development Plan 2018 with slight delays. In all other scenarios, the optimization can expand power transmission network within certain capacity limits. A complete list of maximum network capacities in the optimization is provided in Appendix D.

7.2.1.3 Renewable power variation

Onshore wind is one of the key power generation technologies in the GHG-neutral electricity system. At the same time, there are acceptance problems for the expansion of wind power plants (Guo et al. 2015). For the design of a robust hydrogen supply infrastructure, this study varies the potential of onshore wind. In the *onshore wind scenario*, only half of the land is available for wind turbine expansion compared to all the other scenarios. A complete list of land use factors for renewable electricity generation is provided in Appendix E.

7.2.2 Methods

The energy system model *Enertile* (Fraunhofer ISI 2021) was used to calculate and analyze the conversion sector and hydrogen supply system. The following paragraphs describe the model's main architecture.

7.2.2.1 Renewable electricity generation potential calculation

Renewable energy potential is an important input for the cost minimization of the energy supply system. *Enertile* uses cost-potential curves determined in detailed bottom-up modeling prior to the energy system optimization and differentiates the technologies of onshore wind, offshore wind, concentrated solar power (CSP), utility scale photovoltaics (PV) and rooftop PV. For this analysis, the world is mapped onto a grid of so-called "tiles" that measure 42.25 km². This grid combines data on land use, weather, and power generation technologies. The high-resolution tile results are summarized as cost-potential curves for the system optimization. The individual stages of these cost-potential curves contain the following information for each technology:

- sum of the generation potential on the tiles,
- average full-load hours on the tiles,

- average generation cost on the tiles, and
- the aggregate weather profile on the tiles.

Enertile subsequently makes autonomous expansion decisions for the individual renewable technologies based on the potential curves in a model region and the expansion targets set in the scenarios. Subsequently, the expansion and dispatch results of the optimization can be re-projected onto the tile grid. This results in a spatially detailed picture of the expansion of renewable energies in the scenarios. A more extensive description of calculating the renewable potential is given in Lux et al. (2021).

The development of the other renewable technologies of hydropower, geothermal power, and wave and tidal power is specified exogenously. For these technologies, endogenous expansion is not appropriate for various reasons, e.g., either the unexploited potential is tightly constrained, as is the case for hydropower in Germany and Europe, or the current costs of these technologies are so high that the model would not expand them endogenously, as is the case for wave, tidal, and geothermal power. This analysis assumes that European countries will realize their existing expansion plans for these technologies, but that no expansion beyond these will take place.

7.2.2.2 Energy system optimization model Enertile

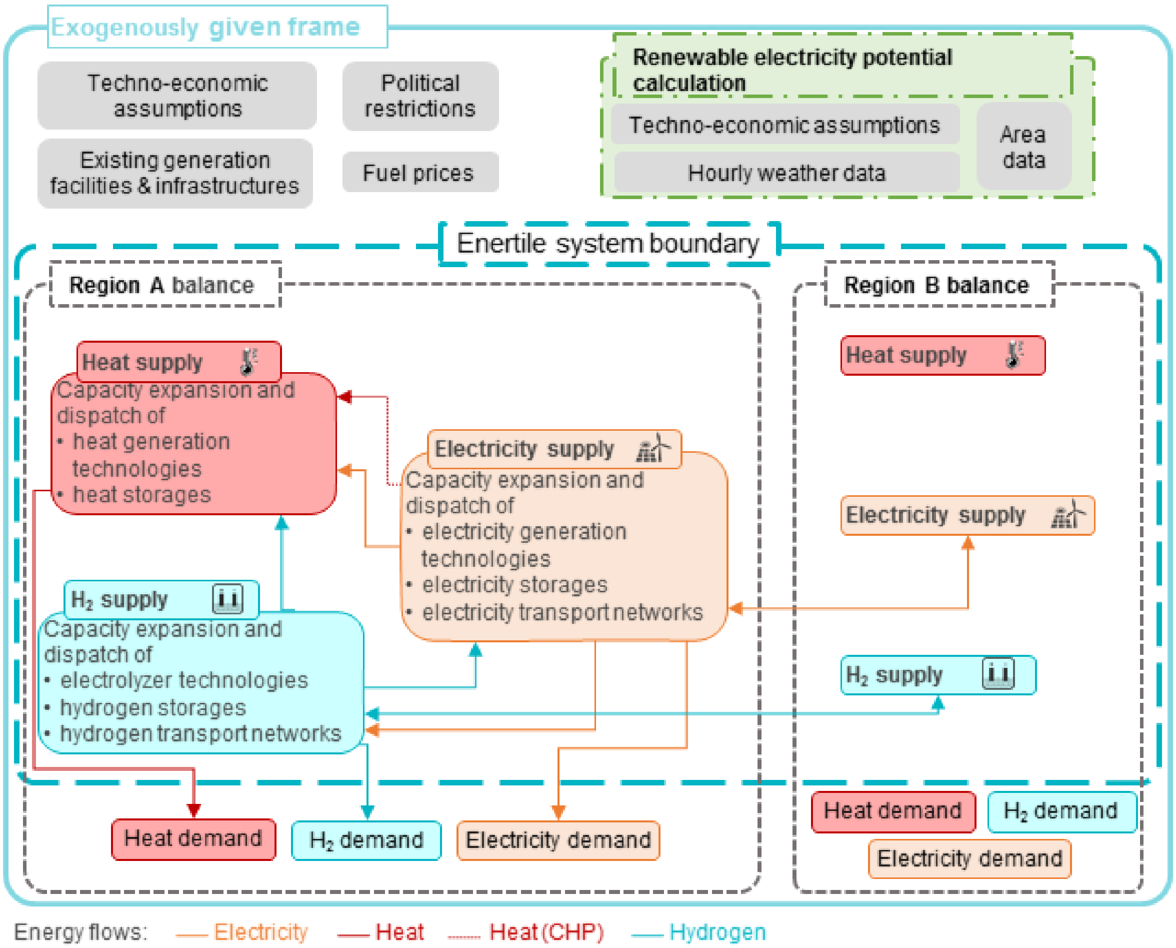

Figure 7-2 Schematic representation of the modeled quantities, interactions, and boundary conditions in the cost minimization of the energy supply-side model *Enertile*.

Modeling the energy supply side is done with the cost minimization model *Enertile*. It simulates the simultaneous supply of electricity, heat in heat grids, and hydrogen. The goal of the optimization is the expansion and dispatch of technologies for the generation, conversion, and distribution of these energy forms to meet exogenously specified demands at least cost. For the supply of electricity, this includes conventional and renewable power generation technologies (including combined heat and power (CHP) plants), storage technologies, and electricity transmission networks. For the supply of heat in heat grids, this includes conventional and renewable heat generation technologies and heat storages. For hydrogen supply, this includes electrolyzer technologies, hydrogen storages, and hydrogen transport pipelines.

Enertile's objective function adds up the fixed and variable costs of the energy system components shown in Figure 7-2. In the linear problem formulation, the decision variables are the installed capacities of the system components and their dispatch.

The key constraints of the linear optimization require that the hourly demand for electricity, heat, and hydrogen is met in each model region. Interactions between the supplies of the different energy forms shown in Figure 7-2 are taken into account. A mathematical formulation of the linear optimization problem is given in Appendix C.

Enertile has a high level of technical, temporal, and spatial detail. The scenario calculations in the conversion sector cover the years 2030, 2040, and 2050 with hourly resolution. The expansion and deployment of infrastructures across all years are jointly considered in a single model run. This means that the model must account for the consequences of a decision in 2030 in subsequent years. Perfect foresight is assumed. In this paper, the modeling of energy supply covers the countries of the European Union (EU), Norway, Switzerland, the United Kingdom, and the Balkan states in all scenarios. This makes it possible to consider cross-regional balancing effects of electricity and hydrogen transport networks. Model regions correspond to either one or more national states (cf. Appendix Appendix C for a definition of the model regions), apart from Germany, which is divided into seven subregions. This regional split is based on potential bottlenecks in the electricity transmission grid. The expansion and use of electricity and hydrogen transport networks between model regions is modeled by means of net transfer capacities.

The model Enertile has already been described and used in many studies for the analysis of energy supply systems. Pfluger (2014) described the modeling of the European electricity system in more detail and investigated different pathways in ambitious climate protection scenarios. Deac (2019) described the coupling of the power and heat system in the model and investigated the impact of heat grids on the integration of renewable energies in Germany. Bernath et al. (2019) examined the sector coupling technology heat pump in the context of a European energy system. The coupling of electricity, heat, and hydrogen generation is described and investigated in Lux et al. (2020) for a European system and in Lux et al. (2021) for a system in the MENA region. Franke et al. (2021) described the model representation of hydrogen grids for the first time and examined a GHG-neutral energy system in China. With its broad coverage of sector coupling options and high technical, temporal, and spatial resolution, Enertile is an appropriate tool for investigating hydrogen supply in Europe. This paper uses the integrated optimization of electricity, heat, and hydrogen supply including hydrogen networks (cf. Figure 7-2) analyzing a European energy system for the first time.

7.2.3 Data

This section provides the input data on energy demands in the different demand scenarios (section 7.2.3.1), on fuel and CO_2 prices (section 7.2.3.2), on constraints to the linear optimization problem (section 7.2.3.3), on utilized parameters on hydrogen infrastructures (section 7.2.3.4), and on renewable electricity potential used in the optimization (section 7.2.3.5).

7.2.3.1 Energy demands

Germany's energy and climate policy goals as of May 2021 require a fundamental restructuring of the energy system that affects all sectors of the economy. The analysis of hydrogen's role in the conversion sector of a GHG-neutral economy in Germany in this paper is based on data from the project 'BMWi Long-term Scenarios' (Fraunhofer ISI et al. 2021). This project uses a series of models representing different sectors and infrastructures and develops consistent scenarios with high technical, spatial and temporal resolution. These scenarios are not intended to predict the future, but show possible developments that are consistent with German energy and climate policy. The overarching goal of the scenarios is to identify robust strategies for achieving GHG neutrality.

The demand for electricity, hydrogen, and district heating in other European countries are based on values taken from the EU Horizon 2020 project "SET-Nav". All SET-Nav pathways achieve a GHG reduction of 85 – 95% across sectors in 2050. This paper's *electrification scenario* and *hydrogen scenario* adopt the demand of the SET-Nav pathway "Directed Vision" for regions outside Germany. The *PtG/PtL scenario* in this paper adopts the energy demand of the SET-Nav pathway "Diversification" for regions outside Germany. These energy demand pathways outside Germany were selected as they have a similar quality in terms of modeling technique and level of detail as the modeling approach for Germany and pursue similar objectives as in the scenario narratives for Germany.

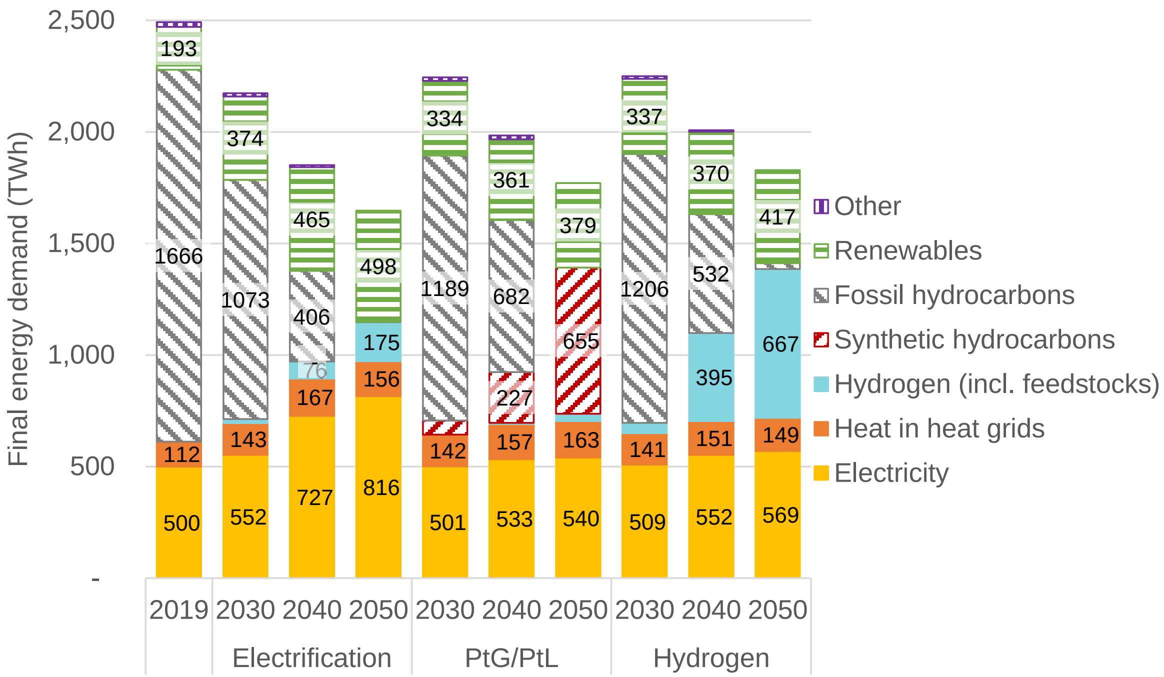

Figure 7-3 Final energy demand of the sectors industry, transport, residential, and services in the three demand variations in Germany. The demand for electricity, heat in heat grids, and hydrogen (including feedstocks) is met by optimizing the energy supply in *Enertile*. Meeting other energy demand is not part of the optimization in *Enertile*. Values for 2019 are taken from (BMWK

2022b), values for the years 2030, 2040, and 2050 are determined by detailed sector models in (Fraunhofer ISI et al. 2021).

Figure 7-3 shows the final energy demand of the demand sectors industry, transport, residential, and services in the three demand variations investigated. The demand for electricity, heat in heat grids, and hydrogen is met by cost minimizing the energy supply in *Enertile*. The demand of other energy forms are balanced externally to *Enertile*.

As the option of GHG reduction via direct electrification is the dominant solution in many applications, electricity demand increases in all three scenarios by 2050. This happens despite substantial energy efficiency improvements in all demand sectors. The increase is most pronounced in the *electrification scenario,* which has a final energy demand for electricity of about 816 TWh_{el} in 2050. Electric heat generation for industrial processes (214 TWh_{el}), heat pumps in buildings (72 TWh_{el}), as well as e-mobility (155 TWh_{el}) are the main drivers of the increased electricity demand in this scenario. In the *hydrogen scenario* and the *PtG/PtL scenario*, the increase in electricity demand is less pronounced. The lowest final energy demand for electricity is in the *PtG/PtL scenario* with about 540 TWh_{el} in 2050.

The importance of heat grids increases substantially in all three scenarios. The final energy demand for district heating increases from 112 TWh_{th} in 2019 (BMWK 2022b) to 149 TWh_{th} in the *hydrogen scenario* and to 163 TWh_{th} in the *PtG/PtL scenario*. For the supply of heat in buildings, the *electrification scenario* differs from the *hydrogen scenario* and the *PtG/PtL scenario* in terms of renovation ambition[13]. In order to realize high shares of electric heat generation, the *electrification scenario* focuses on high building efficiency through insulation, ventilation systems with heat recovery, and ambitious new building standards. There are lower ambitions for building efficiency in both the *PtG/PtL scenario* and the *hydrogen scenario*. The differences in renovation depth have implications for using heat grids to supply heat in buildings. The amount of heat provided in buildings by heat grids increases by 79% to 109 TWh_{th} between 2020 and 2050 in the *electrification scenario*. In the *PtG/PtL scenario* and the *hydrogen scenario*, the amount of heat provided by heat grids in buildings increases by 54% to 94 TWh_{th} between 2020 and 2050. In all scenarios, the number of buildings connected to heat grids increases due to both densification in areas where heat grids already exist and through the construction of new heat grids. The remaining demand for district heating comes from the industrial sector for the provision of process heat.

The final energy demand for hydrogen (including feedstocks for industrial processes) differs significantly in the different scenario narratives. Additional hydrogen demand results from the use of hydrogen as a storage medium in the conversion sector[14]. The utilization of hydrogen as a storage

[13] This aspect of the scenario design accounts for one of the central arguments for the use of PtG and hydrogen for heating as an alternative to the renovations measures that are, at least to some extent, required for an efficient electrification of heat demand in buildings.

[14] Since synthetic hydrocarbons are imported from outside Europe, the hydrogen demand does not include an intermediate product in synthetic fuel production.

medium is calculated endogenously when minimizing supply costs and is discussed in the results section 7.3.2. The *hydrogen scenario* has the highest final energy demand for hydrogen with a total of 667 TWh_{H2} in 2050. The *PtG/PtL scenario* has the lowest final energy demand for hydrogen at 34 TWh_{H2}. The *electrification scenario* is in-between these two extreme positions with a hydrogen demand of 175 TWh_{H2} in 2050. The different hydrogen demand levels in the scenarios are due to different types of use. In the *PtG/PtL scenario*, the final energy demand for hydrogen is limited to the transport sector. Here, a relatively low diffusion of fuel cell vehicles is assumed. This demand amounts to 34 TWh_{H2} in 2050. The other demand sectors in this scenario rely on synthetic, carbon-based energy carriers instead of hydrogen to achieve climate neutrality. These synthetic energy carriers are imported as defined in the scenario and the hydrogen required for their production is not generated in Germany. In the *electrification scenario*, hydrogen demand from the transport sector is supplemented by demand from industry. Hydrogen is used, for example, in the chemical industry as a feedstock or in the steel industry as a reducing agent. In 2050, the hydrogen demand amounts to 20 TWh_{H2} in the transport sector and 156 TWh_{H2} in industry. Only in the *hydrogen scenario* is hydrogen used for heating buildings as well. In 2050, 359 TWh_{H2} of hydrogen demand is accounted for by industry, 129 TWh_{H2} by transport, and 178 TWh_{H2} by heating buildings. The complete hydrogen balances - including model endogenous demands from the conversion sector and hydrogen supply - are shown in Figure 7-6 in the results.

7.2.3.2 Fuel and carbon dioxide prices

Fuel and CO_2 prices are key input parameters in energy system modeling. The level and interaction of fuel prices have a direct impact on the expansion and dispatch decisions for technologies in Enertile. All scenarios assume the same price developments for natural gas, hard coal, lignite, oil, hydrogen imports from outside Europe, and CO_2 certificates. Only the *PtG/PtL scenario* uses synthetic energy carriers. Table 7-1 shows the prices used in this analysis.

Price trends for hard coal, oil, and natural gas are based on the Sustainable Development Scenario of the World Energy Outlook 2019 (IEA 2019). The World Energy Outlook only shows prices up to 2040; for this analysis, prices were extrapolated to 2050 based on previous trends. The conversion of prices to euros is based on the average interbank exchange rate of 2018. In general, the prices of hard coal (6 €/MWh) and natural gas (22 €/MWh) remain at constant levels. The oil price decreases slightly, from 32 €/MWh in 2030 to 29 €/MWh in 2050. For lignite, a flat price of 4 €/MWh is assumed in all scenario years. Overall, the importance of fossil fuel prices decreases in ambitious climate change mitigation scenarios.

To reduce fossil fuels, a key steering parameter in supply side modeling is the CO_2 price. This CO_2 price penalizes emissions from the use of oil, hard coal, lignite, and natural gas for electricity and heat generation. To realize GHG-neutrality by mid-century, the CO_2 price increases from 75 €/t_{CO2} in 2030 to 500 €/t_{CO2} in 2050 in all scenarios.

The electricity and heat supply modeling in Enertile can use hydrogen and synthetic methane as GHG-neutral energy carriers. In addition to the model's endogenous production and distribution of hydrogen within Europe, GHG-neutral hydrogen can also be imported from outside Europe at fixed prices. The hydrogen import price decreases from 101 €/MWh in 2030 to 81 €/MWh in 2050. Synthetic methane is only used in the *PtG/PtL scenario* and is successively blended with natural gas. The assumed blending rates are 5% in 2030, 25% in 2040 and 100% in 2050. Synthetic methane is imported from outside Europe and the import price drops from 126 €/MWh in 2030 to 94 €/MWh in 2050. The import price time series of hydrogen and synthetic methane are based on modeling work for the MENA region (Lux et al. 2021). The time series from Lux et al. (2021) were adjusted to the WACC of 2% generally assumed in this paper.

Table 7-1 Fuel and CO_2 prices used in the different scenarios and simulation years.

Scenario	Category	Unit	2030	2040	2050
All	Natural gas	€/MWh	22	22	22
	Hard coal	€/MWh	6	6	6
	Lignite	€/MWh	4	4	4
	Oil	€/MWh	32	31	29
	Hydrogen (from outside Europe)	€/MWh	101	91	81
	CO_2	€/t	75	125	500
PtG/PtL scenario	Synthetic methane (from outside Europe)	€/MWh	126	110	94

7.2.3.3 Constraints

In all scenarios, the system change towards a GHG-neutral energy supply follows guiding principles that are formulated as constraints in the optimization. These constraints reflect, among other aspects, some basic tenets of Germany's energy and climate legislation. However, not all legislation is implemented to allow the model to make decisions in the optimization. For example, the statutory sector targets for the year 2030 are not reflected in the scenarios.

In all scenarios, the phase-out of nuclear energy by 2022 (Bundestag 2011) and the step-wise phase-out of coal until 2038 (Bundestag 2020) are implemented as stipulated in the respective laws.

Renewable energy expansion corridors are also specified for Germany. For 2030, between 71 GW_{el} and 80 GW_{el} of onshore wind capacity must be installed. For offshore wind, an installed capacity of at least 20 GW_{el} must be reached in 2030 and must increase to at least 40 GW_{el} until 2040. The photovoltaic target sets a minimum expansion to 100 GW_{el} by 2030.

The National Hydrogen Strategy in Germany (BMWi 2020) is implemented in all scenarios. This requires electrolyzer capacities in Germany of at least 5 GW_{el} by 2030 and of at least 10 GW_{el} by 2040. The utilization of these capacities – i.e., the production of hydrogen – can be optimized freely by the model.

Due to the limited availability of sustainable biomass and sectoral competition for the available biomass, the conversion sector quasi-exits the use of biomass for electricity and heat generation after 2030 in all scenarios. Existing biomass power plants leave the system depending on their technical lifetime and year of installation. The only remaining plants are those that run on waste landfill and sewage gas. As a consequence, the capacity of biomass power plants is reduced to 800 MW_{el} in the conversion sector by 2050.

Electricity imports from other European countries are indirectly limited in order to prevent an electricity import dependency exceeding the level perceived as politically feasible. For this purpose, different minimum generation quantities of renewable electricity are defined in the scenarios for the year 2050. This defines a minimum generation within Germany that cannot be replaced with imports. In the *electrification scenario* and the *hydrogen scenario*, a minimum of 900 TWh_{el} of renewable electricity must be generated in Germany in the year 2050. In the *PtG/PtL scenario*, the overall electricity demand is lower and there is a national minimum renewable electricity generation of 650 TWh_{el} in the year 2050.

Fossil fuels may no longer be used for electricity and heat generation in 2050. In all scenarios except the *PtG/PtL scenario*, natural gas-based conversion technologies are no longer part of the technology portfolio. In the *PtG/PtL scenario*, gas technologies are still allowed, but the gas used must be completely GHG-neutral. The phase-out of oil and coal-based electricity generation already happens before 2040.

7.2.3.4 Hydrogen infrastructures

For the expansion and use of hydrogen infrastructure in the cost minimization, its techno-economic parameterization is of central importance. Table 7-2 summarizes the assumptions regarding specific investments, variable operation and maintenance costs (O&M), fixed O&M, technical lifetimes, and the system efficiencies of hydrogen technologies available in the model. All scenarios assume the same price developments for these technologies.

Costs resulting from investments are considered in the cost optimization based on annuities. When calculating these annuities, a weighted average cost of capital of 2% is assumed for all technologies, regions, and simulation years.

The parameterization of hydrogen-based heat and power generation technologies (i.e., hydrogen turbines (CHP and non-CHP), combined cycle turbines (CHP and non-CHP), hydrogen boilers) is based on the techno-economic parameters of natural gas-based technologies. Hydrogen-based technologies are not yet available on an industrial scale today. This paper assumes that the existing extensive experience with combustion units of natural gas can provide benefits, and that hydrogen technologies with similar technical characteristics will be developed.

In electrolytic hydrogen production, a distinction can be made between low-temperature and high-temperature electrolyzers. High-temperature electrolyzers can achieve high electrical efficiencies if the heat supplied from other sources is available at a high temperature level. If there is no high-temperature source available and the heat has to be provided by auxiliary electrical heating, high-temperature electrolysis processes are not more efficient than low-temperature processes. In order to be independent of external heat sources in the siting decision of electrolyzers, electrolysis parameters of the low-temperature technologies alkaline electrolysis (AEL) and polymer electrolyte membrane electrolysis (PEMEL) are used in this paper. These technologies are already more advanced and thus less expensive than high-temperature electrolyzers. The energy system model *Enertile* cannot sufficiently resolve the technical differences between AEL and PEMEL to decide between the two technologies. Therefore, the model parameterization assumes values averaged between these technologies. More detailed reviews on the techno-economic properties of the different electrolyzer technologies are given in (Buttler et al. 2018).

At present, hydrogen pipelines are only used for short point-to-point connections or in relatively small grids connecting industrial clusters; i.e., there is no transnational pipeline-based hydrogen infrastructure in Europe. Potentially, parts of the existing European natural gas transport network could be repurposed into a hydrogen network if fossil gas is phased out. However, which pipelines will be available at which point in the future depends on multiple parameters, including the natural gas supply and demand structures for Europe. Therefore, this paper conservatively assumes a greenfield approach to the development of hydrogen transport pipelines in Europe. The parameters for pipeline construction are based on (Ball et al. 2010).

Table 7-2 Parametrization of hydrogen infrastructures in the scenario runs.

Technology	**Parameter**	**Unit**	**2030**	**2040**	**2050**
Electrolyzer (low temperature)	Efficiency	%	66	68	71
	Specific investment	€/kW_{el}	575	481	388
	Lifetime	a	20	20	20
	Fix OPEX	€/kW_{el}	16.00	15.75	15.50
Hydrogen turbine	Efficiency	%	41	41	41
	Specific investment	€/kW_{el}	400	400	400
	Lifetime	a	30	30	30
	Fix OPEX	€/kW_{el}	7.5	7.5	7.5
	Var OPEX	€/kWh_{el}	1.5	1.5	1.5
Hydrogen turbine (CHP)	Efficiency (el)	%	33	33	33
	Efficiency (CHP)	%	85	85	85
	Specific investment	€/kW_{el}	730	730	730
	Lifetime	a	30	30	30
	Fix OPEX	€/kW_{el}	30	30	30
	Var OPEX	€/kWh_{el}	2.7	2.7	2.7
Combined cycle hydrogen turbine	Efficiency	%	59	60	61
	Specific investment	€/kW_{el}	775	750	750
	Lifetime	a	30	30	30
	Fix OPEX	€/kW_{el}	11.63	11.25	11.25
Hydrogen boiler	Efficiency (th)	%	104	104	104
	Specific investment	€/kW_{th}	50	50	50
	Lifetime	a	25	25	25
	Fix OPEX	€/kW_{th}	1.8	1.8	1.8
	Var OPEX	€/kWh_{th}	0.9	0.9	0.9

Technology	**Parameter**	**Unit**	**2030**	**2040**	**2050**
Combined cycle hydrogen turbine (CHP)	Efficiency (el)	%	48	48	48
	Efficiency (CHP)	%	88	88	88
	Specific investment	€/kW$_{el}$	950	950	950
	Lifetime	a	30	30	30
	Fix OPEX	€/kW$_{el}$	30	30	30
	Var OPEX	€/kWh$_{el}$	3.00	3.00	3.00
Hydrogen pipeline	Specific investment	€/(km MW$_{H2}$)	1120	1120	1120
	Fix OPEX	% of invest	1	1	1

7.2.3.5 Electricity generation potential of renewable energies

a) Germany, all scenarios except onshore wind scenario

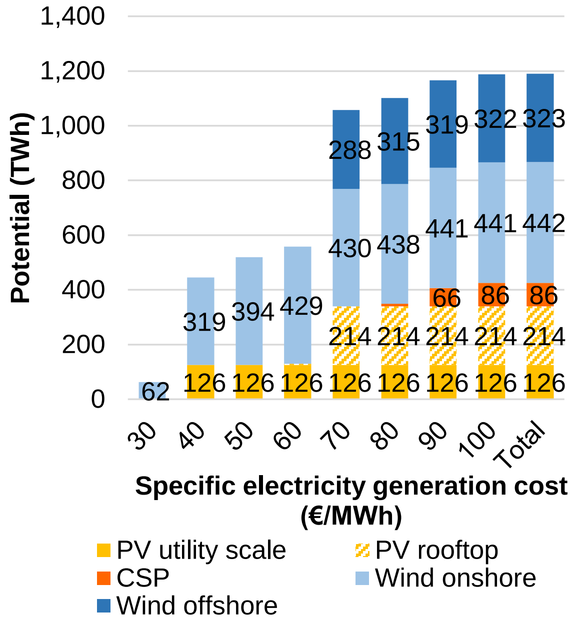

b) Germany, onshore wind scenario

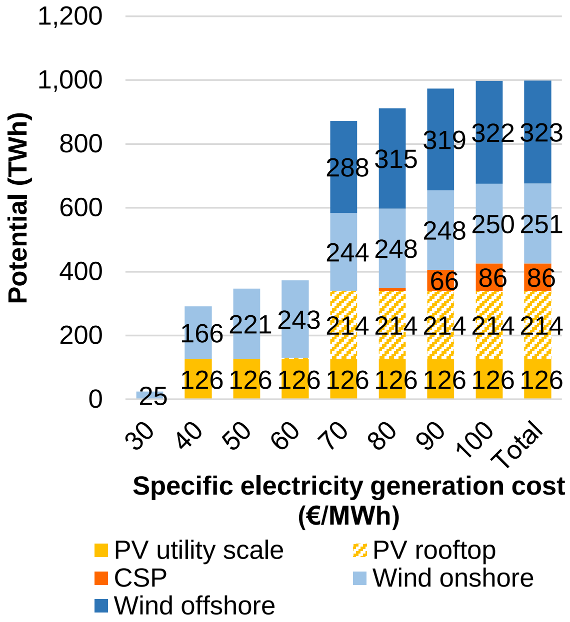

c) Europe, all scenarios except onshore wind scenario

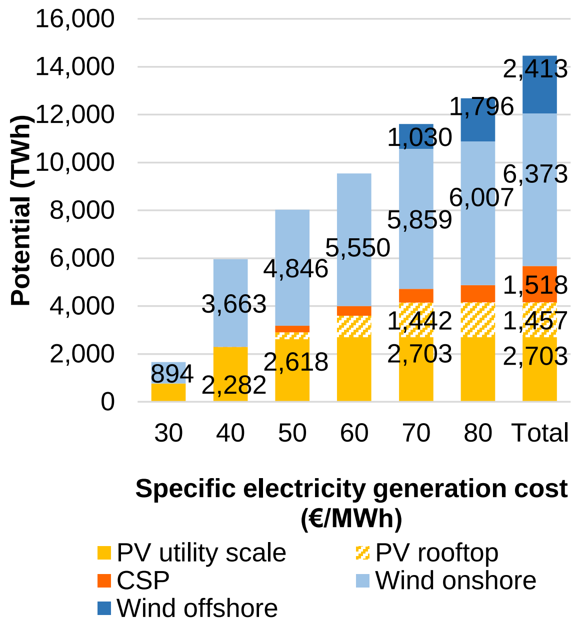

d) Europe, onshore wind scenario

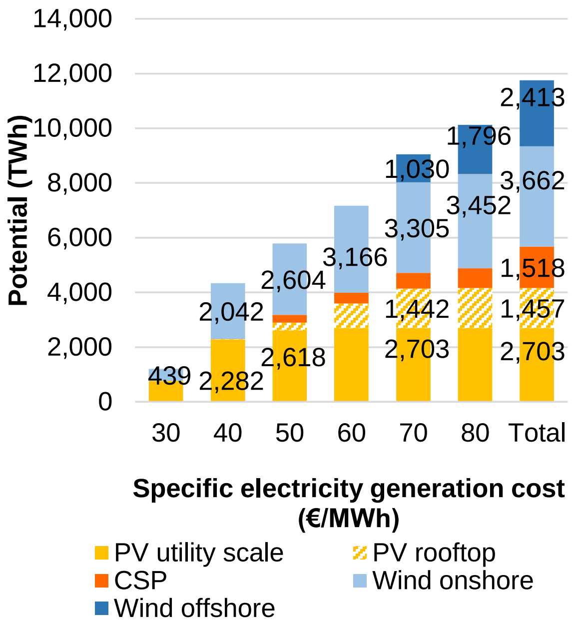

Figure 7-4 Electricity generation potential of the technologies onshore wind, offshore wind, CSP, PV utility scale, and PV rooftop in Germany and Europe in 2050. The potential for the *onshore wind scenario* (b) & (d), and all other scenarios (a) & (c) is displayed.

Figure 7-4 shows the renewable electricity generation potential of the renewable technologies onshore wind, offshore wind, CSP, utility scale PV, and rooftop PV for Germany and Europe in 2050. These potentials serve as input for the energy system optimization in Enertile. In all scenarios except the onshore wind scenario, the renewable potential in Germany totals about 1,200 TWh. There are mainly onshore wind and utility scale PV potentials at electricity generation costs below 60 €/MWh. Offshore wind and rooftop PV show higher electricity generation costs. Onshore wind has the greatest potential at 442 TWh. The potential in Europe amounts to over 14,000 TWh. Onshore wind has the highest potential with 6,373 TWh. In the *onshore wind scenario*, the onshore wind potential decreases to 251 TWh in Germany and 3,662 TWh in Europe.

7.3 Results

This section describes the results of the energy supply optimization for the different scenario variants. These focus on the underlying electricity systems (section 7.3.1), the hydrogen balances in Germany (section 7.3.2), the geographical distribution of hydrogen production and demand within Germany (section 7.3.3), the European hydrogen transport flows (section 7.3.4), the deployment of hydrogen infrastructures over the course of the year (section 7.3.5), and the overall system costs (section 7.3.6).

7.3.1 Electricity supply

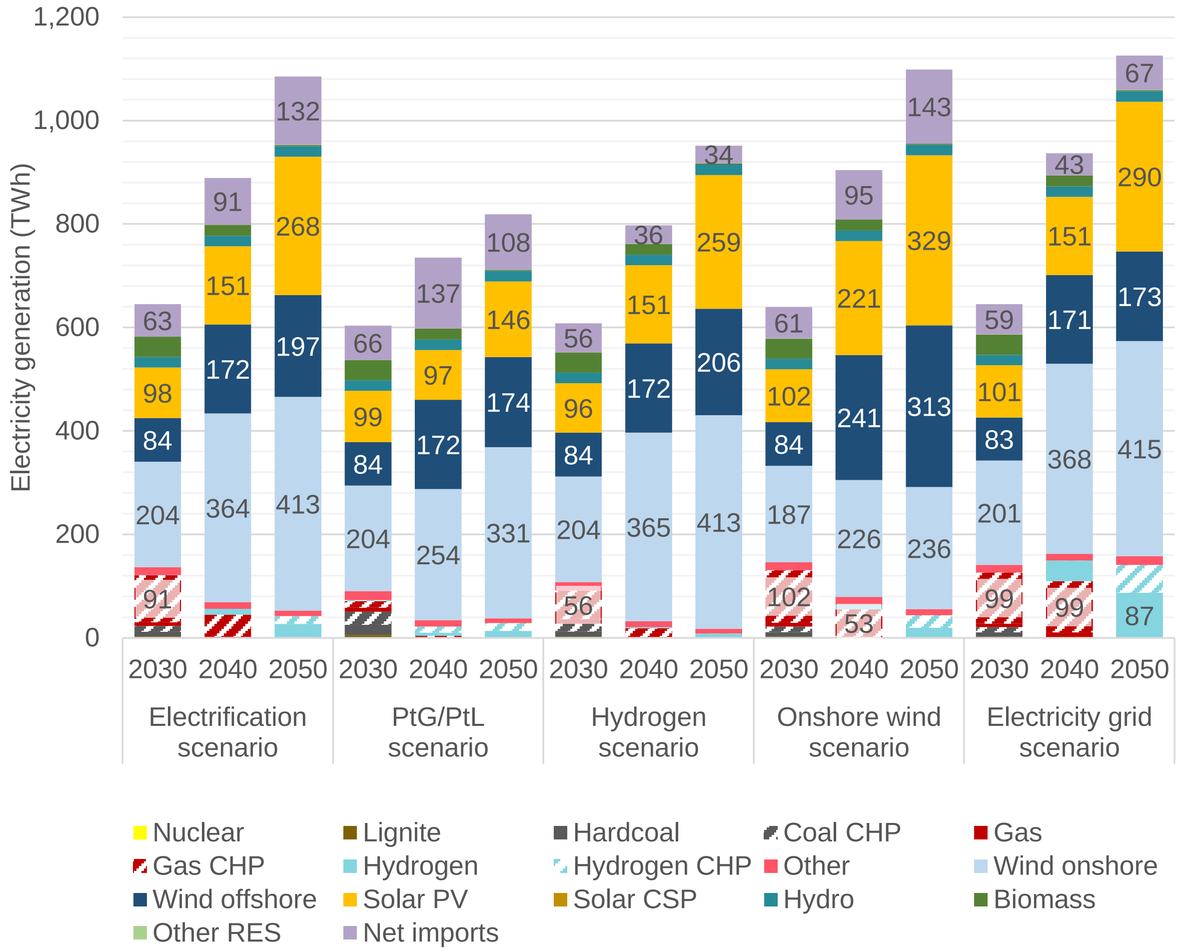

Figure 7-5 Development of electricity supply in the optimization results of the different scenarios up to the year 2050.

Since more than half of Germany's power is currently generated by fossil energy sources, the German power sector is subject to major changes in all analyzed paths to GHG neutrality. Figure 7-5 shows the developments of electricity supply in the optimization results up to the year 2050. Several trends can be observed.

First, the increased demand for electricity requires a substantial increase in electricity supply over time in all scenarios. There are two underlying reasons for this increase: Firstly, the sectoral electricity demand determined by the simulation models increases for all three underlying demand scenario variants over time (cf. section 7.2.3.1). This increase is most pronounced in the *electrification scenario*, *onshore wind scenario*, and *electricity grid scenario*, which are all based on the demand variation focused on an electrification of end-use applications. This type of electricity demand is an exogenous input into the *Enertile* model. Secondly, the electricity supply in Figure 7-5 also covers the increasing and partly model-endogenous electricity demand of heat pumps and electric boilers for the provision of heat in district heating grids, of electrolyzers, as well as grid losses, and storage losses. Especially the electricity consumption of power-to-hydrogen in 2050 increases to between 130 TWh in the *electrification scenario* and 257 TWh in the *hydrogen scenario*. Similarly, the electricity consumption of power-to-heat in 2050 increases to between 110 TWh in the *PtG/PtL scenario* and 131 TWh in the electrification scenario. In total, electricity supply in 2050 ranges between 819 TWh_{el} in the *PtG/PtL scenario* and 1,126 TWh_{el} in the *electricity grid scenario.*

A second major trend is that renewables increasingly dominate electricity supply. In all scenarios, except the *PtG/PtL scenario*, minimum renewable generation levels are implemented as implicit import restrictions. In these scenarios, renewable electricity generation increases up to 900 TWh_{el} in 2050. In the *PtG/PtL scenario,* renewable generation exceeds the minimum target of 650 TWh_{el} and reaches 674 TWh_{el} in 2050. Onshore wind dominates the electricity mix in the optimization results unless its potentials are constrained by scenario design in the *onshore wind scenario*. In all scenarios, except the *PtG/PtL scenario,* the available onshore wind potentials in Germany are almost fully exploited. In all scenarios, except the *onshore wind scenario*, this onshore wind potential amounts to 442 TWh_{el} in 2050; the more restricted configuration in the *onshore wind scenario* totals 251 TWh_{el} in 2050. The *PtG/PtL scenario* also reaches a high level of onshore wind generation with 331 TWh_{el} in 2050. In all scenarios except the *PtG/PtL scenario*, PV is the second most important generation technology. This contributes between 146 TWh_{el} in the *PtG/PtL scenario* and 329 TWh_{el} in the *onshore wind scenario* to the power generation mix. Especially the potential of ground mounted PV is almost fully exploited in all scenarios except the *PtG/PtL scenario*. Offshore wind, as a relatively expensive technology, is only expanded beyond the specified minimum policy target of 40 GW_{el} in the *electrifications scenario*, the *hydrogen scenario*, and the *onshore wind scenario*. In these scenarios, generation from offshore wind reaches 197 TWh_{el}, 206 TWh_{el}, and 313 TWh_{el} respectively. In all other scenario variants, offshore wind contributes only 174 TWh_{el} in 2050. Especially in all scenarios based on the demand variations focused on electrification and hydrogen, the available renewable electricity generation potential in Germany is strongly exploited by 2050. The *PtG/PtL scenario* meets its goal of lower utilization of the German renewable electricity generation potential.

A third trend is that Germany becomes a net importer of electricity in all scenarios. In 2050, imports increase to between 34 TWh_{el} in the *hydrogen scenario* and 143 TWh in the *onshore wind scenario*. Electricity imports increase strongly between 2030 and 2050, and remain constant only in the *hydrogen scenario* and the *electricity grid scenario*. If there were no implicit import restrictions for Germany, the electricity imports from other European countries would be even higher in all scenarios in 2050 except the *PtG/PtL scenario*. These electricity imports are accompanied in the modeling results by a corresponding increase in electricity generation capacities in the exporting European countries.

A fourth major trend is that flexible and controllable electricity generation units change from gas to hydrogen in all scenarios. The capacity of hydrogen power plants in 2050 ranges between

26 GW_{el} in the *hydrogen scenario* and 82 GW_{el} in the *electricity grid variation*. It is noteworthy that, even in the *PtG/PtL scenario*, gas-fired power plants using synthetic methane are displaced by hydrogen power plants in 2050.

7.3.2 Hydrogen balances

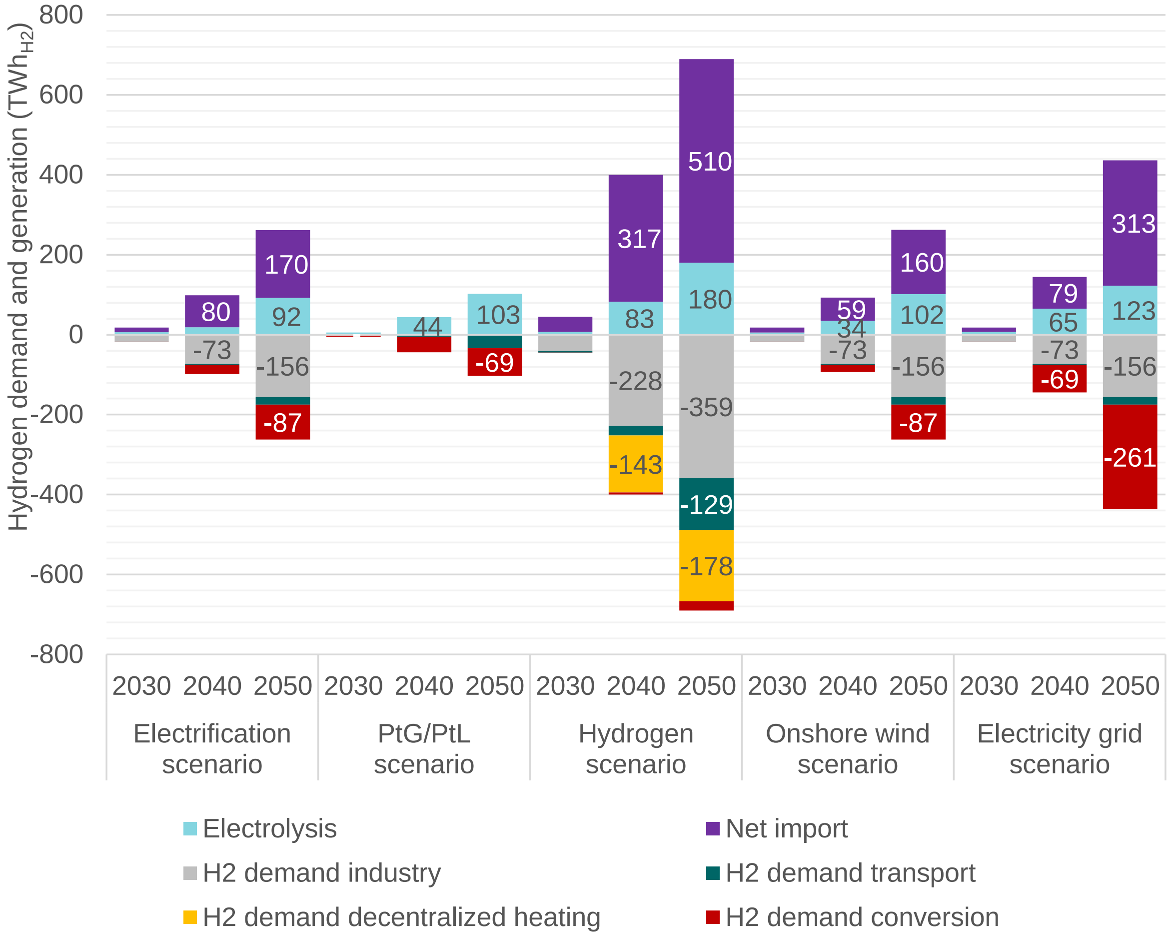

Figure 7-6 Annual hydrogen balances for all scenarios in Germany. Demand from the sectors industry, transport, and tertiary is exogenous. The use of hydrogen in the conversion sector is a modeling decision. Hydrogen imports and electrolytic hydrogen production in Germany are optimization results.

Figure 7-6 shows the German hydrogen balances in all scenarios for the different simulation years. The hydrogen demand of the sectors industry, transport, and decentralized building heat is given exogenously and varies greatly in the underlying demand variations (cf. section 7.2.3.1). The hydrogen supply and the use of hydrogen in the conversion sector for the generation of electricity and heat for heat grids result from modeling decisions in the cost optimization. In contrast to all other scenarios, hydrogen imports from neighboring European countries are not permitted in the

PtG/PtL scenario[15]. Overall, the supply of electricity-based hydrogen in Germany increases to between 103 TWh_{H2} in the *PtG/PtL scenario* and 690 TWh_{H2} in the *hydrogen scenario* in 2050.

The comparison between the scenarios shows clear differences with regard to the use of hydrogen in the conversion sector. Three realizations in the optimization results may be distinguished: firstly, in the electrification scenario 87 TWh_{H2} of hydrogen are used to generate electricity and heat in heating networks. In comparison, a variation in the onshore wind potentials or a shift of energy demands towards PtG/PtL in the demand sectors show only minor impacts on the hydrogen utilization in the conversion sector. Secondly, a substantial increase of hydrogen utilization in the conversion sector results from a reduced provision of flexibility by the electricity transport network. In the *electricity grid scenario*, 261 TWh_{H2} of hydrogen are converted to electricity and heat in heat networks. Thirdly, hydrogen use in the conversion sector is significantly reduced in the *hydrogen scenario* with 23 TWh_{H2}. The reason for the reduced use of hydrogen in electricity and heat generation in this scenario is the overall higher hydrogen demand level from the other sectors. The high hydrogen demand results in an increased model endogenous hydrogen price – 68 €/MWh_{H2}[16] in the *hydrogen scenario* vs. 59 €/MWh_{H2} in the *PtG/PtL scenario* – making a utilization in the conversion sector less attractive for the optimization.

If the model has the option of expanding a European hydrogen network, it meets the main part of the German hydrogen demand with imports from Europe. In the *electrification scenario*, about 170 TWh_{H2} of hydrogen are imported from other European countries. In comparison to the *electrification scenario*, reduced onshore wind potentials do not have a substantial impact on the level of hydrogen imports. As more processes and applications are converted to the use of hydrogen in the *hydrogen scenario* and the sectoral demands in Germany are consequently increased, the highest hydrogen imports of 510 TWh_{H2} can be observed. If electricity imports are limited by a reduced electricity network expansion, the model deviates to hydrogen imports. In the *electricity grid scenario*, hydrogen imports of 313 TWh_{H2} are higher than in the electrification scenario. In the *PtG/PtL scenario*, imports are not included in the scenario design. The remaining hydrogen demand is provided through electrolytic hydrogen production within Germany.

In the *electrification scenario*, the domestic electrolyzer capacity in 2050 amounts to 41 GW_{el}. Due to the lack of a European hydrogen transport infrastructure in the *PtG/PtL scenario*, the required hydrogen must be produced in Germany and the electrolyzer capacity is slightly increased to 43 GW_{el}. In the *onshore wind scenario*, a substantial part of the reduced electricity generation with onshore wind is replaced by PV (cf. section 7.3.1). To integrate the increased PV midday peaks, the electrolyzer capacity is increased to 54 GW_{el} in this scenario. In the *electricity grid scenario*, the optimization increases the electrolyzer capacity to 61 GW_{el} to compensate for the reduced integra-

[15] It is assumed that with the continued strong usage of methane networks an international hydrogen backbone spanning the continent will not be established.

[16] Model endogenous hydrogen prices can be read as shadow prices from the optimization results of the hydrogen demand constraints.

tion capability of the grid with respect to renewable energy by a flexible consumer. The increased demand for hydrogen in the *hydrogen scenario* is met by an increased electrolyzer capacity of 75 GW_{el} alongside a substantial increase in imports. The full load hours of these electrolyzers range between 2,700 h in the *onshore wind scenario* and 3,500 h in the *hydrogen scenario*.

7.3.3 Geographical distribution of hydrogen demand and generation

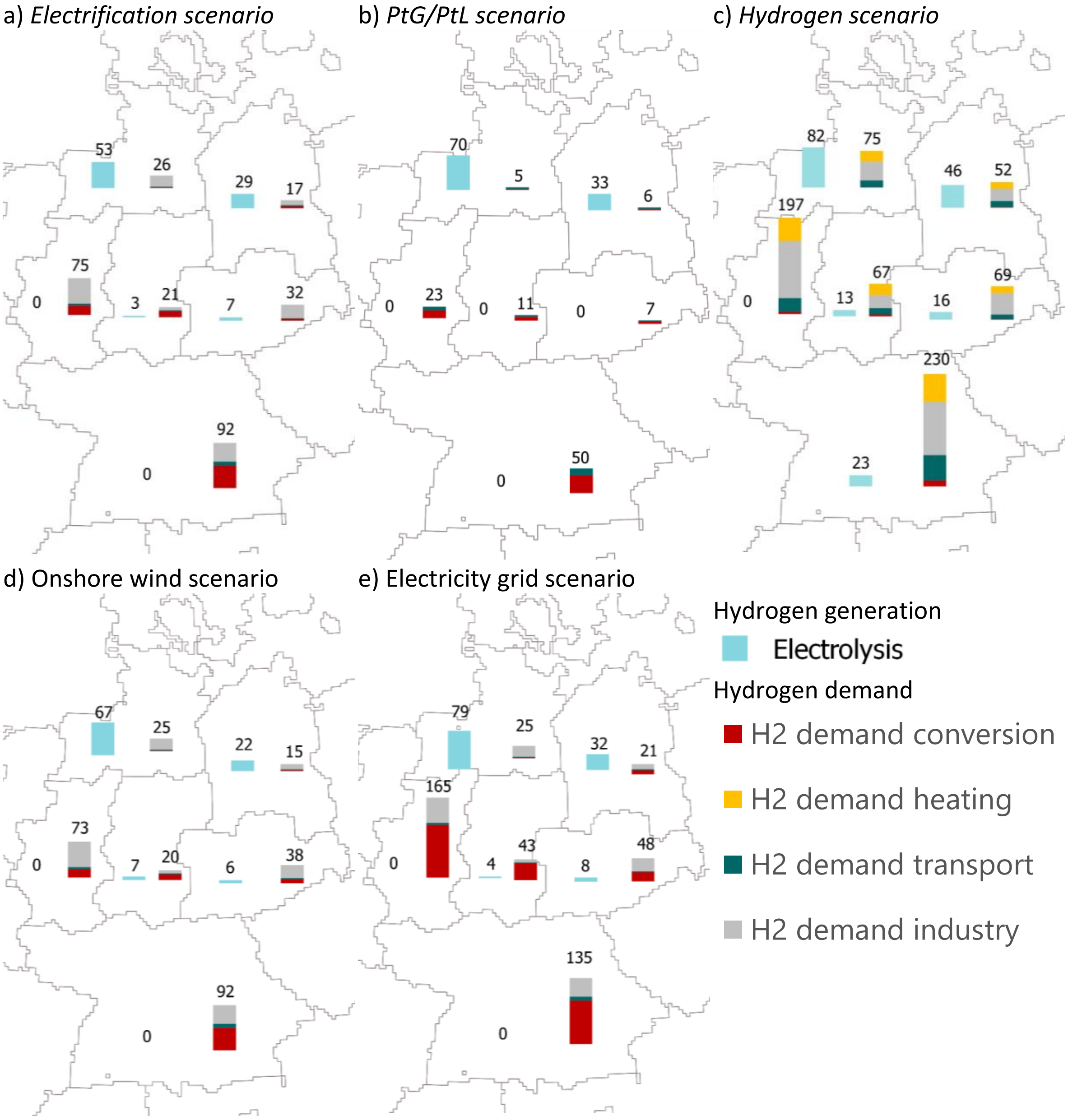

Figure 7-7 Regional distribution of hydrogen production via electrolysis and hydrogen demand by various sectors in 2050 in Germany for the a) electrification scenario, b) PtG/PtL scenario, c) hydrogen scenario, d) onshore wind scenario, and e) electricity grid scenario. Demand from the sectors industry, transport, and heating in buildings is given exogenously. The use of hydrogen in the conversion sector and the electrolytic hydrogen production is a modeling decision.

For all scenarios, Figure 7-7 shows a concentration of electrolytic hydrogen production in the northern coastal regions in 2050. At least 71% of the total German hydrogen production in 2050 takes place at the North Sea and the Baltic Sea, independent of the underlying scenario. The joint absolute hydrogen production volumes of these two regions range between 83 TWh_{H2} in the *electrification scenario* and 129 TWh_{H2} in the *hydrogen scenario*. To produce these amounts of hydrogen via electrolysis, a total electrolyzer capacity of between 37 GW_{el} in the *electrification scenario* and 55 GW_{el} in the *hydrogen scenario* are installed in these northern German regions by the year 2050. The concentration of electrolyzer capacities allows the model to integrate high capacities of wind power at the coast, which would otherwise require greater expansion of the electricity grid.

The scenario comparison in Figure 7-7 shows that with increasing hydrogen demand, hydrogen production increasingly takes place in central and southern Germany as well. In the *PtG/PtL scenario* – with the lowest hydrogen demand of 103 TWh_{H2} – electrolysis takes place exclusively in the two coastal regions. With a higher hydrogen demand of 262 TWh_{H2} in the *electrification scenario*, there is also hydrogen production totaling 10 TWh_{H2} in central and eastern Germany. In the *hydrogen scenario* – with the highest hydrogen demand of 690 TWh_{H2} – hydrogen is produced everywhere except western Germany, which is the region with the lowest renewable electricity generation potential compared to its electricity demand. With rising hydrogen demand, increasingly expensive renewable electricity potential must be used for hydrogen production in regions with already high electricity loads.

Hydrogen demand is concentrated in western and southern Germany in all scenarios. This includes both the exogenous hydrogen demand from the sectors industry, transport, and heating buildings, and the model-endogenous hydrogen demand from the conversion sector. Regardless of the underlying scenario, the hydrogen demand of the two model regions in western and southern Germany account for at least 59% of the total hydrogen demand in 2050. Compared to the electrification scenario, reduced expansion of the electricity transmission grid in the *electricity grid scenario* substantially increases hydrogen use in the conversion sector in western and southern Germany. Due to their high electricity demand and low renewable potential, these regions are dependent on energy imports. If these cannot be realized via the electricity grid, the model converts hydrogen imports into electricity.

7.3.4 European hydrogen transport flows

Depending on the scenario, regional deviations of hydrogen demand and production can be compensated supra-regionally by hydrogen pipeline networks. Due to the low hydrogen demand compared to all other scenarios, the hydrogen transport network in the *PtG/PtL scenario* is limited to hydrogen trade flows between the different German sub-regions by design. In all other scenarios, hydrogen demand and supply can be additionally balanced via a European hydrogen network.

Figure 7-8 shows that there is a stable hydrogen transport route from the coast in the north to western Germany in all scenarios. Similarly, the optimization results show pronounced hydrogen transport flows from the two coastal regions to southern Germany in all scenario variants except the onshore wind variation. These optimization results balance the high hydrogen demand in southern and western Germany and high hydrogen production at the German coast (cf. Figure 7-7). The net hydrogen trade flows leaving the coastal region to the southwest range between 23 TWh_{H2} in the *PtG/PtL scenario* and 154 TWh in the *electricity grid scenario*. The associated hydrogen transport capacities amount to between 3 GW_{H2} and 18 GW_{H2}. Excluding the onshore wind scenario, the net hydrogen flows departing the two northern German zones southwards amount to between 68 TWh_{H2} in the *PtG/PtL scenario* and 164 TWh_{H2} in the *hydrogen scenario* in 2050. The associated hydrogen transport capacities departing Northern Germany southwards lie between 8 GW_{H2} and 19 GW_{H2}. In the *hydrogen scenario*, some of the hydrogen required is not produced in these two regions, but transits Northern Germany from the British Isles and Scandinavia. A reduced availability of onshore wind in the *onshore wind scenario* shifts hydrogen production across Europe towards available PV potentials and thereby changes the hydrogen transport infrastructure. As a result, the north-south link in Germany is less pronounced. The hydrogen transport capacities departing the two northern German zones southwards amount to 2 GW_{H2} transporting 14 TWh_{H2} in 2050 in this scenario.

In all scenarios that allow the expansion of a European hydrogen transport infrastructure, the optimization makes use of this option. Excluding the *PtG/PtL scenario*, by 2050, Germany has a total interconnection capacity with other European countries of between 18 GW_{H2} in the *onshore wind scenario* and 58 GW_{H2} in the *hydrogen scenario*. All these scenarios show pronounced net hydrogen flows from the edges of Europe towards Central Europe. Based on the scenario comparison in Figure 7-8, four major hydrogen transport routes can be identified: Firstly, if wind onshore potentials are not restricted, the British Isles become the largest net exporter of hydrogen. These exports contribute predominantly to meeting hydrogen demand in Germany. Net hydrogen flows between 147 TWh_{H2} in the *electrification scenario* and 220 TWh_{H2} in the *hydrogen scenario* are transmitted from the British Isles to Germany in 2050. With constant hydrogen flows over the year (cf. section 7.3.5), the hydrogen interconnector capacity for these amounts is between 17 GW_{H2} in the *electrification scenario* and 25 GW_{H2} in the *hydrogen scenario*. As most of the hydrogen on the British Isles is produced using wind power, this transport route is considerably reduced in the *onshore wind scenario*: With a transport capacity of 1 GW_{H2}, only 9 TWh_{H2} hydrogen are exported to Germany. Secondly, the Scandinavian countries generate export surpluses to supply Central Europe in all scenarios. In the electrification scenario, Norway, Sweden, Finland, and Denmark provide a total of 162 TWh_{H2} to supply the Benelux Union and Germany in 2050. In the *hydrogen scenario,* the supply to Central Europe along this route increases to 280 TWh_{H2}. Thirdly, the Iberian Peninsula is connected to the European hydrogen supply via France. In the *electrification scenario*, the Iberian Peninsula provides 44 TWh_{H2} to meet hydrogen demand in France and Italy. In the *hydrogen scenario*, the net hydrogen exports from the Iberian Peninsula increase to 100 TWh_{H2}. In addition to France and Italy, Germany benefits from these higher exports. In the *onshore wind scenario*, the Iberian Peninsula becomes the largest hydrogen exporter due to its abundant and low-cost PV power generation potential. A net hydrogen trade volume of 194 TWh_{H2} is exported via France to supply Central Europe. Fourthly, high hydrogen demand in the *hydrogen scenario* results in hydrogen flows from the Baltic States and Poland to Central Europe. In total, these Eastern European countries provide 121 TWh_{H2} to supply Germany, the Czech Republic and Austria. Increased trade flows can also be observed on this route in the *onshore wind scenario*: In the *electrification scenario*, there is still untapped PV potential in Eastern Europe that is exploited in this scenario. Route-independent, hydrogen trade flows from the edges of Europe towards Central Europe increase in the *electricity grid scenario* compared to the *electrification scenario*.

For a deeper understanding of hydrogen trade flows in Europe, Figure 7-9 shows the relationship between electricity demand and cumulative renewable electricity generation potentials in the *electrification scenario* in 2050. The electricity demand includes the exogenously specified electricity demand and the electricity equivalents of the hydrogen demand in the different model regions. The total renewable electricity generation potential is the sum of the individual potentials for onshore wind, offshore wind, PV, and CSP. This graph does not provide information on the balancing of hourly supply and demand profiles, the use of storage, or electricity trade flows between the model regions. The figure illustrates that energy imports are very attractive for Germany. Compared to other European countries, Germany is characterized by its high demand for electricity and hydrogen and its limited, low-cost potential for renewable electricity generation. If Germany had to meet its electricity demand autonomously using its own renewable potential, this would incur electricity production costs of 100 €/MWh and reach the limits of its potential. In contrast, the hydrogen exporting regions on all four identified main transport routes to Germany have available renewable potential at levelized cost of electricity of 40 €/MWh even after domestic electricity demands are met. In the optimization result, these regions therefore contribute to the German hydrogen supply via a European hydrogen transport grid.

In the analyzed scenarios, hydrogen demand is met only by domestic European hydrogen production, there are no hydrogen imports from outside Europe.

a) *Electrification scenario*

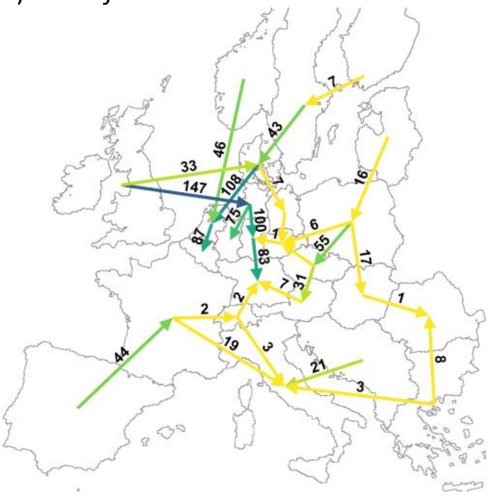

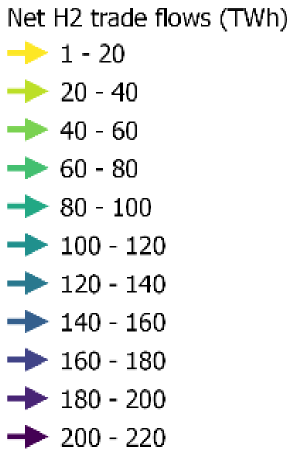

b) *PtG/PtL scenario*

c) *Hydrogen scenario*

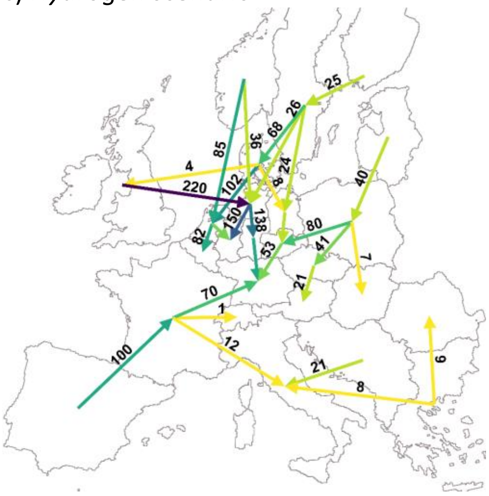

d) *Onshore wind scenario*

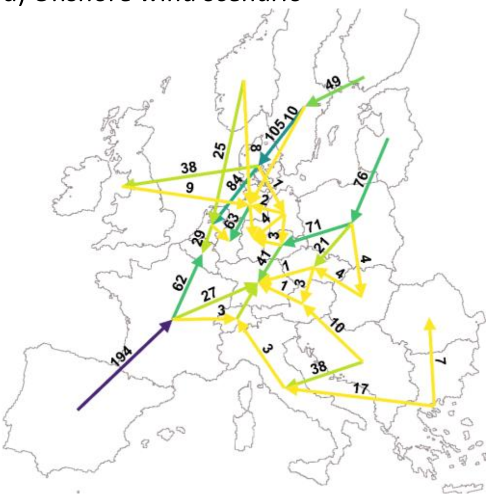

e) *Electricity grid scenario*

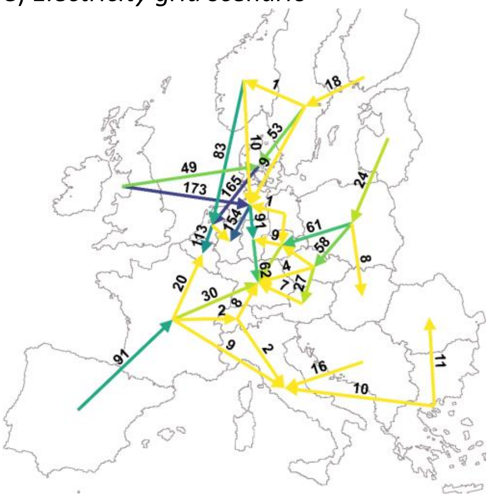

Figure 7-8 Net hydrogen trade flows in 2050 in the a) electrification scenario, b) PtG/PtL scenario, and c) hydrogen scenario, d) onshore wind scenario, and d) electricity grid scenario.

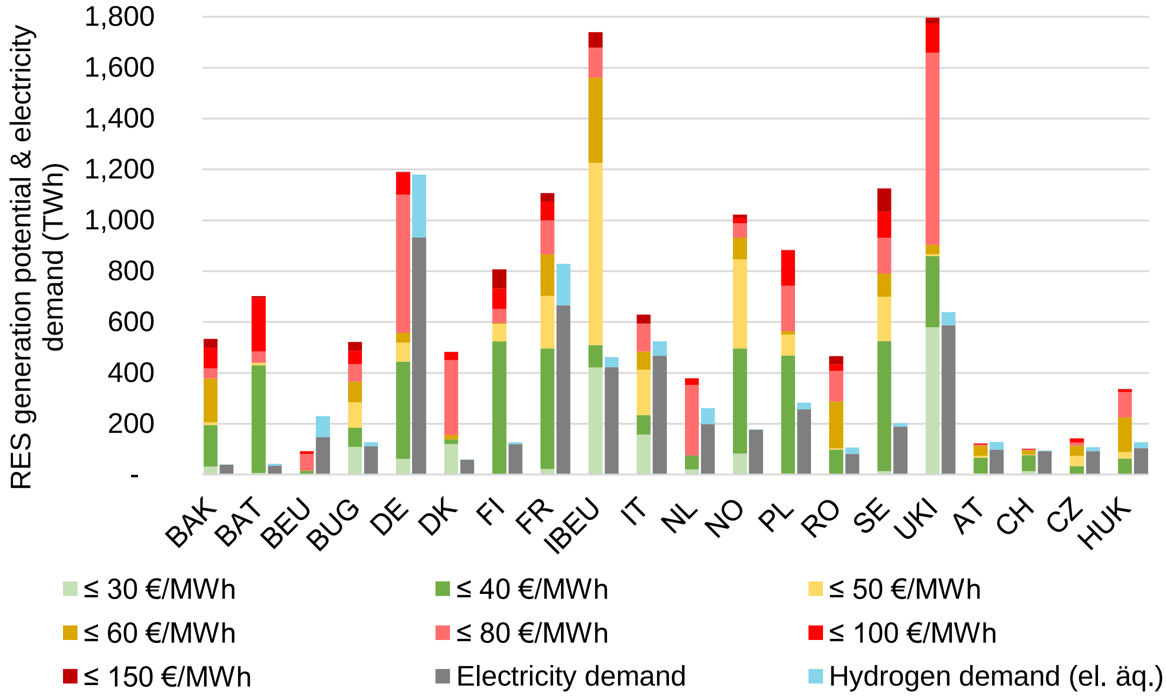

Figure 7-9 Comparison of renewable electricity generation potential and electricity demand in the different model regions (cf. Figure A1) in the *electrification scenario* for the year 2050. The electricity demand includes the exogenous electricity demand of the demand sectors, the electricity usage for heat generation and the electricity equivalent of hydrogen demand. This representation does not take into account storage losses or infrastructure requirements for cross-regional electricity or hydrogen trade.

7.3.5 Hourly dispatch and seasonal hydrogen storage management

Hydrogen serves as a long-term energy storage medium in all scenarios. Figure 7-10 shows a working gas volume of 68 TWh_{H2} hydrogen storage in the electrification scenario. This hydrogen storage is reduced in both demand variations. In the *PtG/PtL scenario*, storage with a working gas volume of 57 TWh_{H2} is sufficient for the optimization due to decreased hydrogen demand. In the *hydrogen scenario*, comparatively little hydrogen is used in the conversion sector to balance residual loads in winter (cf. Figure 7-10). In addition, a large part of the increased sectoral demand is met by imports (cf. section 7.3.2). Both lead to a reduced demand for hydrogen storage with a working gas volume of 42 TWh_{H2}. In the *onshore wind scenario*, the hydrogen storage required for Germany in 2050 increases to a working gas volume of 78 TWh_{H2}. This results from the electrolyzers integrating higher PV capacities in summer and the slightly increased use of hydrogen for electricity and heat generation in winter (cf. Figure 7-10). The highest hydrogen storage demand with 104 TWh_{H2} is shown in the optimization results for the *electricity grid scenario*. If the scenario design limits the use of the electricity grid as a central flexibility option, the optimization deviates to the alternative, more expensive flexibility option of storing hydrogen.

Figure 7-10 shows that the utilization of hydrogen storage in the optimization results has a pronounced seasonal profile in all scenarios. In winter, hydrogen demand exceeds hydrogen supply and storage facilities are emptied. In spring and fall, hydrogen reservoirs are refilled. In summer, the scenarios differ slightly. While in the *hydrogen scenario,* the storage status remains almost unchanged from May to August, all other scenarios show a slight rise in hydrogen storage levels. Hence, seasonal energy storage in the form of hydrogen helps to balance a GHG-neutral energy system throughout the year.

The decrease in the hydrogen storage level in winter can be explained in all scenarios by lower renewable electricity feed-in. As an example, Figure 7-11 shows low electricity generation from solar and wind energy due to fewer hours of sunshine and lower wind levels for calendar week 5 (weather year 2010) in the *electrification scenario*. At the same time, there is an increase in both electricity demand – driven in particular by the use of domestic heat pumps – and heat demand in district heating networks. As a result, electricity becomes a scarce resource and inflexible electricity consumers are preferentially supplied rather than electrolyzers. This reduced renewable electricity generation is partially offset by the use of hydrogen technologies. In all scenarios except the *hydrogen scenario*, substantial amounts of stored hydrogen are converted into electricity and heat in November, December, January, and February (cf. Figure 7-10). Together, these effects are responsible for the depletion of hydrogen storage facilities. Except for the *electricity grid scenario*, there is almost no hydrogen utilization in the conversion sector in the remaining months of the year. In the *electricity grid scenario*, hydrogen is used for power generation throughout the year to compensate for bottlenecks in the power grid.

The optimization results show a higher deployment of electrolyzers in spring and fall months than in the remaining months of the year in all scenarios (cf. Figure 7-10). Figure 7-11 shows that these seasons are characterized by high feed-in of onshore wind power. This wind power, which in some cases occurs constantly over several days, is integrated via electrolyzers. Since very little hydrogen is needed to stabilize the conversion sector, the seasonal hydrogen storage facilities are replenished during these months.

Figure 7-11 shows that the main use of electrolyzers in summer is to integrate high PV generation peaks. In a few low-wind nighttime hours, hydrogen power plants have to balance the electricity system in the absence of imports. Overall, there is less wind in the summer than in the spring and fall for the weather year 2010, which is typical for Germany. Hydrogen production from electrolysis therefore decreases somewhat in a seasonal comparison.

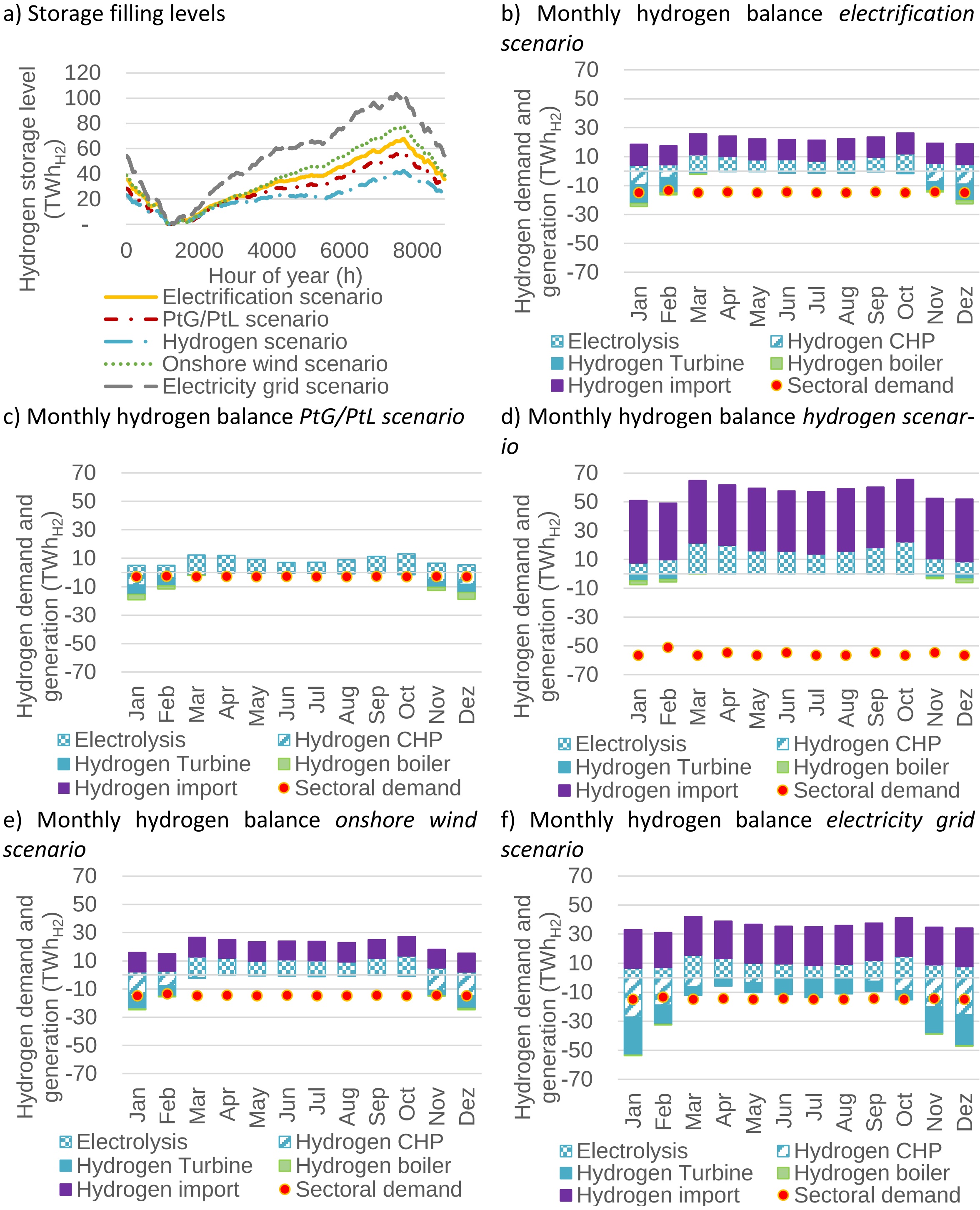

Figure 7-10 Hydrogen storage management in the optimization results for Germany in 2050. a) Storage level for all scenarios over 8,760 hours of the year 2050. Monthly hydrogen demand and supply in the b) *electrification scenario*, c) *PtG/PtL scenario*, and d) *hydrogen scenario*, e) *onshore wind scenario*, f) *electricity grid scenario*.

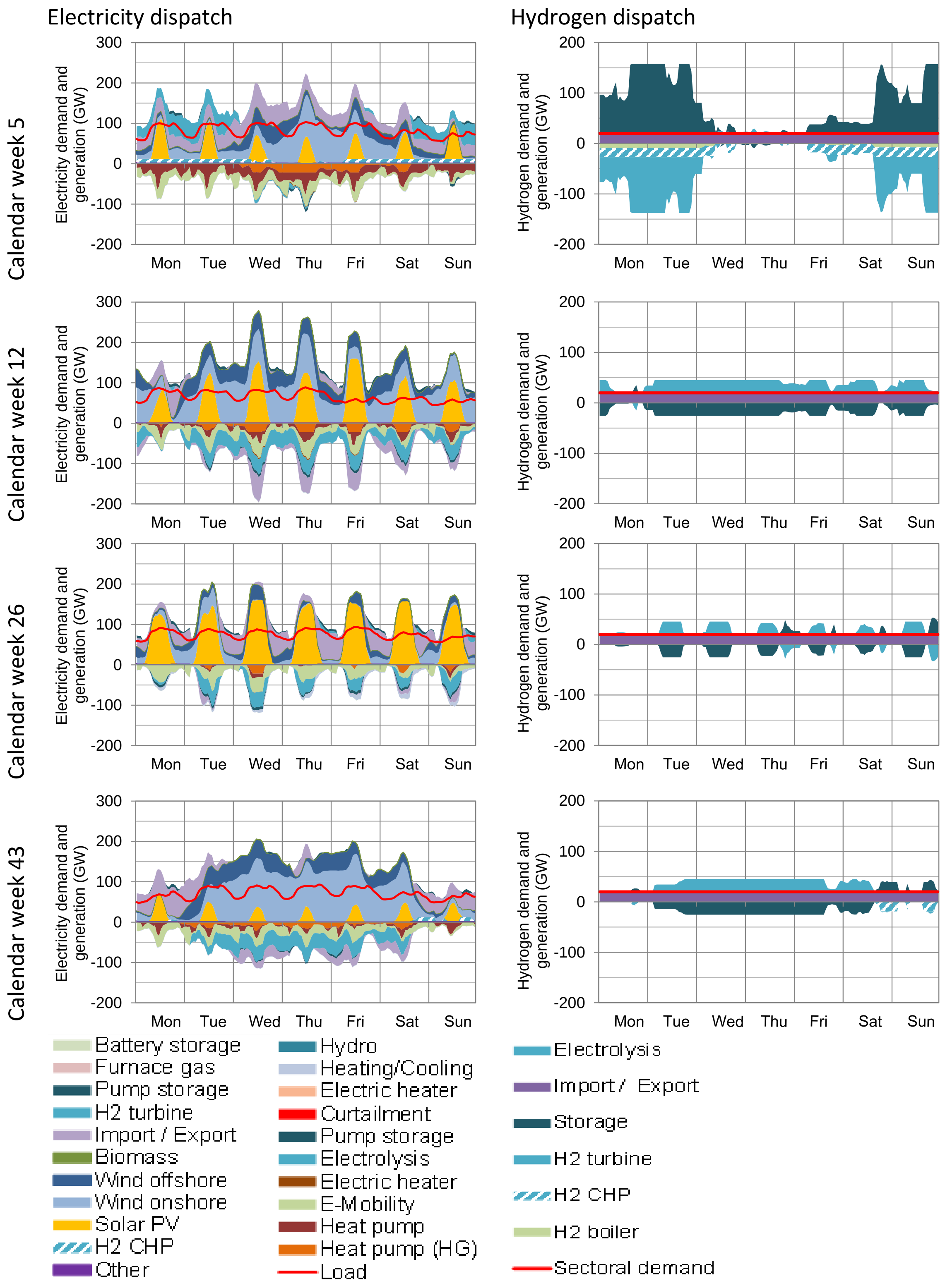

Figure 7-11 Hourly electricity and hydrogen balances in the *electrification scenario* for selected weeks of the simulation year 2050 covering all four seasons.

7.3.6 System costs

All the scenarios shown in this paper achieve GHG-neutrality in Germany by 2050. While the energy demand input data was calculated along consistent scenarios with simulation models, the energy supply in this paper is cost-optimized. Taking all sectors into account, the cost comparison identifies the *electrification scenario* as the most cost-efficient path to GHG-neutrality. An alternative, increased use of synthetic hydrocarbons in the *PtG/PtL scenario* increases the cumulative system costs by 359 billion euros in Germany by 2050. Similarly, an alternative, increased use of hydrogen in end-use applications and processes in the *hydrogen scenario* leads to cumulative additional system cost of 246 billion euros by 2050. The *electrification scenario* will become more expensive if the expansion of the electricity transmission grid is inhibited or less space is available for the expansion of onshore wind. In the *electricity grid scenario*, the cumulative system costs increase by 82 billion euros by 2050 compared to the *electrification scenario*. Similarly, the *onshore wind scenario* results in cumulative additional costs of 197 billion euros compared to the *electrification scenario*.

7.4 Discussion

The optimization results in all scenarios show substantial and rapid increases in renewable electricity capacity. The average net expansion rate of PV, onshore wind, and offshore wind combined in Germany in the scenario results for the period between 2020 and 2050 is between 6.4 GW/a in the *PtG/PtL scenario* and 13.6 GW/a in the *onshore wind scenario*. However, these capacity increases contrast with the expansion rates in Germany in recent years: The average net expansion rate of PV, onshore wind, and offshore wind combined in Germany was 6.4 GW/a between 2015 and 2020 (BMWK 2022a). It is therefore ambitious to realize the expansion rates shown in the optimization results. These rates are, however, necessary to achieve the GHG-neutrality target.

Compared to today, the use of CHP is significantly reduced in the optimization results and shows a dispatch profile with fewer full-load hours. In the overall cost optimization of energy systems for electricity, heat and hydrogen, CHP is used when there is a positive residual electricity load and simultaneous heat demand. CHP always competes with other cost-efficient and emission-free technologies for electricity or heat generation. Consequently, two sides are relevant for CHP utilization: heat demand, and electricity demand. In summer, there is usually low heat demand and high PV generation on the electricity side (cf. Figure 7-11). This means that there is no potential for the cost-efficient use of CHP. In winter, there is higher heat demand and less PV generation. If there is little wind feed-in as well, there is a resulting shortage on the electricity supply side and CHP can then therefore efficiently cover electricity and heat demand. Even today CHP plants are experiencing decreasing hours of operation in electricity systems with a high penetration of intermittent renewables (Sorknæs et al. 2015). Hence, the use of CHP in an optimized GHG-neutral energy supply system is limited and hydrogen CHP plants have between 1,200 and 2,500 full-load hours in the optimization results.

In the scenario results, the demand for geological hydrogen storage in Germany is between 42 and 104 TWh_{H2}. Caglayan et al. (2020) estimate Germany's hydrogen storage potential in salt caverns to be 94 PWh_{H2}. Currently, natural gas storage facilities with a working gas capacity of 240 $TWh_{naturalgas}$ (Kühn et al. 2020) are operated in geological subsurface structures in Germany. Salt caverns are considered especially suitable for storing hydrogen (Caglayan et al. 2020). About 62% (Kühn et al. 2020) of the subsurface natural gas storages are caverns in salt structures with a total working gas capacity of 149 $TWh_{naturalgas}$. If rededicated, the existing salt caverns could only store about 45 TWh_{H2} of hydrogen due to the lower volumetric energy density of hydrogen. In principle, the storage potential is therefore sufficiently large to meet the hydrogen storage requirement in all scenarios. However, even if the demand for natural gas storage decreases fast enough, the reallocation of such storage facilities can only partially cover the hydrogen storage demand in the scenario results; the construction of new cavern storage facilities is necessary. The storage potential is concentrated in northern Germany (Caglayan et al. 2020) and therefore close to the electrolyzer sites in the scenario results (cf. Figure 7-7).

In the modeling, the exogenously specified hydrogen demand is assumed to be uniformly distributed over the year. The requirement and use of hydrogen as a seasonal storage medium in the model results is therefore shaped by the seasonal conditions in the conversion sector. In reality, seasonal fluctuations in hydrogen demand from other sectors would potentially increase the seasonality of the storage profile.

In all scenario results, Germany is an energy importer. Except for the *onshore wind scenario*, most hydrogen is imported from the British Isles. A study by Clees et al. (2021), modeling gas and hydrogen networks, shows that operating a hydrogen-only network benefits from this hydrogen flow direction. In light of Brexit, it seems however questionable whether the population in the UK would tolerate a substantial expansion of wind turbines dedicated to producing hydrogen for export to mainland Europe. Still, as an optimization result, it shows the economic potential of the region in this regard.

In line with the findings in Lux et al. (2021), the results of the optimization in this paper show that an inner-European hydrogen supply is more cost-efficient than imports from the MENA region. The advantages of the MENA region in terms of renewable power generation are offset by the costs of transporting hydrogen to Europe. If the expansion of renewable energies in Europe stagnates due to acceptance problems, imports from outside Europe may still become necessary.

7.5 Conclusions

In a scenario study, this paper examined the supply of hydrogen and its potential use in the conversion sector on different pathways to greenhouse gas neutrality in Germany. The scenarios were deliberately designed to address uncertain and influential drivers of the future energy system: Firstly, consistent variations in energy demand in the demand sectors industry, transport, households, and services illuminate the corners of the possible solution space. Three different pathways to achieve climate neutrality were modeled assuming a high deployment of either electricity, or hydrogen or synthetic hydrocarbons. Secondly, the renewable energy portfolio was varied by limiting the onshore wind potential in one case. Thirdly, in another case, a key flexibility option in the future electricity system was varied by limiting the expansion of the electricity transmission grid. The analysis was carried out using the cost-minimizing energy system model *Enertile* and focused on Germany, but in the context of a European energy system. The aim of the analysis is to support a concretization of the German hydrogen strategy using model calculations to answer three research questions.

The first research question addressed the need for and utilization of hydrogen storage facilities over the course of a year. A robust result of the energy supply optimization is the utilization of hydrogen as a storage medium in the conversion sector with a pronounced seasonal profile. Primarily, this use of hydrogen can shift high electricity generation from onshore wind in spring and fall into the winter when there is lower renewable supply from solar energy and increased electricity and heat demands. To function as this seasonal storage, the scenario results calculated a hydrogen storage volume in the range of 42 TWh_{H2} to 104 TWh_{H2}. High storage volumes are mainly caused by a lack of flexibility in the power transmission grid. Repurposing suitable, currently operated natural gas storage facilities in salt caverns could cover about 45 TWh_{H2} of this hydrogen storage requirement. For storage demands beyond this, new hydrogen cavern storage facilities would have to be built. There is a sufficiently large geological potential of 94 PWh_{H2} available.

Hydrogen storage is used in the scenario results as a flexibility provider in the conversion sector on both the supply and demand side. On the electricity demand side, electrolyzers, in particular, help to integrate high PV peaks and high wind onshore feed-in. In the scenario results, electrolyzer capacities between 41 GW_{el} and 75 GW_{el} are used in Germany in the long term. On the electricity supply side, hydrogen turbines and hydrogen CHP compensate for shortfalls in renewable power generation or bottlenecks in the electricity transmission network. Hydrogen power plants replace gas-fired power plants, even if these are switched to synthetic methane. In the scenario results, hydrogen power plant capacities between 26 GW_{el} and 82 GW_{el} are used in Germany in the long run. This requires the construction of electrolyzers and hydrogen power plants in Germany.

The second research question is dedicated to the site selection of electrolyzers. In the scenarios, hydrogen demand from both industry and the conversion sector mainly occurs in southern and western Germany. Despite this, electrolytic hydrogen production is almost exclusively concentrated in northern Germany in the cost minimization results. At least 71% of hydrogen production takes place at the German coasts in the scenario results. The optimization follows the available low-cost electricity generation potential when selecting electrolyzer site locations and therefore decides against locating hydrogen production close to its consumption. The electrolyzers at the North Sea and the Baltic Sea are able to integrate high volumes of wind power.

The third research question concerned the contribution of a German or European hydrogen transport infrastructure to a cost-efficient energy supply system. Within Germany, the cost minimization results show that a hydrogen transport infrastructure between northern Germany and southern or western Germany is economically efficient to balance hydrogen supply via electrolysis and hydrogen demand. According to the scenario results, this requires the construction of hydrogen transport pipelines from northern Germany to the southwest with a transport capacity between 3 GW_{H2} and 18 GW_{H2}. If onshore wind expansion is not inhibited by factors beyond techno-economic drivers, a north-south pipeline link within Germany is a robust optimization result. In the scenario variants, the capacity of this link ranges between 8 GW_{H2} and 19 GW_{H2}.

Connecting Germany to a European hydrogen transport network is a robust optimization result in scenarios with substantial hydrogen demand in Germany. The ratio of electricity demand and low-cost renewable electricity generation potential is less favorable in Germany than in many other European countries. In the scenario results, Germany therefore imports most of its hydrogen demand from other European countries. Hydrogen imports are particularly pronounced if many end-use applications are converted to hydrogen and hydrogen demand in Germany is consequently very high, or if electricity imports from other European countries are inhibited. The main hydrogen export regions are the British Isles, Scandinavia, and the Iberian Peninsula. These trade flows require the construction of a European hydrogen pipeline network. Due to declining fossil gas demand, it might be possible to convert existing natural gas pipelines for this purpose. Germany's interconnection capacity to other European countries ranges between 18 GW_{H2} and 58 GW_{H2} in the scenario results. In the model results, no hydrogen is imported from outside Europe. The optimization model favors a domestic European hydrogen supply over imports from the MENA region due to the associated transportation costs and decreasing absolute cost benefits of renewable power generation in this region in the long run. From a cost perspective, trading partners in Europe are the primary candidates.

Overall, hydrogen will play an important role on the supply side of the energy system. The optimization results show the range in which electrolyzers, hydrogen storage facilities, and hydrogen transport networks may be used. However, the scenario results also demonstrate that hydrogen is an expensive form of energy due to the high conversion losses in its production. In the optimization, the use of hydrogen in the conversion sector for power and heat generation is price-sensitive.

CRediT authorship contribution statement

Benjamin Lux: Conceptualization, Methodology, Software, Investigation, Data curation, Visualization, Writing - original draft and review.

Gerda Deac: Software, Data curation.

Christoph Kiefer: Visualization, Investigation.

Christoph Kleinschmitt: Software, Data Curation.

Christiane Bernath: Software, Data Curation.

Katja Franke: Software, Data Curation.

Benjamin Pfluger: Writing - original draft, Supervision.

Sebastian Willemsen: Methodology, Data Curation.

Frank Sensfuß: Conceptualization, Supervision, Funding acquisition.

Declaration of Interest statement

Declarations of interest: none.

Acknowledgements

The main content of this manuscript is closely related to the research conducted in the project 'Langfristszenarien für die Transformation des Energiesystems in Deutschland', which received funding from the German Federal Ministry for Economic Affairs and Climate Action (formerly the German Federal Ministry for Economic Affairs and Energy).

The authors are indebted to the project partners for their modeling, expertise, and feedback:

- Fraunhofer Institute for Systems and Innovation Research ISI: Heike Brugger; Tobias Fleiter; Matthias Rehfeldt; Andrea Herbst; Pia Manz; Marius Neuwirth; Martin Wietschel; Till Gnann; Daniel Speth; Michael Krail; Joshua Fragoso García
- ifeu – Institut für Energie- und Umweltforschung Heidelberg gGmbH: Peter Mellwig; Sebastian Blömer
- consentec GmbH: Bernd Tersteegen; Christoph Maurer; Alexander Ladermann; Tom Dröscher
- Technische Universität Berlin, Chair for the Management of Energy and Resources: Joachim Müller-Kirchenbauer; Johannes Giehl; Mélissa Hilaire; Sarah Schöngart; Ashlen Kurre; Jeremias Hollnagel; Flora von Mikulicz-Radecki

Funding

This work was supported with funding from the German Federal Ministry for Economic Affairs and Climate Action (formerly the German Federal Ministry for Economic Affairs and Energy) [03MAP392].

7.6 Appendix

Appendix A.Abbreviations

Table 7-3 Abbreviations.

Abbreviation	Explanation
AEL	Alkaline electrolysis
CCS	Carbon capture and storage
CHP	Combined heat and power
CSP	Concentrated solar power
EC	European Commission
el	Electric
EU	European Union
GHG	Greenhouse gas
MENA	Middle East and North Africa
O&M	Operation and maintenance
PEMEL	Polymer electrolyte membrane electrolysis
PtG	Power-to-Gas
PtL	Power-to-Liquid
PV	Photovoltaics
th	thermal

Appendix B. Enertile model regions

Figure 7-12 Map of model regions in *Enertile*.

Table 7-4 Definition of regions as used in Enertile.

***Enertile* region code**	**Countries**
AT	Austria
CH	Switzerland
DE_1 - DE_6, DE_1O	Germany
FR_0	France
IBEU_0	Spain, Portugal
BEU_0	Belgium, Luxembourg
HUK_0	Hungary, Slovakia

Enertile **region code**	**Countries**
UKI_0	United Kingdom, Ireland
PL_0	Poland
BUG_0	Bulgaria, Greece
BAK_0	Slovenia, Croatia, Bosnia and Herzegovina, Serbia, Kosovo, Montenegro, Albania, North Macedonia
BAT_0	Estonia, Lithuania, Latvia
CZ_0	Czech Republic
DK_0	Denmark
IT_0	Italy
NO_0	Norway
RO_0	Romania
SE_0	Sweden
NL_0	Netherlands

Appendix C. Linear optimization problem in Enertile

The objective function in Enertile of the linear cost minimization problem for supplying electricity el, heat ht, hydrogen $H2$ in an energy system is formulated in equation (16). It sums the cost of all included generation, transmission, and storage infrastructures in all regions $r \in R$ and all hours $h \in H$ of all considered simulation years $a \in A$. There are two types of decision variables in the objective function: First $\vec{X}$ describing installed capacities of considered infrastructures, and second $\vec{x}$ describing the unit dispatch of these infrastructures. Costs for the supply of electricity, heat, and hydrogen are the coefficients of the various decision variables and are grouped into fixed costs and variable costs. Fixed cost $c_{\{i,j,k\}}^{fix}$ contain annuitized investments, capital cost, and fixed operation and maintenance cost of respective technologies. Variable cost $c_{\{i,j,k\}}^{var}$ contain fuel cost, CO_2 emission certificate cost, and variable operation and maintenance cost. The technology portfolio I for the provision of electricity contains conventional electricity generation technologies (including

CHP and hydrogen power plants), renewable electricity generation technologies, electricity storage technologies, and simplified electricity transmission networks. The set of technologies J for the provision of heat contains conventional heat generation technologies (including hydrogen boilers), renewable heat generation technologies, electric heat generators, and heat storages. The technology set K for the provision of hydrogen contains electrolyzers, hydrogen storage technologies, and simplified hydrogen transport networks.

$$\min_{\vec{X},\vec{x},\vec{y}} \sum_{a \in A} \left[\sum_{r \in R} \left\{ \sum_{i \in I} \left(\underbrace{\left(c_{a,i}^{fix} \cdot X_{a,r,i}^{el} \right)}_{capacity\ expansion\ electricity\ supply} + \underbrace{\sum_{h \in H} c_{a,i}^{var} \cdot x_{a,r,i.h}^{el}}_{electricity\ generation} \right) + \sum_{j \in J} \left(\underbrace{\left(c_{a,j}^{fix} \cdot X_{a,r,j}^{ht} \right)}_{capacity\ expansion\ heat\ supply} + \underbrace{\sum_{h \in H} c_{a,j}^{var} \cdot x_{a,r,j,h}^{ht}}_{heat\ generation} \right) + \sum_{k \in K} \left(\underbrace{\left(c_{a,k}^{fix} \cdot X_{a,r,k}^{H2} \right)}_{capacity\ expansion\ H2\ supply} + \underbrace{\sum_{h \in H} c_{a,k}^{var} \cdot x_{a,r,k.h}^{H2}}_{H2\ generation} \right) \right\} \right] \quad (16)$$

The central constraints of the cost minimization – so called demand-supply equations $DS_{\{el,hg,b,H2\}}$ – are region- and hour-specific balancing equations for electricity, heat, hydrogen. These equations ensure that the demands of these goods are met. There are two types of demands: Firstly, exogenous demands from other sectors for electricity D^{el}, heat $D^{ht}_{\{hg,b\}}$ in heat grids hg and buildings b, and hydrogen D^{H2}. Secondly, model endogenous demands that result from interdependencies of the different balancing spaces modelled in Enertile.

Equation (17) shows the electricity demand-supply equation DS_{el}. It ensures that the sum of model endogenous electricity demands for heat supply in heat girds and buildings, and for hydrogen supply via electrolysis along with the exogenously specified electricity demand D^{el} is met for each hour h of a simulation year a and each region r by the net electricity generation of technologies I. Supplying heat in heat grids HG or buildings B with electrical technologies increases electricity demands. Electric boilers eb convert electricity into heat with efficiency γ_{eb}. The electric conversion efficiencies $\gamma_{\{hpg,hpb\}}$ of both heat pumps for heat grids hpg and buildings hpb depend on the prevailing ambient temperature. The supply of hydrogen with electrolyzers ely increases the electricity demand as a function of the electrolyzer efficiency γ_{ely}.

[DS$_{el}$]
$$\sum_{i\in I} x^{el}_{a,r,i,h} = D^{el}_{a,r,h} + \sum_{hg\in HG}\left(\frac{1}{\gamma_{a,r,hpg,h}}\cdot x^{ht}_{a,r,hg,hpg,h} + \frac{1}{\gamma_{a,eb}}\cdot x^{ht}_{a,r,hg,eb,h}\right) + \sum_{b\in B}\frac{1}{\gamma_{a,r,hpb,h}}\cdot x^{ht}_{r,b,hpb,h} + \sum_{ely}\frac{1}{\gamma_{a,ely}}\cdot x^{H2}_{a,r,ely,h} \qquad \forall a,r,h \qquad (17)$$

Equations (18) and (19) show the heat demand-supply equations. The demand-supply equation for heat in heat grids DS$_{hg}$ (18) ensures that the exogenously specified heat demand in heat grids D^{ht}_{hg} is met for each hour h of a simulation year a and each region r by the net heat generation of technologies $N \subset J$ and $Q \subset I$. The technology set N includes pure heat generation technologies and heat storage systems suitable for the use in heat grids; the technology set Q includes hydrogen CHP plants whose heat generation for heat grids is coupled to electricity generation via the power-to-heat ratio $\gamma^{chp,ht}_{q}$. The demand-supply equation for heat in buildings DS$_{b}$ (19)ensures that the exogenously specified heat demand in buildings D^{ht}_{b} is met for each hour h of a simulation year a and each region r by the net heat generation of the subset of heating technologies $O \subset J$ suitable for supplying buildings.

[DS$_{hg}$]
$$\sum_{n\in N} x^{ht}_{a,r,hg,n,h} + \sum_{q\in Q}\gamma^{chp,ht}_{a,q}\cdot x^{el,chp}_{a,r,q,h} = D^{ht}_{a,r,hg,h} \qquad \forall a,r,hg,h \qquad (18)$$

[DS$_{b}$]
$$\sum_{o\in O} x^{ht}_{a,r,b,o,h} = D^{ht}_{a,r,b,h} \qquad \forall a,r,b,h \qquad (19)$$

Equation (20) shows the hydrogen demand supply equation DS$_{H2}$. It ensures for each hour h of a simulation year a and each region r that the net hydrogen supply of technology portfolio K meets the model endogenous hydrogen demands and either explicitly specified exogenous hydrogen demands from other sectors D^{H2} or implicitly imposed hydrogen demands. Endogenous hydrogen demands include the provision of heat in heat grids HG using hydrogen boilers $hyb \in N$ with conversion efficiency γ_{hyb}, the reconversion of hydrogen into electricity using the portfolio of pure hydrogen-to-electricity reconversion technologies $P \subset I$ with associated conversion efficiencies γ_{p}, and the co-generation of electricity and heat using the portfolio of CHP reconversion technologies $Q \subset I$ with associated conversion efficiencies $\gamma^{chp,H2}_{q}$.

[DS$_{H2}$]
$$\sum_{k\in K} x^{H2}_{a,r,k,h} = \sum_{hg\in HG}\frac{1}{\gamma_{a,hyb}}\cdot x^{ht}_{a,r,hg,hyb,h} + \sum_{p\in P}\frac{1}{\gamma_{a,p}}\cdot x^{el}_{a,r,p,h} + \sum_{q\in Q}\frac{1}{\gamma^{chp,H2}_{a,q}}\cdot x^{el,chp}_{a,r,q,h} + D^{H2}_{a,r,h} \qquad \forall a,r,h \qquad (20)$$

Appendix D. Boundaries for the electricity transmission grid capacities

Table 7-5 Boundaries for the electricity transmission grid capacities in the system optimization.

		Electricity grid scenario			All other scenarios		
Region 1	Region 2	2030 (MW, fixed)	2040 (MW, max)	2050 (MW, max)	2030 (MW, fixed)	2040 (MW, max)	2050 (MW, max)
AT_0	BAK_0	950	950	950	950	3950	7900
AT_0	CH_0	870	870	870	870	3870	7740
AT_0	CZ_0	800	800	800	800	3800	7600
AT_0	HUK_0	1550	1550	1550	1550	4550	9100
AT_0	IT_0	1335	1800	1800	1800	4800	9600
BAK_0	HUK_0	190	190	190	190	3190	6380
BAK_0	RO_0	500	500	500	500	3500	7000
BAT_0	FI_0	1000	1000	1000	1000	4000	8000
BAT_0	PL_0	3500	3500	3500	3500	7000	14000
BEU_0	FR_0	3000	3000	3000	3000	6000	12000
BEU_0	NL_0	2400	2400	2400	2400	5400	10800
BUG_0	BAK_0	1268	1268	1268	1268	4268	8536
BUG_0	LY_0	0	0	0	0	3000	6000
BUG_0	RO_0	510	510	510	510	3510	7020
CH_0	FR_0	2850	3150	3150	3150	6300	12600
CH_0	IT_0	3700	4000	4000	4000	8000	16000
CZ_0	HUK_0	1150	1150	1150	1150	4150	8300
CZ_0	PL_0	1300	1300	1300	1300	4300	8600
DE_1	DE_2	3121	3506	3506	3506	7012	14024
DE_1	DE_3	5006	8006	8006	8006	15506	26506
DE_1	DE_4	1305	1466	1466	1466	4466	8932
DE_1	DE_6	3560	4000	4000	4000	4000	4000
DE_1	DK_0	1780	2000	2000	2000	5000	10000
DE_1	NL_0	846	950	950	950	3950	7900
DE_1	NO_0	1246	1400	1400	1400	4400	8800
DE_1	SE_0	534	600	600	600	3600	7200
DE_1	UKI_0	1246	1400	1400	1400	4400	8800
DE_1O	DE_1	30000	37500	48500	30000	37500	48500

		Electricity grid scenario			All other scenarios		
Region 1	Region 2	2030 (MW, fixed)	2040 (MW, max)	2050 (MW, max)	2030 (MW, fixed)	2040 (MW, max)	2050 (MW, max)
DE_1O	DE_3	0	0	0	0	5000	15000
DE_1O	DE_6	0	0	0	0	5000	15000
DE_1O	DK_0	0	0	0	0	5000	15000
DE_1O	NL_0	0	0	0	0	5000	15000
DE_1O	NO_0	0	0	0	0	5000	15000
DE_1O	UKI_0	0	0	0	0	5000	15000
DE_2	DE_4	1235	1388	1388	1388	4388	8776
DE_2	DE_5	5485	6163	6163	6163	12324	23324
DE_2	DE_6	1780	2000	2000	2000	2000	2000
DE_2	DK_0	534	600	600	600	3600	7200
DE_2	PL_0	1335	1500	1500	1500	4500	9000
DE_2	SE_0	623	700	700	700	3700	7400
DE_3	BEU_0	890	1000	1000	1000	4000	8000
DE_3	DE_4	1513	1700	1700	1700	4700	9400
DE_3	DE_6	3293	3700	3700	3700	7400	14800
DE_3	NL_0	534	600	600	600	3600	7200
DE_4	DE_5	2648	2975	2975	2975	5975	11950
DE_4	DE_6	3783	4250	4250	4250	8500	17000
DE_5	CZ_0	445	500	500	500	3500	7000
DE_5	DE_6	5340	6000	6000	6000	12000	23000
DE_5	PL_0	645	725	725	725	3725	7450
DE_6	AT_0	5896	6625	6625	6625	13250	24250
DE_6	BEU_0	2715	3050	3050	3050	6100	12200
DE_6	CH_0	4450	5000	5000	5000	10000	20000
DE_6	CZ_0	668	750	750	750	3750	7500
DE_6	FR_0	2670	3000	3000	3000	6000	12000
DK_0	UKI_0	980	1400	1400	1400	4400	8800
HUK_0	PL_0	600	600	600	600	3600	7200
HUK_0	RO_0	900	900	900	900	3900	7800
IBEU_0	DZ_0	0	0	0	0	3000	6000
IBEU_0	FR_0	4000	4000	4000	4000	8000	16000

		Electricity grid scenario			All other scenarios		
Region 1	Region 2	2030 (MW, fixed)	2040 (MW, max)	2050 (MW, max)	2030 (MW, fixed)	2040 (MW, max)	2050 (MW, max)
IBEU_0	MA_0	650	650	650	650	3650	7300
IT_0	BAK_0	1840	2200	2200	2200	5200	10400
IT_0	BUG_0	500	500	500	500	3500	7000
IT_0	FR_0	2700	2700	2700	2700	5700	11400
IT_0	TN_0	1000	1000	1000	1000	4000	8000
NL_0	DK_0	700	700	700	700	3700	7400
NO_0	DK_0	1640	1640	1640	1640	4640	9280
NO_0	FI_0	925	925	925	925	3925	7850
NO_0	NL_0	700	700	700	700	3700	7400
SE_0	DK_0	2440	2440	2440	2440	5440	10880
SE_0	FI_0	2650	2650	2650	2650	5650	11300
SE_0	NO_0	4995	4995	4995	4995	9990	19980
SE_0	PL_0	600	600	600	600	3600	7200
UKI_0	BEU_0	1000	1000	1000	1000	4000	8000
UKI_0	FR_0	7690	9700	9700	9700	17200	28200
UKI_0	NL_0	1000	1000	1000	1000	4000	8000
UKI_0	NO_0	980	1400	1400	1400	4400	8400

Appendix E. Land use factors for renewable electricity generation

Table 7-6 Land use factors in the potential calculation of renewable electricity generation technologies. Values in parentheses show the deviations in the *onshore wind scenario* from all other scenarios.

Category	**PV rooftop**	**PV utility scale**	**CSP**	**Onshore wind**
Barren	0%	16%	12%	18.0% (9.0%)
Cropland	0%	2%	2%	14.4% (7.2%)
Forest	0%	0%	0%	10.8% (5.4%)
Grassland	0%	2%	2%	18.0% (6.0%)

Category	PV rooftop	PV utility scale	CSP	Onshore wind
Savannah	0%	2%	12%	18.0% (9.0%)
Shrubland	0%	2%	12%	18.0% (9.0%)
Snow and ice	0%	4%	0%	10.8% (9.0%)
Urban	16%	0%	0%	0.0% (0.0%)
Water	0%	0%	0%	0.0% (0.0%)
Wetlands	0%	0%	0%	0.0% (0.0%)

References

Ball, M.; Wietschel, M. (Eds.) (2010): The hydrogen economy. Opportunities and challenges. Cambridge: Cambridge University Press. https://doi.org/10.1017/CBO9780511635359.

Bernath, C.; Deac, G.; Sensfuss, F. (2019): Influence of heat pumps on renewable electricity integration: Germany in a European context. In: Energy Strategy Reviews, 26, p. 100389. https://doi.org/10.1016/j.esr.2019.100389.

Bundesministerium der Justiz und für Verbraucherschutz; Bundesamt für Justiz (Eds.) (2021): Bundes-Klimaschutzgesetz. KSG. Available at https://www.gesetze-im-internet.de/ksg/BJNR251310019.html.

Bundesministerium für Umwelt, Naturschutz und nukleare Sicherheit (2016): Klimaschutzplan 2050 - Klimaschutzpolitische Grundsätze und Ziele der Bundesregierung.

Bundesministerium für Wirtschaft und Energie (Ed.) (2020): Die Nationale Wasserstoffstrategie. Available at https://www.bmwi.de/Redaktion/DE/Publikationen/Energie/die-nationale-wasserstoffstrategie.pdf?__blob=publicationFile&v=20, accessed 29.01.2021.

Bundesministerium für Wirtschaft und Klimaschutz (Ed.) (2022a): Entwicklung der erneuerbaren Energien in Deutschland im Jahr 2021. Grafiken und Diagramme unter Verwendung aktueller Daten der Arbeitsgruppe Erneuerbare Energien-Statistik (AGEE-Stat). Available at https://www.erneuerbare-energien.de/EE/Navigation/DE/Service/Erneuerbare_Energien_in_Zahlen/Entwicklung/entwicklung-der-erneuerbaren-energien-in-deutschland.html, accessed 31.07.2022.

Bundesministerium für Wirtschaft und Klimaschutz (2022b): Zahlen und Fakten: Energiedaten. Nationale und internationale Entwicklung. Available at https://www.bmwi.de/Redaktion/DE/Artikel/Energie/energiedaten-gesamtausgabe.html, accessed 16.03.2022.

Bundestag (Ed.) (2011): Gesetz über die friedliche Verwendung der Kernenergie und den Schutz gegen ihre Gefahren (Atomgesetz). AtG.

Bundestag (Ed.) (2020): Gesetz zur Reduzierung und zur Beendigung der Kohleverstromung und zur Änderung weiterer Gesetze (Kohleausstiegsgesetz).

Buttler, A.; Spliethoff, H. (2018): Current status of water electrolysis for energy storage, grid balancing and sector coupling via power-to-gas and power-to-liquids: A review. In: Renewable and Sustainable Energy Reviews, 82, pp. 2440–2454. https://doi.org/10.1016/j.rser.2017.09.003.

Caglayan, D. G.; Weber, N.; Heinrichs, H. U.; Linßen, J.; Robinius, M.; Kukla, P. A.; Stolten, D. (2020): Technical potential of salt caverns for hydrogen storage in Europe. In: International Journal of Hydrogen Energy, 45 (11), pp. 6793–6805. https://doi.org/10.1016/j.ijhydene.2019.12.161.

Capurso, T.; Stefanizzi, M.; Torresi, M.; Camporeale, S. M. (2022): Perspective of the role of hydrogen in the 21st century energy transition. In: Energy Conversion and Management, 251, p. 114898. https://doi.org/10.1016/j.enconman.2021.114898.

Chen, H.; Song, J.; Zhao, J. (2021): Synergies between power and hydrogen carriers using fuel-cell hybrid electrical vehicle and power-to-gas storage as new coupling points. In: Energy Conversion and Management, 246, p. 114670. https://doi.org/10.1016/j.enconman.2021.114670.

Clees, T.; Baldin, A.; Klaassen, B.; Nikitina, L.; Nikitin, I.; Spelten, P. (2021): Efficient method for simulation of long-distance gas transport networks with large amounts of hydrogen injection. In: Energy Conversion and Management, 234, p. 113984. https://doi.org/10.1016/j.enconman.2021.113984.

Davis, S. J.; Lewis, N. S.; Shaner, M.; Aggarwal, S.; Arent, D.; Azevedo, I. L.; Benson, S. M.; Bradley, T.; Brouwer, J.; Chiang, Y.-M.; Clack, C. T. M.; Cohen, A.; Doig, S.; Edmonds, J.; Fennell, P.; Field, C. B.; Hannegan, B.; Hodge, B.-M.; Hoffert, M. I.; Ingersoll, E.; Jaramillo, P.; Lackner, K. S.; Mach, K. J.; Mastrandrea, M.; Ogden, J.; Peterson, P. F.; Sanchez, D. L.; Sperling, D.; Stagner, J.; Trancik, J. E.; Yang, C.-J.; Caldeira, K. (2018): Net-zero emissions energy systems. In: Science (New York, N.Y.), 360 (6396). https://doi.org/10.1126/science.aas9793.

Deac, G. (2019): Auswirkung der Kopplung von Strom- und Wärmemarkt auf die künftige Integration der erneurbaren Energien und die CO2-Emissionen in Deutschland.

European Commission (Ed.) (2019): The European Green Deal. Brussels.

Franke, K.; Sensfuss, F.; Bernath, C.; Lux, B. (2021): Carbon-neutral energy systems and the importance of flexibility options: A case study in China. In: Computers & Industrial Engineering, p. 107712. https://doi.org/10.1016/j.cie.2021.107712.

Fraunhofer Institut für System- und Innovationsforschung (2021): Enertile. Available at https://www.enertile.eu/enertile-en/index.php.

Fraunhofer Institut für System- und Innovationsforschung; Consentec GmbH (Consentec); ifeu - Institut für Energie- und Umweltforschung Heidelberg GmbH; Lehrstuhl für Energie- und Ressourcenmanagement der TU Berlin (2021): Langfristszenarien. Available at https://www.langfristszenarien.de/enertile-explorer-de/, accessed 17.06.2021.

Gils, H. C.; Gardian, H.; Schmugge, J. (2021): Interaction of hydrogen infrastructures with other sector coupling options towards a zero-emission energy system in Germany. In: Renewable Energy, 180, pp. 140–156. https://doi.org/10.1016/j.renene.2021.08.016.

Guo, Y.; Ru, P.; Su, J.; Anadon, L. D. (2015): Not in my backyard, but not far away from me: Local acceptance of wind power in China. In: Energy, 82, pp. 722–733. https://doi.org/10.1016/j.energy.2015.01.082.

Husarek, D.; Schmugge, J.; Niessen, S. (2021): Hydrogen supply chain scenarios for the decarbonisation of a German multi-modal energy system. In: International Journal of Hydrogen Energy. https://doi.org/10.1016/j.ijhydene.2021.09.041.

International Energy Agency (Ed.) (2019): World Energy Outlook 2019. Available at https://www.iea.org/reports/world-energy-outlook-2019, accessed 19.11.2021.

Kondziella, H.; Bruckner, T. (2016): Flexibility requirements of renewable energy based electricity systems – a review of research results and methodologies. In: Renewable and Sustainable Energy Reviews, 53, pp. 10–22. https://doi.org/10.1016/j.rser.2015.07.199.

Kühn, M.; Nakaten, N. C.; Kempka, T. (2020): Geological storage capacity for green excess energy readily available in Germany. In: Advances in Geosciences, 54, pp. 173–178. https://doi.org/10.5194/adgeo-54-173-2020.

Lux, B.; Gegenheimer, J.; Franke, K.; Sensfuss, F.; Pfluger, B. (2021): Supply curves of electricity-based gaseous fuels in the MENA region. In: Computers & Industrial Engineering, p. 107647. https://doi.org/10.1016/j.cie.2021.107647.

Lux, B.; Pfluger, B. (2020): A supply curve of electricity-based hydrogen in a decarbonized European energy system in 2050. In: Applied Energy, 269, p. 115011. https://doi.org/10.1016/j.apenergy.2020.115011.

Neuwirth, M.; Fleiter, T.; Manz, P.; Hofmann, R. (2022): The future potential hydrogen demand in energy-intensive industries - a site-specific approach applied to Germany. In: Energy Conversion and Management, 252, p. 115052. https://doi.org/10.1016/j.enconman.2021.115052.

Pfluger, B. (2014): Assessment of least-cost pathways for decarbonising Europe's power supply. A model-based long-term scenario analysis accounting for the characteristics of renewable energies. Karlsruhe.

Sens, L.; Piguel, Y.; Neuling, U.; Timmerberg, S.; Wilbrand, K.; Kaltschmitt, M. (2022): Cost minimized hydrogen from solar and wind – Production and supply in the European catchment area. In: Energy Conversion and Management, 265, p. 115742. https://doi.org/10.1016/j.enconman.2022.115742.

Sorknæs, P.; Lund, H.; Andersen, A. N. (2015): Future power market and sustainable energy solutions – The treatment of uncertainties in the daily operation of combined heat and power plants. In: Applied Energy, 144, pp. 129–138. https://doi.org/10.1016/j.apenergy.2015.02.041.

United Nations (Ed.) (2015): Paris Agreement. Available at https://unfccc.int/sites/default/files/english_paris_agreement.pdf.

Welder, L.; Ryberg, D.; Kotzur, L.; Grube, T.; Robinius, M.; Stolten, D. (2018): Spatio-temporal optimization of a future energy system for power-to-hydrogen applications in Germany. In: Energy, 158, pp. 1130–1149. https://doi.org/10.1016/j.energy.2018.05.059.

Wietschel, M.; Zheng, L.; Arens, M.; Hebling, C.; Ranzmeyer, O.; Schaadt, A.; Hank, C.; Sternberg, A.; Herkel, S.; Kost, C.; Ragwitz, M.; Herrmann, U.; Pfluger, B. (2021): Metastudie Wasserstoff – Auswertung von Energiesystemstudien. Studie im Auftrag des Nationalen Wasserstoffrats. Karlsruhe.

[End of Paper 3]

8 Potentials of direct air capture and storage in a greenhouse gas neutral European energy system

[Start of Paper 4]

Potentials of direct air capture and storage in a greenhouse gas neutral European energy system

Benjamin Lux[1*], Niklas Schneck[1], Benjamin Pfluger[2], Wolfgang Männer[1], and Frank Sensfuß[1]

1 Fraunhofer Institute for Systems and Innovation Research ISI, Breslauer Straße 48, 76139 Karlsruhe, Germany

2 Fraunhofer Research Institution for Energy Infrastructures and Geothermal Systems IEG, Breslauer Straße 48, 76139 Karlsruhe, Germany

*corresponding author: Benjamin Lux, benjamin.lux@isi.fraunhofer.de, phone: +49-721-6809-474

Published in:

Energy Strategy Reviews 45, Article No. 101012, DOI: 10.1016/j.esr.2022.101012

Abstract

Negative emission technologies will likely be needed to achieve the European Commission's goal of greenhouse gas neutrality by 2050. This article investigates the potential of reducing greenhouse gases in the atmosphere via the DACCS pathway, i.e., to capture CO2 from the ambient air and permanently store it in geological formations. Since the capture of CO2 from ambient air is energy-intensive, this study particularly models the integration of DACCS plants into a greenhouse gas-neutral European energy system. The model results show that DACCS in Europe 2050 could cost between 160 €/tCO2 and 270 €/tCO2 with very conservative techno-economic assumptions and between 60 €/tCO2 and 140 €/tCO2 using more progressive parameters. Annually capturing 5% of Europe's 1990 emissions with a fully electric DACCS system would increase the capacities of on-shore wind by 80 to 119 GWel and PV by 85 to 126 GWel. In the model results, Sweden, the Iberian Peninsula, Norway, and Finland incorporate the essential characteristics for a successful deployment of capturing and storing CO2 from ambient air: Sufficiently large geological CO2 storage capacities and relatively low-cost, vacant renewable power generation potentials. The low DACCS costs could minimize the cost of combating climate change and prevent the implementation of more expensive mitigation strategies. On the other hand, a DACCS-based climate protection strat-

egy is fraught with the risks of CO2 storage leaks, acceptance problems for the additional required expansion of renewable energies, and premature depletion of global CO2 storage potentials.

Keywords: Direct air capture and storage (DACCS); Carbon dioxide removal (CDR); Negative emission technology (NET); Energy system modeling; GHG neutrality;

Highlights:

- DACCS costs between 60 and 140€/t_{CO2} in Europe in 2050 with progressive parameters
- Sweden, the Iberian Peninsula, and Norway show the best DACCS potentials
- Energy costs are the main component of CDR costs using DACCS
- Europe has a geological CO_2 storage potential of over 100 Gt_{CO2}
- Annually capturing 5% of Europe's 1990 emissions increases RES capacity by 5-8%

8.1 Introduction

The United Nations Sustainable Development Goals name climate change a major challenge for our and future generations (UN 2015b). To reduce the impact of climate change, the Paris Agreement (UN 2015a) sets the target to keep the global temperature increase preferably below 1.5 °C compared to pre-industrial times. To achieve this objective, the European Commission (EC) presented its "European Green Deal" in 2019 (EC 2019), which aims to achieve an economy with net-zero greenhouse gas (GHG) emissions in 2050 in the European Union (EU).

Various studies conclude that despite rigorous decarbonization efforts across sectors, negative emission technologies (NETs) will likely be needed to achieve net-zero GHG emissions by 2050 (Fasihi et al. 2019; Realmonte et al. 2019; Wohland et al. 2018). In the Special Report on Global Warming of 1.5 °C by the Intergovernmental Panel on Climate Change (IPCC), all analyzed 1.5 °C pathways with limited or no overshoot include carbon dioxide removal (CDR) of the order of 100 – 1,000 Gt_{CO2} in the 21st century (Rogelj et al. 2018). CDR is likely necessary since some economic processes like cement production or social habits like meat consumption are related to the generation of GHG emissions. It is neither from a technical nor from a political viability perspective possible to (completely) substitute these with emission-free alternatives. As a consequence, a need for strategies to compensate for the remaining emissions emerges.

There are a variety of NETs that can be used to remove CO_2 from the atmosphere. Minx et al. (2018) classify the different technical approaches in a taxonomy and identify seven major groups of NETs: afforestation and reforestation (AR), biochar, soil carbon sequestration (SCS), enhanced weathering on land and in oceans (EW), ocean fertilization (OF), bioenergy combined with carbon capture and storage (BECCS), and direct air capture and storage (DACCS). Previous studies carried out with integrated assessment models (IAMs) have focused mainly on the options of afforestation, reforestation, and BECCS (Rogelj et al. 2018). However, there are concerns regarding both sustainability and competition for food and water associated with biomass-based strategies (Smith et al. 2013; Smith et al. 2016). Therefore, technical options that chemically remove CO_2 from the atmosphere rather than through photosynthesis are increasingly a topic of discussion. Facilities that use chemical solvents and sorbents to remove CO_2 directly from the ambient air are called direct air capture (DAC) plants. If the captured CO_2 is permanently stored, this overall process is referred to as DACCS. Geological formations such as depleted oil and gas fields or saline aquifers can serve as long-term CO_2 storage. If powered by carbon-neutral energies, DACCS has the potential to lower the CO_2 concentration in the atmosphere. Compared to conventional carbon capture and storage (CCS), DACCS has the advantage that CO_2 can be captured independently of the location and the process of a point source. Therefore, it can capture distributed emissions, such as transport or aviation. The major challenge for DAC technologies to become integral to a climate protection strategy is the high energy consumption for capturing CO_2 from the ambient air. Since the CO_2 concentration in the atmosphere is low – 421 ppm (parts per million) as measured by the Mauna Loa Observatory Hawaii in May 2022 (Thoning et al. 2022) – large volumes of air must be processed, and a substantial amount of energy must be used to extract the CO_2 (Fuhrman et al.

2020). In order to guarantee a beneficial impact of the DAC technologies, this additional energy demand would have to be accompanied by further expansions of renewable power technologies and may compete with other electrification strategies.

Today, DAC has been mainly researched from a technological perspective. Fasihi et al. (2019) provide a comprehensive literature review on the techno-economic properties of DAC plants and make projections for the development of these parameters up to the year 2050. Their analysis focuses on relevant parameters from an energy system perspective without analyzing the interactions between DACCS and the system level. Few studies have analyzed DACCS in the context of energy systems using a model-based approach. Existing works (Chen et al. 2013; Galán-Martín et al. 2021; Marcucci et al. 2017; Realmonte et al. 2019; Strefler et al. 2018) use IAMs or energy system models that take a global perspective or cover long time horizons, such as until 2100. This spatial and temporal broadness in their modeling approaches entails relatively low spatial or temporal resolutions. However, to achieve GHG neutrality, DACCS technologies will most likely need to be integrated into energy systems that have high shares of weather-dependent renewable energies. Taking into account the interactions or competition with other energy demands for these fluctuating sources requires using models with high technological, spatial, and temporal resolution. Modelling DACCS in such a setup allows for a more realistic economic analysis.

The EC aims to become GHG-neutral by the year 2050. This paper examines the integration of DACCS plants into a European energy system to serve potential CDR needs in Europe. Ultimately, the GHG balance must be globally even to limit the temperature increase. This implies that European CO_2 emissions could be offset beyond Europe's borders in regions with favorable conditions. Nevertheless, DACCS plants outside Europe need to be integrated into the respective conditions of the energy system at hand. In this respect, the analyses in this paper are a case study for offsetting GHG emissions through DACCS locally. They can provide insight into fundamentally beneficial energy systems for using DACCS.

The central research questions of this article are:

- What is the techno-economic carbon dioxide removal potential of DACCS in a GHG-neutral European energy system?
- What are the implications of DACCS deployment on the power sector?
- Which European countries offer the most favorable conditions for DACCS?

These research questions are addressed using a new extension of the energy system model *Enertile.* From this approach, several practical implications can be derived. By taking an economic system perspective, this analysis provides insights on DACCS primarily for policymakers, who allocate research funding and establish legislative regulations as part of climate change mitigation strategies.

8.2 Methods and data

8.2.1 Methods

The techno-economic potential of DACCS in Europe is determined using a novel extension of the energy system model *Enertile* (Fraunhofer ISI 2021). *Enertile* is a software package aimed at analyzing the cost-optimal energy supply for a given geographical region. The regional focus of previous analyses has been on Europe (Bernath et al. 2021; Lux et al. 2020; Lux et al. 2022; Pfluger 2014). However, the model has also been used for studies in China (Franke et al. 2021) and the Middle East and North Africa (Lux et al. 2021).

Enertile is a bottom-up optimization model for large, coupled energy systems. The objective of the model is to minimize the cost of energy conversion, transmission, and storage up to the year 2050. The model covers the interlinked supply of electricity, heat, hydrogen, and synthetic fuels. Exogenous and endogenous demands of these energy forms have to be met by optimizing capacity expansions of relevant infrastructures and their hourly dispatch. Taxes and levies are not included in *Enertile*, as the model focuses on an overall economic perspective and not on individual market actors and their behavior. All investments related to capacity expansions are assigned a weighted average cost of capital (WACC) of 2%. A more detailed and formal description of the linear optimization problem in the base version of *Enertile* is given in (Bernath et al. 2019; Deac 2019; Lux et al. 2020; Lux et al. 2021; Pfluger 2014).

Technologically, spatially, and temporally highly resolved electricity generation potentials of the renewable technologies ground-mounted photovoltaics (PV), roof-top PV, onshore wind, offshore wind, and concentrated solar power (CSP) are key characteristics of the model Enertile. For these technologies, installable capacities, hourly generation profiles, and electricity generation costs are determined on a grid with an edge length of 6.5 x 6.5 km across Europe. The determination of renewable energy potentials includes techno-economic parameters of the individual renewable power generation technologies, re-analysis weather data of the year 2010 (Bollmeyer et al. 2015), land use data (EEA 2018), and geographic information such as elevation and slope (Danielson et al. 2011). Appendix C summarizes the most important techno-economic input parameters of the individual renewable technologies. In sum, this results in a detailed picture of the potential of renewable energies used in energy system optimization. More detailed documentation of the potential calculation can be found in (Fraunhofer ISI et al. 2021a; Lux et al. 2021; Sensfuss et al. 2021a, 2021b).

The central extension of *Enertile* in this paper provides a model representation of capturing and permanently storing CO_2 from ambient air to include DACCS technology in the optimization decisions. There are two mechanisms in the model that allow to evaluate DACCS technology within an energy system economically. Both approaches are shown in Figure 8-1. Firstly, the model is offered a selling price for captured and stored CO_2. In cost optimization, *Enertile* decides how much CO_2 it will capture and store at that given price. This mechanism can represent potential CO_2 compensation demands from the sectors of agriculture, industry, transport, residential, and services. The CO_2 compensation demand is indirectly introduced to the model in the form of a selling price that reflects the willingness to pay for captured and sequestered CO_2 of these demand sectors. Technically, the sale of sequestrated CO_2 reduces the energy system cost in the objective function. The model installs and uses additional electricity supply infrastructure and DAC and sequestration units as long as incurred costs are covered by the revenues of selling the compensated CO_2. The last ton of compensated CO_2 provided and sold creates marginal costs at the applied sales price. Applying different sales prices in different model runs generates supply curves for CDR via the DACCS pathway. These supply curves interrelate with the rest of the energy system in the scenario design. Secondly, an exogenous CDR demand is directly imposed on *Enertile*. The model installs and uses additional electricity supply infrastructure and DACCS units until the specified demand is met. This CDR demand represents the remaining emissions from other sectors. Both approaches are used to investigate different aspects of DACCS potentials in Europe.

In addition to these two methods to incentivize CO_2 capture and storage exogenously, model endogenous CO_2 compensation demands may arise. Fossil technologies can be used by *Enertile* to meet given electricity and heat demands. The emissions released in these processes create a CO_2 compensation demand that must be met through the DACCS pathway. In this way, GHG neutrality of the conversion sector is ensured. The decision of whether this combined electricity and heat supply strategy with fossil fuel utilization and CO_2 emission compensation is used to meet exogenously given energy demands is subject to cost minimization.

To generate negative emissions provided by DACCS technologies, costs and energy demands arise within *Enertile*. The DACCS pathway is modeled as a black box requiring electricity as input and providing captured and sequestrated CO_2 from ambient air as an output (cf. Figure 8-1). Potential heat requirements of the DAC technology are accounted for using electricity equivalents. In the modeling, it is conservatively assumed that an electric heater provides this heat (cf. section 8.2.2.5).

Since CO_2 mixes rapidly in the atmosphere (Snæbjörnsdóttir et al. 2020), DAC units are not geographically bound to emission sources. In the modeling, it is assumed that DACCS plants can be operated close to suitable geological CO_2 reservoirs or advantageous locations for renewable power generation across Europe. To provide this regional flexibility in *Enertile*, compensated CO_2 can be exchanged between the balances of model regions (cf. Figure 8-1). For example, emissions released in Austria can be captured from the ambient air and sequestered in Norway.

Enertile has a high temporal and spatial resolution. Renewable energy potentials are determined on a grid with a tile size of 42.25 km^2. The spatial resolution for the balancing of energy supply and demand in the optimization is mostly at the country level. The definition of model regions is shown in Appendix B. Geographically covered are the member states of the EU, Norway, Switzerland, the United Kingdom, and other Balkan states. For simplicity, the geographic area covered in the scenario calculations is referred to as "Europe" in the remainder of this paper. For the analyses in this article, the year 2050 is considered in hourly resolution. The modeling approach uses perfect foresight, i.e., the model has perfect information about all time steps considered when determining the system cost minimum.

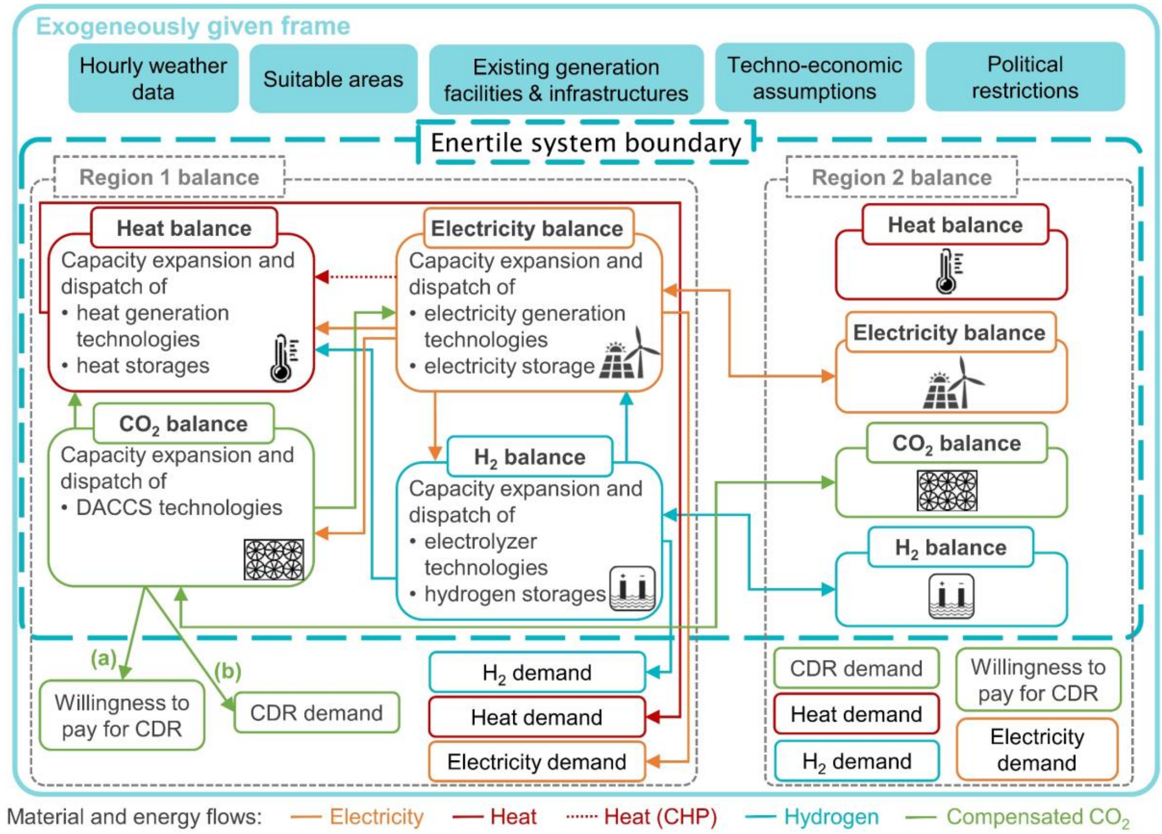

Figure 8-1 Simplified representation of energy and material flows in the energy system model *Enertile*. The model extension for this article is the CO_2 balance. Model endogenously, *Enertile* decides on the compensation of CO_2 emissions from the use of fossil fuels for electricity and heat generation and on the exchange of compensated CO_2 between model regions. Model exogenously CO_2 capture and storage can be incentivized through two mechanisms: a) through a selling price of carbon dioxide removal (CDR) in €/t_{CO2} that represents the willingness to pay for compensated CO_2 of demand sectors. b) through explicitly specified CDR demands in t_{CO2}.

8.2.2 Data

8.2.2.1 Scenario design

The analysis of DACCS potentials in Europe is based on the scenario framework *long-term scenarios* of the German Federal Ministry for Economic Affairs and Energy (Fraunhofer ISI et al. 2021b). In this framework, a research consortium has investigated highly ambitious GHG reduction pathways for the European economic system up to the year 2050. This analysis framework is appropriate because the DACCS option can be studied alongside other extensive GHG mitigation measures. This approach considers that the electricity demands of DACCS plants will be integrated into an electricity system that is exposed to high loads caused by the electrification of applications on the one hand but is also more flexible through sector coupling options on the other. By calculating different scenario variants on this basis, ceteris paribus model responses to CDR requirements can be evaluated.

The energy demands in the sectors industry, transport, residential, and services are taken from the electrification scenario ("TN-Strom") and are the basis for the calculations of the energy supply and provision of compensated CO_2 in *Enertile* for this article. In this scenario, GHG emission reductions in the demand sectors are realized through the electrification of processes and applications whenever possible. This strategy includes, for example, the use of trolley trucks in heavy-duty transport and the use of electrode boilers to provide process heat in industry. This strategy to reduce GHGs across sectors results in relatively high electricity demands that must be met in *Enertile* (cf. section 8.2.2.2)

For the conversion sector in 2050, it is assumed that electricity, heat in heat grids, and hydrogen must be provided GHG-neutral. Therefore, fossil-based electricity and heat generation technologies are prohibited in the model parameterization, except for the utilization of waste. The gross electricity production from non-renewable waste in the scenario runs is fixed to estimates of waste utilization in power generation in the year 2018 (Observ'ER et al. 2020). The resulting emissions of waste-to-energy in the conversion sector must be compensated using DACCS; this results in a model-endogenous CDR demand (cf. Figure 8-1).

In other sectors, certain emissions remain in the selected scenario, which have to be compensated either inside or outside of Europe to achieve GHG neutrality. These remaining emissions include, for example, process-related CO_2 emissions in the cement industry or GHG emissions in agriculture from livestock farming, soil fertilization, or rice cultivation. To analyze the DACCS potential in Europe, the two incentive mechanisms for CO_2 capture and storage in *Enertile* presented in section 8.2.1 are used:

- In the case where a selling price for compensated CO_2 is offered to the model, different variants for the parameterization of the DAC technology (cf. section 8.2.2.5) and different selling prices are investigated. Three parameter variants for DAC are distinguished: *Current2020*, C*ons2050*, and *Base2050* (cf. section 8.2.2.5). As a result, a CDR supply curve is calculated for each DAC parameter variant. The results obtained using this approach are presented in section 8.3.1.
- In the case where the model needs to meet explicit CDR demands, the analysis focuses on three main scenarios. The scenarios differ in the model's degree of freedom to meet CDR demands. One, the *No CDR demand scenario* defines an anchor point for a scenario comparison. No exogenous CDR demands are specified in this scenario, and the model only needs to compensate for endogenous CO_2 emissions. Two, in the *Loc bound scenario,* each country must offset its emissions. In this scenario, there is no CDR exchange between model regions. Three, in the *Loc opt scenario*, the model can decide on the location of the carbon capture in a cost-optimal way. In this scenario, Norway, for example, can meet CDR demands from Austria if this decision results in lower system costs. In all cases, geological

CO_2 storage potentials must not be violated (cf. section 8.2.2.6). The *Loc opt,* and *Loc bound scenarios* are calculated using two different DAC parameterizations: *Cons2050* and *Base2050* (cf. section 8.2.2.5). Region-specific CDR demands are defined in section 8.2.2.3. The complete scenario tree for this approach is specified in . The corresponding results are shown in section 8.3.2.

Table 8-1 Scenario variants for the analysis method where DACCS is incentivized by explicit CDR demands. The *No CDR demand* scenario serves as a reference without exogenously specified carbon dioxide removal demands. In this scenario, only the model endogenous CO_2 emissions from waste-to-energy have to be captured and stored.

Scenario name	Model's degree of freedom to meet CDR demands	DAC parametrization	CDR demand
No CDR demand	n.a.	*Base2050*	none
Loc opt - DAC Cons2050	*Loc opt*, i.e., cost-optimal location	*Cons2050*	active
Loc opt - DAC Base2050	*Loc opt*, i.e., cost-optimal location	*Base2050*	active
Loc bound - DAC Cons2050	*Loc bound*, i.e., each country must offset its emissions	*Cons2050*	active
Loc bound - DAC Base2050	*Loc bound*, i.e., each country must offset its emissions	*Base2050*	active

8.2.2.2 Energy demands

The exogenous energy demands from the sectors of industry, transport, residential, and services are central assumptions of the scenario design with a strong influence on the energy supply optimization. The energy demands for electricity, heat, and hydrogen in the model regions are adopted from the electrification scenario "TN-Strom" of the *long term scenarios* (Fraunhofer ISI et al. 2021b). A flat distribution grid loss of 5.5% is applied to the electricity demands of the demand sectors for the supply optimization, while losses on the transport grid are calculated endogenously. The district heating demands are subject to heat grid losses of 10%.

Figure 8-2 summarizes the final energy demands covered in the supply optimization in *Enertile* for the year 2050 in all model regions. Despite significant efficiency improvements in applications, the electricity demand increases to 4,699 TWh in 2050. This is due to new electricity consumers such as e-mobility. The European heat demand in heat grids amounts to 524 TWh in 2050. The hydrogen demand increases to 619 TWh because processes such as steel production are converted to the use of hydrogen in the scenario design.

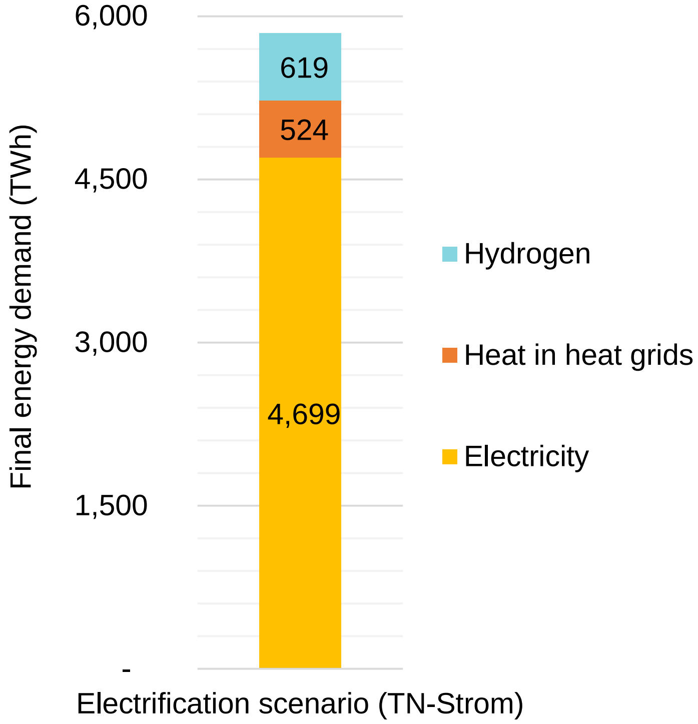

Figure 8-2 Energy demands of the demand sectors industry, transport, residential, and services in 2050 for all model regions in the electrification scenario (TN-Strom) of the *long term scenarios* (Fraunhofer ISI et al. 2021b) framework. In *Enertile*, the demands for electricity, heat in heat grids, and hydrogen are met by energy supply optimization.

8.2.2.3 Carbon dioxide removal demands

In the case where DACCS in the model is induced by a fixed CDR demand, assumptions are needed as to how high this CO_2 compensation demand is. In the analysis of this paper, the estimation of the CDR demand for each scenario region is based on the countries' GHG emission level[17] of 1990 in CO_2 equivalents (BMUV 2020; UNCC 2021). It is assumed that 5% of the 1990 emissions have to be compensated in 2050. Based on the figures of (2020; UNCC 2021), this results in a total European CDR demand of 288 Mt_{CO2}/a. Figure 8-3 visualizes the regional distribution of the assumed CDR demands in the case where (a) each model region must compensate for its emissions[18] (*loc bound*) and (b) no spatial constraints are imposed for offsetting emissions (*loc opt*).

[17] Without land use, land-use change, and forestry (LULUCF).

[18] Given the framework conditions of this study, Austria, Switzerland, the Czech Republic, the Baltic States, and the Benelux Union do not have sufficiently large geological CO_2 storage potentials to meet their own CDR demands (cf. section 8.2.2.6). In order to keep the sum of annual CO_2 capture volumes between the *loc bound* and *loc opt* scenarios equal, exceeding CDR demands in these regions are shifted to the country with the largest geological storage potential: Norway offsets about 15 Mt_{CO2} more than its own demand in the loc bound scenarios.

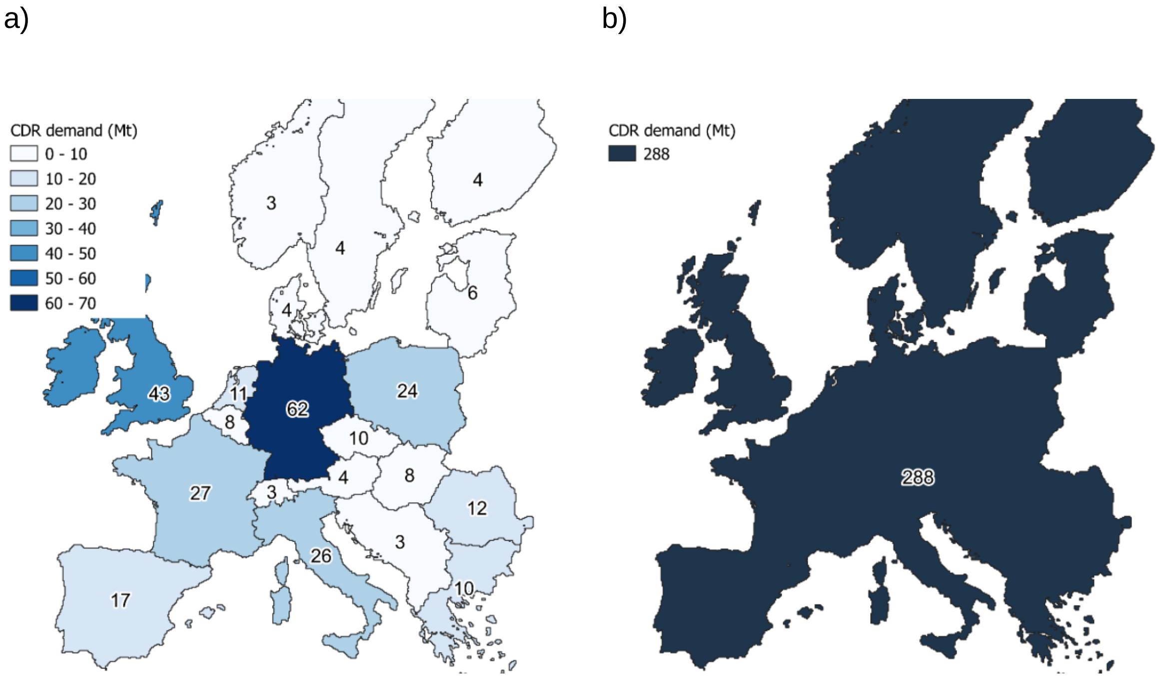

Figure 8-3 The assumed CDR demands in 2050 equal 5% of 1990 GHG emissions (BMUV 2020; UNCC 2021). a) *Loc bound:* Each model region must offset its emissions. b) *Loc opt*: The CDR demand must be met within Europe, but the optimizer decides on the location of DACCS.

8.2.2.4 Renewable energy source potentials

An important input to supply-side energy system optimization is the potential of renewable energy sources (RES). Figure 8-4 shows the result of the renewable potential calculation described in section 8.2.1: aggregated techno-economic generation potentials of the different renewable technologies as a function of the generation costs. The figure shows that the renewable electricity generation potential included in the cost minimization of the European energy supply system is about 14,000 TWh. The potential of about 6,000 TWh has a levelized cost of electricity (LCOE) of 35 €/MWh; the potential of 8,000 TWh is available at an LCOE of about 50 €/MWh. Onshore wind and ground-mounted PV dominate the low-cost potential in Europe in 2050. Offshore wind, rooftop PV, and concentrated solar power (CSP) have smaller potentials and higher generation costs.

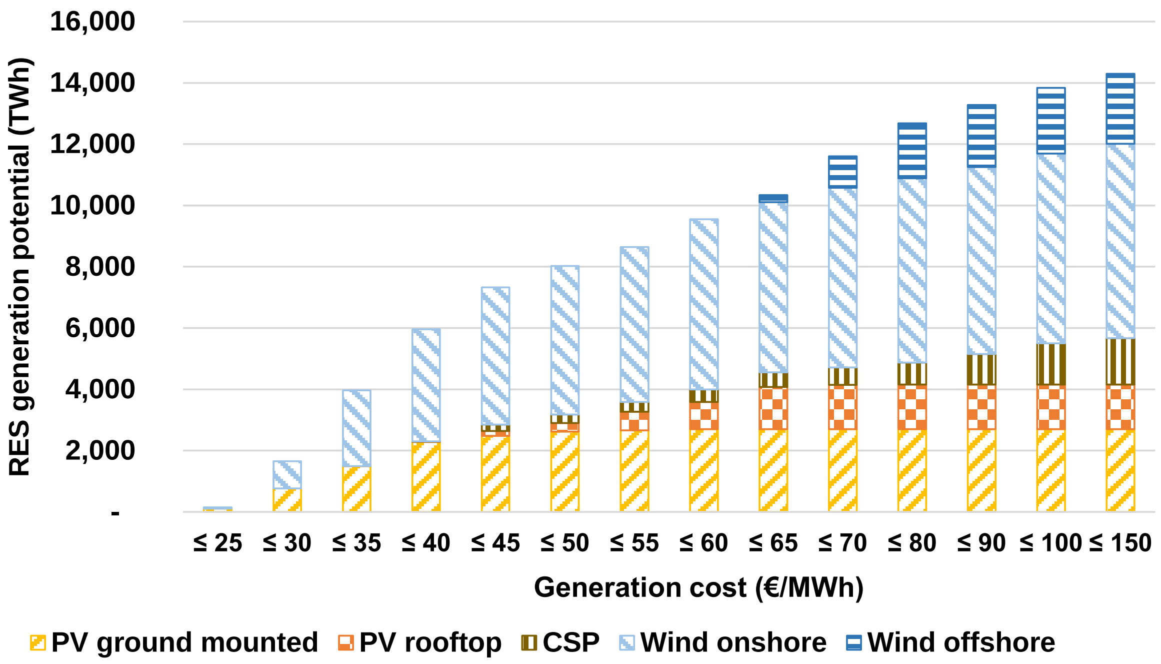

Figure 8-4 Aggregated renewable electricity cost-potential curve for Europe in 2050 (Fraunhofer ISI et al. 2021b).

8.2.2.5 Direct air capture technology

DAC is a relatively new technology, with currently 19 plants operating worldwide (IEA 2021). Climeworks launched the largest DACCS plant to date, with a CO_2 capture capacity of 4,000 t_{CO2}/a in Iceland in 2021 (Skydsgaard 2021). The technology is, therefore, subject to greater uncertainties regarding its development. Viebahn et al. (2019) analyze the current development stage of different DAC technologies and classify low-temperature DAC systems (LT DAC) with a technology readiness level (TRL) of 6 and high-temperature DAC systems (HT DAC) with a TRL of 5.

Fasihi et al. (2019) reviewed the literature on DAC and found that the stated or estimated energy consumptions and costs of the technology vary widely. To account for the high uncertainty and different data in the literature regarding the techno-economic development of DAC technologies until the year 2050, three parameter sets, *Base2050*, *Cons2050*, and *Current2020,* varying in cost, energy demand, and lifetime, are defined for the analysis in this paper in Table 8-2. The *Current2020* parameter set represents state-of-the-art DAC systems as currently reported (Fasihi et al. 2019). This parameterization assumes that DAC technology will not be substantially developed in the future and serves as a lower bound. Based on a log-linear learning curve approach and techno-economic parameters assumed for 2020, Fasihi et al. (2019) estimate the evolution of capital expenditures (CAPEX) for DAC until the year 2050. In the *Cons2050* parameter set, CAPEX are estimated to be 222 €/t_{CO2} a for HT DAC and 199 €/t_{CO2} a for LT DAC. In the *Base2050* parameter set, CAPEX are decreased to 93 €/t_{CO2} a for HT DAC and 84 €/t_{CO2} a for LT DAC. Fasihi et al. (2019) also assume an increase in lifetime and a decrease in energy demand as a result of technological learning until 2050. However, in their DAC parameter scenarios, the authors only differentiate the investments – but not the energy consumption and lifetime – between their "base" and "conservative" scenarios. In this work, the *Cons2050* scenario is calculated with half the learning rate in energy consumption (5%/10 a electricity consumption, 7.2%/10 a heat consumption) and half the increase in lifetime (5 a) compared to the original data. The *Base2050* scenario in this paper adopts the "base" scenario from Fasihi et al. (2019) (Fasihi et al. 2019). Breyer et al. (2020) caveat that these future cost levels can only be achieved via technological learning if DAC systems are scaled up early in the energy system. Fixed operating expenditures (OPEX) are assumed to be 4% of CAPEX for all parameter sets. Since the electricity costs are included and optimized endogenously in the model *Enertile*, no other variable costs are assumed. Since HT DAC systems are reported to have higher costs, we only consider LT DAC systems in this paper.

For both HT DAC and LT DAC, the major part of a DAC plant's energy demand is heat for dissolving captured CO_2 from solvents or sorbents. While for HT DAC primarily natural gas has been used for the heat supply so far, the literature for LT DAC shows different heat sources – waste heat being the most economically attractive one (Fasihi et al. 2019). This paper examines DACCS plants in deep decarbonization scenarios. This limits the selection of suitable or available heat sources. Fasihi et al. (2019) elaborate that natural gas and renewable synthetic methane are not sustainable or efficient for supplying heat in DAC plants. Renewable heat sources such as solar thermal, geothermal, or biomass may be suitable; however, their potential is bound to certain regions and, in the case of biomass, is limited by land use restrictions. Waste heat is locally bound too and, in GHG-neutral energy systems, subject to increasing competition for utilization. Consequently, electricity-based heat supply is expected to become an important decarbonization measure (e.g. (Barnes et al. 2020; Bloess et al. 2018; Lowes et al. 2020)). Aiming at robust results, the modeling approach in this paper conservatively assumes full electric DAC systems. It is conservatively assumed that heat is provided by electric heaters and heat demands of DAC plants are converted into electricity demands. Depending on the parameter set, an LT DAC system requires between 1,339 kWh_{el} and 2,088 kWh_{el} of electricity to capture one ton of CO_2. A lifetime between 20 and 30 years is assumed in the respective parameter sets.

Table 8-2 DAC parameter sets used in the energy system optimization model *Enertile*.

Scenario	CAPEX (€/t_{CO2}h) [a]	OPEX		Electricity demand (kWh_{el}/t_{CO2})	Life-time (a)	Data source
		Fix (% of CAPEX)	Variable (€/t_{CO2})			
Base2050	672,000	4	0	1,339	30	(Fasihi et al. 2019)
Cons2050	1,592,000	4	0	1,685 [b]	25 [b]	(Fasihi et al. 2019)[b]
Current2020	5,840,000	4	0	2,088	20	(Fasihi et al. 2019)

[a] To receive the CAPEX, the reported investments – e.g., 199 €/t_{CO2} a for the conservative parameter set – were multiplied by 8,000 full load hours (FLH) based on results for large-scale DAC systems in Fasihi et al. (2019) and Breyer et al. (2020).
[b] In their DAC parameter scenarios, Fasihi et al. (2019) differentiate only the investments – but not the energy consumption and lifetime – between the scenarios Base and Conservative. In this work, the *Cons2050* scenario is calculated with half the learning rate in energy consumption (5%/10 a electricity consumption, 7.2%/10 a heat consumption) and half the increase in lifetime (5 a) compared to the original data.

8.2.2.6 CO_2 sequestration technology and storage capacities

Deep geological formations into which CO_2 can actively be injected by wells are important for DACCS. Zhang and Song (2014) assume a sequestration site is suitable if it stores the CO_2 for at least 1,000 years with a leakage rate of less than 0.1% per year. The captured CO_2 is preferably compressed and injected in a supercritical state into 800 m to 2,000 m deep geological formations like deep saline aquifers, hydrocarbon fields, or coal fields (d'Amore et al. 2017; Zhang et al. 2014). Depending on the sequestration site, different trapping mechanisms exist to store CO_2 in the gaseous, liquid, or supercritical state. Low-permeability cap rock is a prerequisite for all storage sites, as it traps the moving CO_2 underneath and prevents leakage before other optional trapping mechanisms, such as mineral trapping, can come into play (Zhang et al. 2014).

The EU GeoCapacity project (EU GeoCapacity 2009) performed a GIS-based assessment of geological formations including the most interesting sequestration sites deep saline aquifers, hydrocarbon fields, and coal fields in 25 European countries (d'Amore et al. 2017). Based on the results of Navigant (2019), the total CO_2 sequestration potential of the scenario regions – including the EU 27 member states, Norway, United Kingdom, Switzerland, and countries of the Balkan Peninsula – account for 134 Gt_{CO2}. Deep saline aquifers account for the largest share of storage capacity with about 80% (EU GeoCapacity 2009). The total storage potential of the scenario regions is shown in Figure 8-5. For the 2050 analysis in this paper, the total capacity is divided by 100 years, as capacity may be needed before and after 2050. This results in an annual storage potential of more than 1 Gt_{CO2}/a and would be sufficient to store a quarter of the EU's annual emissions in 2018 (UNCC 2021).

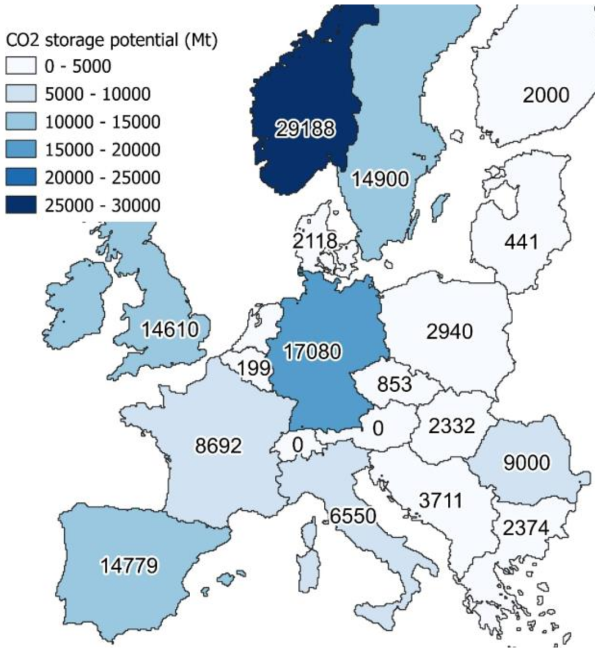

Figure 8-5 Regional CO_2 storage potentials for all scenario regions. Own illustration based on data from (EU GeoCapacity 2009; Navigant 2019).

CO_2 sequestration costs highly depend on the type of storage site. NAVIGANT (2019) estimates storage costs between 1 €/t_{CO2} for low-cost onshore depleted oil or gas fields and 22 €/t_{CO2} for high-cost offshore saline aquifers. Based on additional literature (Budinis et al. 2018; Fasihi et al. 2019), final OPEX of 10 €/t_{CO2} for CO_2 sequestration are assumed in this study.

8.3 Results

The techno-economic DACCS potential in a GHG-neutral European energy system is analyzed using both modeling approaches presented in section 8.2.1. The results of the CDR sales instance supplied by DACCS units are presented in section 8.3.1. European supply curves of captured and sequestrated CO_2 and a cost decomposition are shown. The results of meeting explicit CO_2 removal demands via the DACCS route are shown in section 8.3.2. This methodological approach is used to analyze the regional distribution of CO_2 removal among European countries and to show the impacts of DACCS on the conversion sector.

8.3.1 Methodology approach A – Carbon dioxide removal sales instance for DACCS units

8.3.1.1 European supply curves for carbon dioxide removal by direct air capture and storage

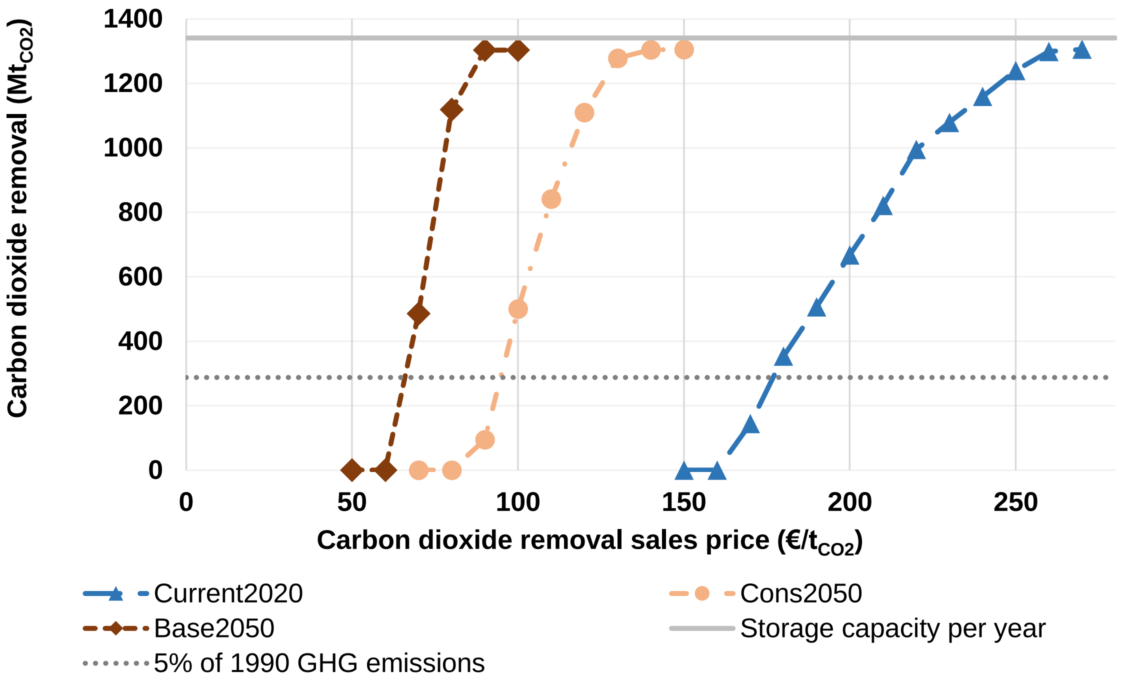

Figure 8-6 Aggregated European DACCS supply curves in 2050 for three different DAC parametrizations. The upper limit of the annual capture volume is set by the geological storage potential. As an order of magnitude, 5% of 1990 GHG emissions are plotted.

Figure 8-6 shows the model results of the DACCS supply curves for Europe in 2050. Three different techno-economic parametrizations of the DAC technology are distinguished. The CDR supplies via the DACCS pathway are an economic European optimum conditioned by regional CO_2 storage potentials and hourly electricity generation costs. The supply curves in Figure 8-6 represent CDR quantities for GHG emissions external to the conversion sector. However, the endogenous CO_2 compensation for waste-to-energy is part of the optimization, accounts for additional 37 Mt_{CO2}/a of CDR requirement, and explains the gap between the maximum values of the supply curves and the upper limit of the annual CO_2 storage capacity.

For all three DAC parametrizations, the optimization results show increasing CDR amounts with increasing sales prices. This means that with a higher willingness to pay for compensated CO_2 in other sectors, additional DACCS plants with higher marginal costs come into play. Assuming that only one-hundredth of the available geological CO_2 storage potential may be used annually and applying the parameter projections for low-temperature DAC plants until 2050, DACCS costs are in the ranges of 60 to 90 €/t_{CO2} for the *Base2050* DAC parameter set and 80 to 140 €/t_{CO2} for the *Cons2050* DAC parameter set. For an upper benchmark, if the presently published key performance indicators of DAC plants are used, DACCS costs in the range of 160 to 270 €/t_{CO2} are obtained for the *Current2020* parameter set. At the upper end of sales prices of 90 €/t_{CO2} (*Base2050*), 140 €/t_{CO2} (*Cons2050*), and 270 €/t_{CO2} (*Current2020*), the respective supply curves reach the predefined maximum annual CO_2 storage capacity.

8.3.1.2 Cost components of DACCS

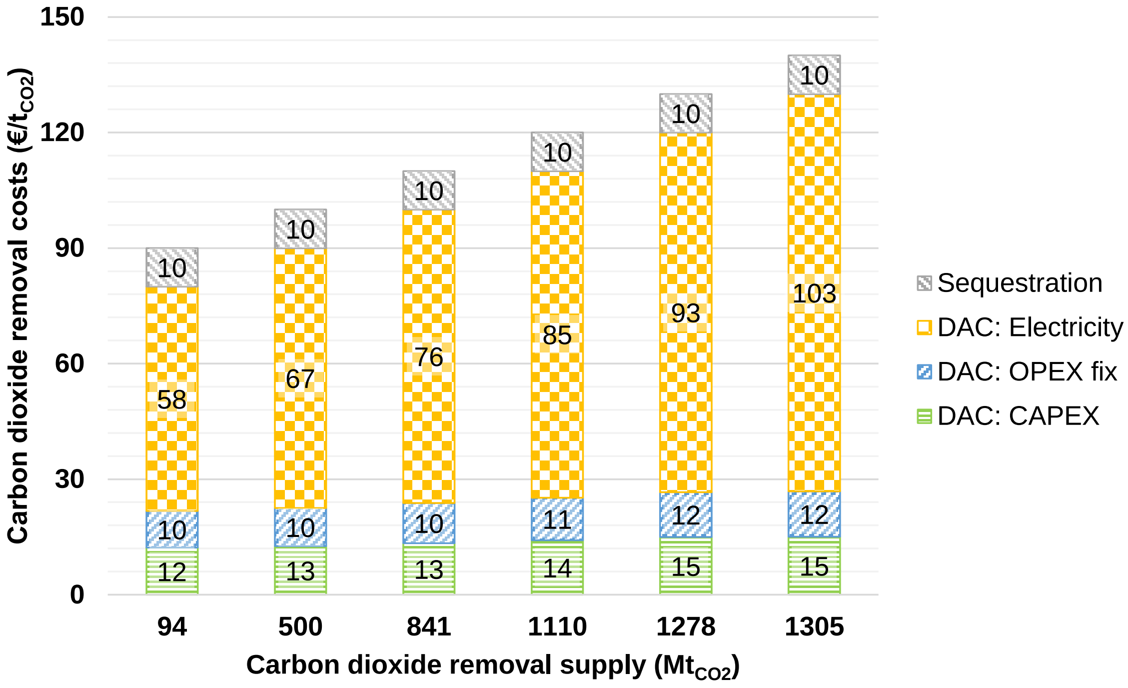

Figure 8-7 Cost decomposition of carbon dioxide removal (CDR) for the DACCS supply curve using the *Cons2050* DAC parameter set.

Figure 8-7 shows the cost decomposition of the DACCS supply curve for the *Cons2050* DACCS technology parametrization. The cost decomposition shows that the dominant cost component for compensating for CO_2 emissions with DACCS is energy costs. With increasing CDR sales prices – and therefore increasing CO_2 compensation amounts – the share of electricity costs for DAC increases from 65% of DACCS costs at a sales price of 90 €/t_{CO2} to 74% at a sales price of 140 €/t_{CO2}. This increase in electricity costs is due to exploiting increasingly expensive RES sites (cf. Figure 8-4) as electricity demands for DACCS increase. Annuitized CAPEX and fixed OPEX of DAC only show moderate increases with increasing CDR sales prices. Depending on the sales prices, these fixed cost components of the DAC unit account for 19% to 24% of the total DACCS cost for the *Cons2050* DAC parameter set. Sequestration costs are assumed to be flat and account for 10 €/t_{CO2} for all points on the supply curve.

The cost decompositions of the *Base2050* and *Current2020* DACCS parametrization scenarios show structurally similar results compared with the *Cons2050* case. For all parametrizations considered, electricity is the dominant cost component of DACCS costs.

8.3.2 Methodology approach B – Meeting explicit regional carbon dioxide removal demands via the DACCS pathway

8.3.2.1 Regional DACCS potential usage

Figure 8-8 shows the regional distribution of CDR via the DACCS route in the scenarios *Loc opt - DAC Base2050* and *Loc opt - DAC Cons2050*. It shows that if the optimizer is given the choice of where to perform DACCS to compensate for European GHG emissions, units are operated only in Sweden, Norway, Finland, the Iberian Peninsula, and the Baltic States. These countries offer sufficient CO_2 sequestration potentials in combination with idle and relatively low-cost renewable electricity generation potentials. In Finland and the Baltic States, the predefined maximum annual sequestration volume is reached in both scenarios. Many countries currently contributing substantially to Europe's GHG emissions, such as Germany, the United Kingdom, France, and Italy (cf. Figure 8-3), do not have favorable conditions to permanently remove CO_2.

The regional distribution of CO_2 capture and storage differs between the two DAC parameterizations. In the *Base2050* DAC parameter scenario, the highest amount of GHG emissions is offset on the Iberian Peninsula amounting to 148 Mt_{CO2}/a. In the parameter scenario *Cons2050* DAC with higher specific investments for DAC plants and higher specific energy consumption for CO_2 capture, the optimizer shifts the capturing of about 50 Mt_{CO2}/a from the Iberian Peninsula to Scandinavia. This shift is especially related to the disproportional increase in specific investments in the *Cons2050* scenario: while the specific investments of DAC units are increased by 137% compared to the *Base2050* scenario, the energy demand per ton of CO_2 captured is only increased by 26%. In consequence, the average full load hours of the DACCS plants in the optimization result increase from 4,878 h in the *Loc opt - DAC Base2050* scenario to 6,633 h in the *Loc opt - DAC Cons2050* scenario. By increasing the full load hours, the increased annuities of the specific investments can be allocated to more hours and thereby reduce the specific DACCS costs. This allocation of the higher investments to more operating hours competes with increased power procurement costs during these additional hours. The renewable expansion results in Figure 8-9 and Figure 8-10 show that these higher full-load hours of DAC units can be realized by onshore wind rather than PV. Therefore, with higher specific investments of DACCS units, the optimizer reduces the expansion of PV capacity on the Iberian Peninsula and increases onshore wind capacity in Scandinavia instead.

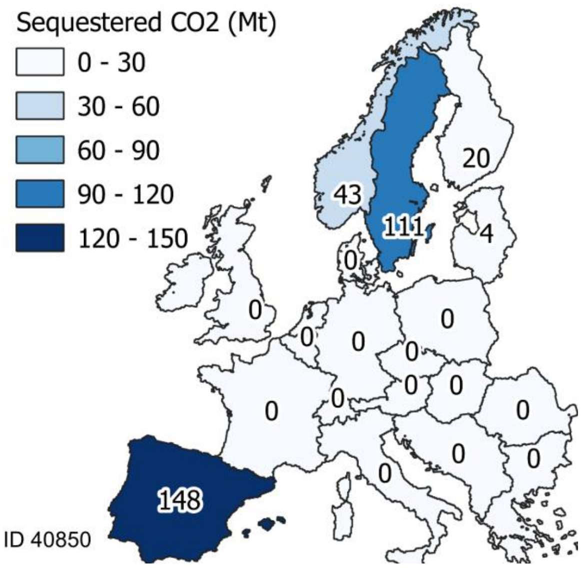

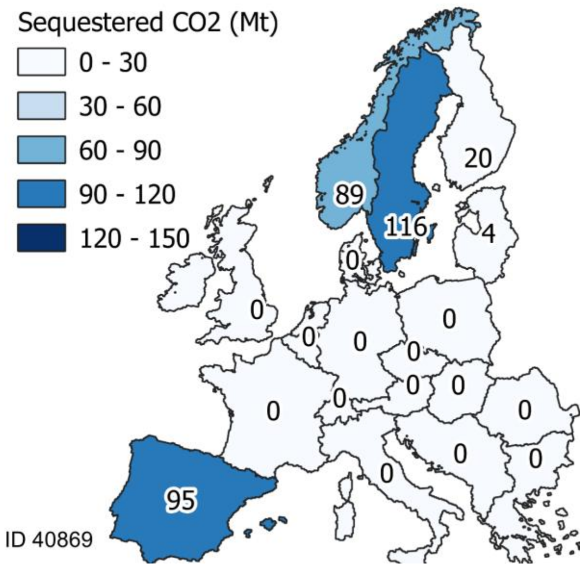

Figure 8-8 Captured and sequestered CO_2 in the scenarios *Loc opt - DAC Base2050* and *Loc opt - DAC Cons2050*. In addition to the model endogenous CDR demands caused by emissions from waste-to-energy within the conversion sector, both scenarios assume that 5% of the 1990 greenhouse gas emissions need to be removed from the atmosphere annually. The total annual CDR demand in the scenarios is about 325 Mt_{CO2}. The optimizer has the choice of where to install and utilize DACCS units across Europe.

8.3.2.2 Impacts of DACCS on the conversion sector

Energy costs are the main component of CDR costs using DACCS technology. This section describes the impacts of DACCS deployment on the electricity system. Figure 8-9 shows the electricity generation, and the associated installed generation capacities in Europe in 2050 for the *No CDR demand* scenario and the change in these quantities for all scenarios with CDR demands defined in Table 8-1. In the reference case of the *No CDR demand* scenario, onshore wind and PV are the dominating electricity generation technologies. Together, they account for 72% of electricity generation and 78% of the installed electricity generation capacity in Europe in 2050.

CO_2 compensation in Europe substantially increases the installed power generation capacities of renewable energies. Compared to the *No CDR demand* scenario, all scenarios with an exogenously given CDR demand of 288 Mt_{CO2}/a show a 5% to 8% increase in power generation capacity. The DAC parameterization has a higher impact on the extent of additional installed capacity than regional constraints on CO_2 capture and storage. Additional electricity generation capacity requirements in the *DAC Cons2050* scenarios range between 206 GW (*Loc opt)* and 228 GW (*Loc bound*), while in the *DAC Base2050* scenarios, they range between 159 GW (*Loc opt*) and 182 GW (*Loc bound*). In both parametrization cases – *DAC Cons2050* and *DAC Base2050* – the free choice of location for offsetting CO_2 emissions within Europe reduces the additional electricity generation capacity by only one percentage point. The capacity expansion for power generation mainly affects onshore wind and PV. Onshore wind capacity increases between 80 GW (*Loc bound - DAC Base2050*) and 119 GW (*Loc bound - DAC Cons2050*); PV capacity increases between 85 GW (*Loc opt - DAC Base2050*) and 126 GW (*Loc bound - DAC Cons2050*). In the *DAC Cons2050* scenarios, the offshore wind capacity is increased by 1 GW; in the *DAC Base2050* scenarios, offshore wind capacity is not increased at all. With the underlying costs assumptions, offshore wind is too expensive to be expanded substantially given the amount of compensated CO_2 required in these scenarios; for higher CRD demands, offshore wind might play a greater role.

Figure 8-10 shows the regional distribution of the potential utilization of the technologies ground-mounted PV, onshore wind, and offshore wind for the scenario *No CDR demand.* In addition, it shows the regional changes in installed electricity generation capacities of these technologies in scenarios with exogenous CDR demands. The figure illustrates that already in the *No CDR demand* scenario, the renewable electricity generation potentials in Central Europe are largely exhausted. Especially in Germany, Denmark, the Czech Republic, the British Isles, and the Benelux Union, the potentials for onshore wind and ground-mounted PV are fully exploited. In the *Loc opt* scenarios, the cost optimization, therefore, mainly selects locations at the “edges” of Europe for the installation of DACCS plants. In these scenarios, onshore wind and ground-mounted PV capacities are expanded mainly on the Iberian Peninsula, Sweden, and Norway. These locations have both a CO_2 storage potential (cf. Figure 8-5) and – equally important – idle and relatively cheap renewable electricity generation potentials. In the *Loc bound* scenarios, there too is a focus of onshore wind and PV expansions on the Iberian Peninsula, in Sweden, Norway, and Finland, but the concentration of the renewable capacity expansion in these regions is not as pronounced. The exploitation of the available renewable potentials is more evenly distributed across Europe. This is based on the scenario-specific restriction that each region must capture and store its own CDR quantity. The required electricity can either be generated within the respective region by renewable energies or imported from other regions. However, imports are limited by transmission grid capacities and are subject to losses. An expansion of the transmission grid is possible in the optimization but is associated with costs. In the optimization result, regions like the Iberian Peninsula or Norway, therefore, export more electricity in the *Loc bound* scenarios than in the *Loc opt* scenarios. On the other hand, regions like Germany and the British Isles, which have already exhausted their potentials for onshore wind and ground-mounted PV in the *No CDR demand* scenario, compensate for the additional energy demands in the *Loc bound* scenarios through their trade balances. Germany imports electricity for CO_2 capture from other European countries. The British Isles reduce their electricity and hydrogen exports to mainland Europe to meet the increased domestic electricity demand. In contrast, Poland is particularly increasing its PV capacity to meet its CDR demand.

All four scenarios with exogenously specified CDR demands show a reduced utilization of hydrogen as a seasonal storage medium in the conversion sector compared to the *No CDR demand* scenario. Figure 8-9 shows that the hydrogen utilization for electricity generation decreases by between 22 TWh_{el} in the *Loc opt - DAC Base2050* scenario and 37 TWh_{el} in the *Loc bound - DAC Cons2050* scenario. Since both electrolysis and DAC technologies have electricity as the main cost driver in this modeling, these technologies compete for low-cost renewable energy and mutually limit one another's uses. As more renewable energy is produced, the need for hydrogen reconversion decreases, while in times of high renewable supply more electricity is used in DAC facilities.

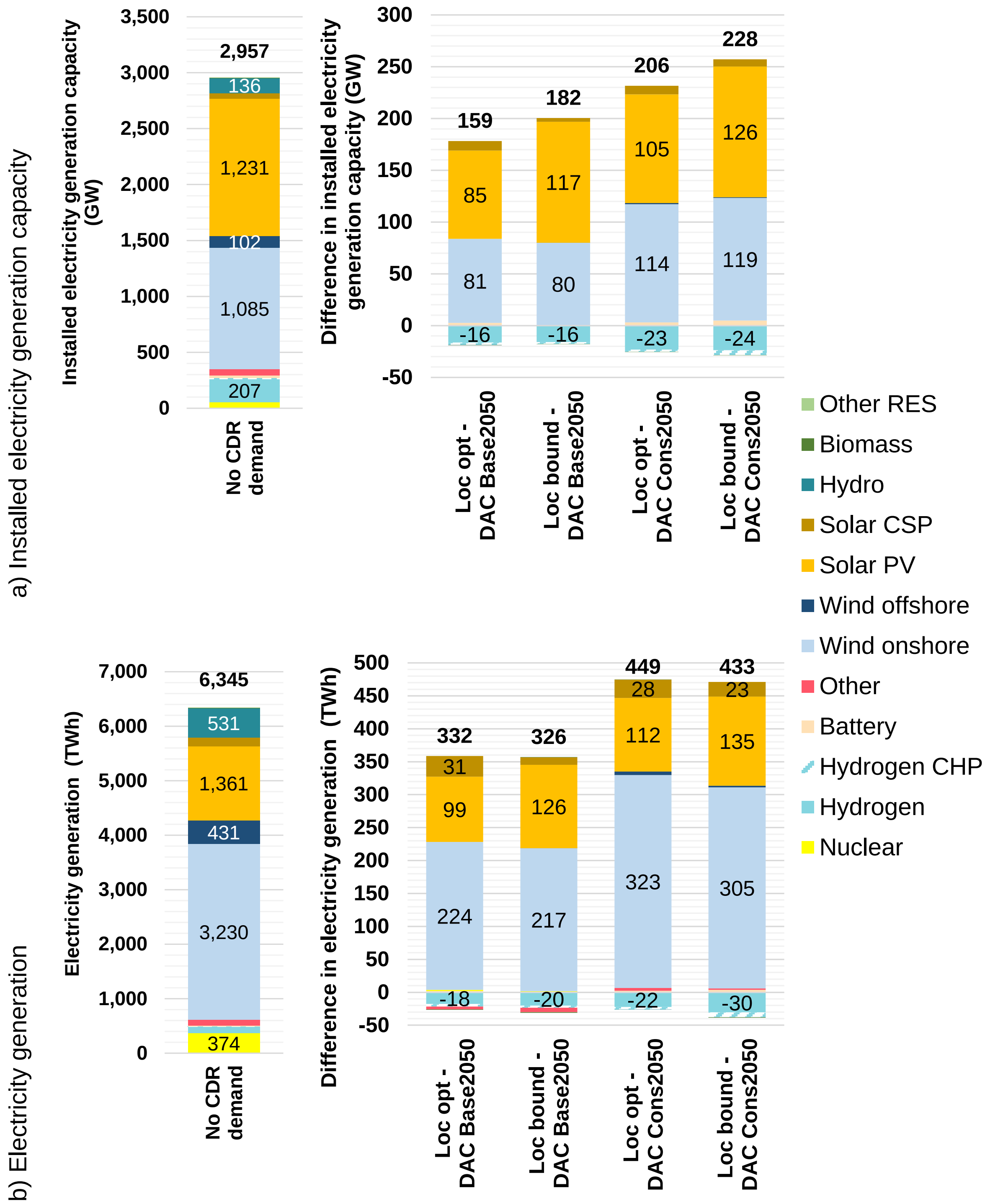

Figure 8-9 Technology-specific installed electricity generation capacities (a) and electricity generation quantities (b) in the European power sector in 2050. The results of the *No CDR demand* scenario and the deviations in the scenarios with CDR demand, as defined in Table 8-1, are distinguished.

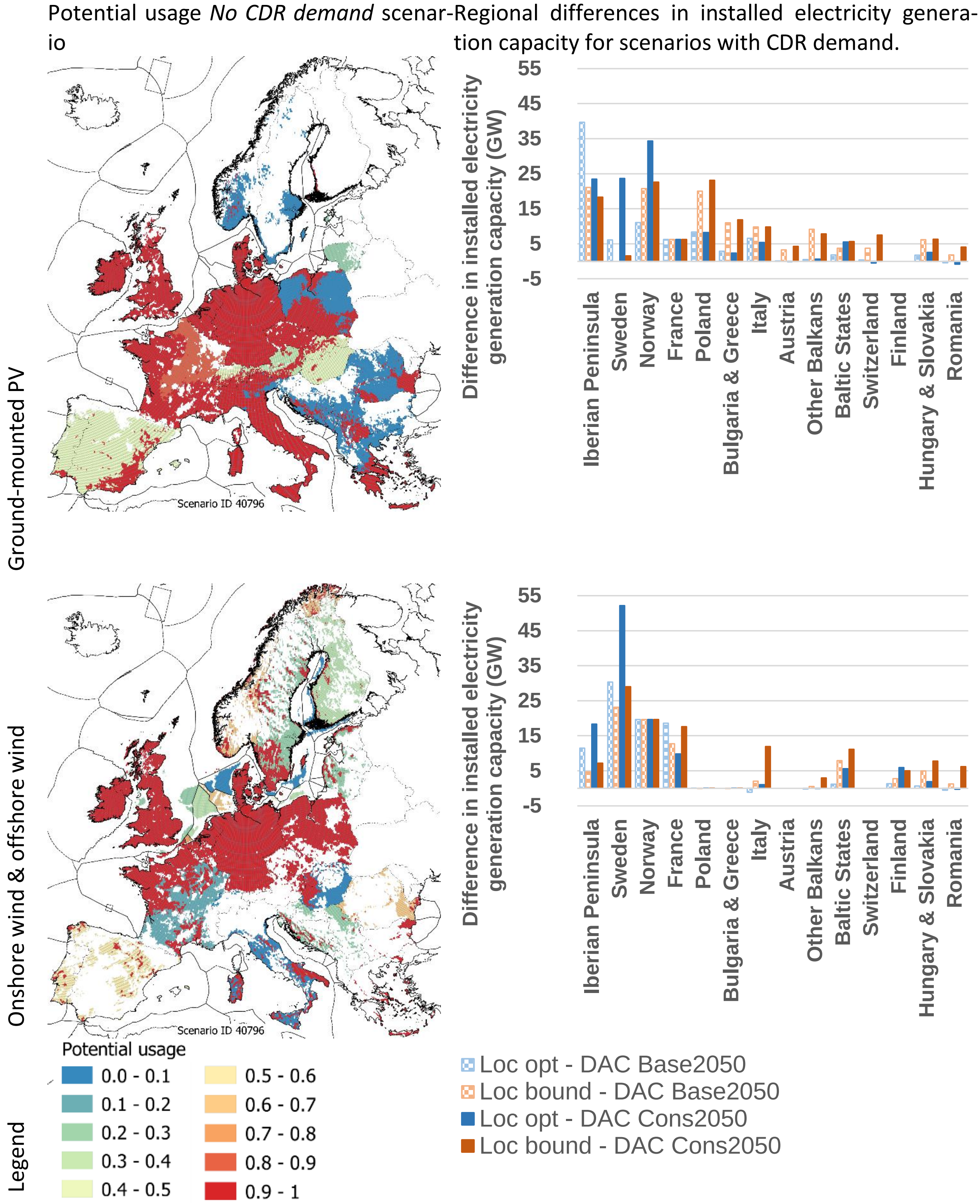

Figure 8-10 Potential utilization of the technologies ground-mounted PV, onshore wind, and offshore wind in the *No CDR demand* scenario in 2050. Deviations in installed wind and PV capacities from the *No CDR demand* scenario are shown for scenarios with CDR demand.

8.3.2.3 Regional DACCS costs

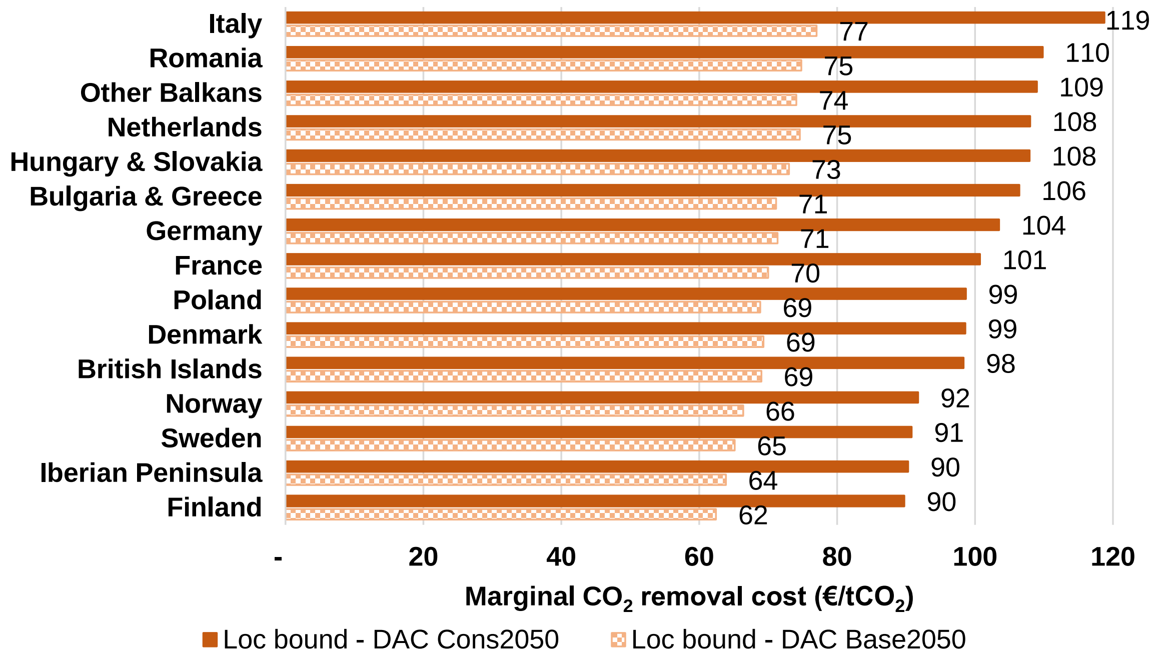

Figure 8-11 Regional DACCS costs in the scenarios *Loc bound - DAC Base2050* and *Loc bound - DAC Cons2050*. DACCS costs are obtained by evaluating the shadow prizes of CDR demand constraints in the optimization results. Austria, Switzerland, the Czech Republic, the Baltic States, and the Benelux Union are excluded because these regions do not have sufficiently large CO_2 storage potential to store their emissions (cf. section 8.2.2.3).

Figure 8-11 shows the regional cost of DACCS in the scenarios *Loc bound - DAC Cons2050* and *Loc bound - DAC Base2050*. Using the methodology approach in which explicit CDR demands must be met, DACCS costs are obtained by evaluating the shadow prices[19] in the optimization results. The regional cost results for the *Loc bound - DAC Cons2050* scenario show that Europe may be categorized into four region clusters: The first cluster consists of Finland, the Iberian Peninsula, Sweden, and Norway and shows the lowest DACCS costs between 90 €/t_{CO2} and 92 €/t_{CO2}. The second cluster consists of the British Isles, Denmark, Poland, and France. This cluster has DACCS costs between 98 €/t_{CO2} and 101 €/t_{CO2}. Germany, Bulgaria and Greece, Hungary and Slovakia, the Netherlands, the Balkan States, and Romania form the third cluster with DACCS costs between 104 €/t_{CO2} and 110 €/t_{CO2}. Italy has the highest DACCS cost compared to all other regions, with 119 €/t_{CO2}, and is the only representative of the fourth cluster. In the *Loc bound - DAC Base2050 scenario*, the clusters are not equally clear-cut and the regional differentiation of DACCS costs is weaker overall. The average DACCS costs in Europe 2050 are 104 €/t_{CO2} in the *Loc bound - DAC Cons2050* scenario and 70 €/t_{CO2} in the *Loc bound - DAC Base2050* scenario.

[19] The shadow prices represent the marginal costs of a constraint, in this case the regional CRD demand, and are retrieved from the dual value of this constraint in the optimization result.

In the *Loc opt* scenarios with an optimization of the DACCS site selection, uniform marginal DACCS costs arise in all model regions for a given CO_2 capture quantity. The optimization approach prevents arbitrage opportunities between the regions. In the *Loc Opt - DAC Base2050* scenario, an effective CDR demand of 325 Mt_{CO2} (including the GHG emission compensation for power-to-waste) results in marginal DACCS costs of 66 €/t_{CO2} in Europe; in the *Loc Opt - DAC Cons2050* scenario, it is 94 €/t_{CO2}. The total European CDR demand in these *Loc opt* scenarios is met by the five model regions with the lowest marginal DACCS costs in the *Loc bound* scenarios.

8.4 Discussion

While NETs are still in their infancy today, they can significantly change pathways to GHG neutrality: cheap NETs may prevent more expensive GHG mitigation strategies. Therefore, the discussion below compares the optimization results for DACCS to existing literature: First, to other DACCS studies (8.4.1); second, to other NET studies (8.4.2); and third, to other GHG mitigation studies in general (8.4.3). Section 8.4.4 discusses the limitation of chosen methodological approach and gives an outlook.

8.4.1 Comparison of the optimization results to other DACCS studies

Fuss et al. (2018) provide a comprehensive literature review on the costs and potentials of NETs. One NET group the review covers is DACCS. The reviewed literature shows a wide CDR cost range from 30 - 1,000 \$/t_{CO2} for DACCS. Due to different boundary conditions in existing studies, the authors emphasize that cost comparisons for DAC are difficult. Based on their understanding of the literature, Fuss et al. estimate the reasonable cost range of widely deployed DACCS plants within 100 - 300 \$/t_{CO2} (Fuss et al. 2018). Fasihi et al. (2019) calculate CO_2 capture costs of LT-DAC for Moroccan conditions in a range of 32 - 54 €/t_{CO2} in 2050, depending on the availability of cost-free waste heat. If waste heat can be deployed, together with low water demand and high modularity, this causes the cost superiority of LT-DAC over HT-DAC technology (Fasihi et al. 2019). Breyer et al. (2020) find that by optimizing operating hours and using low-cost heat, DACCS costs can decrease to around 40 €/t_{CO2}. Lackner and Azarabadi (2021)calculate DACCS cost well below 100 \$/t_{CO2} and close to 50 \$/t_{CO2} if a progressive capacity expansion is assumed. According to a comparative technical assessment of Sabatino et al. (2021), costs for CO_2 capture of less than 200 \$/t_{CO2} are possible for various LT-DAC technologies under optimized process conditions. The company Climeworks currently offers negative emissions using already existing DACCS plants for 1,000 €/t_{CO2} (Climeworks). The system cost minimization results in this manuscript show DACCS costs in Europe 2050 ranging within 60 - 140 €/t_{CO2} with progressive techno-economic assumptions and 160 - 270 €/t_{CO2} with a conservative parameter set. These DACCS costs are, therefore, of the order of magnitude in the current literature. While existing studies were either rather technically oriented or had a high-level perspective using integrated assessment models, this study closes the gap and focuses on the integration of DACCS into a renewables-based European energy system.

8.4.2 Comparison of DACCS to other negative emission technologies

Besides DACCS, Fuss et al. (2018) review other NETs. This section compares this detailed literature evaluation on the costs and potentials of six other NETs to the DACCS results obtained in this paper. One, AR describes the creation of new forests and the regeneration or recreation of former woodlands. This approach uses photosynthesis to convert and store atmospheric CO_2 in additional biomass, i.e., trees. For AR, the authors of the review estimate costs in 2050 in the range of 5 - 50 $/$t_{CO2}$ with a global carbon removal potential of 0.5 - 5 Gt_{CO2}/a. Two, Biochar is produced via pyrolysis, i.e., the thermal decomposition of organic material in a low-oxygen environment. In Fuss et al.'s review, Carbon removal by biochar production and storage in soils have estimated costs within a range of 30 - 120 $/$t_{CO2}$ at a global potential of 0.5 - 2 Gt_{CO2}/a. Three, SCS describes ways of land management in order to increase carbon absorption or decrease carbon losses of soils. SCS is associated with costs of 30 - 120 $/$t_{CO2}$ and a global carbon removal potential of 2 - 5 Gt_{CO2}/a. Four, EW on land and in oceans artificially accelerates the natural weathering of rocks. Rock material is ground to speed up the chemical reaction of atmospheric carbon dioxide with water and air. For EW, Fuss et al. estimate costs of 50 - 200 $/$t_{CO2}$ and a global potential of 2 - 4 Gt_{CO2}/a. Five, OF is a type of geo- or climate engineering that is based on the deliberate addition of plant nutrients to the upper ocean waters. It is in an attempt to remove CO_2 from the atmosphere by increasing phytoplankton production. Fuss et al. consider OF to have an extremely limited potential and give, therefore, no reasonable cost range. Six, BECCS provides negative emissions by combusting sustainable biomass in industrial or power plants and subsequently capturing and storing the resulting carbon dioxide. Fuss et al. estimate the costs of BECCS in the range of 100 - 200 $/$t_{CO2}$ with a global carbon removal potential of 0.5 - 5 Gt_{CO2}/a. The DACCS costs identified in Figure 8-6 tend to be higher than or equal to the costs of alternative NETs in the literature.

However, according to Fuss et al. (2018), all alternative NETs come with negative side effects that are not captured in their costs: For EW, local air pollution and heavy metal pollution in soils are anticipated. SCS and biochar are permanently at risk of a rapid release in case of a turnaround in land management decisions. With increasing scale, BECCS and AR programs involve substantial demand for land. Changes in land use could result in direct and indirect GHG emissions and impacts on biodiversity and soil nutrition. As DACCS is a relatively new technology, literature has not yet systematically discussed its risk of negative side effects.

8.4.3 Comparison of DACCS to other CO_2 abatement options

In addition to offsetting unavoidable remaining emissions, DACCS could play a role in GHG-neutral energy systems when alternative mitigation strategies have higher costs. Below, two approaches are presented to compare the costs of DACCS to other abatement strategies in the literature. The reference for this comparison is the maximum DACCS costs of 270 €/t_{CO2} in Europe in 2050, shown in the DACS supply curves in Figure 8-6. The first approach relies on so-called marginal abatement cost curves (MACCs). MACCs sort various GHG mitigation options according to their costs and show the corresponding saving potential. Gerbert et al. (2018) developed such a curve with measures to achieve a 95% GHG reduction in Germany. Across sectors, it shows mitigation options above 270 €/t_{CO2} with an annual saving potential of 60 Mt_{CO2}. The transport sector has the greatest savings potential within these high-cost options. The most expensive measure in this MACC is the use of synthetic hydrocarbons for electricity generation with abatement costs of 400 €/t_{CO2}. Della Vigna et al. (2021) show comparable curves taking a global perspective. Assuming a ramp-up of currently available abatement technologies until 2030, the study estimates a GHG emission abatement potential of about 2 Gt_{CO2} above costs of 270 €/t_{CO2}. This study sees options with high abatement costs primarily in the buildings and transport sectors. The MACCs in the literature show that most GHG abatement options are less expensive than DACCS. However, there is a substantial portion of abatement strategies significantly more expensive than the DACCS costs identified in this paper. The second approach uses the modeling results of mitigation pathways developed in the latest IPCC report (Lecocq et al. 2022): calculations with global models find median CO_2 prices of 578 \$/t_{CO2} for pathways reaching GHG neutrality by mid-century. This CO_2 price level is significantly above the DACCS costs in this paper.

One central challenge for DACCS is the low CO_2 concentration in the atmosphere (cf. section 8.1). Conventional CCS technologies, therefore, capture emissions at point sources such as power or industrial plants with higher CO_2 concentrations in the flue gas. Wilberforce et al. (2021) estimate the costs of post-combustion CCS in power plants in 2050 in the range of 30 - 270 \$/t_{CO2}, depending on the type of the power plant. In addition to capture costs, PSCC increases the electricity production costs by 0.01 - 0.05 \$/kWh compared to a reference power plant (Wilberforce et al. 2021). For industrial applications, Leeson et al. (2017) project PSCC costs for avoided CO_2 in 2050 to 40 \$/t_{CO2} for iron and steel production, 42.9 \$/t_{CO2} in refineries, and 19.9 \$/t_{CO2} in cement plants. The IEA (2021) lists several current post-combustion CCS projects generally focused on energy production and processing rather than industry. However, the scenario design for this paper prohibits power plants with direct CO_2 emissions in 2050. Literature values of PSCC costs in industry are lower than the DACCS costs obtained in this paper. Since PSCC is not a NET, it is not entirely accurate to compare PSCC and DACCS solely by their costs. PSCC can only reduce (in case of carbon capture and sequestration) or postpone (in case of carbon capture and use, e.g., in synthetic fuel production) fossil CO_2 emissions. In contrast, DACCS can reduce the CO_2 concentration in the atmosphere. As PSCC is locally bound to point sources, it additionally requires the transport of captured CO_2 to a storage site. However, for processes where CO_2 emissions are unavoidable, PSCC and DAC could compete for market shares in terms of capture costs and efficiency (Fasihi et al. 2019).

8.4.4 Limitations of the analytical approach and outlook

In this paper, the central analytical approach to assessing DACCS potentials is cost minimization of the European energy supply system. This approach has structural limitations. Although certain interactions with demand sectors are modeled, e.g., load shifts in charging e-mobiles, it is a partial model, and there is no detailed interaction with other parts of the economy. Furthermore, the modeling approach assumes perfect competition in markets, which does not occur in reality. A well-known characteristic of optimization models is the so-called "penny-switching" effect. It means that small changes in parameterization can lead to fundamentally different results.

A key limitation in computer-based models is computational power. Therefore, aggregations are necessary. For example, the regional resolution in the optimization is limited to national states. Possible power system bottlenecks within a region are therefore not taken into account. This may impact the locations of DACCS plants.

The applied model has a techno-economic focus. Public perception and technology acceptance can only be reflected to a very limited extent. In reality, there may be barriers that prevent the exploitation of the derived DACCS potential in this work. Dütschke et al. (2016) found that real CCS projects raised public concerns. The societal objection may result in existing geological storage potentials not being used. Furthermore, due to favorable conditions, cost minimization concentrates DACCS units in a few countries. This leads to substantial increases in renewable power generation capacity in these regions. In reality, there may be opposition to additional wind power plants for CO_2 compensation for other countries.

In this paper, flat CO_2 sequestration costs are assumed. Future work could develop and consider a pricing mechanism for the finite resource of geologic storage.

This study focuses on the integration of DACCS plants into a GHG-neutral European energy system. However, DACCS has the advantage that it can reduce CO_2 concentration regardless of the emission source. Breyer et al. (2019) show that the global south, in particular, has low-cost DAC potential. The integration of DACCS plants into non-European energy systems remains a task for future studies.

8.5 Summary and conclusions

Negative emission technologies will likely be needed to achieve the climate protection goals of the European Commission by 2050. This article investigates the potential of reducing GHGs in the atmosphere via the DACCS pathway. Since the capture of CO_2 from ambient air is energy-intensive, this study particularly considers the integration of DACCS plants into a GHG-neutral European energy system. The analyses were conducted using a new model extension of the energy system optimization model *Enertile*. Relying on a high technological, temporal and spatial resolution for renewable energy potentials, this modeling approach considers for the first time the interactions of DACCS with weather-dependent power generation technologies, flexible and inflexible power consumers, and sector coupling technologies in the context of the European energy system. Applying different evaluation approaches, the European techno-economic DACCS potential is determined and examined.

Literature shows that there are large geological CO_2 storage capacities of over 100 Gt_{CO2} in Europe. How long this storage capacity could last depends on the rate at which GHGs are extracted from the atmosphere and stored underground. If current emissions of about 4 Gt_{CO2}/a (UNCC 2021) must be removed every year, the CO_2 storage potential is exploited after 27 years. If yearly GHG emissions were reduced to 5% of 1990 emissions, the compensation of these remaining emissions through capture and storage would be possible for over 350 years.

The model results show that there is a potential for DACCS in the framework of a GHG-neutral European energy system. Assuming – in a very conservative approach – that the techno-economic properties of DAC technology do not improve by 2050 and limiting the annual CO_2 capture amount to a hundredth of the geological storage potential (about 1 Gt_{CO2}/a), the cost range for DACCS in the optimization results is between 160 €/t_{CO2} and 270 €/t_{CO2}. This cost range marks the upper limit of DACCS costs in Europe 2050 in the model results. By contrast, assuming technological progress of DAC plants, DACCS costs could be in the range of 60 €/t_{CO2} to 140 €/t_{CO2} by 2050.

The model results show that energy supply is key for the deployment of DACCS units. Firstly, energy costs are the dominant cost driver in CDR costs via DACCS. Secondly, the capture of CO_2 from ambient air is associated with substantial energy demands. Applying fully electric DAC systems and using current projections of the technological development of DAC and CO_2 storage technologies, the removal of about 288 Mt_{CO2}/a (i.e., 5% of European GHG emissions in 1990) increases the electricity demand in 2050 by 385 TWh_{el} to 495 TWh_{el} in Europe. This increase in electricity demand for DAC can be met by a 5% to 8% increase in renewable power generation capacities compared to an energy system without exogenously specified CDR demands. The capacity expansion for power generation mainly increases onshore wind and PV capacities. These required increases in power generation capacity are critical because the expansion of renewables on the path to GHG neutrality in the underlying scenario is enormous in any case. Especially in Germany, Denmark, the Czech Republic, the British Isles, and the Benelux Union, the potentials for onshore wind and ground-mounted PV are fully exploited before the energy demands for DACCS are taken into account. Germany and the British Isles, in particular, are characterized by high absolute CO_2 emissions in the past.

If cheaper heat sources – e. g., waste heat or geothermal energy – were available, lower DACCS costs and a lower additional expansion of renewable power generation technologies would be possible.

The model results show that – given a free choice of location – cost optimization favors Finland, Sweden, Norway, and the Iberian Peninsula for CO_2 capture and storage. These countries on the periphery of Europe are characterized by large geological CO_2 storage capacities and relatively low-cost, vacant renewable power generation potentials. These two characteristics are key for the future deployment of DACCS.

Even applying a conservative set of input parameters, the resulting costs for DACCS appear to be very competitive compared to the abatement costs of other climate change mitigation strategies across sectors. Many alternative CO_2 abatement strategies have been estimated to cost more than 270 €/t_{CO2} and are thus more expensive than the DACCS cost calculated in this article. This can be interpreted from two perspectives: On the one hand, from a cost-minimization perspective, DACCS could be a valuable option for minimizing the cost of combating climate change. It would essentially act as a backstop technology, pushing the necessity of using more expensive options into the future for at least several decades. On the other hand, there are substantial risks when pursuing a strategy that relies heavily on DACCS for fighting climate change, e.g., risks associated with CO_2 storage leakages, the acceptance of the required additional renewable energy capacities, or the chance that DACCS might be used excessively while still relying on fossil fuels, exhausting global storages too quickly. From this perspective, there are valid arguments that DACCS should be reserved for the compensation of unavoidable emissions, e.g., from agriculture and for cleaning up legacy emissions. Nonetheless, even from that perspective, the economic pressure for using DACCS will likely increase once costlier decarbonization options have to be pursued. From both perspectives, it is essential to research, understand, and evaluate DACCS options in greater detail and to decide and regulate their role in the strategies to fight climate change.

CRediT authorship contribution statement

Benjamin Lux: Conceptualization, Methodology, Software, Investigation, Data curation, Visualization, Writing - original draft & review.

Niklas Schneck: Software, Investigation.

Benjamin Pfluger: Writing - original draft, Supervision.

Wolfgang Männer: Writing - review.

Frank Sensfuß: Supervision.

Declaration of Interest statement

Declarations of interest: none.

Acknowledgments

The authors are indebted to Joshua Fragoso García, Christoph P. Kiefer, Christoph Kleinschmitt, Christiane Bernath, Gerda Deac, and Katja Franke for their modeling, expertise, and feedback.

Funding

This research did not receive any specific grant from funding agencies in the public, commercial, or not-for-profit sectors.

8.6 Appendix

Appendix A.Abbreviations

Table 8-3 Abbreviations.

Abbreviation	Explanation
AR	Afforestation and reforestation
BECCS	Bioenergy with carbon capture and storage
CAPEX	Capital expenditure
CCS	Carbon capture and storage
CDR	Carbon dioxide removal
CSP	Concentrating solar power
DAC	Direct air capture
DACCS	Direct air capture and storage
EC	European Commission
EU	European Union
el	electrical
e-fuels	Electricity-based fuels
EW	Enhanced weathering
FLH	Full load hours
GHG	Greenhouse gas
HT DAC	High-temperature direct air capture
IPCC	Intergovernmental Panel on Climate Change
LCOE	Levelized cost of electricity
LT DAC	Low-temperature direct air capture
NET	Negative emission technology

Abbreviation	Explanation
O&M	Operation and maintenance cost
OF	Ocean fertilization
OPEX	Operating expenditure
ppm	Parts per million
PV	Photovoltaics
RES	Renewable energy source
SCS	Soil carbon sequestration
TRL	Technology readiness level
WACC	Weighted average cost of capital

Appendix B. Model regions

Figure 8-12 Map of model regions in Enertile.

Table 8-4 Definition of regions as used in *Enertile*.

***Enertile* region code**	**Countries**	**Term used in the text**
AT	Austria	Austria
CH	Switzerland	Switzerland
DE	Germany	Germany
FR	France	France
IBEU	Spain, Portugal	Iberian Peninsula
BEU	Belgium, Luxembourg	Benelux Union
HUK	Hungary, Slovakia	Hungary & Slovakia
UKI	United Kingdom, Ireland	British Islands
PL	Poland	Poland
BUG	Bulgaria, Greece	Bulgaria & Greece
BAK	Slovenia, Croatia, Bosnia and Herzegovina, Serbia, Kosovo, Montenegro, Albania, North Macedonia	Other Balkans
BAT	Estonia, Lithuania, Latvia	Baltic States
CZ	Czech Republic	Czech Republic
DK	Denmark	Denmark
IT	Italy	Italy
NO	Norway	Norway
RO	Romania	Romania
SE	Sweden	Sweden
NL	Netherlands	Benelux Union

Appendix C. Key assumptions for the renewable potential calculation

The onshore wind potential calculations take 59 different turbine configurations into account. In 2050, hub heights in the range of 80 - 160 m and specific area outputs in the range of 270 - 500 W/m² are considered. Table 8-5 shows specific investments, fixed operation and maintenance costs, and technical lifetimes of representative combinations. The full data set is available online (Fraunhofer ISI et al. 2021a).

Table 8-5 Hub height, rotor diameter, specific investments, fixed operation and maintenance costs, and technical lifetimes of 8 representative onshore wind turbines in the potential calculation for 2050 (Fraunhofer ISI et al. 2021a).

Turbine	Hub height (m)	Specific area power (W/m²)	Specific investment (€/kW$_{el}$)	Fixed operation and maintenance cost (€/kW$_{el}$)	Technical lifetime (a)
1	120	270	1,293	23.21	20
2	120	280	1,277	22.97	20
3	120	290	1,261	22.73	20
4	140	350	1,229	22.89	20
5	150	280	1,374	25.37	20
6	150	350	1,262	23.70	20
7	160	270	1,423	26.41	20
8	160	350	1,294	24.49	20

The offshore wind potential calculations take 16 different turbine configurations into account. In 2050, hub heights in the range of 100 - 120 m and specific area outputs in the range of 370 - 450 W/m² are considered. Table 8-6 shows specific investments and fixed operation and maintenance costs of representative combinations. The full data set is available online (Fraunhofer ISI et al. 2021a).

Table 8-6 Hub height, rotor diameter, specific investments, fixed operation and maintenance costs, and technical lifetimes of 3 representative offshore wind turbines in the potential calculation for 2050.

Turbine	**Hub height (m)**	**Specific area power (W/m^2)**	**Specific investment (€/kW_{el})**	**Fixed operation and maintenance cost (€/kW_{el})**	**Technical lifetime (a)**
1	120	370	3,559	66.51	20
2	120	380	3,542	66.27	20
3	120	390	3,526	663	20

Table 8-7 shows specific investments, fixed operation and maintenance costs, and technical lifetimes of the solar technologies considered in the renewable potential calculation.

Table 8-7 Specific investments, fixed operation and maintenance costs, and technical lifetimes for different solar technologies in 2050.

	Specific investment (€/kW_{el})	**Fixed operation and maintenance cost (€/kW_{el})**	**Technical lifetime (a)**
Technology			
Ground-mounted PV	500	5,00	20
Roof-top PV	764	11,00	20
CSP	2410	40,00	30

Table 8-8 shows land use factors of all relevant technologies in the renewable potential calculation.

Table 8-8 Land use factors in the potential calculation of renewable electricity generation technologies.

Category	**Roof-top PV**	**Ground-mounted PV**	**CSP**	**Onshore wind**
Barren	0%	16%	12%	18.0%
Cropland	0%	2%	2%	14.4%
Forest	0%	0%	0%	10.8%
Grassland	0%	2%	2%	18.0%
Savannah	0%	2%	12%	18.0%

Category	Roof-top PV	Ground-mounted PV	CSP	Onshore wind
Shrubland	0%	2%	12%	18.0%
Snow and ice	0%	4%	0%	10.8%
Urban	16%	0%	0%	0.0%
Water	0%	0%	0%	0.0%
Wetlands	0%	0%	0%	0.0%

References

Barnes, J.; Bhagavathy, S. M. (2020): The economics of heat pumps and the (un)intended consequences of government policy. In: Energy Policy, 138, p. 111198. https://doi.org/10.1016/j.enpol.2019.111198.

Bernath, C.; Deac, G.; Sensfuss, F. (2019): Influence of heat pumps on renewable electricity integration: Germany in a European context. In: Energy Strategy Reviews, 26, p. 100389. https://doi.org/10.1016/j.esr.2019.100389.

Bernath, C.; Deac, G.; Sensfuss, F. (2021): Impact of sector coupling on the market value of renewable energies – A model-based scenario analysis. In: Applied Energy, 281, p. 115985. https://doi.org/10.1016/j.apenergy.2020.115985.

Bloess, A.; Schill, W.-P.; Zerrahn, A. (2018): Power-to-heat for renewable energy integration: A review of technologies, modeling approaches, and flexibility potentials. In: Applied Energy, 212, pp. 1611–1626. https://doi.org/10.1016/j.apenergy.2017.12.073.

Bollmeyer, C.; Keller, J. D.; Ohlwein, C.; Wahl, S.; Crewell, S.; Friederichs, P.; Hense, A.; Keune, J.; Kneifel, S.; Pscheidt, I.; Redl, S.; Steinke, S. (2015): Towards a high-resolution regional re-analysis for the European CORDEX domain. https://doi.org/10.1002/qj.2486.

Breyer, C.; Fasihi, M.; Aghahosseini, A. (2020): Carbon dioxide direct air capture for effective climate change mitigation based on renewable electricity: a new type of energy system sector coupling. In: Mitigation and Adaptation Strategies for Global Change, 25 (1), pp. 43–65. https://doi.org/10.1007/s11027-019-9847-y.

Breyer, C.; Fasihi, M.; Bajamundi, C.; Creutzig, F. (2019): Direct Air Capture of CO2: A Key Technology for Ambitious Climate Change Mitigation. In: Joule, 3 (9), pp. 2053–2057. https://doi.org/10.1016/j.joule.2019.08.010.

Budinis, S.; Krevor, S.; Dowell, N. M.; Brandon, N.; Hawkes, A. (2018): An assessment of CCS costs, barriers and potential. In: Energy Strategy Reviews, 22, pp. 61–81. https://doi.org/10.1016/j.esr.2018.08.003.

Bundesministerium für Umwelt, Naturschutz und nukleare Sicherheit (2020): Treibhausgas-Emissionen der Europäischen Union in Millionen Tonnen Kohlendioxid-Äquivalenten. Available at https://www.umweltbundesamt.de/sites/default/files/medien/384/bilder/dateien/2_tab_thg-emi-eu_2020-08-25.pdf, accessed 24.04.2021.

Chen, C.; Tavoni, M. (2013): Direct air capture of CO2 and climate stabilization: A model based assessment. In: Climatic Change, 118 (1), pp. 59–72. https://doi.org/10.1007/s10584-013-0714-7.

Climeworks: Climeworks website. Available at https://climeworks.com/, accessed 15.10.2022.

d'Amore, F.; Bezzo, F. (2017): Economic optimisation of European supply chains for CO 2 capture, transport and sequestration. In: International Journal of Greenhouse Gas Control, 65, pp. 99–116. https://doi.org/10.1016/j.ijggc.2017.08.015.

Danielson, J. J.; Gesch, D. B. (2011): Global multi-resolution terrain elevation data 2010 (GMTED2010). In: Open-File Report, (2011-1073). https://doi.org/10.3133/ofr20111073.

Deac, G. (2019): Auswirkung der Kopplung von Strom- und Wärmemarkt auf die künftige Integration der erneurbaren Energien und die CO2-Emissionen in Deutschland.

Della Vigna, M.; Stavrinou, Z.; Gandolfi, A.; Snowdon, N.; Young, P.; Tylenda, E.; Chetwode, S.; Singer, B.; Bingham, D. R.; Jones, E. (2021): Carbonomics. Introducing the GS net zero carbon models and sector frameworks.

Dütschke, E.; Wohlfarth, K.; Höller, S.; Viebahn, P.; Schumann, D.; Pietzner, K. (2016): Differences in the public perception of CCS in Germany depending on CO 2 source, transport option and storage location. In: International Journal of Greenhouse Gas Control, 53, pp. 149–159. https://doi.org/10.1016/j.ijggc.2016.07.043.

EU GeoCapacity (2009): Assessing European Capacity for Geological Storage of Carbon Dioxide. D16 WP2 Report. Available at http://www.geology.cz/geocapacity/publications.

European Commission (Ed.) (2019): The European Green Deal. Brussels.

European Environment Agency (2018): CORINE Land Cover. Available at https://land.copernicus.eu/pan-european/corine-land-cover, accessed 29.06.2022.

Fasihi, M.; Efimova, O.; Breyer, C. (2019): Techno-economic assessment of CO2 direct air capture plants. In: Journal of Cleaner Production, 224, pp. 957–980. https://doi.org/10.1016/j.jclepro.2019.03.086.

Franke, K.; Sensfuss, F.; Bernath, C.; Lux, B. (2021): Carbon-neutral energy systems and the importance of flexibility options: A case study in China. In: Computers & Industrial Engineering, p. 107712. https://doi.org/10.1016/j.cie.2021.107712.

Fraunhofer Institut für System- und Innovationsforschung (2021): Enertile. Available at https://www.enertile.eu/enertile-en/index.php.

Fraunhofer Institut für System- und Innovationsforschung; Consentec GmbH (Consentec); ifeu - Institut für Energie- und Umweltforschung Heidelberg GmbH; Lehrstuhl für Energie- und Ressourcenmanagement der TU Berlin (2021a): Dashboards Erneuerbare Energien TN-Szenarien. Langfristszenarien. Available at https://www.langfristszenarien.de/enertile-explorer-de/szenario-explorer/erneuerbare.php, accessed 29.06.2022.

Fraunhofer Institut für System- und Innovationsforschung; Consentec GmbH (Consentec); ifeu - Institut für Energie- und Umweltforschung Heidelberg GmbH; Lehrstuhl für Energie- und Ressourcenmanagement der TU Berlin (2021b): Langfristszenarien. Available at https://www.langfristszenarien.de/enertile-explorer-de/, accessed 17.06.2021.

Fuhrman, J.; McJeon, H.; Patel, P.; Doney, S. C.; Shobe, W. M.; Clarens, A. F. (2020): Food–energy–water implications of negative emissions technologies in a +1.5 °C future. In: Nature Climate Change, 10 (10), pp. 920–927. https://doi.org/10.1038/s41558-020-0876-z.

Fuss, S.; Lamb, W. F.; Callaghan, M. W.; Hilaire, J.; Creutzig, F.; Amann, T.; Beringer, T.; Oliveira Garcia, W. de; Hartmann, J.; Khanna, T.; Luderer, G.; Nemet, G. F.; Rogelj, J.; Smith, P.; Vicente, J. L. V.; Wilcox, J.; del Mar Zamora Dominguez, M.; Minx, J. C. (2018): Negative emissions—Part 2: Costs, potentials and side effects. In: Environmental Research Letters, 13 (6), p. 63002. https://doi.org/10.1088/1748-9326/aabf9f.

Galán-Martín, Á.; Vázquez, D.; Cobo, S.; Mac Dowell, N.; Caballero, J. A.; Guillén-Gosálbez, G. (2021): Delaying carbon dioxide removal in the European Union puts climate targets at risk. In: Nature communications, 12 (1), p. 6490. https://doi.org/10.1038/s41467-021-26680-3.

Gerbert, P.; Herhold, P.; Burchardt, J.; Schönberger, S.; Rechenmacher, F.; Kirchner, A.; Kemmler, A.; Wünsch, M. (2018): Klimapfade für Deutschland.

IEA International Energy Agency (2021): Direct Air Capture. Available at https://www.iea.org/reports/direct-air-capture, accessed 28.12.2021.

Lackner, K. S.; Azarabadi, H. (2021): Buying down the Cost of Direct Air Capture. In: Industrial & Engineering Chemistry Research, 60 (22), pp. 8196–8208. https://doi.org/10.1021/acs.iecr.0c04839.

Lecocq, F.; Winkler, H.; Daka, J. P.; Gerber, J.; Kartha, S.; Krey, V.; Lofgren, H.; Masui, T.; Mathur, R.; Pereira, J. P.; Sovacool, B.; Zhou, N. (2022): Mitigation and development pathways in the near- to mid-term. In: IPCC Intergovernmental Panel on Climate Change (Ed.): Climate Change 2022: Mitigation of Climate Change. Contribution of Working Group III to the Sixth Assessment Report of the Intergovernmental Panel on Climate Change. Cambridge, UK: Cambridge University Press. https://doi.org/10.1017/9781009157926.006.

Leeson, D.; Mac Dowell, N.; Shah, N.; Petit, C.; Fennell, P. S. (2017): A Techno-economic analysis and systematic review of carbon capture and storage (CCS) applied to the iron and steel, cement, oil refining and pulp and paper industries, as well as other high purity sources. In: International Journal of Greenhouse Gas Control, 61, pp. 71–84. https://doi.org/10.1016/j.ijggc.2017.03.020.

Lowes, R.; Rosenow, J.; Qadrdan, M.; Wu, J. (2020): Hot stuff: Research and policy principles for heat decarbonisation through smart electrification. In: Energy research & social science, 70, p. 101735. https://doi.org/10.1016/j.erss.2020.101735.

Lux, B.; Deac, G.; Kiefer, C. P.; Kleinschmitt, C.; Bernath, C.; Franke, K.; Pfluger, B.; Willemsen, S.; Sensfuss, F. (2022): The role of hydrogen in a greenhouse gas-neutral energy supply system in Germany. In: Energy Conversion and Management, 270, p. 116188. https://doi.org/10.1016/j.enconman.2022.116188.

Lux, B.; Gegenheimer, J.; Franke, K.; Sensfuss, F.; Pfluger, B. (2021): Supply curves of electricity-based gaseous fuels in the MENA region. In: Computers & Industrial Engineering, p. 107647. https://doi.org/10.1016/j.cie.2021.107647.

Lux, B.; Pfluger, B. (2020): A supply curve of electricity-based hydrogen in a decarbonized European energy system in 2050. In: Applied Energy, 269, p. 115011. https://doi.org/10.1016/j.apenergy.2020.115011.

Marcucci, A.; Kypreos, S.; Panos, E. (2017): The road to achieving the long-term Paris targets: energy transition and the role of direct air capture. In: Climatic Change, 144 (2), pp. 181–193. https://doi.org/10.1007/s10584-017-2051-8.

Minx, J. C.; Lamb, W. F.; Callaghan, M. W.; Fuss, S.; Hilaire, J.; Creutzig, F.; Amann, T.; Beringer, T.; Oliveira Garcia, W. de; Hartmann, J.; Khanna, T.; Lenzi, D.; Luderer, G.; Nemet, G. F.; Rogelj, J.; Smith, P.; Vicente Vicente, J. L.; Wilcox, J.; del Mar Zamora Dominguez, M. (2018): Negative emissions—Part 1: Research landscape and synthesis. In: Environmental Research Letters, 13 (6), p. 63001. https://doi.org/10.1088/1748-9326/aabf9b.

Navigant (2019): Gas for Climate. The optimal role for gas in a net zero emissions energy system. Available at https://gasforclimate2050.eu/wp-content/uploads/2020/03/Navigant-Gas-for-Climate-The-optimal-role-for-gas-in-a-net-zero-emissions-energy-system-March-2019.pdf, accessed 25.02.2021.

Observ'ER; TNO; RENAC; Frankfurt School of Finance and Management; Fraunhofer Institut für System- und Innovationsforschung; Statistics Netherlands (2020): The state of renewable energies in Europe. Edition 2019 19th EurObserv'ER Report.

Pfluger, B. (2014): Assessment of least-cost pathways for decarbonising Europe's power supply. A model-based long-term scenario analysis accounting for the characteristics of renewable energies. Karlsruhe.

Realmonte, G.; Drouet, L.; Gambhir, A.; Glynn, J.; Hawkes, A.; Köberle, A. C.; Tavoni, M. (2019): An inter-model assessment of the role of direct air capture in deep mitigation pathways. In: Nature communications, 10 (1), p. 3277. https://doi.org/10.1038/s41467-019-10842-5.

Rogelj, J.; Shindell, D.; Jiang, K.; Fifita, S.; Forster, P.; Ginzburg, V.; Handa, C.; Kheshgi, H.; Kobayashi, S.; Kriegler, E.; Mundaca, L.; Séférian, R.; Vilarino, M. V. (2018): Mitigation Pathways Compatible with 1.5°C in the Context of Sustainable Development.

Sabatino, F.; Grimm, A.; Gallucci, F.; van Sint Annaland, M.; Kramer, G. J.; Gazzani, M. (2021): A comparative energy and costs assessment and optimization for direct air capture technologies. In: Joule, 5 (8), pp. 2047–2076. https://doi.org/10.1016/j.joule.2021.05.023.

Sensfuss, F.; Franke, K.; Kleinschmitt, C. (2021a): Langfristszenarien für die Transformation des Energiesystems in Deutschland 3. Potentiale der Windenergie auf See Datensatz 127. Available at https://www.langfristszenarien.de/enertile-explorer-de/dokumente/, accessed 29.06.2022.

Sensfuss, F.; Franke, K.; Kleinschmitt, C. (2021b): Langfristszenarien für die Transformation des Energiesystems in Deutschland 3. Potentiale Windenergie an Land Datensatz 174. Available at https://www.langfristszenarien.de/enertile-explorer-de/dokumente/, accessed 29.06.2022.

Skydsgaard, N. (9/14/2021): World's largest plant capturing carbon from air starts in Iceland. In: Reuters Media. Available at https://www.reuters.com/business/environment/worlds-largest-plant-capturing-carbon-air-starts-iceland-2021-09-08/, accessed 28.12.2021.

Smith, L. J.; Torn, M. S. (2013): Ecological limits to terrestrial biological carbon dioxide removal. In: Climatic Change, 118 (1), pp. 89–103. https://doi.org/10.1007/s10584-012-0682-3.

Smith, P.; Davis, S. J.; Creutzig, F.; Fuss, S.; Minx, J. C.; Gabrielle, B.; Kato, E.; Jackson, R. B.; Cowie, A.; Kriegler, E.; van Vuuren, D. P.; Rogelj, J.; Ciais, P.; Milne, J.; Canadell, J. G.; McCollum, D.; Peters, G.; Andrew, R.; Krey, V.; Shrestha, G.; Friedlingstein, P.; Gasser, T.; Grübler, A.; Heidug, W. K.; Jonas, M.; Jones, C. D.; Kraxner, F.; Littleton, E.; Lowe, J.; Moreira, J. R.; Nakicenovic, N.; Obersteiner, M.; Patwardhan, A.; Rogner, M.; Rubin, E.; Sharifi, A.; Torvanger, A.; Yamagata, Y.; Edmonds, J.; Yongsung, C. (2016): Biophysical and economic limits to negative CO2 emissions. In: Nature Climate Change, 6 (1), pp. 42–50. https://doi.org/10.1038/nclimate2870.

Snæbjörnsdóttir, S. Ó.; Sigfússon, B.; Marieni, C.; Goldberg, D.; Gislason, S. R.; Oelkers, E. H. (2020): Carbon dioxide storage through mineral carbonation. In: Nature Reviews Earth & Environment, 1 (2), pp. 90–102. https://doi.org/10.1038/s43017-019-0011-8.

Strefler, J.; Bauer, N.; Kriegler, E.; Popp, A.; Giannousakis, A.; Edenhofer, O. (2018): Between Scylla and Charybdis: Delayed mitigation narrows the passage between large-scale CDR and high costs. In: Environmental Research Letters, 13 (4), p. 44015. https://doi.org/10.1088/1748-9326/aab2ba.

Thoning, K. W.; Crotwell, A. M.; Mund, J. W. (2022): Atmospheric Carbon Dioxide Dry Air Mole Fractions from continuous measurements at Mauna Loa, Hawaii, Barrow, Alaska, American Samoa and South Pole. Boulder, Colorado, USA: National Oceanic and Atmospheric Administration; Global Monitoring Laboratory. https://doi.org/10.15138/yaf1-bk21.

United Nation Climate Change (2021): GHG inventory database. Available at https://di.unfccc.int/time_series, accessed 22.04.2021.

United Nations (Ed.) (2015a): Paris Agreement. Available at https://unfccc.int/sites/default/files/english_paris_agreement.pdf.

United Nations (2015b): Transforming our world: the 2030 Agenda for Sustainable Development, Viebahn, P.; Scholz, A.; Zelt, O. (2019): The Potential Role of Direct Air Capture in the German Energy Research Program--Results of a Multi-Dimensional Analysis. In: Energies, 12 (18), p. 3443. https://doi.org/10.3390/en12183443.

Wilberforce, T.; Olabi, A. G.; Sayed, E. T.; Elsaid, K.; Abdelkareem, M. A. (2021): Progress in carbon capture technologies. In: The Science of the total environment, 761, p. 143203. https://doi.org/10.1016/j.scitotenv.2020.143203.

Wohland, J.; Witthaut, D.; Schleussner, C.-F. (2018): Negative Emission Potential of Direct Air Capture Powered by Renewable Excess Electricity in Europe. In: Earth's Future, 6 (10), pp. 1380–1384. https://doi.org/10.1029/2018EF000954.

Zhang, D.; Song, J. (2014): Mechanisms for Geological Carbon Sequestration. In: Procedia IUTAM, 10, pp. 319–327. https://doi.org/10.1016/j.piutam.2014.01.027.

[End of Paper 4]

List of publications

Peer-reviewed publications

Lux, Benjamin; Poslowsky, Stefan; Pfluger, Benjamin (2019): The economics of possible CO2 utilization pathways in a highly decarbonized European energy system. In: *2019 16th International Conference on the European Energy Market (EEM)*. IEEE. Piscataway. NJ. DOI: 10.1109/EEM.2019.8916453.

Lux, Benjamin; Pfluger, Benjamin (2020): A supply curve of electricity-based hydrogen in a decarbonized European energy system in 2050. In: *Applied Energy 269*, p. 115011. DOI: 10.1016/j.apenergy.2020.115011.

Lux, Benjamin; Gegenheimer, Johanna; Franke, Katja; Sensfuß, Frank; Pfluger, Benjamin (2021): Supply curves of electricity-based gaseous fuels in the MENA region. In: *Computers & Industrial Engineering 162*, p. 107647. DOI: 10.1016/j.cie.2021.107647.

Franke, Katja; Sensfuß, Frank; Bernath, Christiane; **Lux, Benjamin** (2021): Carbon-neutral energy systems and the importance of flexibility options: a case study in china. In: *Computers & Industrial Engineering 162*, p. 107712. DOI: 10.1016/j.cie.2021.107712.

Lux, Benjamin; Deac, Gerda; Kiefer, Christoph P.; Kleinschmitt, Christoph; Bernath, Christiane; Franke, Katja et al. (2022): The role of hydrogen in a greenhouse gas-neutral energy supply system in Germany. In: *Energy Conversion and Management 270*, p. 116188. DOI: 10.1016/j.enconman.2022.116188.

Lux, Benjamin; Schneck, Niklas; Pfluger, Benjamin; Männer, Wolfgang; Sensfuß, Frank (2023): Potentials of direct air capture and storage in a greenhouse gas-neutral European energy system. In: *Energy Strategy Reviews 45,* p. 101012. DOI: 10.1016/j.esr.2022.101012.

Further publications

Lux, Benjamin; Pfluger, Benjamin; Sensfuss, Frank (2018): Wasserstoff als Flexibilitätsoption im europäischen Stromsektor. In: *15. Symposium Energieinnovation (EnInnov2018)*. Online available: https://www.tugraz.at/fileadmin/user_upload/Events/Eninnov2018/files/lf/Session_G2/824_LF_Lux.pdf, zuletzt geprüft am 04.02.2022.

Franke, Katja; Sensfuß, Frank; Deac, Gerda; Pfluger, Benjamin; Bernath, Christiane; **Lux, Benjamin** (2019): Modellgestützte Analyse optimaler Anpassungsreaktionen des europäischen Stromsystems an unterschiedliche Wettersituationen. In: *11. Internationale Energiewirtschaftstagung an der TU Wien (IEWT2019)*.

Böttger, Diana; Kost, Christoph; Wrede, Daniel; **Lux, Benjamin**; Fleiter, Tobias; Pfluger, Benjamin; Heilig, Judith; Gerhardt, Norman; Haendel, Michael (2021): Interaction of Energy Storage Technologies and Synthetic Fuels in Long-Term Decarbonization Scenarios. In: *Proceedings of the 14th International Renewable Energy Storage Conference 2020 (IRES 2020)*. DOI: 10.2991/ahe.k.210202.009.

Breitschopf, Barbara; **Lux, Benjamin**; Neuner, Felix; Wietschel, Martin (2022): Länderrisiken adäquat berücksichtigen. In: *BWK 74 (5-6)*, pp. 56-59. DOI: 10.37544/1618-193X-2022-5-6-56.

List of Tables

List of Figures

List of Abbreviations

Abbreviation	Explanation
AEL	Alkaline electrolysis
AR	Afforestation and reforestation
BECCS	Bioenergy with carbon capture and storage
BEV	Battery electric vehicles
BfJ	Bundesamt für Justiz
BMJ	Bundesministerium der Justiz und für Verbraucherschutz
BMUV	Bundesministerium für Umwelt, Naturschutz, nukleare Sicherheit und Verbraucherschutz
BMWK	Bundesministerium für Wirtschaft und Klimaschutz
BoL	Begin of life
CAPEX	Capital expenditure
CCS	Carbon capture and storage
CDR	Carbon dioxide removal
CH_4	Methane
CHP	Combined heat and power
CO_2	Carbon dioxide
CSP	Concentrating solar power
DAC	Direct air capture, CO_2 separation from ambient air
DACCS	Direct air capture and storage
DS	Demand-supply equation
e-fuels	Electricity-based energy carriers
EC	European Commission

el	Electric
EU	European Union
EW	Enhanced weathering
FLH	Full load hours
GHG	Greenhouse gas
H_2	Hydrogen
HT DAC	High-temperature direct air capture
IEA	International Energy Agency
IPCC	Intergovernmental Panel on Climate Change
L-hydrogen	Liquefied hydrogen
L-methane	Liquefied methane
LCOE	Levelized cost of electricity
LHV	Lower heating value
LNG	Liquefied natural gas
LT DAC	Low-temperature direct air capture
MACC	Marginal abatement cost curve
MENA	Middle East and North Africa
NET	Negative emission technology
NTC	Net transfer capacity
O&M	Operation and maintenance cost
OF	Ocean fertilization
OPEX	Operating expenditure
PEM	Polymer electrolyte membrane
PEMEL	Polymer electrolyte membrane electrolysis

PHEV	Plug-in hybrid electric vehicles
ppm	Parts per million
$PtCH_4$	Power-to-Methane
PtG	Power-to-Gas
PtH_2	Power-to-Hydrogen
PtL	Power-to-Liquid
PtX	Power-to-X
PV	Photovoltaics
RES	Renewable energy source
SCS	Soil carbon sequestration
SED	Specific energy demand
SOEL	Solid oxide electrolysis
STP	Standard temperature and pressure (T_{STP} = 0 °C, p_{STP} =1.01325 bar).
th	thermal
TRL	Technology readiness level
UN	United Nations
UNFCC	United Nations Framework Convention on Climate Change
WACC	Weighted average cost of capital
wt	weight